From the Institut for Immunology
Center for Infection, Inflammation, and Immunity

Executive Director: Prof. Dr. Stefan Bauer

of the Faculty of Medicine of the Philipps-Universität Marburg

Impact of the Transcription Factor HoxA9 on Toll-like Receptor-Mediated Innate Immune Responses and Development of Dendritic Cells and Macrophages

Inaugural-Dissertation
For the Degree Doctor of Medicine

Submitted to the Faculty of Medicine of the Philipps-Universität Marburg

by
Tobias Mischa Bleyl
from Erlabrunn

Marburg, 2018

Aus dem Institut für Immunologie
Zentrum für Infektion, Entzündung und Immunität

Geschäftsführender Direktor: Prof. Dr. Stefan Bauer

des Fachbereichs Medizin der Philipps-Universität Marburg

Einfluss des Transkriptionsfaktors HoxA9 auf Toll-like Rezeptor-vermittelte Reaktionen des angeborenen Immunsystems und die Entwicklung von dendritischen Zellen und Makrophagen

Inaugural-Dissertation
zur Erlangung des Doktorgrades der Humanmedizin

dem Fachbereich Medizin der Philipps-Universität Marburg

vorgelegt von
Tobias Mischa Bleyl
aus Erlabrunn

Marburg, 2018

Angenommen vom Fachbereich Medizin der Philipps-Universität Marburg am: 10.07.2018

Gedruckt mit Genehmigung des Fachbereichs

Dekan: Prof. Dr. Helmut Schäfer
Referent: Prof. Dr. Stefan Bauer
1. Korreferentin: Prof. Dr. Adriana del Rey

Dedicated to my *beloved* parents Karla & Fritz Bleyl and my *wonderful* wife Jessica Bleyl

ABSTRACT

Purpose of this work: Toll-like receptors (TLRs) are sensors of the innate immune system that perceive evolutionary conserved microbial structures and act as first line defense mechanisms against bacteria, viruses, fungi, and parasites. As a subset of the TLR family, intracellular TLRs reside in endosomal compartments to encounter their ligands comprising different types of nucleic acids. Important members are TLR3, 7, 8, and 9 recognizing double-stranded RNA (dsRNA), single-stranded RNA (ssRNA), again ssRNA, and unmethylated CpG-motif containing DNA, respectively. Innate immune cells including dendritic cells (DCs) and macrophages (MΦs) show different expression profiles and varying functions of intracellular TLRs. In mice, conventional dendritic cells (cDCs) and MΦs express TLR3, 7, and 9, which predominantly induce secretion of proinflammatory cytokines such as IL-6 after activation, whereas type I interferons (IFNs) are only upregulated upon ligation of TLR3 in these cell types. A rare subset of DCs referred to as plasmacytoid dendritic cells (pDCs) uniquely possesses the ability to massively induce Interferon-α and -β (IFN-α/-β; type I IFNs) upon stimulation of TLR7 and 9. Furthermore, murine pDCs have been shown to sense DNA via TLR9 in a CpG-motif independent way. However, the molecular mechanisms of cell type-dependent functional variations of intracellular TLRs are not fully understood and mostly remain elusive. Besides involvement in embryonic tissue patterning, the homeodomain-containing transcription factor HoxA9 is known to play essential roles in normal and malignant hematopoietic processes such as maintaining the stem cell status, leukemogenesis, and the generation of B cell progenitors. The latter circumstance has been partly linked to transcriptional regulation of the cytokine receptor fms-like tyrosine kinase 3 (Flt3) in hematopoietic progenitors. However, Flt3 and its ligand Flt3L are also crucial signals for the development and homeostasis of DCs. Moreover, prominent mRNA expression levels of *hoxa9* upon stimulation of TLR9 in murine pDCs (unpublished data) suggest participation of this transcription factor in TLR9 biology particularly in pDCs. The impact of HoxA9 on the function of intracellular TLRs as well as development of DCs and MΦs was therefore investigated in this study using HoxA9 knockout (KO) mice.

Hypothesis: Upregulation of HoxA9 upon activation of TLR9 in pDCs and involvement in B cell differentiation via Flt3 suggests a prominent role of this gene in TLR-mediated

immune responses as well as development of DCs and MΦs.

Results: HoxA9$^{-/-}$ mice displayed an insignificant hypocellularity of total nucleated bone marrow (BM) cells, which was reported before by several other groups. FACS analyses of total BM cells *ex vivo* revealed significantly reduced B cell counts but normal quantities of mature DC subsets in HoxA9-deficient mice, again confirming previous studies. TLR stimulation experiments of HoxA9$^{-/-}$ total BM cells as well as FACS-sorted pDC fractions *ex vivo* exhibited statistically significant impaired IFN-α responses upon TLR7 and 9 activation, whereas FACS-sorted cDCs did not show significant alterations in TLR function. Moreover, *in vitro* generated HoxA9-deficient Flt3L-induced DC cultures, which contain pDCs and cDCs, displayed almost completely abolished IFN-α levels and clearly reduced IL-6 levels upon TLR7/9 stimulation compared to wild type (WT). Importantly, Flt3L-induced DC cultures generated from BM cells of HoxA9-deficient animals presented notably reduced amounts of differentiated cells after the maturation period, a higher rate of dead cells, and a shifted pDC/cDC ratio in comparison to WT littermates. Conversely, *in vitro* generated GM-CSF-induced cDCs and M-CSF-induced MΦs demonstrated no significant differences in surface marker expression and TLR-mediated cytokine responses in the KO cultures. Primary splenocytes of HoxA9-deficient and WT animals showed equal quantities of both DC subsets regarding surface markers measured by FACS. Nonetheless, TLR7/9-mediated IFN-α levels of HoxA9$^{-/-}$ splenic pDCs displayed reductions similarly to those found in the BM. Finally, genome-wide microarray expression profiling of FACS-sorted BM-derived pDCs revealed differential expression of several genes between KO and WT including the HoxA9 co-factor Meis1.

Conclusions: Collectively, these results implicate a pivotal role for HoxA9 in TLR7/9-mediated pDC-specific immunity especially impacting on IFN-α responses. TLR biology of cDCs and MΦs is apparently not affected by the HoxA9 knockout. DC development among HoxA9$^{-/-}$ BM cells is partly impaired *in vitro*. However, this effect is compensated *in vivo*. The emerging evidence that pDCs play central roles in the pathogenesis of numerous human disorders such as viral infections, autoimmune diseases, and the tumorigenesis of various types of cancer underlines the importance of these cells and emphasizes the fact that HoxA9 could serve as a potential therapeutic target.

ZUSAMMENFASSUNG

Ziel dieser Arbeit: Toll-like Rezeptoren (TLRs) sind Sensoren des angeborenen Immunsystems, welche durch die Evolution konservierte mikrobielle Strukturen erkennen und als Mechanismen der ersten Verteidigungslinie gegen Bakterien, Viren, Pilze und Parasiten zu betrachten sind. Eine Subfamilie stellen die intrazellulären TLRs dar, welche sich in unterschiedlichen endosomalen Kompartimenten befinden, um dort ihre Liganden, bestehend aus verschiedenen Typen von Nukleinsäuren, zu erkennen. Zu den intrazellulären TLRs gehören TLR3, 7, 8 und 9. TLR3 erkennt doppelsträngige RNA (dsRNA), TLR7 und 8 erkennen einzelsträngige RNA (ssRNA) und TLR9 wird durch DNA aktiviert, welche unmethylierte CpG-Sequenzen enthält. Zellen des angeborenen Immunsystems, wie dendritische Zellen (DCs) und Makrophagen, zeigen unterschiedliche Expressionsprofile intrazellulärer TLRs. Zudem kann die Funktion der einzelnen TLRs je nach Zelltyp variieren. Konventionelle dendritische Zellen (cDCs) und Makrophagen in Mäusen exprimieren TLR3, 7 und 9. Nach Aktivierung der TLRs mit dem jeweiligen Ligand kommt es zur Bildung und Sekretion von proinflammatorischen Zytokinen wie IL-6. Zusätzlich wird bei der Aktivierung von TLR3 die Freisetzung von Typ I Interferonen, wie Interferon-α und -β (IFN-α/-β), induziert. Eine selten vorkommende Subpopulation von dendritischen Zellen, genannt plasmazytoide dendritische Zellen (pDCs), hat die außergewöhnliche Fähigkeit, eine enorme Menge an IFN-α und -β nach Aktivierung von TLR7 und 9 freizusetzen. Zudem konnte an murinen pDCs gezeigt werden, dass TLR9 in diesem Zelltyp auch DNA ohne unmethylierte CpG-Sequenzen erkennen kann. Die molekularen Mechanismen zelltypabhängiger funktioneller Unterschiede von intrazellulären TLRs werden bisher noch nicht gut verstanden. Der Transkriptionsfaktor HoxA9, welcher eine Homöodomäne besitzt, spielt verschiedene wichtige Rollen in der Embryogenese und bei diversen Prozessen im Rahmen der Hämatopoese, wie beispielsweise die Erhaltung des Stammzellenstatus, Bildung von Progenitor-Zellen der B-Zell Reihe und bei der Entstehung von Leukämien. Der Einfluss auf die Entwicklung von B-Zellen wurde teilweise auf die transkriptionelle Regulierung des Zytokinrezeptors fms-like tyrosinkinase 3 (Flt3) in hämatopoetischen Progenitor-Zellen zurückgeführt. Flt3 und der passende Ligand Flt3L spielen jedoch auch eine entscheidende Rolle im Rahmen der Entwicklung und Homöostase von DCs. Unveröffentlichte Daten zeigten eine deutliche Überexpression der *hoxa9* mRNA in murinen pDCs nach Aktivierung von TLR9. Basierend auf diesen Daten wird in dieser

Studie der Einfluss des Transkriptionsfaktors HoxA9 auf die Funktion intrazellulärer TLRs sowie die Entwicklung von DCs und Makrophagen untersucht. Hierfür wurden HoxA9 Knockout (KO) Mäuse verwendet.

Hypothese: Die Hochregulierung von HoxA9 in pDCs unter Aktivierung von TLR9 lässt einen Einfluss dieses Gens auf die TLR-vermittelte Funktion von DCs und Makrophagen vermuten. Die bekannte transkriptionelle Regulierung des Zytokinrezeptors Flt3 in Progenitor-Zellen der B-Zell Reihe durch HoxA9 könnte ebenfalls im Rahmen der DC Differenzierung eine Rolle spielen.

Ergebnisse: HoxA9$^{-/-}$ Mäuse zeigten eine geringe, statistisch nicht signifikante, Hypozellularität der gesamten kernhaltigen Knochenmarkszellen. Dies bestätigte die Ergebnisse von anderen Arbeitsgruppen. In FACS-Analysen der gesamten Knochenmarkszellen konnte *ex vivo* eine signifikante Reduktion der Anzahl von B-Zellen, inklusive der B-Vorläuferzellen, bei HoxA9-defizienten Mäusen im Vergleich zum Wildtyp (WT) beobachtet werden. Vergleiche der unterschiedlichen DC Subpopulationen ergaben jedoch zwischen KO und WT keine Unterschiede, passend zu den Ergebnissen früherer Studien. TLR Stimulations-Experimente von gesamten Knochenmarkszellen und aus Knochenmark FACS-gesorteten pDCs zeigten in der KO-Gruppe eine deutlich gestörte IFN-α Sekretion nach Aktivierung von TLR7 und 9 *ex vivo*, welche statistisch signifikant war. FACS-gesortete cDCs waren jedoch, bezogen auf die TLR-Funktion, nicht verändert. Zudem konnten in *in vitro* generierten Flt3L-induzierten DC Kulturen, welche sowohl pDCs als auch cDCs enthalten, eine fast vollständig fehlende Sekretion von IFN-α sowie eine reduzierte Sekretion von IL-6 nach Aktivierung von TLR7 und 9 beobachtet werden. Darüber hinaus zeigte sich in den HoxA9-defizienten Flt3L-induzierten Kulturen im Vergleich zum WT eine leicht reduzierte Rate an differenzierten Zellen, eine erhöhte Rate an toten Zellen sowie eine veränderte pDC/cDC Ratio. Die *in vitro* generierten HoxA9$^{-/-}$ GM-CSF-induzierten cDCs sowie die M-CSF-induzierten Makrophagen waren weder in den FACS-Analysen noch in den TLR Stimulations-Experimenten verändert, verglichen zum WT. Die Anzahl von pDCs und cDCs in primären Milzzellen mit HoxA9-Knockout zeigte sich in den FACS-Analysen unverändert zum WT. Die Sekretion von IFN-α war hingegen, ähnlich wie im Knochenmark, nach Stimulation von TLR7 und 9 im Vergleich zum WT reduziert. Eine genomweite Microarray-Analyse von *ex vivo* FACS-gesorteten pDCs aus dem

Knochenmark, konnte eine veränderte Expression multipler Gene, z.B. des HoxA9 Kofaktors Meis1, bei HoxA9-Defizienz nachweisen.

Fazit: Die Ergebnisse dieser Studie lassen auf eine essenzielle Rolle von HoxA9 im Rahmen der TLR-vermittelten IFN-α Sekretion von pDCs schließen. Hingegen kann kein Einfluss von HoxA9 auf die TLR-induzierten Immunreaktionen von cDCs und Makrophagen gezeigt werden. Die Differenzierung von DCs unter HoxA9-defizienten Bedingungen ist *in vitro* teilweise verändert. Dieser Effekt scheint jedoch *in vivo* kompensiert zu sein. Zunehmende Hinweise zeigen, dass pDCs bei unterschiedlichen Erkrankungen wie Virusinfektionen, Autoimmunerkrankungen und im Rahmen der Tumorgenese von verschiedenen Krebserkrankungen eine wichtige Rolle einnehmen. Dies unterstreicht die Wichtigkeit dieser Immunzellen. Der Transkriptionsfaktor HoxA9 rückt damit als ein potenzielles therapeutisches Ziel in den Fokus.

TABLE OF CONTENTS

ABBREVIATIONS

#	numbers
Ab	antibody
AEP	asparagine endopeptidase
AGS	Aicardi-Goutières-Syndrome
AIM2	absent in melanoma 2 protein
Akt	v-akt murine thymoma viral oncogene homolog
ALL	acute lymphoid leukemia
ALRs	AIM2-like receptors
AML	acute myeloid leukemia
AP-1	activator protein 1
AP-3	adapter-related protein complex-3
APC	allophycocyanine
APCs	antigen-presenting cells
ASC	apoptosis-associated speck-like protein containing a CARD
Atg	autophagy protein
BAD	Bcl2-associated agonist of cell death
Batf3	basic leucine zipper transcription factor, ATF-like 3
Bcl2	B cell leukemia/lymphoma 2
BCR	B cell receptor
BDCA	blood dendritic cell antigen
BIM	Bcl2 interacting mediator of cell death
BLOC	biogenesis of lysosome-related organelle complex
BM	bone marrow
bp	base pair
BSA	bovine serum albumin
BST2	bone marrow stromal antigen 2
B220	tyrosine phosphatase also known as CD45R
CARD	caspase activation and recruitment domain
CCR	chemokine (C-C motif) receptor
CD	cluster of differentiation
cDCs	conventional/classical dendritic cells

CDNs	cyclic dinucleotides
CDPs	common dendritic cell progenitors
CDX	caudal type homeobox
cGAMP	cyclic GMP-AMP
cGAS	cyclic GMP-AMP synthase
CHO	chinese hamster ovary
c-kit	v-kit Hardy-Zuckerman 4 feline sarcoma viral oncogene homolog
CLPs	common lymphoid progenitors
CLRs	C-type lectin receptors
CMPs	common myeloid progenitors
c-Myb	myeloblastosis oncogene
CpG	cytosine-phosphatidyl-guanine
CpG-ODNs	cytosine-phosphatidyl-guanine oligodeoxynucleotides
CREB	cAMP responsive element binding protein
c-rel	v-rel reticuloendotheliosis viral oncogene homolog
CTLD	C-type lectin-like domain
C/EBPα	CCAAT/enhancer-binding protein alpha
DAI	DNA-dependent activator of IFN-regulatory factors
DAMPs	damage- or danger-associated molecular patterns
DAP12	DNAX activation protein 12
DCP2	decapping complex catalytic subunit 2
DC-SIGN	dendritic cell-specific intercellular adhesion molecule-3-grabbing non-integrin
DCs	dendritic cells
DD	death domain
DEAF1	deformed epidermal autoregulatory factor 1
Dm	drosophila melanogaster
dNTPs	deoxynucleotide triphosphates
Dock2	dedicator of cytokinesis protein 2
DOTAP	1,2-dioleoyloxy-3-trimethylammonium-propane
dsDNA	double-stranded deoxyribonucleic acid
dsRNA	double-stranded ribonucleic acid

EAM	experimental autoimmune myocarditis
EBV	Epstein-Barr virus
EDTA	ethylenediaminetetraacetate
EGR1	early growth response 1
Ehmt2	euchromatic histone lysine N-methyltransferase 2
ELISA	enzyme-linked immunosorbent assay
EMCV	encephalomyocarditis virus
ER	endoplasmic reticulum
ERV	endogenous retrovirus
Erms	erythromycin resistance methylases
EtBr	ethidiumbromide
Exd	extradenticle
E2-2	basic helix-loop-helix transcription factor
FACS	fluorescence activated cell sorting/sorter
FBS	fetal bovine serum
Fc	fragment, crystallizable
FcεRI	Fc receptor for IgE
FCS	fetal calf serum
FITC	fluorescein isothiocyanate
Flt3	fms-like tyrosine kinase 3
Flt3L	fms-like tyrosine kinase 3 ligand
FOXO3	forkhead box O3
fp	forward primer
FSC	forward scatter
GATA6	GATA binding protein 6
GM-CSF	granulocyte-macrophage colony-stimulating factor
GM-CSFR	GM-CSF receptor
GMPs	granulocyte/macrophage progenitors
gp96	glycoprotein 96
HAT	histone acetyltransferase
HDAC	histone deacetylase
HHV8	human herpesvirus 8
HIV-1	human immunodeficiency virus type 1
HLA-DR	human leucocyte antigen locus DR

HMGB1	high mobility group box 1
Hox	homeobox
HoxA9	hox (homeobox) protein A9
Hsp5	Hermansky-Pudlak syndrome 5
HRP	horseradish peroxidase
Hs	humans
Hsp90b1	heat shock protein 90 kDa beta member 1
HSCs	hematopoietic stems cells
HSV	herpes simplex virus
HTC	high-throughput cDNA
HX	hexapeptide
H5N1	Influenza A virus subtype H5N1; also known as A(H5N1) or H5N1
ICOS-L	inducible T-cell co-stimulator ligand
Id2	inhibitor of DNA binding 2
IFI16	Interferon-gamma induced protein 16
IFNAR	type I IFN receptor
IFNs	interferons
IFN-α	interferon-α
IFN-β	interferon-β
Ig	immunoglobulin
IκB	inhibitor of nuclear factor κB
IKDCs	interferon-producing killer dendritic cells
IKK	inhibitor of nuclear factor κB kinase
IL	interleukin
IL-6	interleukin 6
ILT7	immunoglobulin-like transcript 7
IL7Rα	interleukin 7 receptor subunit alpha
iMO	inflammatory monocytes
iNOS	inducible nitric oxide synthase
int	intermediate
IRAK	IL-1R-associated kinase
IRF	interferon regulatory factor
ISGs	interferon-stimulated genes

ITAMs	immunoreceptor tyrosine-based activation motifs
ITGAM	integrin alpha M
ITIMs	immunoreceptor tyrosine-based inhibitory motifs
JNKs	Jun kinases
kDa	kilo Dalton
KLF4	Kruppel-like factor 4
KRAS	v-Ki-ras2 Kirsten rat sarcoma viral oncogene homolog
LAM	lipoarabinomannan
LAMP1	lysosome-associated membrane protein 1
LBP	lipopolysaccharide binding protein
LCMV	lymphocytic choriomeningitis virus
LCs	Langerhans cells
LGP2	laboratory of genetics and physiology 2
LMPPs	lymphoid-primed multipotent progenitors
LMP2A	latent membrane protein 2A
LPDCs	lamina propria dendritic cells
LPG	lipophosphoglycan
LPS	lipopolysaccharide
LRO	lysosome-related organelles
LRRs	leucin-rich repeats
LXR	liver x receptor
Ly	lymphocyte antigen
MΦs	macrophages
MAb	monoclonal antibody
Mal	myelin and lymphocyte protein
MAP	mitogen-activated protein
MAPKs	mitogen-activated protein kinases
MCMV	murine cytomegalovirus
M-CSF	macrophage colony-stimulating factor
M-CSFR	M-CSF receptor
MDA5	melanoma differentiation-associated gene 5
mDCs	myeloid dendritic cells
MDPs	macrophage/dendritic cell progenitors

MD2	myeloid differentiation factor 2
Meis	myeloid ectopic insertion proteins
MEM	minimal essential medium
MEPs	megakaryocyte/erythrocyte progenitors
MHC-I	major histocompatibility complex I
MHC-II	major histocompatibility complex II
min	minutes
miRNA	micro ribonucleic acid
MLL	mixed lineage leukemia
MLS antibiotics	macrolides, lincosamides, and streptogramin Antibiotics
Mm	mus musculus
MMTV	mammary tumor virus
MOF	males absent on the first
mPDCA-1	mouse pDC antigen 1
MPPs	multipotential progenitors
mTOR	mechanistic/mammalian target of rapamycin
MV	measles virus
MyD88	myeloid differentiation primary response protein 88
NAP1	NAK-associated protein 1
n.d.	not detectable
NEMO	NFκB essential modulator
NFAT	nuclear factor of activated T cells
NFκB	nuclear factor κB
NGS	next-generation sequencing
NK cells	natural killer cells
NLRs	NOD-like receptors
NO	nitride oxide
NOD	nucleotide-binding oligomerization domain
NOS-2	nitride oxide (NO) synthase 2
NPM1	nucleophosmin 1
n.s.	not significant
NUP98	nucleoporin 98
ODC	ornithine decarboxylase

ODN	oligodeoxynucleotide
OPD	o-Phenyl-Diamin
OPNi	intracellular osteopontin
OxPL	oxidized phospholipids
PAb	polyclonal antibody
PACSIN1	protein kinase C and casein kinase substrate in neurons 1
PAMPs	pathogen-associated molecular patterns
Pam3CSK4	Pam3CysSerLys4; also known as Pam3Cys
Pam3Cys	see Pam3CSK4
PBS	phosphate buffered saline
Pbx	pre-B-cell leukemia proteins
PCNA	proliferating cell nuclear antigen
PCR	polymerase chain reaction
PD	phosphodiester
pDCs	plasmacytoid dendritic cells
pDC-TREM	pDC-triggering receptor expressed in myeloid cells
PE	phycoerythrin
PIN1	peptidyl-prolyl cis-trans isomerase NIMA interacting 1
PI3K	phosphatidylinositol-3 kinase
PLSCR1	phospholipid scramblase 1
POD	peroxidase
Pol III	RNA Polymerase III
Poly-dT	polyT deoxynucleotides
Poly I:C	polyinosinic-polycytidylic acid
PPAR	peroxisome proliferator-activated receptor
PRAT4A	protein associated with TLR4 a
Pre-cDCs	BM-derived DC precursors, also called Pre-DC
Pre-DCs	BM-derived DC precursors, also called Pre-cDCs
Pre-mNK cells	precursors of mature NK cells
PS	phosphorothioate
PRRs	pattern recognition receptors
PYHIN	Pyrin and HIN domain

RAUL	RTA-associated ubiquitin ligase
RAG	recombination activating genes
RefSeq	reference sequence
RIG-I	retinoid acid-inducible gene I
RIP	receptor-interacting protein
RLRs	RIG-I-like receptors
RNA	ribonucleic acid
RNPs	ribonucleoproteins
ROS	reactive oxygen species
rp	reverse primer
RPMI	Roswell Park Memorial Institute
rRNA	ribosomal ribonucleic acid
RSV	respiratory syncytial virus
RT	room temperature
Runx2	runt related transcription factor 2
R837	imiquimod
R848	resiquimod
SARM	sterile-alpha and Armadillo motif-containing protein
SCR	sex combs reduced
Sema6D	semaphorin-6D
SD	standard deviation
SDS	sodium dodecyl sulfate
SHP	family of protein tyrosine phosphatases
SINTBAD	similar to NAP1 TBK1 adapter
SiglecH	sialic acid binding Ig-like lectin H
siRNA	short interfering ribonucleic acid
SLE	systemic lupus erythematosus
snRNA	small nuclear ribonucleic acid
snoRNA	small nucleolar ribonucleic acid
SpiB	Spi-B transcription factor (also known as Spi-1/PU.1 related)
SREBPs	sterol regulatory element-binding proteins
SSC	side scatter

ssDNA	single-stranded deoxyribonucleic acid
ssRNA	single-stranded ribonucleic acid
STAT	signal transducer and activator of transcription
Std	standard
STING	stimulator of interferon genes
SYK	spleen tyrosine kinase
TAE	tris-acetate-EDTA
TAB	TAK1-bindig protein
TAG	TRAM adaptor with GOLD domain
TALE	three amino acid long loop
TAM	tumor-associated macrophages
TANK	TRAF family member-associated NFκB activator
TAK1	TGF-β-activated kinase 1
TBK1	TANK-binding kinase 1
TCR	T cell receptor
TCF4	transcription factor 4
TfR	transferrin receptor
tGPI-mucin	Glycosylphosphatidylinositol-anchored mucin-like glycoproteins from Trypanosoma cruzi trypomastigotes
Th1	Th1 helper cells
Th17	Th17 helper cells
TICAM-1	toll/interleukin-1 receptor domain containing adaptor molecule 1
ROS	toll/interleukin-1 receptor
TIRAP	toll/interleukin-1 receptor domain containing adaptor protein
TLR	Toll-like receptor
TLRs	Toll-like receptors
TNF	tumor necrosis factor
TNF-α	tumor necrosis factor α
TRADD	TNF receptor-associated death domain protein
TRAF6	TNF receptor-associated factor 6
TRAM	TRIF-related adaptor molecule

TREX1	three prime repair exonuclease 1
TRIF	toll/interleukin-1 receptor domain containing adaptor inducing IFN-β
tRNA	transfer ribonucleic acid
Ubc13	ubiquitin-conjugating enzyme 13
Ubx	ultrabithorax
Uev1A	ubiquitin-conjugating enzyme E2 variant 1
UNC93B1	Unc-93 homolog B1
VEGF	vascular endothelial growth factor
VSV	vesicular stomatitis virus
VLRs	variable lymphocyte receptors
WNV	west nile virus
Zbp1	Z-DNA binding protein 1

List of Figures

LIST OF TABLES

1. INTRODUCTION

1.1 THE IMMUNE SYSTEM

1.1.1 CLASSIFICATION AND FEATURES OF THE IMMUNE SYSTEM

The presence of infectious pathogenic microorganisms like bacteria, viruses, fungi, and parasites in the environment of human beings leads to the necessity of specific defense mechanisms against attacking microbes (Murphy et al., 2012). These defense mechanisms are driven by cells and molecules of the human immune system, which comprises an innate and adaptive part. Both, innate and adaptive immunity, consist of cellular and humoral (non-cellular) components, which cooperate to eliminate foreign invaders. The adjusted and coordinated response of an organism against the invasion of infectious microbes is called the immune response (Abbas et al., 2007). The immune system is further capable to identify and kill malignantly transformed cells, thus, another main function is prevention from emerging cancer diseases. Under pathological conditions even noninfectious foreign substances are able to elicit immune responses resulting in allergic diseases. Furthermore, immune defense mechanisms directed against components of the host itself can cause massive inflammation, which leads to the origin of autoimmune diseases. Deficient self-tolerance mechanisms are believed to be responsible for the latter. Interestingly, it seems that there is an inverse relation between autoimmune disorders or allergic diseases on one hand (e.g. Crohn's disease, Multiple sclerosis, Type I diabetes, or Asthma) and infectious diseases on the other hand (e.g. Measles, Mumps, Tuberculosis, or Hepatitis A) in industrialized countries (Bach, 2002). The decline of infectious diseases in Western countries is accompanied by a fast increase of allergy and autoimmune disorders.

The human immune system can be subdivided into innate and adaptive immunity, as mentioned before. Rapid immune responses are prompted by cells and molecules of the innate immune system, whereas adaptive immunity is responsible for later reactions that drive long-lasting highly specific defense mechanisms (Abbas et al., 2007). Important components of innate immunity are several cell types including MΦs, DCs, neutrophils, and natural killer (NK) cells and physical or chemical barriers such as epithelial cells of the skin and all mucosal membranes that produce antimicrobial peptides. Further, proteins of the complement system that circulate in the blood stream and all kinds of cytokines

and chemokines that regulate and coordinate immune cells are components of innate immunity (Abbas et al., 2007). T and B lymphocytes are the cellular part of the adaptive immune system, which are able to develop powerful defense mechanisms that "adapt" to the particular pathogen by targeting distinct antigens with highly specific antibodies (Abbas et al., 2007; Murphy et al., 2012).

To efficiently fight acute infections and induce long-lasting protection, the human immune system requires at least four main features, which are pathogen recognition, effector mechanisms, immune regulation, and immunological memory (Murphy et al., 2012). The task of identifying infection is done by cells of the innate immune system using specific receptors that recognize conserved structures shared by groups of related microbes (Abbas et al., 2007) called pattern recognition receptors (PRRs) including the TLR family. And further by lymphocytes of the adaptive immune system which recognize specific antigens of particular pathogens using their B and T cell receptor (BCR, TCR) that are randomly generated by complex processes called gene rearrangement and somatic hypermutation (Flajnik and Du Pasquier, 2004; Murphy et al., 2012). Once detected, several humoral and cellular effector functions of innate and adaptive immunity such as phagocytosis by MΦs or DCs, cytotoxic activities of specific T lymphocytes ($CD8^+$ T cells), antibodies produced by plasma cells, or the complement system collectively intend to keep infection under control and completely destroy all pathogens if possible. To prevent an exaggerated immune reaction and falsely induced immune responses to structures of the host itself, diverse regulatory self-tolerance mechanisms are needed (Abbas et al., 2007; Murphy et al., 2012). As already mentioned above, dysfunctions in immune regulation and self-tolerance result in allergic and autoimmune diseases. Long-lasting protection to avoid recurring infections by the same microbe is mediated by the adaptive immune system, which is able to memorize highly defined structures of pathogens and induce immediate immune responses when re-infection occurs (Murphy et al., 2012).

All cells of the immune system originate from pluripotent hematopoietic stem cells (HSCs) in the bone marrow (Murphy et al., 2012). Most cell types of innate immunity arise from the common myeloid progenitors (CMPs) such as monocytes, MΦs, most DCs, all kinds of granulocytes, and mast cells. NK cells derive from the common lymphoid progenitors (CLPs) and belong to the family of lymphocytes. DCs can also arise from CLPs. B cells and T cells, the cellular part of the adaptive immune system, are also lymphocytes and emerge from CLPs (Murphy et al., 2012).

Understanding physiological as well as pathological mechanisms of the immune system is essential to improve existing and develop novel therapies or diagnostics of almost all kinds of diseases to further advance average life expectancy and assure the basic right of physical and mental health of all human beings. Thus, investigating the immune system and its properties is of utmost importance for all disciplines of medicine and plays an integral role in biomedical research.

1.1.2 ORIGIN AND EVOLUTION OF THE IMMUNE SYSTEM

Some sort of innate immune system can be found in all multicellular organisms (metazoans), whereas adaptive immunity is only present in vertebrates (Abbas et al., 2007) that firstly appeared in jawed vertebrates (gnathostomes; e.g. sharks) (Abbas et al., 2007; Flajnik and Du Pasquier, 2004). Different kinds of phagocytes are present in all metazoans. Their capability to engulf microbes and kill them makes these cells effective defenders of innate immunity (Abbas et al., 2007). Humoral components of the innate immune system in invertebrates comprise different antimicrobial molecules, whereas the complement system and antibodies as well as antibody-producing lymphocytes are not existing in these creatures (Abbas et al., 2007). Different PRRs and especially TLRs are found in all metazoans and seem to be a very old efficient solution to recognize infection, which was therefore highly conserved. Interestingly, species without adaptive immunity possess a larger diversity of TLRs (e.g. Echinodermata hold 222 TLRs) than vertebrates (e.g. mammals possess 10 – 13 TLRs) (Ward and Rosenthal, 2014), indicating that the presents of adaptive immune mechanisms might have led to negative selection of TLRs (Ward and Rosenthal, 2014). However, the fact that adaptive immune responses are actually triggered by innate immune cells using pathogen recognition by TLRs among others and the emerging evidence that TLRs are also expressed in B and T lymphocytes providing other important functions (Michallet et al., 2013) complicates former reflections and shows that innate and adaptive immunity cannot be sharply separated. Moreover, professional antigen-presenting cells (APCs) like DCs might have evolved from phagocytes together with the adaptive immune system that actually provided the need for antigen-presentation (Schmid et al., 2010).

The most established theory of the origin of the adaptive immune system is that a transposon containing the gene for the RAG (recombination activating genes) recombinase was inserted into a immunoglobulin gene member in an ancestor of jawed

vertebrates (Abbas et al., 2007; Flajnik, 2014). Latest findings demonstrated additional adaptive immune mechanisms even in jawless vertebrates, for instance the so-called variable lymphocyte receptors (VLRs) (Flajnik, 2014; Ward and Rosenthal, 2014). Of note, VLRs contain leucine rich repeats (LRRs) which are also found in the ectodomains of TLRs, hence, it is possible that VLRs could have developed from TLRs (Litman et al., 2005).

For decades, most immunologists put their focus on analyzing the complex mechanisms of the adaptive immune system, which basically started with a dispute between the founding fathers of immunology at the end of the 19th century whether Metchnikoff's phagocytes or Ehrlich's antibodies were more important and ended up with a victory of the latter (Silverstein, 2003). The discovery of TLRs in the late 1990s led to a new perspective on innate immunity and substantially changed the field of immunology. The findings concerning innate immunity in recent years provided remarkable new insights showing a far more complex system that has ever been expected. Strict separation of adaptive and innate immunity seems to be not possible and both are definitely necessary for efficient immune responses in mammals.

1.1.3 INNATE IMMUNITY

Properties that are attributed to the innate immune system exist already before organisms are exposed to microbes and can act rapidly in order to combat infection and induce further immunity mediated by the adaptive immune system (Abbas et al., 2007). Immune responses basically occur in three steps (Murphy et al., 2012). Natural barriers like the epithelium of the skin and the mucosa of the respiratory and gastrointestinal tracts are components of innate immunity that prevent invasion of intruders physically and chemically by arranging a certain antimicrobial milieu (e.g. by establishing a low pH hard to live for most microbes or producing antimicrobial molecules) (Abbas et al., 2007; Murphy et al., 2012). A broad range of molecules present in the blood stream, several extracellular fluids, and the surface of epithelia are able to digest or lyse bacterial cell walls (e.g. lysozyme or defensins) and/or mark bacteria for phagocytosis by phagocytes such as MΦs or DCs including proteins of the complements system (Murphy et al., 2012). Many infections can be stopped by these mechanisms. Microbes that overcome those preventive actions are recognized by pattern recognition receptors (PRRs) of innate immune cells that sense evolutionary conserved structures occurring only in pathogens

(often essential for survival) and not the host itself called pathogen-associate molecular patterns (PAMPs) (Abbas et al., 2007; Janeway and Medzhitov, 2002; Murphy et al., 2012). By recognizing PAMPs through PRRs, innate immune cells are activated and a number of effector mechanisms are launched. Complex signaling cascades induce transcription factors that subsequently migrate to the nucleus to activate the transcription of multiple genes resulting in production and secretion of several cytokines and chemokines that initiate a state of inflammation (Kumar et al., 2011). Among other things, these molecules prompt an acute-phase reaction and promote attraction of further immune cells such as monocytes and neutrophils that circulate in the blood stream by dilatation and higher permeability of local vessels and increased expression of adhesion molecules by epithelial cells (Murphy et al., 2012). Additionally, soluble factors of innate immunity from the blood are able to enter sites of infection. Activated blood clotting in local vessels further prevents that microbes can quickly spread through the blood stream (Murphy et al., 2012). Moreover, the activation of MΦs and DCs by PRRs facilitates antigen presentation of molecules derived from phagocytosed pathogens to naïve T lymphocytes and thus initiates highly efficient adaptive immunity (Abbas et al., 2007; Kumar et al., 2011; Murphy et al., 2012). The last aspect reflects the third step of immune responses, which is necessary when the first two lines of defense have been overwhelmed (Murphy et al., 2012).

The basic purposes of innate immunity consist of prevention of a potential or rapid control and elimination of an ongoing infection by inducing inflammation. If these mechanisms are not effective enough to clear attacking microbes, another important function is to trigger adaptive immune responses and further facilitate the appropriate type of adaptive immunity, which is different depending on the particular pathogen (Abbas et al., 2007).

1.2 PATTERN RECOGNITION RECEPTORS (PRRS)

1.2.1 THE ROLE OF PRRS IN THE INNATE IMMUNE SYSTEM

As mentioned above, microbial invaders such as bacteria, viruses, fungi, and protozoan parasites cause infection and activate cells of the innate immune system including DCs, MΦs, and others (Kumar et al., 2011). Highly conserved PAMPs are sensed by transmembrane or cytoplasmic proteins referred to as PRRs (Kawai and Akira, 2010). In addition, endogenous molecules released from damaged cells, named damage- or danger-associated molecular patterns (DAMPs), do as well contribute to PRR activation (Takeuchi and Akira, 2010). Four different families of PRRs have been identified so far. Toll-like receptors (TLRs) and C-type lectin receptors (CLRs) are transmembrane proteins whereas RIG-I-like receptors (RLRs) and NOD-like receptors (NLRs) encounter their ligands in the cytoplasm. Thus, intracellular as well as extracellular recognition of numerous pathogenic molecules including lipids, proteins, lipoproteins, carbohydrates, and nucleic acids provides a wide range of detecting infection (Kawai and Akira, 2010; Kumar et al., 2011). Different cellular compartments such as the plasma membrane, the cytosol, endosomes, lysosomes, endolysosomes, and phagosomes are sites of this action (Blasius and Beutler, 2010). Sensing of PAMPs and DAMPs by PRRs of innate immune cells rapidly triggers complex intracellular signaling pathways that initiate transcriptional expression of various proinflammatory cytokines, type I IFNs, chemokines, and antimicrobial peptides (Kawai and Akira, 2011; Kumar et al., 2011). Moreover, activation of PRRs primes DC maturation, which in turn is important for prompting T cell mediated adaptive immune responses (Kawai and Akira, 2011).

Taken together, PRR signaling immediately starts an innate immune response and elicits antigen-specific adaptive immunity in order to eliminate invading infectious agents (Kawai and Akira, 2011; Kumar et al., 2011). On one hand, pathogens mostly activate several PRRs simultaneously due to multiple PAMP composition of each species. On the other hand, different PRRs can recognize the same PAMP (Kawai and Akira, 2011). The particular expression of various PRRs depends on the immunological cell type and very importantly, the crosstalk between diverse PRRs seems to be essential for mounting proper immune responses and is tailored to the certain infecting microbes (Kawai and Akira, 2010). In addition, PRRs can be found in several nonprofessional immune cells such as endothelial cells or fibroblasts (Takeuchi and Akira, 2010).

1.2.2 DIFFERENT TYPES OF PRRS

1.2.2.1 RIG-I-LIKE RECEPTORS (RLRS)

This work is focusing on members of the TLR family, which are discussed in detail in section 1.2.3. Besides TLRs, the most prominent members of PRRs, other PRR families were identified and extensively studied in the last couple of years. One of them is the family of RIG-I-like receptors (RLRs), which consists of the RNA helicases RIG-I, MDA5, and LGP2 that sense genomic dsRNA of dsRNA viruses and dsRNA replication intermediates of ssRNA viruses in the cytoplasm of infected cells (Takeuchi and Akira, 2010). Activation of these receptors leads to production of proinflammatory cytokines that initiate inflammation and attract DCs and MΦs to sites of inflammation and type I IFNs inducing an antiviral state in infected and healthy cells via an autocrine and paracrine way (Kumar et al., 2011; Takeuchi and Akira, 2010). RIG-I detects short dsRNA which is considerably enhanced when including a 5' triphosphate, whereas MDA5 senses long dsRNA including the synthetic dsRNA analog Poly I:C (Takeuchi and Akira, 2010). LGP2 was initially believed to serve as a negative regulator of RIG-I and MDA5, but instead turned out as a positive regulator (Gürtler and Bowie, 2013; Kumar et al., 2011).

1.2.2.2 NOD-LIKE RECEPTORS (NLRS)

Another PRR family that senses their ligands in the cytosol are NLRs, consisting of more than 20 members in humans and more than 30 in mice (Kumar et al., 2011). They recognize a broad range of PAMPs mainly derived from bacteria, but also viral and fungal structures. The two most prominent members are NOD1 and NOD2, which perceive peptidoglycans from various bacteria (Takeuchi and Akira, 2010). Interestingly, genetic variants of NOD1 and NOD2 have been linked to allergic diseases like asthma or atopic dermatitis and Crohn's disease, an autoimmune disorder affecting the gastrointestinal tract, respectively (Kumar et al., 2011). Upon ligation, proinflammatory cytokines are upregulated via the transcription factor NFκB and the MAP kinase pathway (Kumar et al., 2011). Some NLRs such as NLRP3 and NLRC4 are part of protein complexes called inflammasomes that are found in DCs and MΦs activated by several PAMPs, together

with other receptors like AIM2 and ASC (see further passages), resulting in production of IL-1β through proteolytic activation of caspase-1 (Kumar et al., 2011).

1.2.2.3 C-TYPE LECTIN RECEPTORS (CLRS)

CLRs are localized to the plasma membrane and recognize different carbohydrates found in viruses, fungi, and bacteria (Takeuchi and Akira, 2010). All members contain at least one C-type lectin-like domain (CTLD) (Dambuza and Brown, 2015). Well known are dectin-1 and dectin-2 that sense *β*–glucans from fungi and have been shown to play an important role in anti-fungal immunity. Their activation leads to induction of proinflammatory cytokines through the transcription factors NFAT and NFκB (Takeuchi and Akira, 2010). However, latest findings showed that also proteins and lipids can serve as ligands and that type I IFNs are induced via activation of IRF5 (Dambuza and Brown, 2015). Interestingly, CLRs have been implicated recently in the regulation of homeostasis, autoimmunity, allergy, and cancer (Dambuza and Brown, 2015).

1.2.2.4 CYTOSOLIC DNA SENSORS

Beside the four PRR families discussed above and in section 1.2.3, several other sensors have been identified in recent years, some of which can not be assigned to a particular PRR family. This section briefly introduces different PRRs that are able to detect DNA in the cytosol of cells. Apart from the well known DNA sensor TLR9, which is restricted to endosomal/endolysosomal compartments, several receptors localized to the cytosol were found to recognize DNA (Gürtler and Bowie, 2013). Double-stranded DNA (dsDNA) derived from pathogens as well as host cells possess immunostimulatory activity when present in the cytoplasm (Gürtler and Bowie, 2013). The PYHIN proteins IFI16 (p204 in mice) and AIM2 sense cytoplasmic dsDNA and use the adaptor proteins STING and ASC, which lead to induction of type I IFNs or IL-1β and IL-18 through caspase-1, respectively (Paludan and Bowie, 2013). These proteins are summarized as AIM2-like receptors (ALRs). Interestingly, the recognition of dsDNA by these receptors is independent of any motifs and is mediated by electrostatic interactions between the sugar phosphate backbone of the DNA and the HIN domain of the receptors (Gürtler and Bowie, 2013). The adaptor molecule STING itself can bind cyclic dinucleotides (CDNs) that serve as second messengers in bacteria and another dsDNA sensor called cGAS

catalyzes the production of cGAMP (cyclic GMP-AMP, a type of endogenous CDNs) after ligation that further activates STING (Gürtler and Bowie, 2013; Sun et al., 2013a; Wu et al., 2013). Several DExD/H box proteins have also been shown to sense cytosolic DNA using different signaling pathways. For instance the members DHX9 and DHX36 are expressed in pDCs and recognize cytosolic CpG DNA leading to production of proinflammatory cytokines and type I IFNs through activation of NFκB and IRF7 via the adaptor molecule MyD88 (Gürtler and Bowie, 2013). Other prominent DNA receptors include the dsDNA recognizing protein DAI and the AT-rich dsDNA (present in some pathogens) sensing RNA Polymerase III (Pol III). The latter transcribes AT-rich DNA to dsRNA containing a 5' triphosphate that is subsequently recognized by RIG-I (Gürtler and Bowie, 2013). Many viruses enforce replication in the nucleus probably to avoid cytosolic DNA sensing, however, some receptors have been shown to recognize microbial DNA even in the nucleus such as IFI16 (Gürtler and Bowie, 2013; Paludan and Bowie, 2013). The fact that host-derived DNA serves as DAMP in the cytosol in contrast to different self RNA species suggests a central role for cytosolic DNA sensors not only in antimicrobial defense mechanism but also in the pathogenesis of autoimmunity and needs to be further elucidated (Gürtler and Bowie, 2013; Paludan and Bowie, 2013). AIM2 and IFI16 are additionally known to be involved in stimulating inflammasome protein complexes (Paludan and Bowie, 2013).

1.2.3 TOLL-LIKE RECEPTORS (TLRS)

1.2.3.1 DISCOVERY, PROPERTIES, AND LOCALIZATION OF TLRS

After the discovery of the Toll protein in *Drosophila melanogaster* (Gay and Keith, 1991; Lemaitre et al., 1996) and its orthologous gene TLR4 (Medzhitov et al., 1997), TLRs were the first family of PRRs to be found in mammals (Kawai and Akira, 2011). They are the largest PRR subgroup and believed to be the most important innate immune sensors (Kumar et al., 2011). Currently, 10 and 12 functional TLRs have been identified in humans and mice, respectively, which are mainly well characterized. TLR1 to TLR9 are expressed in both species whereas TLR10 is only functional in humans due to an endogenous retrovirus insertion that causes a stop codon in the murine TLR10 gene (Kawai and Akira, 2010; Kumar et al., 2011). Moreover, the gene of TLR11 in humans

is dysfunctional and TLR12 and TLR13 are considered to be completely lost from the human genome (Roach et al., 2005).

TLRs are type I transmembrane glycoproteins consisting of an ectodomain that contains 16 to 28 leucin-rich repeats (LRRs) (Matsushima et al., 2007) required for PAMP/DAMP recognition, a transmembrane region, and a cytoplasmic Toll/interleukin-1 receptor (TIR) domain prerequisite for initiation of intracellular signal transduction (Kawai and Akira, 2011). The crystal structure of the ectodomain of several TLRs reveals a "horseshoe" or "m" shaped architecture. After ligand binding, the ectodomain forms a dimer either with the same TLR type (homodimers) or other TLRs (heterodimers) depending on the particular receptor (Jin and Lee, 2008).

The family of TLRs can be largely divided into 2 subgroups according to their localization and PAMP recognition. Primarily cell surface localized TLR1, TLR2, TLR4, TLR5, and TLR6 sense bacterial, fungal, and parasitic membrane components whereas TLR3, TLR7, TLR8, and TLR9 are restricted to intracellular compartments (endoplasmic reticulum (ER), endosomes, lysosomes, and endolysosomes) and predominantly recognize nucleic acids derived from several bacteria and viruses or infected cells after internalization (Blasius and Beutler, 2010; Kumar et al., 2011). The latter are sequestered in the ER and transported to the endosome/endolysosome via the Golgi apparatus prior to ligand encounter (Blasius and Beutler, 2010). Distinction of foreign nucleic acids from host nucleotides might be the reason of the endolysosomal localization of this TLR subgroup, considering that host nucleic acids are usually not present in these compartments (Barton et al., 2006; Blasius and Beutler, 2010). The localizations of TLR10 to TLR13 are discussed in several studies presenting diverse results. Human TLR10 shares a common locus on chromosome 4p14 and has sequence similarity to TLR1 and TLR6 (Hasan et al., 2005) and is therefore believed to be mainly expressed on the cell surface (Blasius and Beutler, 2010). TLR11, which is a relative to TLR5 (Kawai and Akira, 2009), is exclusively expressed in mice and senses its ligands on the cell surface (Blasius and Beutler, 2010; Kumar et al., 2009; Takeuchi and Akira, 2010). Nevertheless, recent findings demonstrate that TLR11 is also expressed within intracellular compartments and TLR11/TLR12 heterodimers recognize the profilin-like protein of the protozoan *Toxoplasma gondii* in an UNC93B1-dependent manner (Andrade et al., 2013; Lee et al., 2013; Pifer et al., 2011). The chaperon UNC93B1, a 12 membrane-spanning protein, physically interacts with intracellular TLRs in both humans and mice in the ER and is crucial for trafficking to the endosome/endolysosome (Casrouge et al.,

2006; Kim et al., 2008; Tabeta et al., 2006). Most recently, TLR13 has been reported to respond to a bacterial ssRNA segment within 23*S* RNA in an UNC93B1-dependent way (Hidmark et al., 2012; Li and Chen, 2012; Oldenburg et al., 2012). Hence, TLR13 is another member of nucleotide-sensing endocytic TLRs. Further on, Lee et al. demonstrated that UNC93B1 is necessary for TLR3, 7, 9, 11, 12, and 13 to leave the ER and join endolysosomal compartments, implicating enlargement of the intracellular TLR subgroup in mice (Lee et al., 2013).

Trafficking of TLRs from the ER to the cell membrane or via the Golgi apparatus to the endosome/lysosome and overall TLR regulation to ensure appropriate function seems to be a complex scenario, since several proteins are involved and cell type dependency was demonstrated (Blasius et al., 2010; Blasius and Beutler, 2010). Apart from UNC93B1, which is indispensable for intracellular TLRs, the proteins gp96 (also known as Hsp90b1) and PRAT4A are essential for proper TLR 1, 2, 4, 5, 7, and 9 localization (Kawai and Akira, 2011). Evidence for gp96 in TLR9 trafficking suggest further roles in conformational stability and involvement in proteolytic processes (Brooks et al., 2012). TLR7 and TLR9 processing and signaling in plasmacytoid dendritic cells is different from those in other cell types and depends on specific lysosomal sorting proteins (for details see chapters 1.2.3.4 and 1.3.1.2). Interestingly, only intracellular TLRs that access acidified endolysosomes are activated, since bafilomycin A1, chloroquine, and ammonium chloride inhibit acidification and abrogate TLR responses (Bauer, 2013; Häcker et al., 1998). Several lysosomal enzymes such as asparagine endopeptidase (AEP) and cathepsins (cathepsin l, k, and s) are involved in processing the N-terminal region of the ectodomains of TLR7 and 9, which enhances ligand binding and is indispensable for efficient signal transduction (Bauer, 2013; Blasius and Beutler, 2010; Ewald et al., 2011). Interestingly, TLR3 seems to be nonparticipating in cleavage processing (Blasius and Beutler, 2010).

1.2.3.2 PATTERN RECOGNITION BY TLRS

As mentioned above, TLRs are activated by numerous molecular structures of many microorganisms. Bacterial PAMPs comprise different cell wall components (e.g. LPS, peptidoglycan), nucleic acids including genomic DNA rich in unmethylated CpG-motifs and bacterial RNA, and the flagellin protein expressed by flagellated bacteria (Kumar et al., 2011). Patterns of viruses detected by several TLRs are nucleic acids (ssRNA,

dsRNA, ssDNA, and dsDNA) and coat proteins (e.g. RSV, MMTV). The recognition of fungal PAMPs including *β*-glucans and mannans involves co-receptors such as dectins, CD14, mannose receptors, and DC-SIGN (Kumar et al., 2011). Infections by protozoans are recognized by TLRs sensing membrane associated patterns (e.g. alkylacylglycerol from *Trypanosoma* or lipophosphoglycan (LPG) from *Leishmania*), genomic DNA, the actin associated profillin-like protein, and hematin crystals (Kumar et al., 2011). The ***TABLES 1.1*** and ***1.2*** depict all currently known ligands and their origin of cell surface and intracellular localized TLRs, respectively.

Besides their important role of recognizing infectious microorganisms, inappropriate TLR responses without negative regulation and sensing of host-derived endogenous structures have been shown to be strongly involved in acute and chronic inflammation, several autoimmune processes, and cancer (Kawai and Akira, 2010). Section 1.2.4 will give some brief insights into this issue.

TLR2 senses multiple PAMPs from bacteria, fungi, and viruses by forming homodimers or heterodimers either with TLR1 or TLR6 on the cell surface (Takeuchi and Akira, 2010). The cell wall of gram-positive bacteria contains peptidoglycan and lipoteichoic acid, which are detected by TLR2 homodimers (Schwandner et al., 1999). These TLR2 homodimers also detect lipoarabinomannan (LAM) from mycobacteria. Diacyl or triacyl lipoproteins are recognized by TLR6/TLR2 or TLR1/TLR2 heterodimers, respectively, from bacteria, mycoplasma, and mycobacteria (Kumar et al., 2009). Additionally, zymosan from fungi, tGPI-mucin from *Trypanosoma cruzi*, and the coat protein of the measles virus termed hemagglutinin is detected by TLR2 (Kawai and Akira, 2010). *In vivo* studies showed important roles for TLR2 and TLR6 in fighting RSV infections (Kawai and Akira, 2010). Stimulation with synthetic TLR2 ligands such as Pam3CSK4 (Pam3Cys), a synthetic triacetylated (tripalmitoylated) lipopeptide that stimulates TLR1/2 heterodimers, induces activation of the transcription factor NFκB (Ozinsky et al., 2000) and subsequent expression of proinflammatory cytokines (e.g. TNF-α, IL-1β, and IL-6) but not type I IFNs in DCs and MΦs (Takeuchi and Akira, 2010). Nevertheless, Barbalat and colleagues described type I IFN induction after viral TLR2 stimulation of inflammatory monocytes, indicating cell type-dependent signaling and function (Barbalat et al., 2009).

TLR3 is part of the intracellular TLR subgroup and identifies double-stranded RNA (dsRNA), which is present in some viruses (Blasius and Beutler, 2010). Polyinosinic-polycytidylic acid (Poly I:C) is structurally similar to dsRNA and represents

a synthetic ligand of TLR3 (Alexopoulou et al., 2001). Further, ssRNA and dsDNA viruses were found to trigger TLR3 activation (see ***TABLE 1.2*** for details) (Blasius and Beutler, 2010). This observation might be due to dsRNA intermediates during positive sense ssRNA virus replication and bidirectional transcription of dsDNA virus genomes resulting in dsRNA sensed by TLR3 (Weber et al., 2006). Activation of TLR3 leads to the expression of type I IFNs and proinflammatory cytokines via IRF3 and NFκB, respectively (Trinchieri, 2010). Furthermore, *in vivo* studies revealed a critical role for TLR3 in IL-12 production (Kato et al., 2006).

Lipopolysaccharide (LPS) is a cell wall component of the outer membrane of gram-negative bacteria and is known to provoke septic shock (Kawai and Akira, 2010; Takeuchi and Akira, 2010). It is recognized by TLR4 in cooperation with the co-receptor myeloid differentiation factor 2 (MD2) on the cell surface (Park et al., 2009). The LPS binding protein (LBP), a serum glycoprotein, extracts LPS from the bacterial outer membrane and transfers it to CD14, which is delivering LPS to the TLR4/MD2 complex (Miyake, 2006). Binding of LPS initiates homodimerization of two TLR4/MD2 complexes and further downstream signaling leading to expression of AP-1, NFκB, and IRF3 associated genes (Park et al., 2009; Takeuchi and Akira, 2010). Moreover, TLR4 recognizes envelope proteins of viruses (see ***TABLE 1.1*** for details) and is participating in the pathogenesis of H5N1 avian influenza virus infection by detecting endogenous oxidized phospholipids (OxPL) (Imai et al., 2008).

Flagellin from flagellated bacteria is the ligand of TLR5, which is highly expressed by DCs of the lamina propria (LPDCs) of the small intestine (Takeuchi and Akira, 2010; Yarovinsky et al., 2005). After recognition of flagellated bacteria by TLR5, LPDCs induce maturation of naïve T cells into Th1 and Th17 cells and the IgA production by activating naïve B cells that differentiate into plasma cells (Uematsu et al., 2008).

Murine TLR7 and human TLR7/8 perceive ssRNA derived from viruses or synthetic ribonucleic acids (Diebold et al., 2004; Heil et al., 2004; Lund et al., 2004). The imidazoquinolines imiquimod (R837) and resiquimod (R848) are synthetic small purine analog compounds and as well able to trigger both human and murine TLR7 and human TLR8 activation (Hemmi et al., 2002; Jurk et al., 2002). Guanine analogs such as loxoribine are also agonists of TLR7 (Heil et al., 2003; Lee et al., 2003). In addition, several bacterial and fungal RNA species (Biondo et al., 2012; Eberle et al., 2009; Jöckel et al., 2012; Mancuso et al., 2009) and short interfering RNA (siRNA) (Hornung et al., 2005) act as TLR7 ligand or in case of bacterial transfer RNA (tRNA) even as inhibitor

depending on the methylation status (Jöckel et al., 2012). Most recently it was shown that a single 2'-O-methylation can turn a TLR7/8 activating RNA sequence from 18s rRNA into a TLR8-specific agonist (Jung et al., 2015). The ligand of murine TLR8 is still unknown and remains elusive, however, imidazoquinolines are capable to trigger murine TLR8 together with polyT deoxynucleotides (poly-dT) (Gorden et al., 2006). Interestingly, TLR7 seems to be very important for the control of endogenous retroviruses (ERV), given the fact that TLR7-deficient mice develop retroviremia and lack sufficient anti-ERV-specific IgG antibodies (Yu et al., 2012). With TLR3 and TLR9 contributing in a currently unclear way, this property of TLR7 is crucial to prevent ERV-induced malignancies (Yu et al., 2012).

Microbial DNA recognition in endosomal/lysosomal compartments is mediated by TLR9 (Bauer et al., 2001; Hemmi et al., 2000; Takeshita et al., 2001). A sequence motif within bacterial and viral DNA called CpG, which contains a hexamer with an unmethylated cytosine-phosphatidyl-guanine dinucleotide bordered by 5' purines and 3' pyrimidines (Bauer, 2013), is four times less abundant in eukaryotic DNA and believed to be the main activator of TLR9-driven immune responses (Blasius and Beutler, 2010). By contrast, recent findings demonstrated a CpG motif-independent stimulation of TLR9 in murine pDCs by natural phosphodiester (PD) DNA (Bauer, 2013). Simply the phosphate-deoxyribose backbone without purine or pyrimidine nucleobases seems to prime TLR9 stimulation in mouse pDCs (Haas et al., 2008; Wagner, 2008). Thus, the idea that intracellular compartmentalization of TLR9 is due to avoid host derived DNA recognition in order to prevent autoimmunity becomes more prevalent (Bauer, 2013; Wagner, 2008). In line with this idea, self-DNA in the extracellular space is normally degraded by nucleases and does not enter intracellular vesicles (Kawai and Akira, 2011). Moreover, self-DNA that somehow accesses endosomal/lysosomal compartments is believed to be degraded by endosomal DNases previously to TLR ligation (Takeuchi and Akira, 2010). Nonetheless, TLR9-dependent DNA detection by leukocytes of humans seems to be more reliant on CpG-motifs than cells of the murine innate immune system (Bauer, 2013). Additionally identified ligands of TLR9 are dsDNA viruses and the DNA of protozoan parasites (see ***TABLE 1.2*** for details). Furthermore, hemozoin, a crystalline metabolite formed of digested hemoglobin from parasites such as *Plasmodium,* acts as carrier for parasitic DNA into the endosome/lysosome and thus enhances TLR9-dependent immune responses (Parroche et al., 2007). However, Coban et al. state that hemozoin directly binds to TLR9 and functions as a TLR9 ligand (Coban et al., 2010). A

fascinating study about circadian rhythmicity in TLR biology revealed a temporal oscillating expression for TLR9 but not for other TLRs, indicating specific circadian control of TLR9-dependent innate immune responses by molecular clock genes (Silver et al., 2012). Interestingly, this time-dependent TLR9 expression was only observed in MΦs and B cells, but was lacking in DCs (Obermann and Bauer, 2012). It is noteworthy, that two classes of synthetic unmethylated CpG-motif containing oligodeoxynucleotides (ODNs) are used for TLR9 stimulation experiments. CpG-A ODNs (also known as D-type ODNs) trigger a much higher IFN-α/β response in pDCs than CpG-B ODNs (also known as K-type ODNs), which mainly induce proinflammatory cytokines via NFκB (see chapter 1.2.2.4. for details) (Hemmi et al., 2003). CpG-A DNA consists of a single CpG-motif and a 3' poly-G tail on both PD- or PS-backbone, whereas CpG-B DNA contains either a single or multiple CpG-motifs on a PD- or PS-backbone (Blasius and Beutler, 2010).

Murine TLR11 is located either on the cell surface or the endosome/lysosome, as noted above, and senses uropathogenic bacteria and the actin associated profiling-like protein of the parasite *Toxoplasma gondii* by forming heterodimers with TLR12 (Andrade et al., 2013; Pifer et al., 2011; Yarovinsky et al., 2005). Ligands of TLR12 homodimers have not been identified so far.

A bacterial ssRNA sequence within 23*S* rRNA of gram-positive and gram-negative bacteria was lately found to trigger TLR13 activation (Hidmark et al., 2012; Li and Chen, 2012; Oldenburg et al., 2012). Remarkably, methylation of a single adenosine by erythromycin resistance methylases (Erms), which are encoded on transposons or plasmids, or natural substitution of the adenosine by guanosine in 28*S* rRNA of eukaryotes, abolishes both TLR13 activation and binding of MLS antibiotics (macrolides, lincosamides, and streptogramin) (Hochrein and Kirschning, 2013; Oldenburg et al., 2012). Accordingly, this sequence-specific detection of bacterial rRNA induces immune responses and prevents autoimmunity in eukaryotes that retained TLR13, but provides an escape mechanism for Erm-possessing bacteria from both MLS antibiotics and TLR13-dependent immunostimulatory activity (Bordon, 2012; Hochrein and Kirschning, 2013). Shi et al. further report that TLR13 expressing cells specifically respond to vesicular stomatitis virus (VSV) infection and that TLR13 knockdown leads to increased vulnerability to VSV (Shi et al., 2011).

***TABLE 1.1** LIGANDS AND THEIR ORIGIN OF TLRS LOCALIZED TO THE PLASMA MEMBRANE*

TLR (CO-RECEPTORS)	LIGAND	ORIGIN
TLR1/2	Triacyl lipopeptides	Bacteria
TLR2 (Dectin-1, C-type lectin)	Peptidoglycan	Gram pos. bacteria
	Lipoarabinomannan (LAM)	Mycobacteria
	Hemagglutinin	Measles virus
	Phospholipomannan	*Candida*
	Glycosylphosphophatidyl inositol mucin	*Trypanosoma*
	Zymosan	*Saccharomyces*
TLR4 (MD2, CD14, LBP)	Lipopolysaccharide (LPS)	Gram neg. bacteria
	Mannan	*Candida*
	Glycoinositolphospholipids	*Trypanosoma*
	Envelope proteins	MMTV, RSV
	Pneumolysin	*Streptococcus pneumonia*
	Endogenous oxidized phospholipids (OxPL)	After H5N1 avian influenza virus infection
	Paclitaxel[#]	pacific yew (*Taxus brevifolia*)
TLR5	Flagellin	Flagellated bacteria
TLR6/2 (CD36)	Diacyl lipopeptides	*Mycoplasma*
	Lipoteichoic acid	*Streptococcus*
TLR10*	Unknown	Unknown

*Shown are currently known ligands, the origin of the ligands, and co-receptors of TLRs localized to the plasma membrane (Kawai and Akira, 2010, 2011; Kumar et al., 2011; Takeuchi and Akira, 2010). RSV, Respiratory syncytial virus; MMTV, Mammary tumor virus; *, only functional in humans; #, only in mice.*

1.2.3.3 SIGNALING PATHWAYS OF TLRS

Engagement of the TLR ectodomain and its LRRs with the appropriate ligand generates dimerization, either with the same TLR or other TLRs depending on the particular receptor, and leads in part to conformational change, which is believed to initialize linkage to the cytosolic TIR domains (Latz et al., 2007). By doing so, adaptor proteins interconnect with their TIR domain to the TLR pertaining TIR domain dimer and launch a signaling cascade resulting in transcriptional expression of distinctive genes (Blasius and Beutler, 2010).

***TABLE 1.2** LIGANDS AND THEIR ORIGIN OF TLRS LOCALIZED TO THE ENDOSOME/LYSOSOME*

TLR	LIGAND	ORIGIN
TLR3	ssRNA	WNV, RSV, EMCV
	dsRNA	Reovirus, Poly I:C
	dsDNA	MCMV, HSV
TLR7	ssRNA (poly-U or GU-rich)	VSV, Influenza virus
		Synthetic
	Bacterial RNA	*Streptococcus*
	Bacterial tRNA	Several bacteria
	Imidazoquinolines (R837, R848)	Purine analog compounds
	siRNA	Synthetic
TLR8*	ssRNA (poly-U or GU-rich)	RNA viruses,
	Imidazoquinolines (R837, R838)	Synthetic
		Purine analog compounds
	siRNA	Synthetic
	2'-O-ribose methylated rRNA	rRNA
TLR9	dsDNA viruses	HSV, MCMV
	CpG motifs	Bacteria and viruses
	Phosphodiester (PD) 2' deoxyribose	DNA including self-DNA
	Hemozoin	*Plasmodium*
	DNA	*Trypanosoma cruzi*
TLR11[#§]	Uropathogenic bacteria	Bacteria
TLR11/12[#]	Profilin-like protein	*Toxoplasma gondii*
TLR12[#]	Unknown	Unknown
TLR13[#]	Bacterial ssRNA segment of 23*S* rRNA ("CGGAAAGACC")	Gram pos. and neg. bacteria
	VSV	VSV

*Shown are currently known ligands and their origin of endosomal/lysosomal localized TLRs (Andrade et al., 2013; Blasius and Beutler, 2010; Jung et al., 2015; Jöckel et al., 2012; Kawai and Akira, 2011; Kumar et al., 2009, 2011; Oldenburg et al., 2012; Pifer et al., 2011; Shi et al., 2011; Takeuchi and Akira, 2010). WNV, West Nile virus; EMCV, Encephalomyocarditis virus; MCMV, Murine cytomegalovirus; VSV, Vesicular stomatitis virus; HSV, Herpes simplex virus; CpG - cytosine-phosphatidyl-guanine; *, only in humans (murine TLR8 ligands are unknown); #, only in mice; §, expressed on the cell surface or/and endosomes/lysosomes.*

A set of five adaptor proteins are containing a TIR domain namely myeloid differentiation primary response protein 88 (MyD88), TIR domain containing adaptor inducing IFN-β

(TRIF) also known as TICAM-1, TRIF-related adaptor molecule (TRAM), TIR domain containing adaptor protein (TIRAP), and sterile-alpha and Armadillo motif-containing protein (SARM) (Takeuchi and Akira, 2010). Two main signaling pathways of TLRs are distinguished in general, the MyD88- and TRIF/TICAM-1-pathway (Takeuchi and Akira, 2010). Besides TLR3, all TLRs require MyD88 to induce at least a complete signaling process, some in fact fully depend on it including TLR7 and 9 (see ***TABLE 1.3***) (Blasius and Beutler, 2010). TLR3 dependently and TLR4 after internalization utilize the TRIF pathway with TRAM needed as a linkage between TLR4 and TRIF (Hoebe et al., 2003; Weighardt et al., 2004; Yamamoto et al., 2003). One study shows a TRIF-associated pathway in intestinal epithelial cells for TLR5 in addition to MyD88 (Choi et al., 2010). Current knowledge suggests that TRIF only signals from intracellular sites whereas MyD88 can do both, cell surface and endocytic regulated signaling. For TLR2 and TLR4 signaling, the adaptor protein TIRAP is necessary to connect TLR and MyD88 (Takeuchi and Akira, 2010). TLR4 is the only TLR that associates with four adaptor proteins and induces both the MyD88- and TRIF-related signaling pathway (Kawai and Akira, 2010).

Interestingly, one study showed recruitment of mitochondria to the phagosomes of macrophages after TLR1/2 and 4 activation, resulting in augmented ROS (reactive oxygen species) production, which was important for adequate anti-bacterial immunity (West et al., 2011). This might implicate mitochondria as a platform for TLR-mediated immune responses against bacteria (Kawai and Akira, 2011).

After MyD88 is recruited to the paired cytoplasmic TIR domains of the activated TLR, the N-terminal death domain (DD) acts together with the DD of IL-1R-associated kinase 4 (IRAK4), a serine/threonine kinase which subsequently phosphorylates its family members IRAK1 and IRAK2 (Kawagoe et al., 2008). Further, the E3 ubiquitin ligase TNF receptor-associated factor 6 (TRAF6) is activated by the IRAK1/IRAK2 complex (that detaches from MyD88) and in turn catalyzes the development of two polyubiquitin chains in cooperation with Ubc13 and Uev1A, one binding directly to TRAF6 itself and one remaining freely in the cytosol (Takeuchi and Akira, 2010). The latter activates a complex consisting of TGF-β-activated kinase 1 (TAK1), TAK1-bindind protein 1 (TAB1), TAB2, and TAB3 which phosphorylates IκB kinase β (IKK-β), a part of the IKK complex consisting of IKK-α, IKK-β, and NFκB essential modulator (NEMO), and activates a cascade of mitogen-activated protein kinases (MAPKs) including MAPKK3, MAPKK6, Jun kinases (JNKs), p38, and CREB (Blasius and Beutler, 2010; Takeuchi and Akira, 2010).

TABLE 1.3 *ADAPTOR PROTEINS AND SIGNALING CASCADES OF TLRS*

TLR	ADAPTOR PROTEIN	TRANSCRIPTION FACTOR	GENE EXPRESSION
TLR1/2	MyD88, TIRAP	NFκB	Proinflammatory cytokines
TLR2	MyD88, TIRAP	NFκB, IRF3, IRF7	Proinflammatory cytokines Type I IFNs
TLR3	TRIF	NFκB, IRF3, IRF7	Proinflammatory cytokines Type I IFNs
TLR4	MyD88, TIRAP TRIF, TRAM	NFκB, IRF3, IRF7	Proinflammatory cytokines Type I IFNs
TLR5	MyD88, TRIF	NFκB	Proinflammatory cytokines
TLR6/2	MyD88, TIRAP	NFκB	Proinflammatory cytokines
TLR7	MyD88	NFκB, IRF7	Proinflammatory cytokines Type I IFNs
TLR8	MyD88	NFκB, IRF7	Proinflammatory cytokines Type I IFNs
TLR9	MyD88	NFκB, IRF7	Proinflammatory cytokines Type I IFNs
TLR11	MyD88	NFκB	Proinflammatory cytokines
TLR12	MyD88?	NFκB?	Proinflammatory cytokines?
TLR13	MyD88	NFκB, IRF7	Proinflammatory cytokines Type I IFNs

Shown are adaptor proteins, activated transcription factors, and resulting gene transcription of TLRs. (Barbalat et al., 2009; Choi et al., 2010; Kawai and Akira, 2011; Kumar et al., 2009; Shi et al., 2011)

The phosphorylated IKK complex promotes phosphorylation of the NFκB inhibiting protein IκB, which therefore degrades, leading to NFκB translocation to the nucleus and further induction of proinflammatory cytokines such as TNF-α, IL-6, IL-12, and IL-1β (Blasius and Beutler, 2010). The MAPKs cascade finally triggers activation of the transcription factor complex AP-1 (activator protein-1) and subsequent cytokine expression (Takeuchi and Akira, 2010).

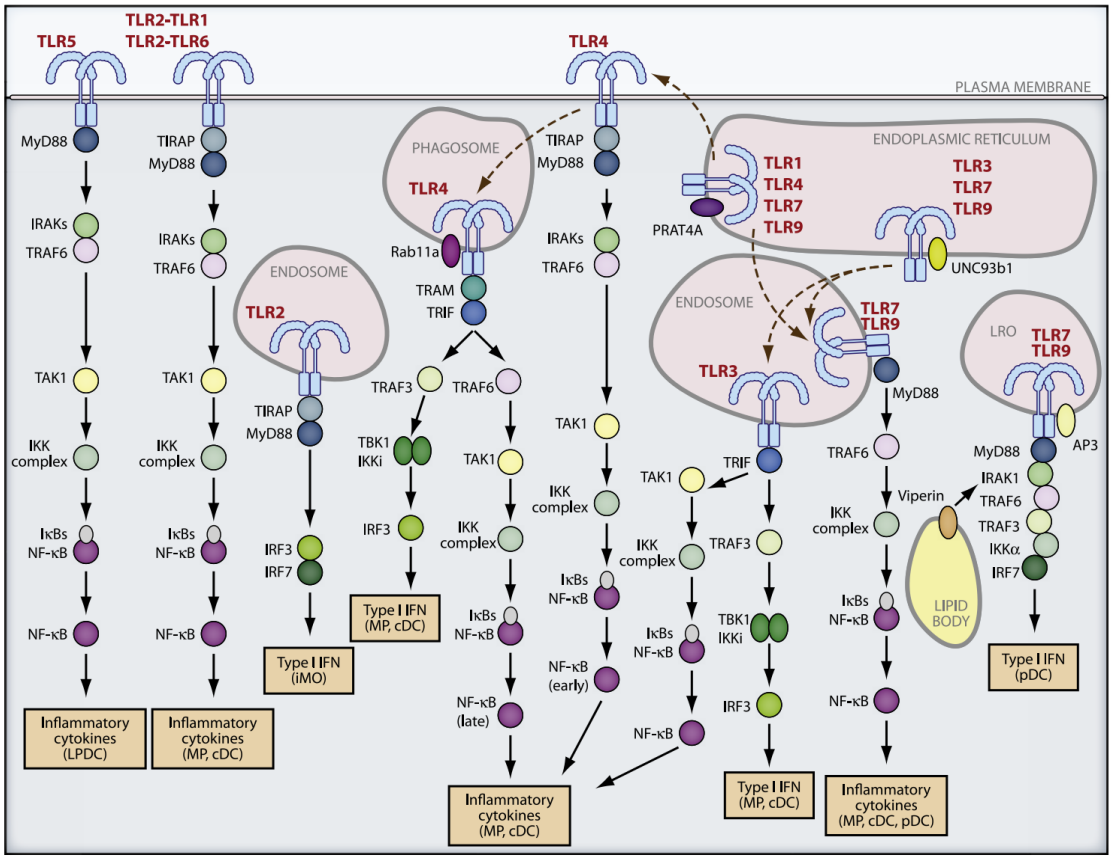

FIGURE 1.1 *LOCALIZATION, TRAFFICKING, AND SIGNALING OF TLRS*
Localization, trafficking, and general signaling pathways of all currently known TLRs (apart from mouse-specific TLR11 – 13) are depicted (Taken from Kawai and Akira, 2011). MP, macrophages; cDC, classical dendritic cells; pDC, plasmacytoid dendritic cells; LPDC, lamina propria dendritic cells; iMO, inflammatory monocytes; LRO, lysosome-related organelles.

The upregulation of type I IFNs upon TLR7 and 9 signaling is completely MyD88 dependent (Takeuchi and Akira, 2010), which especially in pDCs forms other complexes as noted above (for details see section below). Moreover, IRF5 binds directly to MyD88 and TRAF6 and seems to be involved in proinflammatory cytokine production such as TNF-α, IL-6, and IL-12 upon TLR9 and TLR4 activation with CpG-DNA and LPS, respectively (Takaoka et al., 2005). IRF1 is induced by IFN-γ and also directly engages with MyD88 in cDCs and MΦs, indicating an important role for MyD88-dependent TLR signaling, since IRF1-deficient cells show impaired IL-12p35, iNOS, and IFN-β expression after TLR9 stimulation (Negishi et al., 2006; Schmitz et al., 2007).

In response to dsRNA and LPS, TLR3 and 4, respectively, recruit the adaptor protein TRIF, with only TLR4 additionally requires TRAM as a linkage in between (O'Neill et al., 2003; Yamamoto et al., 2003). In case of TLR4, ligand recognition takes place at the cell surface with MyD88-dependent signaling cascade activation. However, TLR4 is internalized after ligand binding and indeed triggers TRIF-dependent signaling

in the early endosome (Tanimura et al., 2008). When TLR4 finally travels to late endosomes, this TRIF-dependent pathway is negatively regulated by a splice variant of TRAM called TRAM adaptor with GOLD domain (TAG) in mice and in humans by the TIR-domain containing protein SARM (Blasius and Beutler, 2010; Kawai and Akira, 2011; Takeuchi and Akira, 2010). After initiation of downstream signaling, TRIF interconnects with its C-terminal domain with receptor-interacting protein 1 (RIP1) and RIP3 as well as with its N-terminal region with TRAF3 and TRAF6 (Blasius and Beutler, 2010). Recruitment of TRAF6 mediates NFκB and MAPKs activation like reported for the MyD88-dependent way (Kawai and Akira, 2011). Furthermore, the TNF receptor-associated death domain protein (TRADD) is required for this signaling pathway, interacting with several other factors in a quite complex way, ultimately resulting in NFκB activation (Kumar et al., 2011; Takeuchi and Akira, 2010). TRAF3, similar to TRAF6, functions as an E3 ubiquitin ligase and activates TANK-binding kinase 1 (TBK1) and IKK-ε (also known as IKK-*i*), which in turn phosphorylate IRF3 and the E3 ubiquitin ligase Pellino1 (Blasius and Beutler, 2010; Enesa et al., 2012; Kumar et al., 2011). IRF3 dimers subsequently translocate to the nucleus and facilitate transcriptional expression of type I interferons and IFN-inducible genes (Takeuchi and Akira, 2010). The E3 ubiquitin ligase Pellino1 interacts with another transcription factor named DEAF1, which binds to the IFN-β promoter and thus seems to be involved in TBK1-associated type I IFN induction (Enesa et al., 2012; Ordureau et al., 2013). IKK-ε additionally phosphorylates STAT1, which is able to trigger some IFN-inducible genes such as *Adar1*, *Ifit3*, and *Irf7* (Tenoever et al., 2007). Finally, a number of proteins control TBK1 and IKK-ε activation including TRAF family member-associated NFκB activator (TANK), NAK-associated protein 1 (NAP1), and similar to NAP1 TBK1 adapter (SINTBAD) (Takeuchi and Akira, 2010). ***FIGURE 1.1*** depicts general signaling pathways of TLRs.

1.2.3.4 TLR7 AND 9 SIGNALING IN PDCS

TLR7 and 9 signaling in pDCs differentiates from those of other immune cells. The MyD88-dependent signaling pathway described above for TLR7 and 9 takes place in MΦs, B cells, cDCs as well as pDCs and culminates in the production of NFκB and MAPKs/AP-1 regulated proinflammatory cytokines (Blasius and Beutler, 2010).

However, an additional pathway in pDCs is responsible for immediate production of vast quantities of type I IFNs in response to coupled TLR7 and 9 signaling (see ***FIGURE 1.2***). Accordingly, MyD88 associates with IRAK4, IKK-α, TRAF3, TRAF6, IRAK1, and IRF7 to form a complex, which phosphorylates IRF7 (mediated by IRAK1 and IKK-α within the complex) and leads to further nuclear translocation of IRF7, followed by gene expression of type I IFNs (Blasius and Beutler, 2010; Honda et al., 2005b; Kawai and Akira, 2011; Takeuchi and Akira, 2010). Thus, IRF7 has turned out to be the master regulator of IFN-α/β induction in pDCs (Honda et al., 2005b). A continuous basal induction of IRF7 is believed to be responsible for the immediate and enormous type I IFN responses of pDCs (Honda et al., 2005b). In addition, other proteins are involved including OPNi (intracellular osteopontin) and Dock2, which also associate with the complex (Cao and Liu, 2006; Gotoh et al., 2010; Shinohara et al., 2006). OPNi is

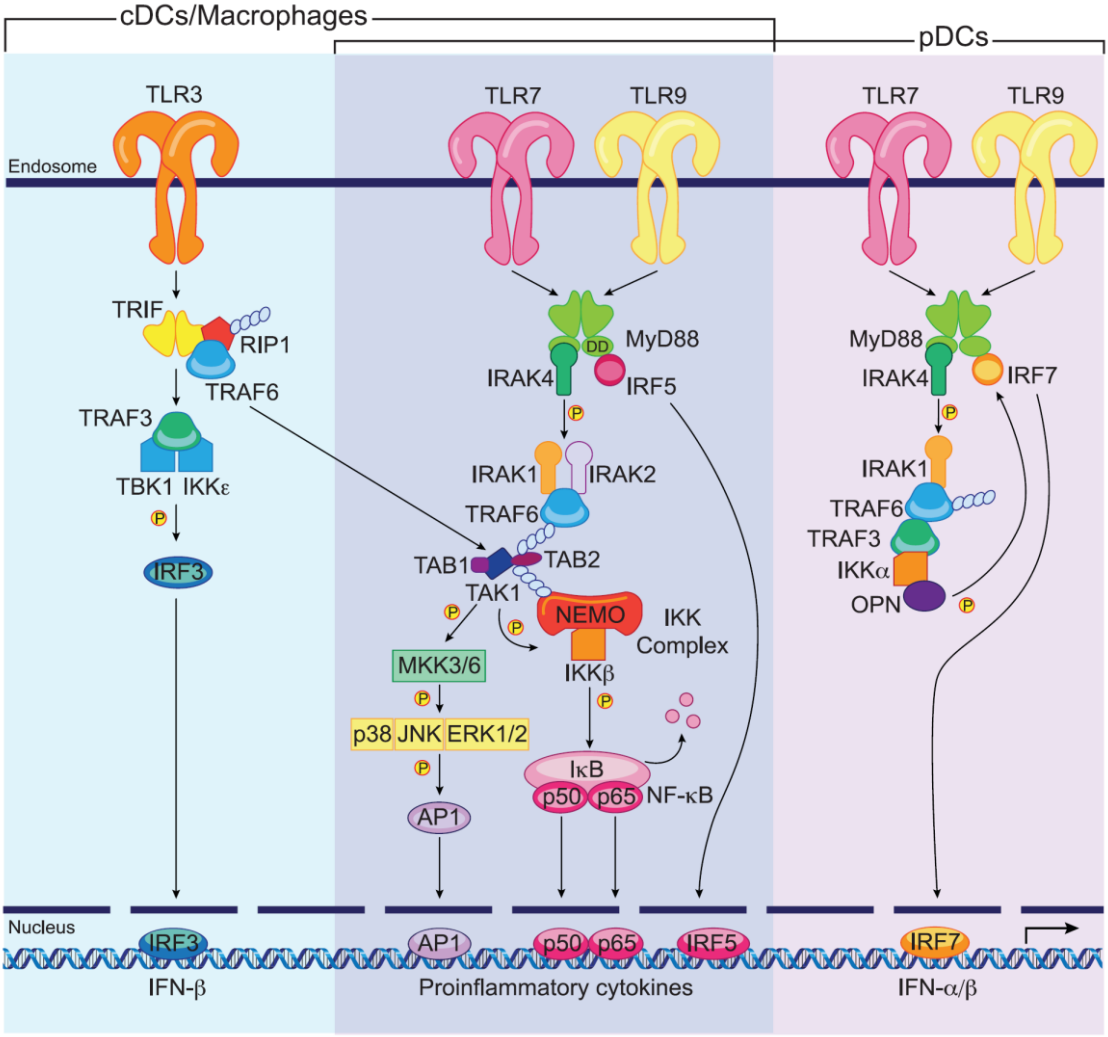

FIGURE 1.2 *SIGNALING PATHWAYS OF TLR3, 7, AND 9 IN PDCS, CDCS, AND MΦS*
Murine cDCs and macrophages possess all three receptors and use signaling pathways resulting in gene expression via IRF3, AP-1, IRF5, and NFκB, whereas pDCs only possess TLR7 and 9 and use an additional pathway for type I IFN expression via IRF7 (Taken from Blasius and Beutler, 2010).

upregulated upon CpG stimulation and directly binds to MyD88 with subsequent increase of type I IFN responses, but surprisingly, proinflammatory cytokine levels remain unaffected (Shinohara et al., 2006). Dock2 regulates the activation of IKK-α and hence influences IRF7 phosphorylation (Gotoh et al., 2010). IKK-β, the second subunit of the IKK complex, appears to be somehow involved in this issue, since inhibitors of this kinase provoke impaired IFN-β secretion of the human pDC cell line Gen2.2 (Pauls et al., 2012). The isomerase Pin1 has lately been found to regulate IRAK1 and its deletion slightly reduced proinflammatory cytokine levels in cDCs after TLR7 and 9 stimulation, but completely abrogated type I IFN responses in pDCs (Tun-Kyi et al., 2011). By probably stabilizing the linkage between TLR9 and MyD88 and influencing translational regulation as well as phosphorylation of IRF7, the mammalian target of rapamycin (mTOR) and further "downstream" targets, such as p70S6K, have been identified as crucial regulators of type I IFN induction in pDCs (Cao et al., 2008). The phosphatidylinositol-3 kinase (PI3K) in turn is involved in the mTOR pathway by indirectly activating mTOR and has similarly been shown to affect nuclear translocation of IRF7 (Guiducci et al., 2008). Hence, the PI3K-mTOR-p70S6K pathway seems to play a pivotal role in TLR7 and 9 mediated IFN-α/β induction in pDCs. In addition to that, a number of molecules are involved in negative IRF7 regulation, including protein modification and translational as well as transcriptional alteration. For instance, the mammalian Dcp2 mRNA-decapping protein supports IRF7 mRNA degradation, the tripartite motif-containing protein 28 causes transcriptional repression, and the K48-linked polyubiquitination of IRF7 through the ubiquitin E3 ligase RAUL leads to proteasome-associated IRF7 degradation (Bao and Liu, 2012; Yu and Hayward, 2010). Further on, a complex comprised of the transcription factor FOXO3, the nuclear co-repressor 2, and the histone deacetylase 3 is able to repress IRF7 transcription, but becomes degraded by the PI3K/Akt pathway after type I IFN induction (Litvak et al., 2012).

1.2.4 THE ROLE OF TLRS AND OTHER PRRS IN AUTOIMMUNITY AND CANCER

In the past decade, TLRs and other PRRs have been implicated in numerous disorders apart from infectious diseases including autoimmune diseases and the tumorigenesis of various cancers (Kawai and Akira, 2009; Nagi et al., 2014; Takeuchi and Akira, 2010). This passage gives just a very brief insight into this issue due to the enormous complexity

and large progress that has been made in this field, indicating again the importance of PRRs and particularly TLRs in the pathogenesis of many diseases.

The innate immune system is capable to discriminate self from non-self under normal physiological conditions and contributes to maintain homeostasis. However, under pathological conditions, permanent activation of PRRs by DAMPs or PAMPs can promote chronic disease (Nagi et al., 2014; Takeuchi and Akira, 2010). For instance, TLR7 and 9 play a central role in the pathogenesis of systemic lupus erythematosus (SLE) and psoriasis by recognizing self-nucleic acids bound to different proteins such as HMGB1, RNPs, antimicrobial peptides (e.g. LL37), or autoantibodies that are internalized into endosomes/lysosomes of pDCs and B cells. In addition, due to inhibited degrading of self-nucleic acids by nucleases, TLR activation can occur (Takeuchi and Akira, 2010). The resulting inflammation mainly driven by type I IFNs but also proinflammatory cytokines causes disease. Defects by mutation or deficiency of the extracellular located self-DNA degrading DNase I also causes SLE-like pathologies (Takeuchi and Akira, 2010). Mutations of the RNA sensor MDA5 leads to resistance against type I diabetes, suggesting a fundamental role of this receptor in the pathogenesis of this autoimmune disease (Takeuchi and Akira, 2010). Further mechanisms involving aberrant pDC-mediated type I IFN production by TLR7 or 9 have been implicated in the generation of type I diabetes and experimental autoimmune myocarditis (EAM) (Ganguly et al., 2013).

Disrupted function of the exonuclease TREX1 leads to accumulation of cytoplasmic DNA and has been linked to the neurodevelopmental disease Aicardi-Goutières-Syndrome (AGS) by overproduction of IFN-α (Paludan and Bowie, 2013; Takeuchi and Akira, 2010). To date, the DNA sensors involved in this pathology have not been found. However, further suggestion that the recognition of accumulated self-DNA in the cytosol leads to autoimmunity comes from the fact that DNase II-knockout embryos die due to massively elevated type I IFN and TNF-α levels (Paludan and Bowie, 2013; Takeuchi and Akira, 2010). DNase II degrades self-DNA in endosomes/lysosomes, which accumulates and is somehow transferred to the cytosol when DNase II is lacking. Interestingly, mice deficient for DNase II and the type I IFN receptor (IFNAR) are rescued, but develop polyarthritis due to increased proinflammatory cytokines such as TNF-α. The evidence that cytosolic DNA sensors must be involved is reinforced by the fact that DNase II and STING double knockout mice are rescued from both lethality and polyarthritis (Paludan and Bowie, 2013). Unravelling innate immune mechanisms will of

course also open new opportunities to fight diverse autoimmune disorders, which are currently increasing in industrialized countries (Bach, 2002).

Concerning the connection between innate immunity and cancer, multiple genes upregulated by certain transcription factors downstream of several PRR-induced signaling cascades play also essential roles for the tumorigenesis and progression of different types of cancer (Nagi et al., 2014). One of the key transcription factors in PRR signaling namely NFκB upregulates anti-apoptotic (e.g. Bcl2) and angiogenic (e.g. angiopoietin, VEGF) proteins besides proinflammatory cytokines. Moreover, induced nitride oxide (NO) synthase 2 (NOS-2)-dependent NO production together with ROS (reactive oxygen species) leads to the death of infected cells which in turn release different DAMPs like self-DNA that again activate PRRs, for example, cytosolic DNA sensors (Nagi et al., 2014). The latter can induce KRAS via TBK1, which again activates NFκB. Further signaling cascades involved in both innate immunity and cancer include STAT pathways, MAPK pathways with induction of AP-1, and different inflammasomes (e.g. AIM-2 inflammasome) (Nagi et al., 2014). Tumor-associated innate immune cells such as TAM (tumor-associated macrophages) have been shown to promote progression, angiogenesis, anti-apoptosis, and tissue-remodeling resulting in enhanced tumor growth and metastasis by PRR activation (Nagi et al., 2014). Deregulated immune cells in tumor tissues as well as tumor cells itself are operating with tools originally meant to fight infections and to repair damaged tissues. The link between inflammation and cancer has already been proposed more than a century ago by Rudolf Virchow (Nagi et al., 2014). Developing our understanding of the innate immune system and its properties including PRRs will also lead to improved understanding of cancer in the future and might result in promising novel therapies and diagnostics.

1.3 DENDRITIC CELLS (DCS) AND MACROPHAGES (MΦS)

1.3.1 DENDRITIC CELLS (DCS)

DCs play a central role in innate immunity. Since the identification of DCs by Steinman and Cohn (Steinman and Cohn, 1973) as the main antigen-presenting cells (APCs) 40 years ago, a lot of research has been done and many different subsets with diverse functions have been discovered (Schraml and Reis e Sousa, 2015; Watowich and Liu, 2010). The name is related to the morphology of these cells that distinguish them from MΦs and is characterized by dendrite-like protrusions or extensions of the plasma membrane that are believed to improve cell-cell contact between DCs and T cells (Schmid et al., 2010; Schraml and Reis e Sousa, 2015; Watowich and Liu, 2010). The latter feature describes the condition that seems to be needed for the main function that is the uptake of antigens in non-lymphoid tissues followed by migration to T cell areas of secondary lymphoid organs to prime naïve T cells through antigen-presentation, thus prompting adaptive immune responses. Apart from other cell types that also possess the ability of antigen-presentation including monocytes, MΦs, and B cells, DCs are believed to be the most professional APCs (Murphy et al., 2012).

The classification of DCs includes several aspects and is still subject of controversial discussions (Schraml and Reis e Sousa, 2015; Steinman and Idoyaga, 2010). Based on morphology, expression of surface markers, and gene expression profiles, DCs are distinguished into conventional/classical dendritic cells (cDCs) on one hand and plasmacytoid dendritic cells (pDCs) on the other hand (Steinman and Idoyaga, 2010). CDCs are also called myeloid dendritic cells (mDCs) initially referring to their ontogeny from myeloid progenitors, which has been proven wrong by several groups showing that both pDCs and cDCs can differentiate from myeloid as well as lymphoid progenitors (for details see the following passages and ***FIGURE 1.3***) (Schmid et al., 2010; Steinman and Idoyaga, 2010). Nevertheless, the term “mDCs” is still used mainly as a counterpart to pDCs, which is in fact wrong and thus the name “cDCs” is used throughout this work. The cDC subset resembles the initially discovered type of DC with typical morphology (see ***FIGURE 1.3 B***) and the capability of professional antigen-presentation and can be further subdivided into various subtypes (see chapter 1.3.1.3 for details). In contrast, the morphology of pDCs is similar to plasma cells with a spherical shape and a large rough endoplasmic reticulum (see ***FIGURE 1.3 A***) that are responsible for the name plasmacytoid

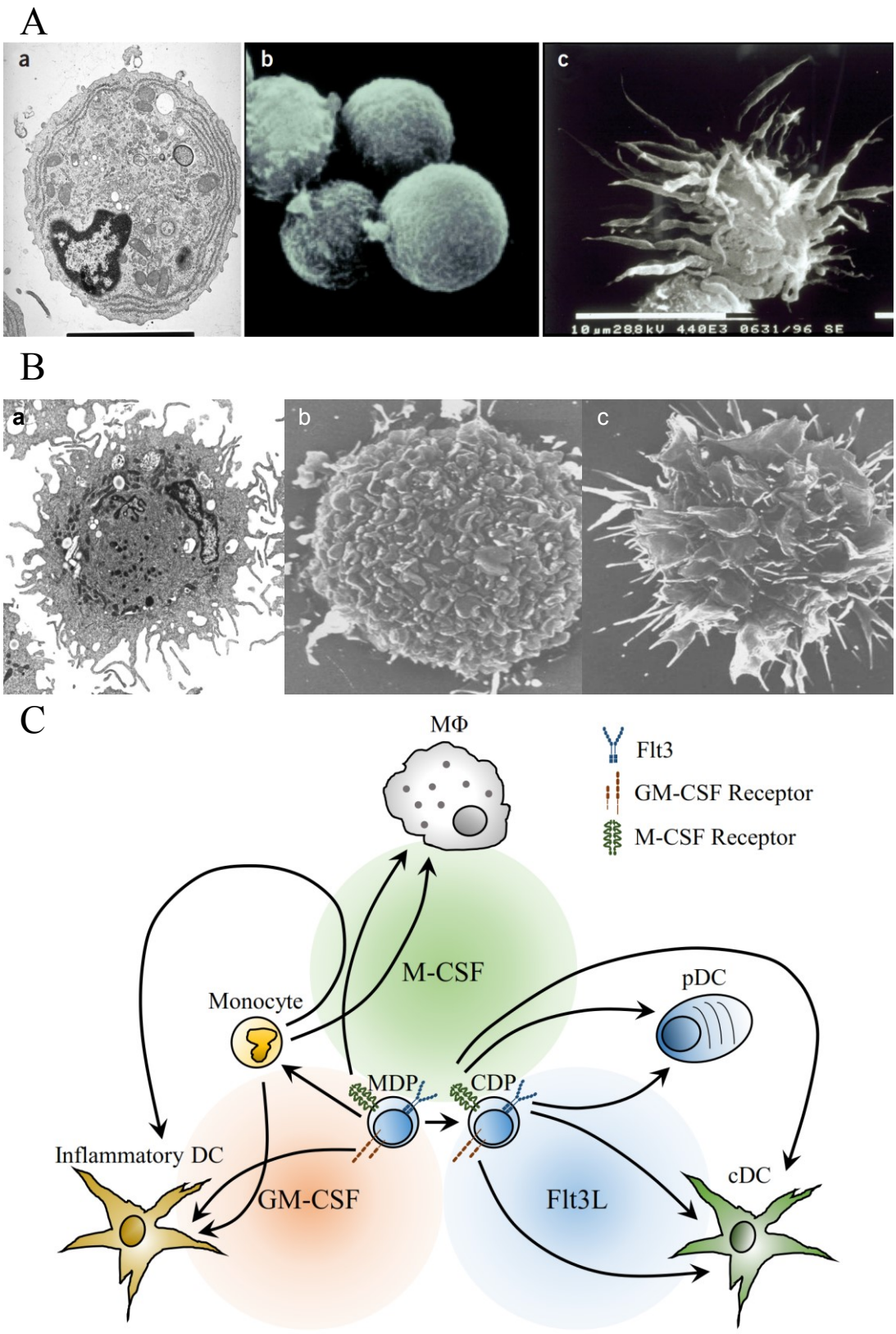

FIGURE 1.3 *MORPHOLOGY AND DIFFERENTIATION OF DCS AND MΦS*
A) *The spherical morphology* ***(b)*** *of inactivated pDCs containing a well developed rough endoplasmic reticulum* ***(a)*** *and CD40L-mediated "dendritic" morphology* ***(c)*** *of activated pDCs is depicted (Taken from Colonna et al., 2004).* ***B)*** *The typical morphology of cDCs with dendritic extensions in an immature* ***(b)*** *and mature state after antigen uptake* ***(a,c)*** *(Taken from Bashyam, 2007 and Bhardwaj and Walker, 2003).* ***C)*** *Simplified model of cytokine-dependent DC and MΦ differentiation. Adapted and modified from Schmid et al., 2010. M-CSF, macrophage colony-stimulating factor; GM-CSF, granulocyte/macrophage colony stimulating factor; Flt3L, fms-like tyrosine kinase 3 ligand; MDP, macrophage/dendritic cell progenitor; CDP, common dendritic cell progenitor; cDC, classical dendritic cell; pDC, plasmacytoid dendritic cell; MΦ, macrophage.*

and reflect the large amounts of type I IFNs produced by pDCs ready to be secreted when activation of TLR7 and 9, mainly by viruses, occurs (Colonna et al., 2004; Schmid et al., 2010). Further classifications are based on location or ontogeny (Schraml and Reis e Sousa, 2015; Steinman and Idoyaga, 2010; Watowich and Liu, 2010). Resident dendritic cells are localized to lymphatic tissues and migratory DCs are present in non-lymphoid peripheral tissues for surveillance and migrate to secondary lymphoid organs upon activation (Watowich and Liu, 2010). Some authors restrict the term cDCs to resident DCs. The type of DCs found at sites of inflammation is different to steady state DCs and is regarded as a separate class, which derives from monocytes circulating in the blood stream and thus is called monocyte-derived DCs or inflammatory DCs. Conversely, DCs which are not derived from monocytes are termed monocyte-independent DCs (Steinman and Idoyaga, 2010).

1.3.1.1 ORIGIN AND DEVELOPMENT OF DENDRITIC CELLS (DCS)

Like all immune cells, DCs arise from HSCs and specific beyond precursors in the BM. The differentiation towards certain subsets of leukocytes is driven by complex signals from the microenvironment. Soluble cytokines that bind to their respective receptors in a paracrine, autocrine, or distant manner via the blood steam or lymph vessels and cell-cell contacts are the basis of interactions that promote differentiation and development (Schmid et al., 2010).

The cytokine granulocyte-macrophage colony-stimulating factor (GM-CSF) was the first cytokine shown to generate differentiation of DCs *in vitro* from BM or monocyte cultures (Inaba et al., 1992). These DCs resemble cDCs derived from monocytes at sites of inflammation and are therefore called inflammatory DCs or monocyte-derived DCs, as already noted above (Schmid et al., 2010; Watowich and Liu, 2010). BM cultures supplemented with the cytokine fms-like tyrosine kinase 3 ligand (Flt3L) comprise both pDCs and cDCs that are believed to resemble splenic steady state DCs and do not differentiate from monocytes but HSCs (Brasel et al., 2000; Schmid et al., 2010; Watowich and Liu, 2010). Interestingly, mice lacking GM-CSF or the GM-CSF receptor (GM-CSFR) exhibit only small reductions in splenic and lymph node cDCs, whereas $Flt3^{-/-}$ and $Flt3L^{-/-}$ mice show a large loss of both pDCs and cDCs and inversely wild type mice treated with Flt3L generate massive quantities of DCs (Schmid et al., 2010; Watowich and Liu, 2010). However, double knockout mice deficient for GM-CSF and Flt3L are still

able to give rise to DCs, but Kingston et al. could show that GM-CSF is essential for a specialized subset of dermal DCs expressing the integrin CD11b (Kingston et al., 2009; Schmid et al., 2010). Of note, GM-CSF has been shown to inhibit Flt3L-dependent generation of pDCs in BM cultures *in vitro* (Gilliet et al., 2002). The third cytokine found to be involved in DC differentiation is macrophage colony-stimulating factor (M-CSF) due to the lack of Langerhans cells (LCs; subset of cDCs in the skin) in mice deficient for its receptor (M-CSFR) and M-CSF supplemented BM cultures that contain pDCs and cDCs (Fancke et al., 2008; Ginhoux et al., 2006; Schmid et al., 2010). Interestingly, mice with a homozygous mutation in the *csf1* gene that encodes for M-CSF ($Csf1^{op/op}$ mice) showed normal LCs in the skin. Another cytokine binding to M-CSFR apart form M-CSF called IL-34 was recently found and seems to clarify this issue (Schmid et al., 2010). However, the major role of IL-34 in DC differentiation needs to be further investigated. The fact that numbers of pDCs and cDCs were increasing in $Flt3L^{-/-}$ mice treated with M-CSF indicates an important role for this cytokine in DC development. However, further cytokines seem to be involved in this scenario since mice lacking several of the previously mentioned cytokines are still able to generate DCs (Watowich and Liu, 2010). Given that IFN-α has been linked to hematopoietic processes lately and the fact that IFN-α and -β have been shown to enhance pDC and restrict cDC differentiation implicates type I IFNs as contributors of DC development in the BM (Essers et al., 2009; Li et al., 2011; Watowich and Liu, 2010). This observation is believed to be utilized as an immune-evading mechanism by viruses (e.g. measles virus (MV) and lymphocytic choriomeningitis virus (LCMV)) (Hahm et al., 2005; Watowich and Liu, 2010). ***FIGURE 1.3 C*** shows the three currently known cytokines involved in DC development and their impact on specific DC lineages as well as MΦs (Schmid et al., 2010).

The differentiation of DCs from HSCs is interposed by several intermediate progenitor subsets. HSCs differentiate either to common lymphoid (CLPs) or myeloid progenitors (CMPs). The latter subset can further develop to granulocyte/macrophage progenitors (GMPs) and megakaryocyte/erythrocyte progenitors (MEPs) (Schmid et al., 2010). In addition, an intermediate subset referred to as lymphoid-primed multipotent progenitors (LMPPs) can give rise to all other progenitors except MEPs. As mentioned above, several groups have demonstrated that DCs can develop from all progenitors apart from MEPs (Schmid et al., 2010). Interestingly, lymphoid and myeloid lineage derived DCs exhibit no differences in surface markers, gene transcription, and function, however,

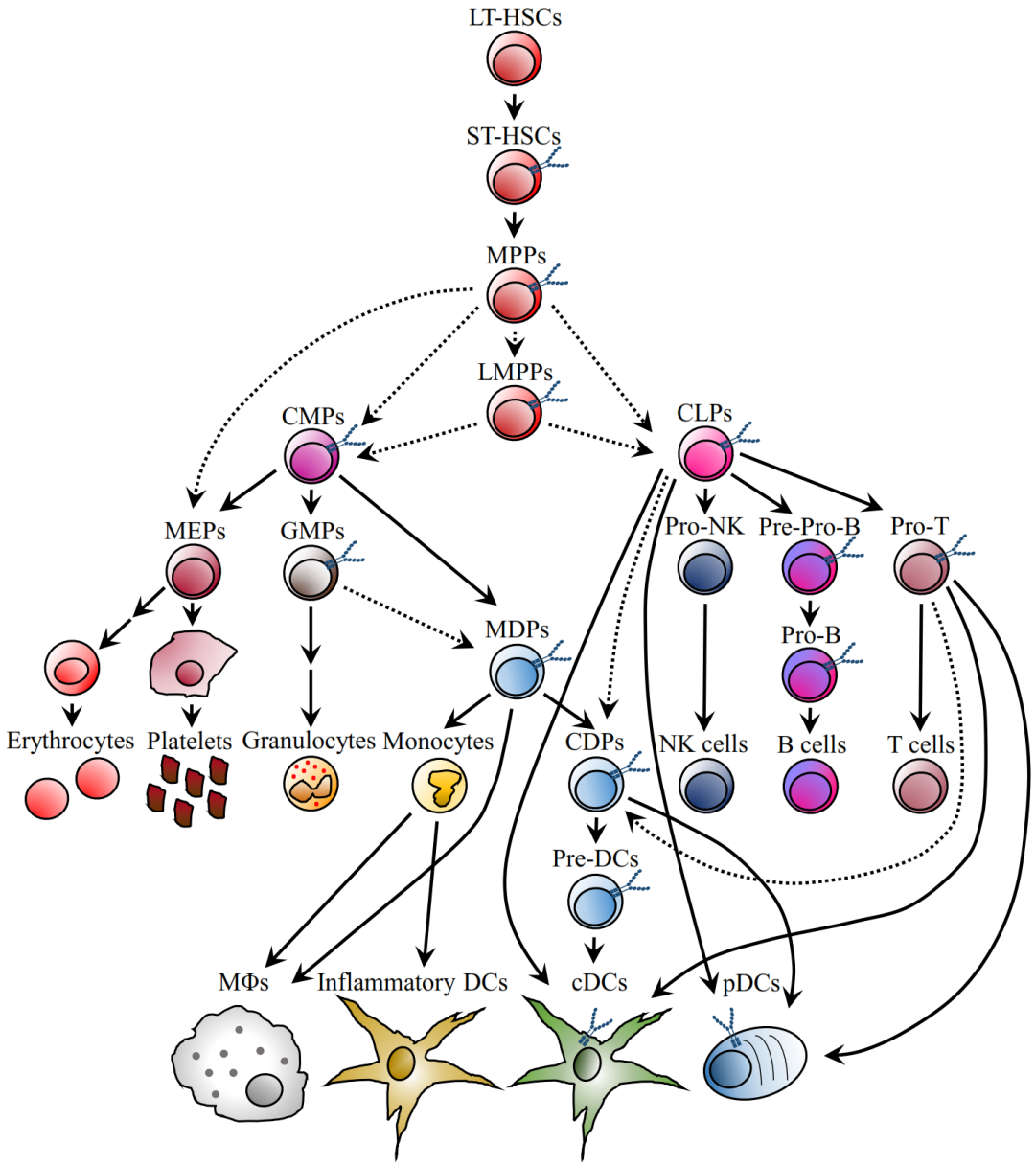

***FIGURE 1.4** HEMATOPOIETIC TREE FOR DEVELOPMENT OF DCS AND MΦS*
Simplified developmental tree of DC and MΦ differentiation in the BM. Model adapted and modified from Schmid et al., 2010. The cytokine receptor Flt3 is illustrated as blue receptor on the cell surface of expressing subsets. Solid arrows depict known pathways and dotted arrows show suggested pathways. LT-HSCs, long-term hematopoietic stem cells; ST-HSCs, short-term HSCs; MPPs, multipotent progenitors; LMPPs, lymphoid-primed MPPs; CMPs, common myeloid progenitors; CLPs, common lymphoid progenitors; MEPs, megakaryocyte/erythrocyte progenitors; GMPs, granulocyte/macrophage progenitors; MDPs, macrophage/dendritic cell progenitor; CDPs, common dendritic cell progenitors; MΦs, macrophages; cDCs, classical dendritic cells; pDCs, plasmacytoid dendritic cells.

the destination to lymphoid organs strongly differs between myeloid and lymphoid primed DCs (Schmid et al., 2010). Downstream of the CMP lineage, progenitors that can give rise to both MΦs and DCs were found called macrophage/dendritic cell progenitors (MDPs). However, direct precursors of DCs that possess the ability to differentiate into pDCs and cDCs were also discovered and termed common dendritic cell progenitors

(CDPs). CDPs have been shown to directly arise from MDPs (Schmid et al., 2010). Whether CDPs can develop from CLPs as well is currently unclear, however, it is known that CLPs can differentiate to pDCs, cDCs, and Pre-DCs (Watowich and Liu, 2010). The latter subset was shown to be the direct precursor of cDCs that lost the potential to differentiate into pDCs (Schmid et al., 2010; Watowich and Liu, 2010). Deficiency of Flt3L alone and significantly enhanced in GM-CSF and Flt3L double knockout mice, caused a strong reduction of the DC precursors MDPs and CDPs, suggesting a synergistic impact of both cytokines on the generation of direct DC precursors. Furthermore, numbers of CLPs were also largely decreased in $Flt3L^{-/-}$ mice (Schmid et al., 2010), showing an important dependency of DC development on this cytokine and on lymphoid progenitors in general (Schmid et al., 2010). One study identified a pDC precursor that possesses the ability to differentiate into cDCs under certain conditions including the presents of GM-CSF or soluble factors secreted by intestinal epithelium (Schlitzer et al., 2011). ***FIGURE 1.4*** depicts all currently known developmental stages from HSCs to DCs.

The hypothesis that different expression or loss of lineage-specific cytokine receptors of precursor cells and the presents of diverse cytokines in varying levels in certain niches of the BM drives differentiation seems to be the most plausible to date (Schmid et al., 2010). However, in contrast to development strongly dependent on cytokines and expression of respective receptors, some authors believe differentiation from HSCs to differentiated cells is a stochastic procedure. The receptor c-kit is continuously less expressed as the differentiation process proceeds. Flt3 and M-CSFR are still expressed in lymphoid progenitors (CLPs), probably maintaining differentiation towards DCs, whereas further differentiated B cell precursors mainly express IL7Rα and downregulate Flt3 and M-CSFR (Schmid et al., 2010). Conversely, myeloid progenitors retain Flt3 and M-CSFR and loos IL7Rα expression. However, further cytokines and receptors seem to be involved and need to be discovered.

Interestingly, Pre-cDCs, also called Pre-DCs, exit the BM and fully mature to different cDC-subsets in peripheral tissues and organs after contacting any antigen, whereas pDCs are known to enter the blood stream from the BM and migrate to peripheral tissues as mature developed cells (Watowich and Liu, 2010). Notably, one recent study showed that CDPs, the direct precursor of pDCs and cDCs, already express TLR2, TLR4, and TLR9 and directly enter the blood stream and migrate to lymph nodes upon TLR activation (Schmid et al., 2011).

1.3.1.2 PLASMACYTOID DENDRITIC CELLS (PDCS)

PDCs are specialized type I IFN-producing cells responding to nucleotides derived from viruses, bacteria, and dead cells via TLR 7 and 9. Their ability of massive IFN-α/β secretion on TLR7 and 9 activation is unique among the mammalian immune system and is especially important for innate immune responses against viral infections (Lande and Gilliet, 2010; Reizis et al., 2011). In humans, only 0.2 – 0.8 % of blood cells are pDCs that are capable to produce approximately 95 % of all type I IFNs upon viral infections (Lande and Gilliet, 2010). Compared to other immune cells, pDC-mediated IFN-α/β responses are up to 1000 times more potent (Reizis et al., 2011). This promotes a complex antiviral state of infected and non-infected cells that limits viral replication and further spread of these pathogens (Lande and Gilliet, 2010). The additional production of proinflammatory cytokines such as IL-6, TNF-α, and IL-12 (only in mice) induces inflammation and regulates several other immune cells in concert with type I IFNs. This includes the generation of cDCs from monocytes, polarization of $CD4^+$ T cells into Th1 cells, differentiation of B cells into plasma cells, promotion of clonal expansion as well as survival of $CD8^+$ cytotoxic T cells, and activation of NK cells (Karrich et al., 2014; Lande and Gilliet, 2010). After TLR-mediated activation and cytokine release, pDCs develop a "classical" DC morphology (see ***FIGURE 1.3 A***) and acquire properties for antigen-presentation to T cells, thus turn into a cDC-like cell (Reizis et al., 2011). This "maturation" seems to be dependent on the activation of NFκB, since mice deficient for NFκB1 and c-Rel secrete type I IFNs and undergo apoptosis after TLR9 stimulation by CpG-DNA (O'Keeffe et al., 2005). Activated pDCs are able to efficiently prime and cross-prime $CD4^+$ and $CD8^+$ T cells, respectively, however with a capacity distinct from cDCs to induce a subset of IL-10 producing regulatory T cells through ICOS-L and thus seem to be also important for negative regulation of self-induced inflammation and immune tolerance in general (Lande and Gilliet, 2010; Reizis et al., 2011). Besides antiviral immunity, pDCs have been linked to various other physiological and pathological processes such as immune tolerance (see above) and cytotoxicity or autoimmunity and cancer, respectively (Ganguly et al., 2013; Karrich et al., 2014; Lande and Gilliet, 2010).

Typical surface expression markers of pDCs in mice are CD11c, B220 (CD45R), low levels of MHC-II, and co-stimulatory molecules (Reizis et al., 2011). However, B220 and CD11c are also expressed on a precursor of NK cells called pre-mNK cells, which have initially been thought to reflect an intermediate cell subset between pDCs and NK

cells named interferon-producing killer dendritic cells (IKDCs) (Blasius et al., 2007; Caminschi et al., 2007; Guimont-Desrochers et al., 2012). Moreover, a CCR9$^-$ precursor of cDCs was also shown to express B220 and CD11c (Segura et al., 2009). The surface markers BST2 (mPDCA-1) and SiglecH have been demonstrated to be highly specific for murine pDCs and are therefore preferentially used. Further pDC-associated receptors in mice include Ly6C (the GR1 antibody binds to Ly6G in granulocytes and Ly6C on pDCs) and Ly49Q, which are less specific (Lande and Gilliet, 2010; Reizis et al., 2011). In humans, BDCA-2, BDCA-4, and ILT7 are typical surface markers. BDCA-2 negatively regulates pDC-function after engagement of respective antibodies (Lande and Gilliet, 2010) and is therefore less appropriate for functional analysis.

The basic helix-loop-helix transcription factor E2-2 (also known as TCF4) was identified as the master regulator of pDC maturation and differentiation (Cisse et al., 2008; Ghosh et al., 2010; Nagasawa et al., 2008). Various pDC-specific genes responsible for differentiation and function are regulated by E2-2 including TLR7, TLR9, IRF8, IRF7, and SpiB (Cisse et al., 2008). Interestingly, deletion of E2-2 in mature peripheral pDCs causes differentiation into cDCs, indicating the integral role of E2-2 in maintaining the pDC fate (Reizis et al., 2011). The E protein inhibitor Id2 was demonstrated as the counterpart of E2-2 in cDCs that is downregulated in pDCs and vice versa, showing a distinct relationship and plasticity between these two cell types (Reizis et al., 2011). Further transcription factors such as IRF8, SpiB, or Runx2 and miRNAs have been shown to be part of the regulatory machine in pDCs (Karrich et al., 2014; Sawai et al., 2013).

Exclusive signaling cascades and currently known contributing molecules of TLR7 and 9 biology in pDCs have already been described in chapter 1.2.3.4. However, various proteins have additionally been identified that are involved in pDC-specific regulation of TLR signaling. The adapter-related protein complex-3 (AP-3), biogenesis of lysosome-related organelle (LRO) complexes (BLOC)-1, BLOC-2, and the peptide-proton symporter channel Slc15a4 are essential for TLR7 and 9 endosomal trafficking in pDCs (Blasius et al., 2010; Sasai et al., 2010). Lately, the IFN-inducible proteins phospholipid scramblase 1 (PLSCR1) and viperin were found to participate in these difficult processes as well (Saitoh et al., 2011; Talukder et al., 2012). PLSCR1 binds to the LRRs of the TLR9 ectodomain and regulates its trafficking to the endosomal compartment (Talukder et al., 2012). The protein viperin was found to promote TLR7 and 9 signaling through forming an IFN-signaling complex consisting of MyD88 associated with IRAK1 and TRAF6 within lipid bodies resulting in nuclear translocation

of IRF7 (Saitoh et al., 2011). Furthermore, autophagy-associated proteins are known to be involved in the regulation of immune responses for quite a while (Saitoh and Akira, 2010). In pDCs, ssRNA virus infection detected by TLR7 was reported to be dependent on the autophagy protein 5 (Atg5), because pDCs lacking this gene showed diminished type I IFN and IL12p40 levels, whereas upon CpG stimulation only IFN but not IL12p40 was reduced (Lee et al., 2007). Another pDC-specific protein called PACSIN1 might play a role for type I IFN induction, since PANSIN1-deficient pDCs show reduced IFN-α levels after TLR9 stimulation and this protein has been demonstrated to regulate vesicle trafficking by connecting membrane trafficking with the cytoskeleton (Esashi et al., 2012). Granulin, the next contributing molecule, activates TLR9 through delivery of CpG-ODNs to TLR9-containing endosomes/lysosomes (Park et al., 2011). Interestingly, upon TLR9 stimulation with CpG-A DNA, the transport from the early endosome to the late endosome or lysosome in pDCs is much more prolongated compared to cDCs. Moreover, artificial ligand retention in cDC endosomes, induced by using the cationic lipid DOTAP, results in abnormal type I IFN responses, suggesting a unique membrane trafficking pathway for TLR9 in pDCs (Honda et al., 2005a). Notably, multimeric CpG-A DNA seems to be longer present in the early endosome according to its tendency of aggregation compared to monomeric CpG-B DNA, which could be an explanation for stronger IFN-α/β activation upon CpG-A DNA stimulation (Kerkmann et al., 2005). Furthermore, the observation that multimeric CpG-A enters transferrin receptor (TfR) positive endosomes rather than lysosome-associated membrane protein 1 (LAMP1) positive lysosomes (monomeric CpG-B occurs in the latter), and the fact that reverse molecular modification of both leading to monomeric CpG-A and multimeric CpG-B results in inverted gene expression, implicates that different TLR9 signaling pathways strongly depend on localization and molecular properties of the engaging ligands (Guiducci et al., 2006). Supporting this idea, Sasai et al. quite recently demonstrated that the two different TLR9 signaling pathways in pDCs depend on different endogenous localizations and occur sequentially instead of simultaneously (Sasai et al., 2010). Thus, early endosome engagement of CpG-A DNA and TLR9 promotes a MyD88-TRAF6-associated activation of NFκB, whereas further travel of CpG-DNA/TLR9 to the so called lysosome-related organelles (LRO) triggers TRAF3-incorporation and promotes IRF7 activation, all governed by AP-3 (Sasai et al., 2010). In murine pDCs, the ITIM-containing cell surface receptor Ly49Q has been shown to be also important for intracellular tasks, supporting appropriate temporal CpG-DNA and TLR9 co-localization

and trafficking to endosomal/lysosomal compartments (Yoshizaki et al., 2009). In summary, proper spatiotemporal engagement of TLR9 ligands, and probably TLR7 ligands, with their receptor and the molecular structure of them seem to be very important determinants of sufficient TLR7/9 activation and different signaling pathways.

The regulation of TLR7 and 9 signaling in pDCs is further mediated by several pDC-specific surface receptors, which are proposed to play an important role in controlling the potentially hazardous massive type I IFN secretion in order to "fine-tune" antiviral host responses and prevent autoimmunity (Bao and Liu, 2012; Reizis et al., 2011). Immunoreceptor tyrosine-based activation motifs (ITAMs) are found within various transmembrane adaptor proteins that primarily function as immune cell activators (Bao and Liu, 2012). ITAMs activate a pathway involving SCR and SYK family tyrosine kinases similar to the BCR signaling cascade (Bao and Liu, 2012; Gilliet et al., 2008). In human pDCs, BDCA-2 (a C-type lectin), immunoglobulin-like transcript 7 (ILT7), and the Fc receptor for IgE (FcεRIα) are associated with the ITAM-containing adaptor molecule FcεRIγ-chain and inhibit TLR7 and 9 signaling after ligand binding (Cao et al., 2006; Dzionek et al., 2001; Schroeder et al., 2005). Respective ligands of these receptors are the HIV-1 encoded envelope glycoprotein gp120, BST2, and IgE (Cao and Bover, 2010). Another ITAM-containing adaptor molecule is DNAX activation protein 12 (DAP12), which also functions mainly as inhibitor of TLR7/9 signaling. The human pDC receptor Nkp44, the murine transmembrane proteins SiglecH (sialic acid-binding Ig-like lectin H), and pDC-TREM (pDC-triggering receptor expressed in myeloid cells 4) in cooperation with Plexin-A1 signal through DAP12 (Cao and Bover, 2010). Nkp44 engages with the hemagglutinin of the influenza virus and the proliferating cell nuclear antigen (PCNA), which is overexpressed in tumors, implicating a role in both negative regulation of viral responses and pDC-inactivation by tumor cells (Bao and Liu, 2012). The murine pDC receptor SiglecH decreases IFN-secretion upon TLR9 activation after binding of specific antibodies, while the natural ligand is currently unknown (Bao and Liu, 2012). Taken together, BDCA-2, ILT7, FcεRIα, Nkp44, and SiglecH use the ITAM-signaling pathway with different adaptor molecules to inhibit pDC-driven IFN-α/β responses. Conversely, pDC-TREM upregulation is mediated by IFN-α, and complexed with Plexin-A1 it enhances type I IFN responses after semaphorin-6D (Sema6D), a ligand of Plexin-A1, engages with the complex (Watarai et al., 2008). Interestingly, several virus-encoded proteins embody ITAMs, suggesting strategies to evade pDC activation or at least to limit anti-viral immunity (Bao and Liu, 2012). Examples are the K1 protein of

the human herpesvirus 8 (HHV8) or the latent membrane protein 2A (LMP2A) of the Epstein-Barr virus (EBV). The latter has been demonstrated to target interferon receptors leading to their degradation, but so far without known ITAM involvement (Shah et al., 2009).

Further on, immunoreceptor tyrosine-based inhibitory motifs (ITIMs) are located within the cytosolic domains of numerous inhibitory surface receptors, including C-type lectins and immunoglobulin superfamily members and use SHP1 and SHP2 or SHIP1 for signaling (Bao and Liu, 2012). PDCs also express ITIM-containing receptors, which positively influence TLR7/9 signaling. In human pDCs, the ITIM-possessing receptor CD300a recognizes phospholipids of the outer membrane of dead cells (phosphatidylethanolamine and phosphatidylserine) after crosslinking with CD300c, and diminishes HLA-DR, TNF-α, and IL-6 expression, but impressively increases IRF7 expression and subsequent IFN-α secretion (Bao and Liu, 2012). A relative in murine pDCs is Ly49Q, member of the C-type lectin natural killer receptor family, which binds type I major histocompatibility complex (MHC-I) and is very important for TLR7/9-depentent IFN-α secretion, since $Ly49Q^{-/-}$ murine pDCs reveal critically reduced cytokine secretion (Tai et al., 2008). Recent work on this issue demonstrates further roles of Ly49Q in IL-12 secretion, MHC-II expression, appropriate T cell activation, and nuclear translocation of IRF7 in murine pDCs (Rahim et al., 2013). Yoshizaki et al. additionally propose an impact of Ly49Q on proper TLR9-CpG engagement and involvement in intracellular trafficking to endosomal/lysosomal compartments (Yoshizaki et al., 2009).

1.3.1.3 CONVENTIONAL DENDRITIC CELLS (CDCS)

The term “cDCs” is mostly used as a counterpart to pDCs, which comprise different subtypes of DC lineages that collectively reflect the main function of highly efficient antigen-presentation of exogenous and endogenous antigens to T cells and possess the typical DC morphology with long extensions of the plasma membrane. As noted before, some authors prefer to use the name cDCs only for resident DCs found in lymphoid organs such as the spleen and lymph nodes in steady state (Watowich and Liu, 2010). Besides resident DCs, further lineages are migratory DCs present in non-lymphoid peripheral tissues (e.g. lung, intestine, or skin), monocyte-derived DCs (also called inflammatory DCs), and Langerhans cells (LCs) (Idoyaga and Steinman, 2011). Resident DCs are further subdivided into $CD8\alpha^{+}$ and $CD8\alpha^{-}$ DCs (or cDCs) showing particular

skills in exogenous antigen-presentation to $CD4^+$ T cells and cross-presentation to cytotoxic $CD8^+$ T cells, respectively (Idoyaga and Steinman, 2011; Reizis et al., 2011). Circulating monocytes in the blood are able to differentiate into monocyte-derived DCs (inflammatory DCs), apart from MΦs (see section 1.3.2 for details), and can prime $CD4^+$ as well as $CD8^+$ T cells. Some monocyte-derived DCs reside in draining lymph nodes of the skin and can rapidly proliferate after LPS-mediated TLR4 activation (Idoyaga and Steinman, 2011). Two major DC subsets are present in the skin, which are LCs and dermal DCs. The latter can be subdivided into $CD103^+CD11b^-$ and $CD103^-CD11b^+$ and further subsets of dermal DCs (Idoyaga and Steinman, 2011). LCs derive from progenitors of the fetal liver or yolk sac, need M-CSF, and are resistant to irradiation, whereas dermal DCs derive from pre-DCs (pre-cDCs) from the blood, are dependent on Flt3L, and are sensitive to irradiation (Idoyaga and Steinman, 2011). Interestingly, similarities in function and transcription factor expression have been found for $CD8\alpha^+$ resident DCs and $CD103^+CD11b^-$ migratory DCs as well as the $CD8\alpha^-$ and the $CD103^-CD11b^+$ subset (Steinman and Idoyaga, 2010). Similar to dermal DCs, either $CD11b^+$ or $CD103^+$ migratory DC subsets have been described in many other tissues. However, a subset expressing both CD103 and CD11b was found in the intestinal lamina propria (Idoyaga and Steinman, 2011).

Apart from the surface receptors mentioned above that discriminate certain DC subsets, expression of the integrin CD11c, high levels of major histocompatibility complex class II (MHC-II), and co-stimulatory molecules including CD80, CD86, and CD40 on the cell surface are characteristic for cDCs in mice (Reizis et al., 2011; Schmid et al., 2010; Schraml and Reis e Sousa, 2015). The receptor B220 found on the cell membrane of pDCs is not expressed in cDCs. The integrin CD11b is expressed on some cDC subsets but not present on pDCs (Reizis et al., 2011). CDCs circulating in the human blood with high MHC-II expression comprise two different types, one with BDCA-1/CD1c and the other with BDCA-3/CD141 expression (Idoyaga and Steinman, 2011). BDCA-3^+ human DCs have been shown to resemble murine $CD8^+$/$CD103^+$ cDCs in function and gene expression (Reizis et al., 2011). Further surface markers of human DCs are CD1a, CD1b, DEC-205 (CD202), and Langerin (CD207) (Steinman and Idoyaga, 2010).

Each cDC subset expresses different surface receptors such as lectins that are involved in the uptake of antigens and presentation or PRRs including TLRs that sense PAMPs or DAMPs. As a result of PRR activation, cDCs are able to produce a wide range

of cytokines and chemokines that regulate either inflammation or self-tolerance (Idoyaga and Steinman, 2011).

Transcriptional regulation of cDCs is controlled by Id2, which inhibits E2-2 and thus prevents pDC fate (see section 1.3.1.2). Moreover, the basic leucine zipper transcription factor Batf3 has recently been demonstrated to be an important regulator of $CD8\alpha^+$ resident DCs and $CD103^+$ migratory DCs but not $CD8\alpha^-$ resident DCs (Watowich and Liu, 2010). Further transcription factors that play important roles in pre-DC and cDC lineages include PU.1, IRF8, RelB, IRF2, and IRF4 (Watowich and Liu, 2010).

1.3.2 ORIGIN, DEVELOPMENT, AND FUNCTIONS OF MACROPHAGES (MΦS)

Blood-circulating monocytes and tissue resident macrophages (MΦs) were the first members of the mononuclear phagocyte system that were described. Ilya Metchnikoff discovered MΦs in the late 19th century, whereas the subpopulation of DCs, which are also part of this family, were discovered about 40 year ago as noted above (Epelman et al., 2014). In the past, all MΦs were believed to arise from monocytes that circulate in the blood stream, which are derived from precursors in the BM (Dey et al., 2014; Epelman et al., 2014). Indeed, $Ly6C^+$ and $Ly6C^-$ monocytes develop in the BM from the myeloid lineage with direct precursors GMPs and MDPs (see chapter 1.3.1.1 and ***FIGURE 1.4***) and start circulating in the blood stream. $Ly6C^-$ monocytes (also called non-classical monocytes) were initially thought to infiltrate tissues and differentiate into resident MΦs. However, recent studies show that these cells directly derive from $Ly6C^+$ monocytes (also termed classical monocytes) and do not enter tissues, instead patrol the intravascular endothelium to clear dying endothelial cells (Dey et al., 2014; Epelman et al., 2014). In contrast, classical monocytes that highly express Ly6C are able to infiltrate and patrol peripheral tissues in steady state and transport pathogens to nearby lymph nodes without differentiation (Epelman et al., 2014). In inflammatory conditions, classical monocytes enter sites of infection and differentiate into MΦs (Epelman et al., 2014). However, several studies showed that most tissue resident MΦs originate independently of blood-monocytes already in embryonic tissues such as the yolk sac and the fetal liver and are able to self-renew their population in peripheral tissues throughout adulthood (Dey et al., 2014; Epelman et al., 2014). For instance, Kupffer cells in the liver, Microglia in the brain, and cardiac tissue MΦs were shown to develop in the yolk sac (Dey et al., 2014). Thus, it appears that monocytes have a patrolling function in steady state and can

differentiate into MΦs and DCs when inflammation occurs, whereas most resident MΦs are derived from embryonic tissues and develop independently from monocytes and BM precursors (Epelman et al., 2014).

MΦs are localized to non-lymphoid and lymphoid tissues and comprise a heterogeneous population of phagocytes that have different functions in homeostasis (e.g. clearing dead cells or producing growth factors) and inflammation depending on the particular tissue (Dey et al., 2014; Geissmann et al., 2010). For instance, alveolar MΦs are involved in surfactant turnover, osteoclasts resorb bone tissue, and splenic red pulp MΦs clear old erythrocytes contributing to iron metabolism (Dey et al., 2014). Moreover, tissue-resident as well as monocyte-derived MΦs can be further polarized into M1 or M2 phenotype. M1 MΦs are effector cells that fight infectious pathogens and clear infected or malignantly transformed cells (Italiani and Boraschi, 2014). The task of maintaining tissue homeostasis through eliminating damaged cells and promoting tissue repair und growth is carried out by M2-like polarized MΦs (Italiani and Boraschi, 2014). The molecular basis of M1/M2 polarization seems to be due to a different arginine metabolism. M2 MΦs produce ornithine and polyamines which are important for cell proliferation and repair via synthesis of collagens and drive fibrosis, whereas citrulline and NO are arginine metabolites in M1 MΦs that are important for killing pathogens and inhibiting cell proliferation (Italiani and Boraschi, 2014). The M1 phenotype can be induced *in vitro* by PAMPs e.g. LPS and cytokines such as TNF-α and IFN-γ (Italiani and Boraschi, 2014). These cells express high levels of IL-12, IL-23, IL-1β, IL-6, and TNF-α and low levels of IL-10, produce toxic molecules including NO and reactive oxygen species (ROS), and trigger adaptive Th1 responses (Italiani and Boraschi, 2014). The cytokines IL-13 and IL-4 are present in Th2 responses and have been shown to polarize MΦs into M2 phenotype together with IL-10, TGF-β, glucocorticoids, activation of Fcγ receptors, and stimulated TLRs (Italiani and Boraschi, 2014). Depending on the activating agents, the M2 phenotype has been subdivided into M2a, M2b, and M2c. Generally, M2-MΦs are characterized by producing high levels of IL-10 and TGF-β and low levels of IL-23 and IL-12. Various scenarios for contribution of M2-MΦs have been demonstrated such as Th2 responses, parasitic infections, allergy, tissue remodeling, angiogenesis, immune tolerance, and promotion of several types of cancers (Italiani and Boraschi, 2014). Numerous other functions and pathologies of both M1 and M2 MΦs and further phenotypes in between have been described. M1 as well as M2 polarized MΦs are well appointed with a broad range of PRRs including TLRs and other receptors such as

scavenger, mannose, and galactose receptors that support phagocytosis and induce various cytokines and chemokines to regulate innate immune responses (Geissmann et al., 2010). Furthermore, MΦs are capable to present antigens and induce and coordinate different adaptive immune responses (Italiani and Boraschi, 2014).

Cytokines that are involved in differentiation, proliferation, and self-renewal of monocytes and MΦs are M-CSF, GM-CSF, IL-34, and IL-4 (Italiani and Boraschi, 2014). Murine BM cultures supplemented with M-CSF lead to large amounts of differentiated adherent MΦs among other cells including pDCs and cDCs found in suspension (Fancke et al., 2008; Stanley et al., 1978). The best known surface receptor of MΦs in mice is F4/80. Further used membrane-bound markers in mice are CD11b, MHC-I, MHC-II, Ly6C, CCR2, Mac3, TRAP, and CD169 among others (Dey et al., 2014). Transcription factors that drive distinct transcriptional programs to mediate specific functional and phenotypic properties in different MΦs are not as well investigated as for DCs and are one interesting part of current research in this field. However, it was shown that yolk sac-derived MΦs depend on PU.1 and do not need c-Myb in contrast to monocyte-derived MΦs that originate from the BM (Italiani and Boraschi, 2014). Further transcription factors implicated in MΦ biology are KLF4, EGR1, IRF8, GATA6, SpiB, SpiC, PPARγ, PPARδ, SREBPs, and LXR (Dey et al., 2014; Epelman et al., 2014; Geissmann et al., 2010; Italiani and Boraschi, 2014).

1.4 HOX GENES

1.4.1 DISCOVERY, ORIGIN, AND PROPERTIES OF HOX GENES

The family of Hox genes can be found in almost all eukaryotes and its members are transcription factors involved in regulating fundamental processes in embryonic tissue patterning by determining cellular identity along several body axes (Holland, 2013; Soshnikova, 2014). Especially the development of limbs and organs along their anterior-posterior axis has been shown to be regulated by Hox genes (Shah and Sukumar, 2010). The identification of their orthologous genes in *drosophila melanogaster* called Hom genes comprising two gene complexes termed bithorax and antennapedia in 1978 and 1980, respectively, led to the discovery of the homeotic or homeobox (Hox) genes and their homeobox DNA-binding domain in many animals including mammals just a few years later (Shah and Sukumar, 2010). The DNA sequences and functions of Hox genes are evolutionary highly conserved and single genes as well as whole genome duplications are believed to be the reason for the expansion of these genes throughout evolution that resulted in 39 Hox genes in mammals. The latter are organized in 4 clusters termed A, B, C, and D (Alharbi et al., 2013; Morgan, 2006; Rezsohazy et al., 2015). Each gene cluster is located on a different chromosome. ***FIGURE 1.5 A*** depicts the homology of the Hom genes in *drosophila melanogaster* and each of the mammalian Hox gene clusters and their chromosome location by colors (Alharbi et al., 2013). The configuration in gene clusters is needed for enhancer sharing that allows exact spatiotemporal expression during developmental processes (Morgan, 2006). The 3' – 5' position of a Hox gene in its cluster determines the spatial expression in development, for example, HoxB1 is earlier expressed than HoxB2 and so forth (Morgan, 2006; Shah and Sukumar, 2010). This means that 3' located genes are expressed in anterior tissues and 5' position leads to expression in posterior tissues, which is called spatial collinearity (Shah and Sukumar, 2010). Further on, temporal collinearity describes that Hox gene expression within one cluster is temporally kept in line exactly from 3' to 5' (Morgan, 2006; Shah and Sukumar, 2010). In addition, posterior (5' positioned) located Hox genes are dominant over anterior (3' positioned) genes, which is referred to as posterior prevalence (Morgan, 2006). All Hox proteins share the homeodomain that consists of a 60 amino acid-containing triple helicoidal motif (3 alpha helices), which facilitates binding to specific DNA-binding sites with the N-terminal arm contacting the minor and helix 3 (recognition helix) binding the

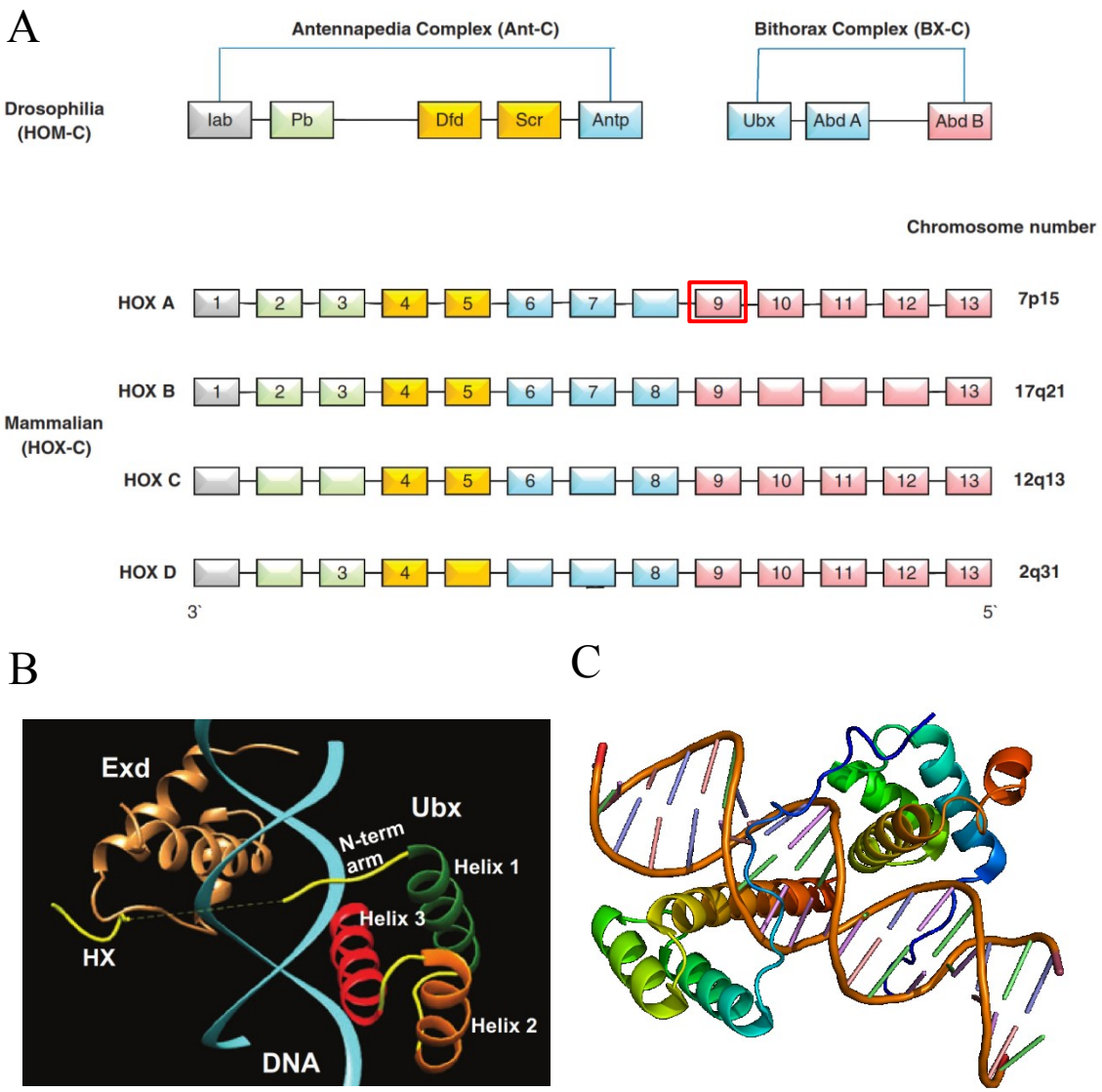

***FIGURE 1.5** HOX GENES*
***A)** Shown are HOM clusters of* Drosophila melanogaster *and the mammalian HOX clusters with their chromosome location. Homology is depicted by colors. HoxA9 is highlighted by a red frame. Taken from Alharbi et al., 2013.* ***B)** Co-binding of the homeodomain protein Ubx and its co-factor Exd of* Drosophila melanogaster *to their DNA sequence. The hexapeptide (HX) motif mediates protein-protein interaction. Taken from Rezsohazy et al., 2015.* ***C)** Crystal structure of the HoxA9 protein bound to DNA. Created with open source software PyMOL; adapted and modified from LaRonde-LeBlanc and Wolberger, 2003.*

major groove of the DNA (Ladam and Sagerström, 2013; Rezsohazy et al., 2015; Svingen and Tonissen, 2006). The core DNA-binding site contains the sequence 5'-TTNAT-3' with N depending on the specific Hox protein (LaRonde-LeBlanc and Wolberger, 2003). However, specificity and selectivity to DNA-binding sites of Hox proteins were shown to be quite poor and thus various co-factors that have been identified seem to enhance both specificity and selectivity and are cell-type dependent (Alharbi et al., 2013; Collins and Hess, 2016; Huang et al., 2012; Rezsohazy et al., 2015). The pre-B-cell leukemia (Pbx) and myeloid ectopic insertion (Meis) families are the most important co-factors

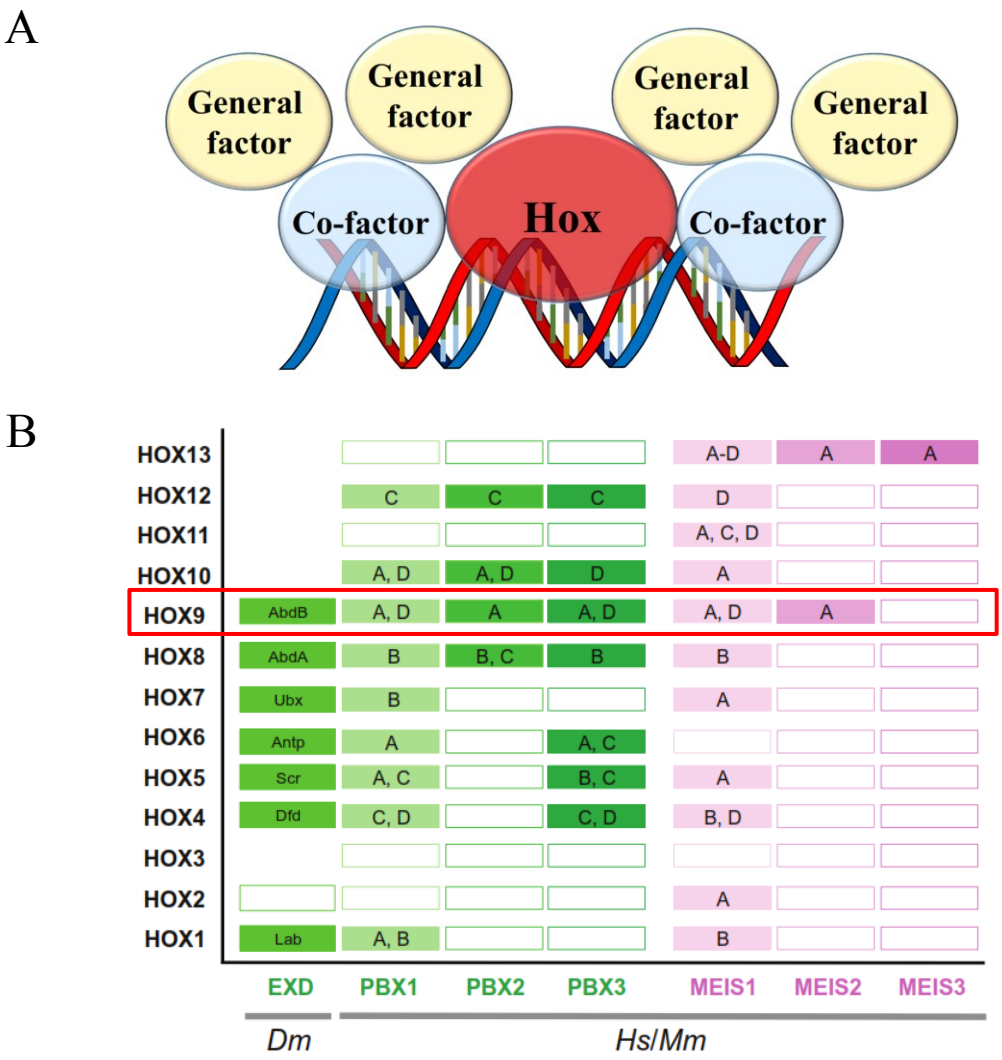

FIGURE 1.6 *STRUCTURE OF HOX PROTEIN COMPLEXES AND KNOWN TALE-CO-FACTORS*
A) *Schematic structure of Hox protein complexes bound to their DNA binding site including the Hox protein itself, co-factors, and additional non-DNA-binding general factors (adapted and modified from Ladam and Sagerström, 2013).* ***B)*** *Currently known TALE-containing co-factors of the Pbx and Meis family and their recruiting Hox proteins. The Hox9 paralogs are highlighted by a red frame. Taken from Rezsohazy et al., 2015.*

(Alharbi et al., 2013), which also possess a homeodomain that differs from the Hox homeodomain by containing a three amino acid long loop between helix 1 and 2 (TALE) (Ladam and Sagerström, 2013). Prominent members are Pbx1 and Meis1 that are both crucial for developmental and hematopoietic functions of Hox proteins (Alharbi et al., 2013). The hexapeptide (HX) motif of Hox proteins was shown to facilitate binding to Pbx proteins (Rezsohazy et al., 2015). ***FIGURE 1.5. B*** depicts the structure of Hox proteins in case of Ubx found in *drosophila* with the 3 alpha helices containing homeodomain and the HX motif that together with a co-factor (Exd) binds to a specific DNA sequence (Rezsohazy et al., 2015). Hox and Pbx proteins together bind the consensus sequence 5'-TGATNNATNN-3', which is longer than the sequence that Hox monomers bind to and increases specificity (Rezsohazy et al., 2015). Furthermore, additional proteins termed

general factors or collaborators that do not directly bind DNA sequences but Hox proteins or co-factors are recruited, leading to multi-protein Hox transcription complexes (Collins and Hess, 2016; Ladam and Sagerström, 2013). Hox proteins and co-factors contain domains that can interact with general factors/collaborators, which are members of the transcription machinery itself and chromatin regulators such as the CBP/p300 histone acetyltransferase or HDAC1 und 3 (histone deacetylases), implicating also epigenetic influences (Huang et al., 2012; Ladam and Sagerström, 2013; Rezsohazy et al., 2015). ***FIGURE 1.6 A*** and ***B*** depict the assembly of Hox complexes and the currently known co-factors that are recruited from different Hox proteins (Ladam and Sagerström, 2013; Rezsohazy et al., 2015). Several studies have shown that the composition of Hox complexes is depending on the cell type and context and cell type dependent further transcription factors are involved in this scenario (Huang et al., 2012; Ladam and Sagerström, 2013; Rezsohazy et al., 2015).

Besides controlling the cellular identity along axes of embryonic developmental processes including limps, the gastrointestinal tract, and the female reproductive tract, numerous other functions of Hox proteins have been described in the last couple of years (Morgan, 2006; Rezsohazy et al., 2015). First it became evident that Hox proteins are not only expressed during embryogenesis, the nested expression of Hox proteins (also called the "Hox code") along body axes was shown to be still active in adult tissues (Morgan, 2006). Moreover, Hox genes are expressed in HSCs and precursors in a similar manner as in embryonic developmental processes showing distinct expression patterns in different lineages (Alharbi et al., 2013) and have been implicated in leukemogenesis as well as tumorigenesis of solid tumors in recent years (see chapter 1.4.2 for details) (Shah and Sukumar, 2010). Involvement in cell shaping, migration, proliferation, apoptosis, and differentiation were shown for various Hox proteins lately (Rezsohazy et al., 2015). For instance, cell shape and migration are influenced by Hox genes through regulating and coordinating cell adhesion, cell-to-cell contacts, the cytoskeleton, and controlling expression of receptors and ligands that interact with the microenvironment that cells are travelling along (Rezsohazy et al., 2015). Another example shows that Hox proteins control cell cycle processes and proliferation by directly regulating cell cycle regulators in concert with other transcription factors (Collins et al., 2014). The question if Hox genes directly influence cellular actions or function as master regulators or both cannot be fully answered currently. However, growing evidence suggests that both situations take place, since Hox genes were shown to orchestrate gene regulatory networks from the very top

through initiation but also influence ongoing networks at several stages and can directly control particular actions (Rezsohazy et al., 2015). Apart from their role as transcription factors, "non-transcriptional" activities have been found for Hox proteins including DNA replication, DNA repair, mRNA translation, and protein degradation (Rezsohazy et al., 2015). Depending on the cell type and context, Hox proteins can adopt multifaceted functions in concert with co-factors and cell type dependent transcription factors, which reflects a high versatility of these regulatory proteins (Huang et al., 2012; Rezsohazy et al., 2015).

1.4.2 The Role of Hox Genes in Hematopoiesis and Cancer

As noted in chapter 1.4.1, many Hox genes (22 of 39) were demonstrated to play crucial roles in normal and malignant hematopoiesis and solid tumors, which is of utmost relevance and thus mentioned here (Alharbi et al., 2013). Similar to their contribution in embryogenesis, Hox genes are expressed in HSCs and certain progenitors with distinct patterns, for instance Hox1-6 paralogs (anterior 3' position) are present in HSCs and early uncommitted progenitors ($CD34^+$ cells) and the posterior Hox genes are stepwise upregulated throughout commitment (Alharbi et al., 2013). Additionally, Hox clusters are related to certain lineages such as HoxA genes are mainly expressed in myeloid cells, HoxB genes in erythoid cells, HoxC genes in lymphoid cells, and HoxD is not expressed in hematopoietic progenitors (Alharbi et al., 2013). Gain of function studies showed that overexpression of most Hox genes results in enlargement of HSCs and progenitors and a differentiation block, e.g. HoxB6 overexpression leads to expansion of HSCs and myeloid progenitors and inhibits erythroid and lymphoid lineages (Alharbi et al., 2013). Some Hox proteins are crucial for maintaining stem cell status and regulate their proliferation such as HoxA9, which was additionally shown to be the most expressed Hox gene in stem cells and early progenitors and is gradually downregulated throughout differentiation (Alharbi et al., 2013; Pineault et al., 2002). Deletion of the complete HoxA cluster results in reduced proliferation of hematopoietic stem and progenitor cells, but has almost no influence on differentiation of these cells (Lebert-Ghali et al., 2016). By inducing overexpression of HoxA9 in $HoxA^{-/-}$ cells, Lebert-Ghali and colleagues were able to rescue the missing proliferation in part, underlining the importance of HoxA9 among the HoxA gene cluster (Lebert-Ghali et al., 2016). Moreover, HoxA9 overexpression in mice drives expansion of HSCs and myeloid progenitors, blocks pre-B-cell differentiation, and

leads to leukemia (Alharbi et al., 2013). Some proteins were found that regulate Hox expression in hematopoiesis including MLL (mixed lineage leukemia) and caudal-type Hox transcription factors (CDX1, CDX2, and CDX4) (Alharbi et al., 2013). Interestingly, Hox proteins were shown to upregulate nearby Hox genes, their own co-factors, and some even positively influence their own expression, e.g. HoxA9 enhances *HoxA7*, *HoxA10*, *Pbx3*, and *Meis1* expression (Alharbi et al., 2013).

The overexpression of many Hox proteins and in particular the presents of fusion-proteins between distinct Hox and other genes such as NUP98 play fundamental roles in the pathogenesis of acute leukemia, especially acute myeloid leukemia (AML) but also acute lymphoid leukemia (ALL) (Alharbi et al., 2013). Several Hox downstream target genes are partakers in cell proliferation and survival including self-renewal or anti-apoptosis, which can promote tumorigenesis. Upstream regulators of Hox genes such as MLL are involved in chromosome rearrangements that result in fusion proteins in leukemia and thus initiate aberrant Hox expression (Alharbi et al., 2013). As a result, differentiation is blocked and cell proliferation heightened. Members of CDX proteins, another family of Hox upstream regulators, namely CDX2 and CDX4 are also overexpressed in AML (Alharbi et al., 2013). A mutation of the NPM1 (nucleophosmin 1) protein was also demonstrated to enhance expression of several Hox proteins and co-factors in AML including HoxA4, HoxA6, HoxA7, HoxA9, HoxB9, and Meis1 (Mullighan et al., 2007). Apart from AML, both T and B cell precursor acute lymphoid leukemia (ALL) possess MLL and other translocations that result in overexpression of several Hox proteins (Ferrando et al., 2003). Interestingly, fusion proteins between Hox members and the T cell receptor (TCR) in T-ALL were identified, leading to elevated Hox expression levels (Alharbi et al., 2013). The dysregulation of Hox proteins in AML is associated with a poor prognosis and therefore used as a prognostic marker (Alharbi et al., 2013). HoxA9 was shown to be the number one gene associated with the worst prognosis, shortest survival, and most frequent relapse rate (Golub et al., 1999). Inversely, low HoxA9 expression was linked to the best therapy response and overall outcome (Andreeff et al., 2008). Apart from HoxA9, low expression of HoxA4 and Meis1 was also shown to correlate with a good prognosis of AML (Alharbi et al., 2013). Interestingly, the highest Hox expression levels were reported for AML types with Flt3 mutations (Alharbi et al., 2013). HoxA9/Meis1-induced leukemia is a murine model of aggressive AML, which displays high Flt3 expression similar to human AML. Latest findings

demonstrated no significant impact of Flt3 overexpression in this model on leukemic progression and suggests a rather passive role of Flt3 in AML (Staffas et al., 2016).

Apart from leukemia, aberrant Hox expression was reported for numerous solid tumors including breast, colon, prostate, thyroid, lung, brain (glioblastomas), bladder, ovarian, and kidney cancers as well as for melanomas (Bhatlekar et al., 2014; Shah and Sukumar, 2010). The most overexpressed Hox genes in solid tumors are HoxA9 and HoxB13 (Bhatlekar et al., 2014). Hox genes were shown to be partakers in both tumorigenesis and metastasis of many solid tumors, with mechanistic impact on spatiotemporal deregulation, gene dominance, and epigenetic deregulation (Shah and Sukumar, 2010). HoxA gene overexpression is often altered in breast and ovarian cancers, HoxB in colon cancer, HoxC in prostate and lung cancers, and HoxD in colon and breast cancers (Bhatlekar et al., 2014). Interestingly, different tumors that arise from the same embryogenic tissues exhibit similar aberrant Hox expression profiles (Bhatlekar et al., 2014). The use of overexpressed Hox proteins in many solid tumors as biomarkers and possible therapeutic targets is currently subject of intense research and some promising results have already been published (Bhatlekar et al., 2014; Shah and Sukumar, 2010).

1.4.3 FUNCTIONS OF HOXA9

The Hox protein A9 has been extensively studied in the context of hematopoiesis and leukemia because of its important roles in these settings. As a key regulator of hematopoiesis, it is involved in self-renewal of HSCs including cell proliferation and cell survival and is therefore important to maintain the stem cell status (Alharbi et al., 2013). Its central role among the HoxA cluster for proliferation of HSCs and precursor cells was shown by Lebert-Ghali et al. by overexpressing HoxA9 in a HoxA cluster knockout model leading to rescue of lost functions to a great extent (Lebert-Ghali et al., 2016). Interestingly, the contribution of HoxA genes in differentiation of hematopoietic cells was only marginal (Lebert-Ghali et al., 2016). HoxA9 has been implicated in the function of myeloid and lymphoid progenitors (Alharbi et al., 2013), with an emphasis on lymphoid-dependent B cell progenitors in concert with its downstream target *Flt3* (Alharbi et al., 2013; Dolence et al., 2014; Gwin et al., 2010; Gwin et al., 2013b).

The expression of HoxA9 is mediated by a large protein called MLL1 (mixed lineage leukemia 1) through its histone methyltransferase activity along the HoxA9 locus, leading to histone H3 lysine 4 trimethylation (H3K4me3) in concert with the co-factors

Menin and LEDGF (Collins and Hess, 2016; Gan et al., 2010). Further involvement of the histone acetyltransferase MOF (males absent on the first) in regulating HoxA9 expression has been reported (Collins and Hess, 2016; Mishra et al., 2014). Several genetic alterations in approximately 50 % of AML and some subsets of ALL result in aberrant upstream regulation of HoxA9 including MLL1 translocations, NUP98-fusion proteins, CDX deregulation, or NPM1 mutations (Collins and Hess, 2016).

Transcriptional downstream targets of HoxA9 were identified by several studies in different cell settings, both in human and murine hematopoietic tissues, which are collectively depicted in ***TABLE 1.4***. HoxA9 controls expression of its target genes through binding at cis-regulatory elements together with co-factors and cell type-dependent general factors/collaborators (see also section 1.4.1) (Collins and Hess, 2016). As mentioned in section 1.4.2, HoxA9 regulates nearby Hox genes such as *HoxA7* and *HoxA10* and its co-factors *Pbx3* and *Meis1* (Faber et al., 2009). *Meis1* was recently shown to be additionally controlled by HoxA9 through regulating the Meis1 regulators *creb1* and *pknox1* (Hu et al., 2009). As part of the fusion protein NUP98-HoxA9, HoxA9 was even shown to positively regulate its own activation (Takeda et al., 2006). The target gene *Pim1* promotes proliferation via *c-Myb*, which in turn was also shown to be directly regulated by HoxA9 in concert with its co-factor Meis1 (Hess et al., 2006). A novel study confirms upregulation of *c-Myb* through HoxA9, Meis1, and PU.1 in murine myeloid progenitors via distal regulation (Zhang et al., 2016). Interestingly, c-Myb, which also functions as transcription factor, was demonstrated to be an important developmental regulator of monocyte-derived MΦs but not monocyte-independent MΦs recently (Italiani and Boraschi, 2014). *Pim1* further supports anti-apoptotic effects by inhibiting the BAD protein (Hu et al., 2007). A whole bunch of genes involved in proliferation that are positively regulated by HoxA9 were found by Huang et al. in hematopoietic cells namely *Flt3, Foxp1, Kit, Gfi1, Lvk, Myb, Lmo, Camk2d, Cdk6, Etv6, and Erg* (Huang et al., 2012). As noted in section 1.3.1.1, the receptor tyrosine kinase Flt3 is also important for the development and maintenance of DCs and was shown to be regulated by HoxA9 in lymphoid progenitors (Gwin et al., 2010; Gwin et al., 2013b; Schmid et al., 2010). Furthermore, high expression levels of Flt3 and a Flt3 mutation were linked to a poor prognosis in AML and studies have shown promising results combining Flt3 inhibitors and standard therapies for AML (Konig and Levis, 2015). HoxA9 further downregulates genes responsible for differentiation and inflammation in hematopoietic progenitors including *Runx1, Ifngr1, Csf2rb, Ccl4, Ccl3, Ifit1, Tlr4, Cd28,* and *Cd33* (Huang et al.,

2012). Important additional target genes are the oncogene Id2, which is enhanced by HoxA9 and is also involved in the fate of cDCs and inhibits pDC differentiation (see section 1.3.1.1 and 1.3.1.2 for details), and the apoptotic factor BIM, that is downregulated by HoxA9 (Nagel et al., 2010). Besides auto-regulatory activity and the upregulation of adjacent Hox proteins as well as co-factors, the fusion protein NUP98-HoxA9 enhances the expression of transcription factors and receptor tyrosine kinases that have important functions in leukemogenesis such as *Evi1, Mef2c, Kit,* and again *Flt3* (Takeda et al., 2006). The HoxA9-mediated transcriptional regulation of cell cycle regulators in concert with the transcription factor CCAAT/enhancer-binding protein alpha (C/EBPα) and the methyltransferase G9a (Ehmt2) was demonstrated in leukemogenesis models (Collins et al., 2014; Lehnertz et al., 2014). The chromatin regulator CBP/p300 (Crebbp/Ep300) histone acetyltransferase (HAT) was shown to be a transcriptional target of HoxA9 (Huang et al., 2012). The numbers of genomic binding sites and regulated genes of HoxA9 in different primary cells and cell lines were ranging between 696 – 6535 and 72 – 7132, respectively, with predicted other transcription factors C/EBPα, CREB, MYB, CAUDAL ETS, MYC, and STAT as additional binding partners (general factors) (Collins et al., 2014; Dorsam et al., 2004; Ferrell et al., 2005; Huang et al., 2012; Rezsohazy et al., 2015; Sun et al., 2013b).

In addition to its function as transcription factor, HoxA9 was shown to positively influence translation of distinct mRNAs through direct interaction with the translation initiation factor eIF4E by using specific binding sites (Topisirovic et al., 2005). The eIF4E-dependent nuclear export of cyclin D1 and ornithine decarboxylase (ODC) mRNAs as well as increased ODC translation efficiency in the cytosol were facilitated by HoxA9 (Topisirovic et al., 2005). Moreover, HoxA9 forms complexes with the ubiquitin ligase core component Roc1-Ddb1-Cul4a and functions as an E3 ligase activator that mediates ubiquitination and thus degradation of the geminin protein (Ohno et al., 2013). Geminin inhibits DNA replication and is normally degraded during the mitotic phase of the cell cycle, therefore, by enhancing degradation of geminin, HoxA9 induces DNA replication important for cell proliferation (Ohno et al., 2013).

TABLE 1.4 *TRANSCRIPTIONAL TARGET GENES OF HOXA9*

HOXA9 PROTEIN (SPECIES)	ACTIVATION	REPRESSION
HoxA9 (human/mouse)	*Pim1, ID2, CYBB, HoxA7, HoxA10, Pbx3, Meis1, Flt3, Creb1, Pknox1, Camk2d, Cdk6, Erg, Foxp1, Gfi1, Kit, Lck, Lmo2, Myb, Sox4, Crebbp, Igf1, mir-21, mir-196b*	*BIM, Itfi1, Tlr4, Ccl3, Ccl4, Csf2rb, Ifngr1, Runx1, Cd28, Cd33, Ink4a*
HoxA9-Meis1 (mouse)	*c-Myb*	
NUP98-HoxA9 (human)	*HoxA7, HoxA9, Meis1, Pbx3, EVI1, MEF2C, Flt3, Kit*	

Shown are currently known downstream targets of transcriptional activation or repression of HoxA9, HoxA9 in concert with the co-factor Meis1, and the fusion protein NUP98-HoxA9 found in leukemia (Alharbi et al., 2013; Bei et al., 2005; Collins et al., 2014; Collins and Hess, 2016; Faber et al., 2009; Gwin et al., 2010; Hess et al., 2006; Hu et al., 2009; Hu et al., 2007; Huang et al., 2012; Morgan, 2006; Nagel et al., 2010; Steger et al., 2015; Takeda et al., 2006; Velu et al., 2014).

1.5 PURPOSE OF THIS WORK

Several reasons encouraged me to investigate the role of the homeodomain-containing transcription factor HoxA9 in the context of TLR biology and development of DCs and MΦs.

Firstly, unpublished data from the former group of Prof. Bauer in the Institute for Medical Microbiology and Hygiene in Munich revealed strikingly high expression levels of *hoxa9* mRNA in gene expression profiles of sorted murine pDCs that were activated by TLR9 ligands. Furthermore, Philipp Kurbel from our group was able to show an upregulation of *hoxa9* in qPCR experiments upon stimulation of Flt3L-induced DCs and splenocytes with the TLR9 agonist ODN 2216 up to 20-fold. The fact that TLR9-driven innate immune responses provided by murine pDCs can be triggered by ODNs without CpG-motifs in contrast to other immune cells (Bauer, 2013; Haas et al., 2008; Wagner, 2008), raises the question whether pDCs possess a unique mechanism. One hypothesis is that TLR9 is supported by a co-factor or even several co-factors only present in pDCs, which co-bind or promote binding of DNA sequences free of CpG-motifs. Increased mRNA expression levels in TLR9-activated mouse pDCs and the DNA-binding properties of HoxA9, as it is a well-known transcription factor, together supported the hypothesis that HoxA9 could acts as co-factor for TLR9 or is at least linked to TLR9 biology in pDCs. Furthermore, if true, other TLRs (intracellular TLRs in particular) or PRRs might be influenced by HoxA9 as well.

Secondly, Hox genes, and above all HoxA9, are known to have essential functions in the maintenance of HSCs and differentiation of hematopoietic precursor cells in a complex way (see section 1.4.2 for details). However, they were shown to be stepwise downregulated in parallel to ongoing differentiation and are generally believed to be silenced in mature differentiated hematopoietic cells (Alharbi et al., 2013). The observation of high HoxA9 mRNA expression levels in TLR9-activated mature murine pDCs is therefore surprising und suggests a role for HoxA9 also in differentiated cells. Regarding the involvement of Hox genes in embryogenesis, the assumption that these genes are completely downregulated in adult cells was proven wrong a couple of years ago (Morgan, 2006). Hence, Hox genes might as well have functions in adult differentiated hematopoietic cells. Following this idea, upregulation of HoxA9 in certain scenarios such as activation of TLRs in matured pDCs or other immune cells might take place.

Besides, it seems natural that HoxA9 as an important player in hematopoietic processes including self-renewal of HSCs and different functions in myeloid und lymphoid progenitors (Alharbi et al., 2013), might be directly involved in differentiation and development of precursors of innate immune cells such as DCs or MΦs. To date, participation in B cell development was shown with a link to the cytokine receptor Flt3 as a direct downstream target of HoxA9 (Gwin et al., 2010; Gwin et al., 2013b), as already mentioned in detail in the latter section as well as section 1.3.1.1. However, Flt3 and its ligand Flt3L play also important roles in DC development (Schmid et al., 2010), which points towards a potential involvement of HoxA9 in the maturation of DC subsets. Id2 was demonstrated by Reizis and colleagues as the main transcription factor responsible for differentiation into cDCs (Reizis et al., 2011), which inhibits its counterpart for pDCs called E2-2 and vice versa (see section 1.3.1.2 for details). HoxA9 was shown to activate expression of Id2 (Huang et al., 2012), hence, this represents another link to DC development. It is believed that mature pDCs in peripheral tissues are long-living cells and can survive for many years (Reizis et al., 2011), though there is still poor knowledge in this field. It seems likely that HoxA9 could promote self-renewal of peripheral differentiated pDCs similarly to HSCs in the BM. Moreover, the transcription factor c-Myb, which was recently shown to be a developmental regulator of monocyte-derived MΦs (Italiani and Boraschi, 2014), is another direct downstream target of HoxA9 together with its co-factor Meis1 or indirectly via Pim1 (Huang et al., 2012). These various connections to development/differentiation of DCs and MΦs encouraged me to investigate BM cells *ex vivo* as well as different cell settings *in vitro*.

Using HoxA9 knockout mice, which were originally generated by Mario Capecchi, who was one of the pioneers of knockout animals and won the Nobel Prize for Physiology or Medicine for this achievement 2007, I tried to find out whether TLR-mediated innate immune responses were different to wild type in various cell settings. These included total BM cells, splenocytes, *in vitro* generated DCs as well as MΦs, and *ex vivo* sorted BM-derived DCs. My focus was initially on BM cells as well as pDCs and TLR9-related immunity. However, after several experiments it was clear that more TLRs as well as cell types could be affected by the knockout, which led to further approaches.

The central purpose of this work was to investigate the influence of the transcription factor HoxA9 on innate immune reactions that are initiated by TLRs with an emphasis on nucleic-acid sensing TLRs, in particular TLR7/9-related cytokine responses in pDCs. The generated data resulted in extension of the used cell settings and

TLR stimuli, taking a broader range of potential impact of the used HoxA9 knockout model into account. Understanding the complex mechanistic coherences of innate immune cells in various physiologic as well as pathologic conditions provides a basis for possible novel strategies to fight diseases like infections, allergies, autoimmunity, and cancer in the future.

2. MATERIALS AND METHODS

2.1 MATERIALS

2.1.1 DEVICES AND EQUIPMENT

***TABLE 2.1** DEVICES AND EQUIPMENT*

DEVICE/EQUIPMENT	MANUFACTURER
Agarose gel chamber	OWL, Weilheim
Biofuge 15	Heraeus, Hanau
CASY®-1 Cell counter	Schärfe System, Reutlingen
Diavert microscope	Leitz, Bielefeld
Electrophoresis power supply	EC 150 – E-C Apparatus Cooperation American Laboratory Trading, USA
Emax microplate spectrophotometer	Molecular Devices, Ismaning
Flow cytometer FACSCalibur™	Becton Dickinson, Heidelberg
Flow cytometer/sorter FACSAria™ III	Becton Dickinson, Heidelberg
Gel photo-imaging system	Mitsubishi, Ratingen
Gel UV-imaging system	Fröbel, Lindau
Hera Cell 240 Incubator	Heraeus, Hanau
Hettich Rotanta Centrifuge	Hettich Lab Technology, Tuttlingen
Manual pipetting aid (Pipetus®)	Hirschmann, Eberstadt
Micropipettes (10µl; 100µl; 1000µl)	Eppendorf, Hamburg
Multifuge 1 L-R	Heraeus, Hanau
Skanwasher 400 Microplate Washer	Molecular Devices, Ismaning
Thermocycler Eppendorf	Eppendorf, Hamburg
Vortexer Reax 2000	Heidolph, Schwabach

Used devices and equipment are listed with name and location of manufacturer.

2.1.2 CHEMICALS

***TABLE 2.2** CHEMICALS*

CHEMICAL	MANUFACTURER
Ethanol	Roth, Karlsruhe
Ethidium bromide	Roth, Karlsruhe
Ethylenediaminetetraacetate (EDTA)	Roth, Karlsruhe
H_2O_2	Roth, Karlsruhe
H_2SO_4	Roth, Karlsruhe
KCL	Roth, Karlsruhe
KH_2PO_4	Roth, Karlsruhe
Isopropanol	Roth, Karlsruhe
NaCl	Roth, Karlsruhe
Na_2HPO_4 x $2H_20$	Roth, Karlsruhe
PBS ^{def} without Ca^{2+}, Mg^{2+}	Biochrom AG, Berlin
Sodium azide (NaN_3)	Roth, Karlsruhe
Tween® 20	Roth, Karlsruhe
Ultra pure water	Biochrom AG, Berlin
β-Mercaptoethanol 50 mM	Gibco, Karlsruhe

Used chemicals listed with name and location of manufacturer.

2.1.3 MEDIA AND SUPPLEMENTED MEDIA

***TABLE 2.3** MEDIA*

MEDIUM	MANUFACTURER
OptiMEM (with L-glutamine)	Gibco, Karlsruhe
RPMI 1640 (with Hepes)	PAA, Cölbe

Used media listed with name and location of manufacturer.

***TABLE 2.4** SUPPLEMENTED MEDIA*

SUPPLEMENTED MEDIUM	SUPPLEMENTS
OptiMEM$^{Suppl.}$	500 ml OptiMEM (with L-Glutamine) 1 % FCS 100 U/ml Penicillin 100 µg/ml Streptomycin 0.05 mM β-Mercaptoethanol
RPMI$^{Suppl.}$	500 ml RPMI 1640 (with Hepes) 10 % FCS 2 mM L-Glutamin 100 U/ml Penicillin 100 µg/ml Streptomycin 0.05 mM β-Mercaptoethanol
Spleen DC isolation medium	500 ml RPMI 1640 (with Hepes) 1 mg/ml Collagenase D 50 µg/ml DNase

Used supplemented media listed with supplements.

2.1.4 MOLECULAR BIOLOGICAL REAGENTS

***TABLE 2.5** MOLECULAR BIOLOGICAL REAGENTS*

REAGENT	MANUFACTURER
6x LoadingDye	Fermentas, St. Leon Rot
Agarose (Electrophoresis grade)	Invitrogen, Karlsruhe
Bovine serum albumin (BSA)	Roth, Karlsruhe
Collagenase D	Roche, Mannheim
DNase	Roche, Mannheim
DOTAP Liposomal Transfection Reagent	Roth, Karlsruhe
Dulbecco's PBS	PAA, Cölbe
Fetal bovine serum (FBS)	Gibco, Karlsruhe
Flt3L	Cell culture supernatant, BMFZ Marburg
Generuler 1 kb DNA Ladder Plus	Fermentas, St. Leon Rot

Generuler 100 bp DNA Ladder Plus	Fermentas, St. Leon Rot
GM-CSF	PeproTech, Rocky Hill, USA
GM-CSF	Cell culture supernatant, BMFZ Marburg
Lipofectamine 2000 Reagent	Invitrogen, Karlsruhe
L-glutamine 200 mM	PAA, Cölbe
LSM 1077 Separation Medium (Ficoll)	PAA, Cölbe
M-CSF	PeproTech, Rocky Hill, USA
o-Phenyl-Diamin (OPD) 20 mg tablet	Sigma-Aldrich, München
Penicillin/Streptamycin	PAA, Cölbe
Proteinase K	Fermentas, St. Leon Rot
Recombinant murine IFN-α (Standard)	HyCult Biotech, Uden, NL
Recombinant murine IL-6 (Standard)	R&D Systems, Wiesbaden
Streptavidin-POD	Roche, Mannheim
Taq PCR Master Mix Kit	Qiagen, Hilden

Used molecular biological reagents listed with name and location of manufacturer.

2.1.5 BUFFERS AND SOLUTIONS

***TABLE 2.6** BUFFERS AND SOLUTIONS*

BUFFER/SOLUTION	COMPONENTS
ELISA blocking buffer 1%	10 g BSA 0.5 ml Tween® 20 Ad 1 L PBS def.
ELISA substrate buffer	7.3 g $C_6H_8O_7$ 11,87 g Na_2HPO_4 x $2H_2O$ Ad 1 L ddH_20
ELISA washing buffer	500 ml 10x PBS 2.5 ml Tween® 20 Ad 5 L ddH_2O

FACS buffer	PBS def. 2 % FCS 0.01 % NaN_3 2 mM EDTA
FACS sorting buffer	PBS def. 2 % FCS 2 mM EDTA
PBS 10x	10 g KCl 10 g KH_2PO_4 400 g NaCl 57.5 g Na_2HPO_4 x $2H_2O$ Ad 5 L ddH_20
TAE DNA-gel running buffer 50x	242 g Tris-Base 57.1 ml concentrated CH_3COOH 100 ml 0.5 M EDTA (pH 8)
Tail lysing buffer	10 mM Tris HCL pH 8.0 25 mM EDTA 100 mM NaCl 0.5 % SDS (10 %)

Used buffers and solutions listed with required components.

2.1.6 MOUSE STRAINS

***TABLE 2.7** MOUSE STRAINS*

MOUSE STRAIN	SOURCE
C57/Bl6 (wild type mice)	Animal facility BMFZ Marburg
HoxA9 knockout mice on C57/Bl6 background	Prof. Dr. Stefanie Dimmeler, Institute of Cardiovascular Regeneration, Goethe-University Frankfurt am Main

Used mouse strains and their source.

2.1.7 ANTIBODIES

***TABLE 2.8** ELISA ANTIBODIES*

ELISA ANTIBODY	MANUFACTURER
Goat IgG biotinylated anti-mouse IL-6 PAb (Detection-Ab)	R&D Systems, Wiesbaden
Goat POD-conjugated anti-rabbit IgG Mab (3.Ab)	Jackson ImmunoResearch, Suffolk, UK
Rabbit anti-mouse IFN-α PAb (Detection-Ab)	PBL, Piscataway, NJ, USA
Rat IgG1 anti-mouse IFN-α MAb (Capture-Ab)	PBL, Piscataway, NJ, USA
Rat IgG1 anti-mouse IL-6 MAb (Capture-Ab)	R&D Systems, Wiesbaden

Used ELISA antibodies listed with name and location of manufacturer.

***TABLE 2.9** FACS ANTIBODIES*

FACS ANTIBODY	MANUFACTURER
ChromePure Rat IgG (Fc blocking)	Jackson ImmunoResearch, Suffolk, UK
Rat anti-mouse BST2-FITC	eBioscience, San Diego, USA
Rat anti-mouse B220-APC	BD Pharmingen, Heidelberg
Rat anti-mouse B220-FITC	BD Pharmingen, Heidelberg
Rat anti-mouse CD11b-APC	eBioscience, San Diego, USA
Rat anti-mouse CD11b-FITC	eBioscience, San Diego, USA
Rat anti-mouse CD11c-APC	eBioscience, San Diego, USA
Rat anti-mouse CD11c-PE	eBioscience, San Diego, USA
Rat anti-mouse Flt3-PE	BD Pharmingen, Heidelberg
Rat anti-mouse F4/80-FITC	eBioscience, San Diego, USA
Rat anti-mouse Ly6C-PE	Miltenyi Biotec, Bergisch Gladbach

Rat anti-mouse MHC-I-PE	eBioscience, San Diego, USA
Rat anti-mouse MHC-II-PE	eBioscience, San Diego, USA
Rat anti-mouse SiglecH-FITC	eBioscience, San Diego, USA
TO-PRO®-3 iodide	Invitrogen, Karlsruhe

Used FACS antibodies listed with name and location of manufacturer.

2.1.8 STIMULI

***TABLE 2.10** STIMULI*

STIMULUS	SEQUENCE 5'- 3' / DESCRIPTION	MANUFACTURER
LPS	Lipopolysaccharide from *Escherichia coli*	DIFCO, Detroit, USA
ODN AP-1 PD	GCTTGATGACTCAGCCGGAA	TIB MOLBIOL, Berlin
ODN 1668 PD	TCCATGACGTTCCTGATGCT	TIB MOLBIOL, Berlin
ODN 1720 PD	TCCATGAGCTTCCTGATGCT	TIB MOLBIOL, Berlin
ODN 2216 PS	GsGsGGGACGATCGTCGsGsGsGsGsG	TIB MOLBIOL, Berlin
POLY I:C	Polyinosinic-polycytidylic acid	InvivoGen, San Diego USA
		GE Healthcare
RNA 40 PD	GCCCGUCUGUUGUGUGACUC	IBA Biologics, Göttingen
R848	Imidazoquinoline compound Resiquimod - selective synthetic ligand for murine TLR7 and human TLR7/8	InvivoGen, San Diego USA
Pam-3-Cys	Pam3CysSerLys4 – synthetic tripalmitoylated lipopeptide which activates TLR2	InvivoGen, San Diego USA

Used stimuli listed with sequence or description and name as well as location of manufacturer. 'G' – guanine; 'C' – cytosine; 'A' – adenine; 'T' – thymine; 'U' – uracil; 's' – phosphorothioate (PS) linkage.

2.1.9 PRIMER

***TABLE 2.11** PRIMER*

PRIMER	SEQUENCE 5'- 3'	MANUFACTURER
hoxa9-fp	CGCTGGAACTGGAGAAGGAGTTTCTG	Metabion, Martinsried
hoxa9-rp	ATCCTGCGGTTCTGGAACCAGATC	Metabion, Martinsried
MC1neo-rp	TCTATCGCCTTCTTGACGAGTTC	Metabion, Martinsried

Used primer listed with sequence and name and location of manufacturer. 'G' – guanine; 'C' – cytosine; 'A' – adenine; 'T' – thymine.

2.1.10 CONSUMPTION ITEMS

***TABLE 2.12** CONSUMPTION ITEMS*

ITEMS	MANUFACTURER
24 G cannula	BD Microlance, Heidelberg
96-well ELISA MaxiSorp microplate	NUNC, Roskilde, Denmark
96-well flat bottom plate	Greiner, Frickenhausen
96-well round bottom plate	Greiner, Frickenhausen
Cell culture dishes BD 10 cm	BD Falcon, Heidelberg
Cell culture dishes BD Primaria 10 cm	BD Falcon, Heidelberg
Cell culture dishes Nunclon surface 10 cm	NUNC, Roskilde, Denmark
Cell strainer 70 µm Nylon	BD Falcon, Heidelberg
	Fisher Scientific, Pittsburgh, USA
FACS tubes sterile 5 ml snap cap (12 x 75 mm)	BD Falcon, Heidelberg
FACS tubes 1.3 ml (8.5 x 44 mm)	Greiner, Frickenhausen
Petri dishes 10cm	Greiner, Frickenhausen
Pipette barrier tips (10 µl; 100 µl; 1000 µl)	Sorenson, Salt Lake City, USA

Pipette tips (10 µl; 100 µl; 1000µl)	Greiner, Frickenhausen
Pipette tips for multipette® (25 µl; 50 µl; 250 µl)	Eppendorf, Hamburg
Plastic pipettes (5 ml; 10 ml; 25 ml)	Greiner, Frickenhausen
Reaction tubes (0.5 ml; 1.5 ml; 2 ml)	Sarstedt, Nümbrecht
Reaction tubes (15 ml; 50 ml)	Greiner, Frickenhausen
Syringe 10 ml	B. Braun, Melsungen
Topseal A for 96-well microplates	PerkinElmer, Zaventem, Belgium

Used consumption items listed with name and location of manufacturer.

2.1.11 SOFTWARE

***TABLE 2.13** SOFTWARE*

SOFTWARE	MANUFACTURER
BD FACSDiva™ 7.0 (for Windows)	BD Bioscience, San Jose, USA
CellQuest Pro, version 5.2.1 (for Macintosh)	BD Bioscience, San Jose, USA
EndNote Web	Thomson Reuters, Carlsbad, USA
FlowJo, version 10.0.7 (for Windows)	Treestar, San Carlos, USA
Microsoft Office 2007, 2010, and 2013	Microsoft, Redmond, USA
GraphPad Prism 6.05	GraphPad Software, La Jolla, USA
SigmaPlot 10.0	Scientific Solutions, Lausanne, Swiss
SoftMax Pro V5	Molecular Devices, Ismaning

Used software listed with name and location of manufacturer.

2.2 METHODS

2.2.1 HOXA9 KNOCKOUT MICE

HoxA9 knockout mice were obtained from Prof. Dr. Stefanie Dimmeler, Institute of Cardiovascular Regeneration, Goethe-University Frankfurt am Main. A targeted disruption of the HoxA9 gene in murine embryonic stem cells was introduced by homologous recombination by Dr. Cynthia Peterson and Dr. Mario Capecchi (Chen and Capecchi, 1997). The MCI *neo* cassette replaced a 1.8 kb *Bg1*/II/*Eco*RI fragment of the HoxA9 gene, containing most of the homeobox and 3' noncoding sequences (Lawrence et al., 1997). Cells of the resulting targeted cell line 3C-3 were injected into C57/Bl6 blastocysts. Chimeric males were crossed with C57/Bl6 females to generate heterozygous offspring. HoxA9$^{-/-}$ and wild type littermates were generated by crossing heterozygotes. Both HoxA9$^{+/-}$ and HoxA9$^{-/-}$ mice appear healthy, are fertile, and weigh the same as their wild type littermates. Furthermore, mice bearing the mutant gene do not appear to be predisposed to infections or develop leukemia although they show statistically significant reductions in both peripheral blood lymphocytes and granulocytes (Lawrence et al., 1997). In addition, HoxA9$^{-/-}$ mice display a slight pancytopenia and hypocellularity in the spleen and thymus (Lawrence et al., 1997).

Procedure:

To distinguish mice bearing the wild type, heterozygous, or the mutant HoxA9 alleles, genomic DNA was isolated from tail clips of weanlings. The tail clips were transferred into a 1.5 ml reaction tube. 495 µl tail lysing buffer and 5 µl Proteinase K (final concentration: 0.1 mg/ml) were added and incubated at 56°C under constant shaking with 300 rpm overnight. After centrifugation at 13000 rpm for 15 min at room temperature (RT), the supernatant of the lysate was transferred into a new reaction tube containing 450 µl of isopropanol for precipitation of genomic DNA. The tube was inverted until the precipitated genomic DNA was visible and caught by a toothpick for transfer into a new reaction tube, which was filled with 300 µl of ultra pure water. After incubation at RT under constant shaking with 300 rpm for 3 h, the genomic DNA was solved and ready for PCR or storage at -20°C until further use.

2.2.2 GENOTYPING OF HOXA9 MICE BY POLYMERASE CHAIN REACTION (PCR)

The PCR allows amplification of small amounts of DNA *in vitro*. It was established in 1983 by Kary Mullis. The number of PCR publications increased exponentially since the first PCR publication in 1985 by Saiki and colleagues (Saiki et al., 1985). The main principle of the PCR is based on denaturation of dsDNA at 92 – 95°C and annealing of specific oligonucleotides (primers), after decreasing the temperature to 50 – 60°C, at the 5'- and 3' end of each side of the DNA sequence to be amplified. These oligonucleotides are elongated by a thermostable DNA polymerase at 68 – 75°C in the presence of deoxynucleotide triphosphates (dNTPs). Elongation of the template takes place until the reaction is stopped or the DNA polymerase 'drops down'. By increasing the temperature to 95°C, the DNA template denatures again and a new cycle begins. As a result, the real length of the DNA template is amplified for the first time. After 25 PCR cycles approximately 3.2 x 10^7 duplicates of the template are synthesized. Time and temperature conditions for each step of the PCR depend on the used DNA polymerase, the DNA template, and the primers. In addition, a buffer containing MG^{2+} as co-factor for the DNA polymerase is necessary.

For genotypic analysis of HoxA9 mice, a PCR with a *Taq* polymerase and a three-primer system was applied. The primers hoxa9-fp and hoxa9-rp were used for amplification of the WT allele and resulted in a 123 bp band, whereas amplification of the targeted allele with primers hoxa9-fp and MC1neo-rp resulted in a 200 bp band (***FIGURE 2.1***). Mice showing both bands were heterozygous.

Procedure:

A total reaction volume of 30 µl was used, containing 15 µl *Taq* PCR MasterMix, 10 µl ultra pure water, 2 µl of genomic DNA, and 1 µl of each primer with a molarity of 100 pmol (final concentration: 0.3 pmol). ***FIGURE 2.1 B*** shows a HoxA9 screening PCR.

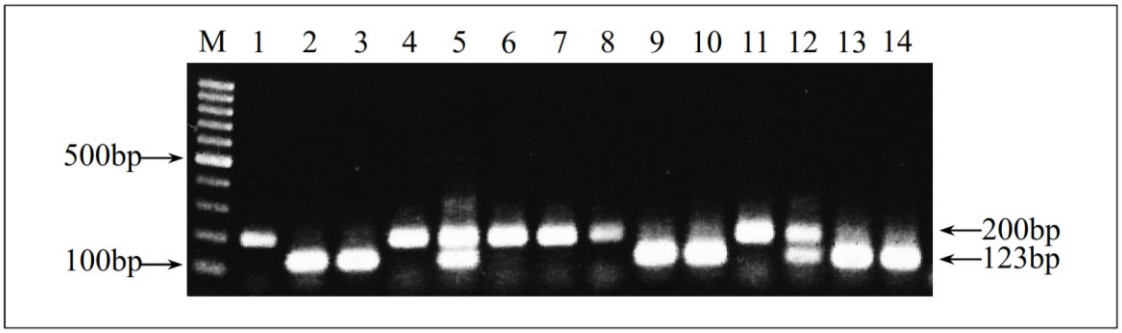

FIGURE 2.1 *GENOTYPING OF HOXA9 KO AND WT MICE BY PCR*
Shown is the HoxA9 screening PCR. Amplification of the wild type allele with primers hoxa9-fp and hoxa9-rp results in the lower 123 bp band, whereas amplification of the targeted allele with primers hoxa9-fp and MC1neo-rp results in the upper 200 bp band. Mice showing both bands are heterozygous. M – 100 bp ladder; Lane 1 – positive control targeted allele; Lane2 – positive control wild type allele; Lanes 3, 9, 10, 13, and 14 - wild type animals; Lanes 4, 6, 7, 8, and 11 – knockout animals; Lanes 5 and 12 - heterozygous animals.

The following PCR program was performed on an Eppendorf Thermocycler:

95°C	5 min	
95°C	40 sec	35 cycles
57°C	35 sec	
72°C	40 sec	
72 °C	5 min	
Hold 4°C		

The visualization of the amplified DNA fragments was carried out by gel electrophoresis. The negatively charged DNA fragments moved through an agarose matrix in an electric field to the positively charged anode. The separation of the fragments depended on the length. Thus, smaller fragments moved faster than longer ones. The concentration of the agarose gel was 1.6 %. Accordingly, 1.6 g of agarose was boiled up in 100 ml of 1 x TAE buffer and filled in a gel slide. After polymerization of the agarose gel, 15 µl of PCR product dissolved in DNA loading dye was pipetted into the small pockets of the gel. After separation by electrophoresis, the gel was stained with the DNA intercalating dye ethidiumbromide (EtBr) (final concentration: 1 µg/ml) and visualized by ultraviolet light.

2.2.3 ISOLATION OF MURINE BONE MARROW (BM) CELLS AND SPLENOCYTES

Mice were killed by cervical dislocation at the age of 6 to 27 weeks. After disinfection with 70 % ethanol and fixation on a preparation board, both femur and tibia were

dissected. The bones were stored in sterile petri dishes on ice. The spleen was isolated and stored in 3 ml of spleen DC isolation medium in a 15 ml tube on ice. A piece of ear of each mouse was cut off and transferred into a 1.5 ml reaction tube and stored at -20°C for DNA isolation and PCR genotyping. The following steps were carried out under a sterile bench of security class 2. The bones were cleaned precisely from all muscles. Shortly after cutting off the epiphysis on each side of the bone, the BM was flushed out of the diaphysis using a sterile syringe (filled with 10 ml OptiMEM$^{Suppl.}$ or RPMI$^{Suppl.}$) and a 24 G cannula. This step was repeated until the bones were completely empty. The obtained BM pieces were pipetted softly up and down (using a 10 ml pipette) in order to achieve a single-cell suspension. The suspended cells were transferred into a 50 ml tube through a 70 µm cell strainer (to separate them from bone pieces) and centrifuged at 1300 rpm for 7 min at 4°C. The supernatant was discarded and the cell pellet was resuspended in 5 ml of red blood cell lysing buffer. After an incubation time of 7 min at RT, the lysis of the erythrocytes was stopped by adding 5 ml OptiMEM$^{Suppl.}$ or RPMI$^{Suppl.}$. Again, the cell suspension was centrifuged at 1300 rpm for 7 min at 4°C and subsequently the supernatant was discarded and the cell pellet was resuspended in 5 ml OptiMEM$^{Suppl.}$ or RPMI$^{Suppl.}$. Now the number of cells was determined by using the CASY®-1 cell counter.

The spleen was cut into small pieces and incubated in spleen isolation medium at 37°C for 45 – 50 min. Sterile EDTA (final concentration: 10 mM) was added and the spleen was mashed through a 70 µm cell strainer using a plunger of a 5 ml syringe. After centrifugation at 1300 rpm for 7 min at 4°C, the supernatant was discarded and the cell pellet was resuspended in 5 ml red blood cell lysing buffer and incubated for 10 min. The lysis was stopped by adding 5 ml of RPMI$^{Suppl.}$. Again, the cell suspension was centrifuged at 1300 rpm for 7 min at 4°C, the supernatant discarded, and the cell pellet was resuspended in 5 ml RPMI$^{Suppl.}$ followed by filtration through a 70 µm cell strainer. By stacking carefully 5 ml of the cell suspension on top of 15 ml ficoll and centrifugation at 2000 rpm for 30 min at RT (brake switched off), the lymphocytes, monocytes, and DCs in the white phase were separated from dead cells, remaining erythrocytes (passing through the ficoll phase), and thrombocytes (stay in the supernatant). The cells in the white interphase between the ficoll phase and the medium were withdrawn carefully and washed twice with 10 – 15 ml RPMI$^{Suppl.}$ followed by centrifugation at 1300 rpm for 7 min at 4°C. Finally, the cell pellet was resuspended in 5 ml RPMI$^{Suppl.}$ and the cell number was determined by the CASY®-1 cell counter.

Isolated BM cells were used for FACS analysis, TLR stimulation experiments, the generation of pDCs and cDCs in Flt3L and GM-CSF supplemented cultures, respectively, and the generation of MΦs in M-CSF supplemented cultures. Isolated splenocytes were used for FACS analysis and TLR stimulation experiments. Moreover, pDCs and cDCs were sorted *ex vivo* from BM cells using a FACSAria™ III flow sorter (see section 2.2.9).

2.2.4 GENERATION OF DCS FROM FLT3L SUPPLEMENTED BM CULTURES

The growth factor fms-like tyrosine kinase 3 ligand (Flt3L) is used for the generation of pDCs as well as cDCs from HSCs *in vitro* (Brasel et al., 2000).

Procedure:

15 x 10^6 freshly isolated BM cells (see chapter 2.2.3) were seeded at a density of 1.5 x 10^6 cells/ml in a 10 cm cell culture dish (BD Primaria). Stefanie Seibert from our working group showed that OptiMEM$^{compl.}$ is the best supplemented medium to achieve high numbers of pDCs in her bachelor thesis. Flt3L (supernatant of a chinese hamster ovary (CHO) transgenic cell line culture) was added to each culture at a ratio of 1:250 (depending on the batch). Flt3L supplemented BM cultures were incubated at 37°C, 5 % CO_2, and 100 % air humidity and cultured for 8 days. The differentiated cells were harvested by aspirating the medium and gently washing the bottom of the 10 cm cell culture dish with a 10 ml pipette. The single-cell suspension was transferred into a 50 ml tube and centrifuged at 1300 rpm for 7 min at 4°C. The cell pellet was resuspended in 5 ml OptiMEM$^{Suppl.}$ and the cells were counted by the CASY®-1 cell counter. The quality, viability, and differentiation into pDCs and cDCs was checked by FACS analysis (see ***FIGURE 2.2***). The viability of the cells after 8 days in culture was 35 – 50 %. Approximately 35 – 80 % of the viable cells differentiated into pDCs and 15 – 35 % into cDCs. PDCs show a B220$^+$ CD11c$^+$ cell surface

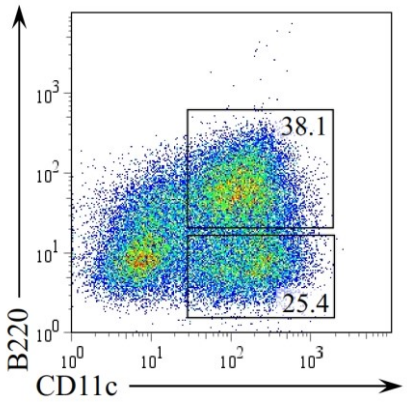

FIGURE 2.2
FACS OF FLT3L CULTURE
FACS analysis of Flt3L supplemented wild type bone marrow culture after 8 days. Viable (ToPro3 iodide negative gated) B220$^+$ CD11c$^+$ cells are pDCs, whereas B220$^-$ CD11c$^+$ cells represent cDCs.

phenotype, whereas cDCs do not express the membrane bound tyrosine phosphatase B220 (also known as CD45R). The harvested cells were used for further FACS analysis and TRL stimulation experiments.

2.2.5 GENERATION OF DCS FROM GM-CSF SUPPLEMENTED BM CULTURES

It was shown that murine BM cells cultured in GM-CSF for 6 – 8 days differentiate into large numbers of mature DCs (Caux et al., 1992; Inaba et al., 1992). These cells most likely represent DCs formed during inflammatory conditions (Randolph et al., 1998). Because GM-CSF inhibits Flt3L dependent pDC development from early BM progenitors, mainly cDCs are found in these cultures (Esashi et al., 2008).

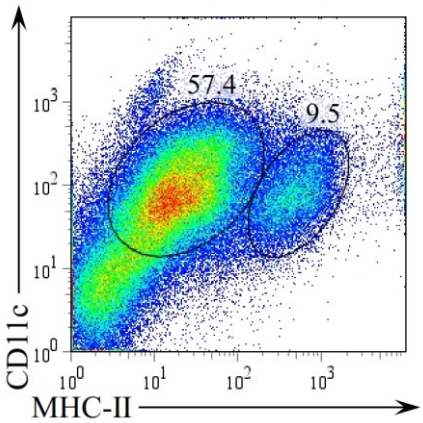

FIGURE 2.3
FACS OF GM-CSF CULTURE
FACS analysis of GM-CSF supplemented wild type bone marrow culture after 7 days. $CD11c^+$ $MHC\text{-}II^{int}$ cells represent nonactivated cDCs, whereas $CD11c^+$ $MHC\text{-}II^{high}$ cells are activated cDCs.

Procedure:

3 – 6 x 10^6 freshly isolated BM cells were cultured in cell culture dishes (Nunclon surface) each containing 10 ml $RPMI^{Suppl.}$ + 10 % GM-CSF (supernatant of X6310 cell line culture). 10 ml of $RPMI^{Suppl.}$ + 10 % GM-CSF were added carefully on day 3 and 6. The differentiated cells were harvested on day 7 by gently aspirating the whole medium. The quality, viability, and differentiation was checked by FACS analysis using antibodies against CD11c and MHC-II (see ***FIGURE 2.3***). Cells were used for FACS analysis and TLR stimulation experiments.

2.2.6 GENERATION OF MΦS FROM M-CSF SUPPLEMENTED BM CULTURES

The differentiation of MΦs *in vitro* from murine BM cells using the growth factor M-CSF was shown by Stanley et al. for the first time (Stanley et al., 1978).

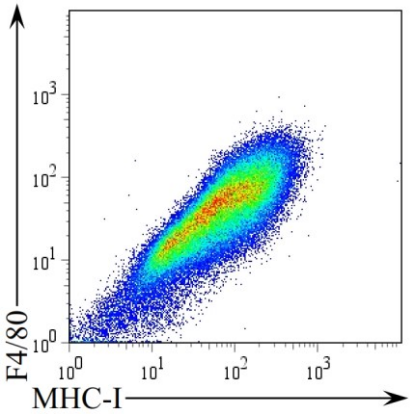

FIGURE 2.4
FACS OF M-CSF CULTURE
FACS analysis of M-CSF supplemented wild type bone marrow culture after 5 days. F4/80 and MHC-I double positive cells represent mature macrophages.

Procedure:

After isolation of BM cells (see chapter 2.2.3), 5 x 10^6 cells were cultured in 10 cm cell culture dishes (BD) containing 10 ml of RPMI$^{Suppl.}$. M-CSF was added to the medium (final concentration: 20 ng/ml) directly after seeding the BM cells and again at day 3. After 5 days of culture at 37°C, 5 % CO_2, and 100 % air humidity, the medium was aspirated and adherent cells were detached by incubation with PBSdef/3 % FCS/2mM EDTA for 15 min at 37°C. The cell suspension was transferred into a 50 ml tube and centrifuged at 1300 rpm for 7 min at 4°C. The cell pellet was resuspended in 5 ml RPMI$^{Suppl.}$ and cells were counted by the CASY®-1 cell counter. The quality was checked by FACS analysis using fluorescence labeled antibodies against F4/80 and MHC-I (***FIGURE 2.4***). Cells were used for FACS analysis and TLR stimulation experiments. The aspirated medium containing a single-cell suspension of non-detached cells was transferred into a 50 ml tube and centrifuged at 1300 rpm for 7 min at 4°C. The cell pellet was resuspended in 5 ml RPMI$^{Suppl.}$ and the cells were counted by the CASY®-1 cell counter. The small proportion of DC subsets in M-CSF supplemented cultures was determined by FACS using fluorescence labeled antibodies against B220, CD11c, SiglecH, BST2, and CD11b. TLR stimulation experiments were carried out to investigate TLR function.

2.2.7 STIMULATION OF CELLS WITH TLR-LIGANDS *IN VITRO*

To activate TLRs and subsequently investigate TLR-mediated cytokine responses, different synthetic stimuli were used, which are explained in the following passage. For basic details of pattern recognition of the various TLRs see chapter 1.2.3.2.

Pam3CSK4 or Pam-3-Cys is a synthetic triacetylated (tripalmitoylated) lipopeptide and a TLR1/2 agonist. It mimics the acetylated amino terminus of bacterial lipoproteins. TLR2 recognizes Pam-3-Cys and induces the signaling cascade in cooperation with the cytoplasmic domain of TLR1, which leads to activation of the transcription factor NFκB (Ozinsky et al., 2000) and subsequent expression of

proinflammatory cytokines (e.g. TNF-α, IL-1, and IL-6). TLR3 senses double-stranded RNA (dsRNA), which is present in some viruses. Poly I:C (Polyinosinic-polycytidylic acid) is structurally similar to dsRNA and represents a synthetic ligand for TLR3. Activation of TLR3 leads to the expression of type I interferons (IFN-α/β) via IRF3 and NFκB mediated proinflammatory cytokines (Trinchieri, 2010). LPS from *Escherichia coli* was used to stimulate TLR4 activation. It is part of the outer membrane of gramnegative bacteria and is recognized by a TLR4-homodimer in cooperation with the protein MD2 (myeloid differentiation factor 2) and CD14. TLR7 senses single-stranded RNA (ssRNA) and leads to expression of type I interferons and NFκB associated proinflammatory cytokines (Heil et al., 2004). The stimulation of this receptor was realized using the ssRNA-oligonucleotide (ODN) RNA40 as phosphodiester (PD) and a synthetic ligand called R848 (Resiquimod). RNA40 was mixed with the transfection reagent DOTAP to enter the endosomal compartment of the stimulated cells (see ***FIGURE 2.5*** for details). R848 is a synthetic immune response modifier which binds to murine TLR7 and human TLR7/8 and acts as vaccine adjuvant, enhances antigen-specific antibody production, and skews immunity towards a Th1 response (Tomai et al., 2007). The endosomal receptor TLR9 is activated by unmethylated CpG-DNA of viruses, bacteria, parasites, and dead cells. The signaling cascade via IRF7 and NFκB is similar to TLR7 and leads to expression of IFN-α/β and NFκB induced proinflammatory cytokines. Different DNA-ODNs were used for TLR9 stimulation experiments. ODN AP-1, ODN 1668, and ODN 1720 were used as phosphodiesters and needed to be mixed with the transfection reagent DOTAP to enter the endosomes of the stimulated cells (see ***FIGURE 2.5*** and ***TABLE 2.15***). ODN 2216 was used with phosphorothioate (PS) internucleotide linkage instead of phosphodiester. Phosphorothioates are DNA sequences in which one of the non-bridging oxygens of the phosphate backbone is replaced by sulfur. The sulfurization reduces the cleaving of ODNs by several enzymes (e.g. exonucleases) dramatically and increases the chance of crossing the cell membrane. Thus, ODN 2216 did not need to be mixed with a transfection reagent for TLR9 stimulation. The ODNs AP-1 and 1720 do not contain CpG-motifs, whereas 1668 and 2216 possess sequences including CpG-motifs.

Procedure:

Cells were seeded into 96-well plates in a volume of 100 µl per well for *in vitro* TLR stimulation. The concentration of the cells depended on the used cell type (see ***TABLE 2.14***). Used stimuli were diluted in 100 µl medium (same medium the cells were solved in) and added carefully on top of the seeded cells. Stimuli that consisted of nucleic acids and did not have a phosphorothioate internucleotide linkage were mixed with the transfection reagent DOTAP. Therefore, the stimulus was diluted in 25 µl OptiMEM or RPMI. 25 µl of the transfection solution (1.5 µl DOTAP + 23.5 µl OptiMEM/RPMI) was added to the stimulus. After 10 min of incubation at RT, 50 µl medium (OptiMEM or RPMI) was added to a final volume of 100 µl (***FIGURE 2.5***). Medium and DOTAP without a stimulus were used for negative controls. The final volume of each well was 200 µl. The stimulated cells were incubated at 37°C and 5 % CO_2 for 18 hours. 190 µl of the supernatant were transferred into a round bottom 96-well plate and stored at -20°C until ELISA was performed.

TABLE 2.14 *CELL TYPES AND FINAL CONCENTRATIONS*

CELL TYPE	CELLS/WELL
BM *ex vivo*	1.5×10^5
Flt3L-induced DCs *in vitro*	1.0×10^5
Sorted BM pDCs/cDCs *ex vivo*	0.5×10^5
M-CSF-induced MΦs *in vitro*	2.0×10^5
M-CSF-induced pDCs *in vitro*	1.5×10^5
GM-CSF-induced cDCs *in vitro*	3.0×10^5
Splenocytes *ex vivo*	2.0×10^5

Used cell types for in vitro *stimulation and their final concentration.*

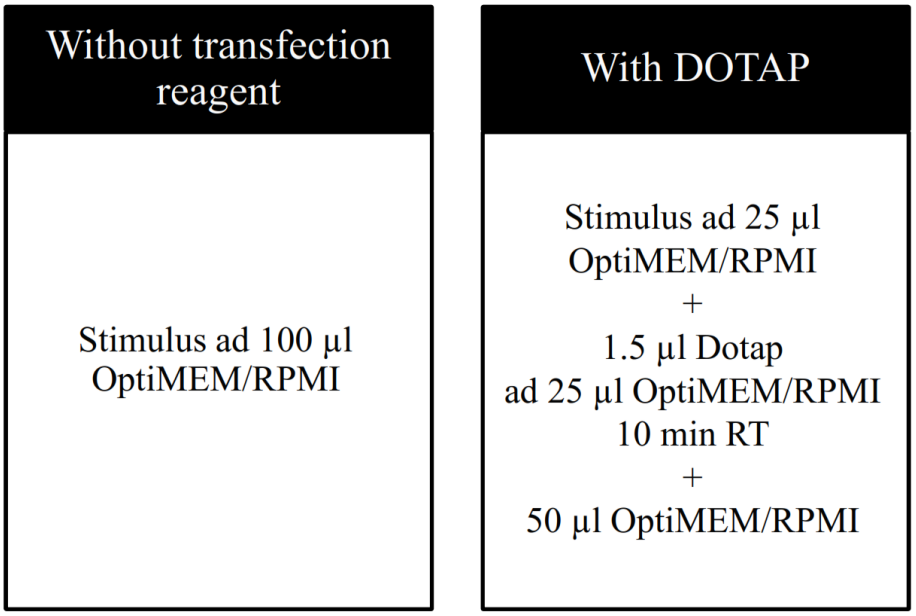

FIGURE 2.5 *STIMULUS PREPARATION*
Algorithm of stimulus preparation with and without the transfection reagent DOTAP.

TABLE 2.15 *FINAL CONCENTRATIONS AND TRANSFECTION OF STIMULI*

STIMULUS	FINAL CONCENTRATION/WELL	TRANSFECTION
LPS	1000 ng/ml	no
ODN AP-1 PD	1 µM	yes
ODN 1668 PD	1 µM	yes
ODN 1720 PD	1 µM	yes
ODN 2216 PS	1 µM	no
POLY I:C	10 µg/ml	yes
RNA40 PD	10 µg/ml	yes
R848	5 µg/ml	no
Pam-3-Cys	5 µg/ml	no

Used stimuli with their final concentration per well and transfection with DOTAP or not.

2.2.8 ENZYME-LINKED IMMUNOSORBENT ASSAY (ELISA)

The Enzyme-linked immunosorbent assay (ELISA) was first described in 1971 by two different groups in France (Avrameas and Guilbert, 1971) and Sweden (Engvall and Perlmann, 1971) at the same time. By searching for an alternative label to replace radioactive isotopes, it was a further development of the Radioimmunoassay (RIA) (Leng et al., 2008). The RIA was the first quantitative immunoassay invented incidentally by Berson and Yalow 1959 (BERSON and YALOW, 1959) by investigating the insulin metabolism. The main principle is a competitive assay. Radioactively labeled antigen is covalently bound to insolubilized antigen-specific antibodies. The binding of labeled antigen is competitively inhibited by unlabeled antigen.

Thus, it can be used for quantitative determination of unlabeled antigen in standard solutions or unknown samples (Avrameas and Guilbert, 1971). The more unlabeled antigen you have in your sample the less radioactivity can be measured.

The ELISA uses enzyme labeled antigen instead of radioactive labeled antigen. By adding the substrate of the used enzyme, a colored reaction product can be photometrically measured. This method is called competitive ELISA. Because of its high sensitivity to detect antigens, the more often used ELISA is the sandwich ELISA. In the typical sandwich ELISA, an antigen-specific antibody (capture-antibody) is attached to the bottom of a microplate (***FIGURE 2.6** and **2.7***). After incubation with the antigen, a second enzyme labeled antibody (detection-antibody) is used for detection. By adding the substrate of the enzyme, the colored reaction product can be measured with a photometer. The more antigen you have in your sample, the more colored reaction product can be photometrically measured. Hence, the measured color intensity is related directly to the quantity of the antigen. The color intensities of serial standard solutions with known concentrations of the antigen are used for comparison with the color intensities of the unknown samples.

The sandwich ELISA usually enables a more sensitive detection (Sensitivity in theory 10^{-15} to 10^{-16} mol/l) of the antigen then the competitive ELISA (Sensitivity in theory 10^{-14} mol/l). However, in practice the sensitivity is always depending on the affinity of the used antibody to its antigen. A big disadvantage of the sandwich ELISA is the necessity of two different epitopes of the antigen to be detected. Therefore, the competitive ELISA is used for detection of small antigens (e.g. haptenes).

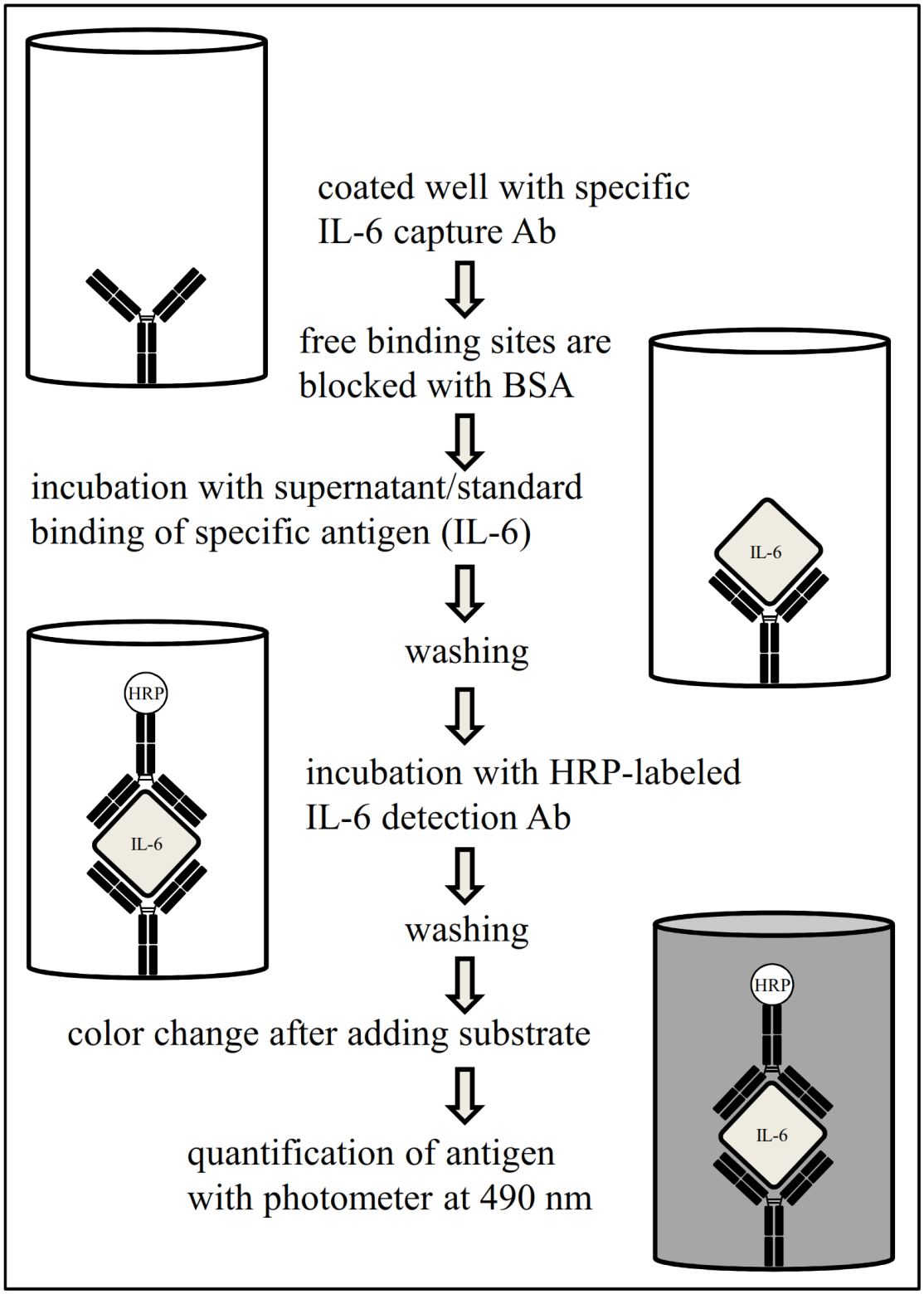

FIGURE 2.6 *SANDWICH ELISA FOR IL-6*
Main principle of the sandwich ELISA for detection of murine IL-6.

In this work, the typical double antibody sandwich ELISA was used for detection of murine IL-6 (***FIGURE 2.6***). To measure murine IFN-α, a slightly modified system was applied. The used enzyme (HRP) was conjugated to a third antibody. This antibody recognized specifically the Fc fragment of the IFN-α detection antibody (***FIGURE 2.7***).

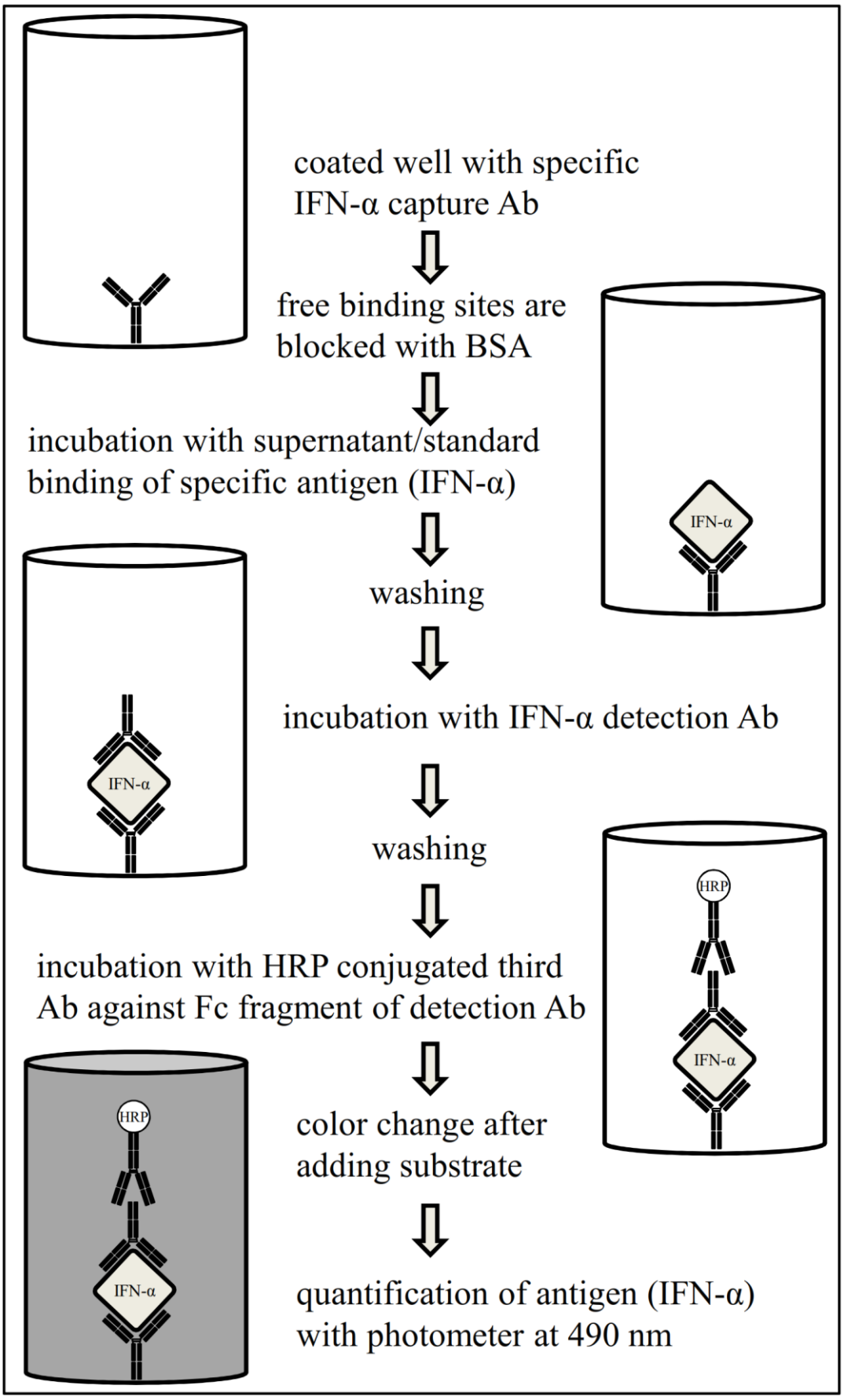

***FIGURE 2.7** SANDWICH ELISA FOR IFN-α*
Main principle of the sandwich ELISA for detection of murine IFN-α.

Procedure:

After diluting the capture antibody with $PBS^{def.}$, it was coated in a 96-well ELISA MaxiSorp microplate (50 µl/well) over night at 4°C. Unbound antibodies were washed out with ELISA washing buffer by using the Skanwasher 400 microplate washer. Remaining binding sites on the microplate were blocked with blocking buffer (250 µl/well), consisting of bovine serum albumin fraction V (BSA) solved in $PBS^{def.}$, for 1 h at RT. The microplate was washed again afterwards. The supernatants of the stimulated cells were added to the microplate as well as serial standard solutions with known concentrations of the antigen to be analyzed (50 µl/well). The supernatants had to be diluted depending on the cell type and cytokine to be detected to achieve concentrations which were covered by the range of the standard curve (***TABLE 2.16***). After 1.5 h at RT, the microplate was washed out. The detection antibody was diluted and added to the microplate (50 µl/well) for 1.5 h and subsequently unbound antibodies were washed out. The IL-6 detection antibody was biotinylated to bind streptavidin conjugated horseradish peroxidase (HRP) (30 min incubation time; this step is not depicted in ***FIGURE 2.6*** for reasons of simplicity), whereas for INF-α detection a third HRP-labeled antibody recognized the detection antibody via an IgG-mediated Fab binding to the Fc fragment of the detection antibody (1 h incubation time). Unbound streptavidin conjugated HRP or HRP-labeled third antibodies were washed out. The substrate solution, consisting of 1 tablet (20 mg) *o*-phenylenediamine (OPD) and 20 µl of 30 % H_2O_2 solved in 20 ml of ELISA substrate buffer, was added to the microplate. HRP reduced H_2O_2 and oxidized OPD leading to a colored reaction product. After stopping the reaction with 2 M H_2SO_4 (25 µl/well) the color change was measured with a photometer at a wavelength of 490 nm. For background determination an additional measurement at a wavelength of 650 nm was performed. The more antigen was bound, the more HRP was bound and the more OPD was oxidized leading to a stronger color change and intensity. Now the color intensities of the serial standard solutions with known concentrations of the antigen were compared with the color intensities of the supernatants in order to determine the unknown concentration of the antigen in the supernatants. All standards and samples were measured in duplicates. The microplate was read out using the Emax microplate spectrophotometer and the SoftMax Pro V5 software. The different used ELISA systems are shown in ***TABLE 2.17***.

***TABLE 2.16** DILUTIONS OF SUPERNATANTS*

CELL TYPE	IFN-ALPHA	IL-6
BM	undiluted	undiluted
Flt3-L-induced DCs	1:3	undiluted
Sorted pDCs/cDCs from BM	1:5	undiluted
M-CSF-induced MΦs	undiluted	undiluted
GM-CSF-induced cDCs	undiluted	1:2
Splenocytes	undiluted	undiluted

Used cell types and dilutions of supernatants.

***TABLE 2.17** ELISA SYSTEMS*

	IFN-ALPHA	IL-6
Standards		
Number:	11 Standards	11 Standards
Concentration:	1.Std: 500 U/ml	1.Std: 10 ng/ml
Incubation time:	1.5 h at RT	1.5 h at RT
Capture Ab		
Type:	Rat IgG1 anti-mouse IFN-α MAb	Rat IgG1 anti-mouse IL-6 MAb
Concenration:	1 µg/ml	1 µg/ml
Incubation time:	over night at 4°C	over night at 4°C
Detection Ab		
Type:	Rabbit anti-mouse IFN-α PAb	Goat IgG biotinylated anti-mouse IL-6 PAb
Concentration:	0.994 µg/ml	100 ng/ml
Incubation time:	1.5 h at RT	1.5 h at RT
Enzyme/3.Ab		
Type:	Goat POD-conjugated anti-rabbit IgG MAb	Streptavidin conjugated HRP
Concentration:	0.16 µg/ml	0.1 U/ml
Incubation time:	1 h at RT	0.5 h at RT
Substrate:	OPD and H_2O_2	OPD and H_2O_2

Used ELISA systems.

2.2.9 FLOW CYTOMETRY / FLUORESCENCE ACTIVATED CELL SORTING (FACS)

The flow cytometry or fluorescence activated cell sorting (FACS) is one of the most important methods used in immunology. It allows distinguishing the many subpopulations of immune cells by their different expression of cell-surface proteins, which can be detected by specific fluorochrome labeled antibodies. Furthermore, it is a highly sophisticated technique for separation of viable cells from distinct populations, achieving very high purity (95 – 100 %) (Basu et al., 2010).

The fluorescence activated cell sorter (FACS) or flow cytometer was invented by Bonner, Sweet, Hulett, Herzenberg, and others at the Herzenberg laboratories at Stanford University (Stanford, United States) in the late 1960s (Herzenberg et al., 2002). It can detect and count single cells in a stream passing through a laser beam. It consists of one or more lasers, a hydrostatic aspiration unit, lenses, multiple fluorescence and light scatter detectors, mirrors, and different filters. The complexity of a FACS device is shown in ***FIGURE 2.8***. Hydrostatic aspiration allows the uptake, separation, and a constant flow rate of the cells to be analyzed. By using the principles of light emission, distraction, and scatter, the morphology of the cells can be detected by the forward (size) and sideward (granularity) scatter detector (FSC/SSC). Moreover, multiple fluorescence detectors enable modern FACS devices to distinguish up to seventeen or even more colors (Perfetto et al., 2004). Fluorescence labeled specific monoclonal antibodies bind to cell-surface or intracellular proteins or glycoproteins and facilitate the discrimination of many subpopulations of leucocytes. The most commonly used fluorochromes are allophycocyanine (APC), phycoerythrin (PE), and fluorescein isothiocyanate (FITC).

For purification of specific subpopulations, a flow cytometer with sorting capacity and the appropriate software is necessary. Stained cells in suspension are passed as a stream through a laser beam in droplets, each containing one single cell. Droplets with cells of interest are charged and can be collected into appropriate collection tubes or microplates by an electrostatic deflection system (***FIGURE 2.8***). Different sorting parameters can be adapted depending on the requirement of purity and yield (Basu et al., 2010). The success of cell-sorting depends on the identifying surface markers and the used fluorescence labeled antibodies. Different sizes of nozzles are used depending on the cell type to be sorted.

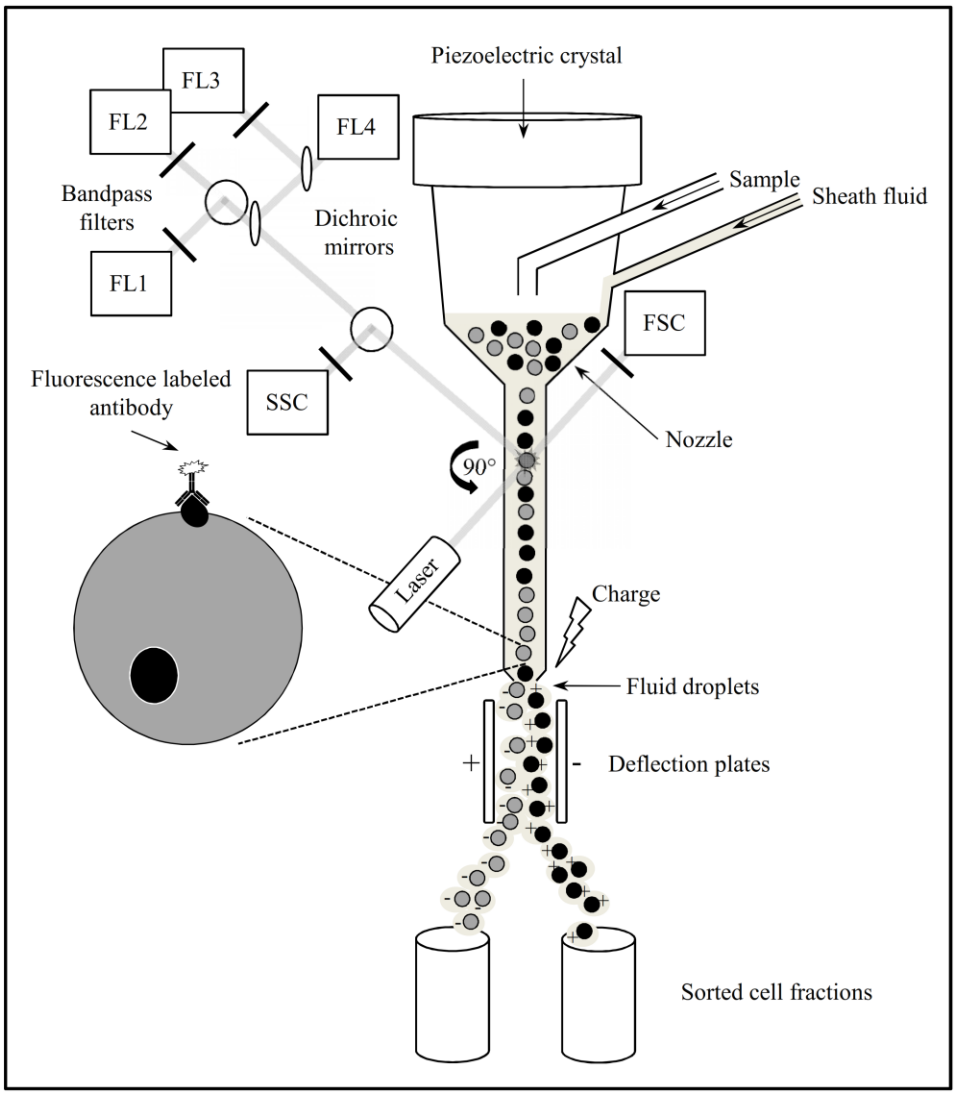

FIGURE 2.8 *STRUCTURE OF A FACS SORTER*
Main structure of a FACS Sorter. Adapted from Herzenberg et al., 2002 and Sabban, 2011.

The flow cytometry was used in this work for differentiation and purity control of DCs and MΦs within mixed cell populations like BM, spleen, and several *in vitro* cell cultures (see chapters 2.2.3 – 2.2.6). All samples were analyzed using the BD FACSCalibur™ flow cytometer, CellQuest Pro software (Version 5.2.1 for Macintosh), and FlowJo software (Version 10.0.7 for Windows). ToPro3 iodide staining was used to indicate the viability of the cells. Only viable cells (ToPro3 iodide negative gated populations) were used for further FACS analysis. For purification of pDCs and cDCs from BM *ex vivo* a BD FACSAria™ III cell sorter and BD FACSDiva™ software (Version 7.0 for Windows) were used. The different used fluorochrome labeled antibodies and their dilutions are shown in ***TABLE 2.18***.

Procedure:

For flow cytometry 0.3 – 0.5 x 10^6 cells were transferred into a small FACS tube (1.2 ml). 1 ml of FACS buffer was added and the cells were centrifuged at 1300 rpm at 4°C for 6 min. The supernatant was discarded and the cells were washed again by adding 1 ml of FACS buffer and centrifugation at 1300 rpm at 4°C for 6 min. The supernatant was discarded up to a final volume of 90 µl. The cells were incubated for 7 min at 4°C with 30 µl of purified rat IgG (stock concentration: 11 mg/ml and final concentration: 27.5 µg/ml) for blocking Fc-receptors to avoid non-specific immune fluorescence. Subsequently, the fluorochrome labeled antibody mix was added (0.2 – 1 µg/ml per Ab) in a final volume of 30 µl (see ***TABLE 2.18*** for dilutions of Abs) and incubated for 30 min at 4°C. The samples were washed twice with 500 µl of FACS buffer and centrifuged at 1300 rpm for 6 min at 4°C. In a final step, the supernatant was discarded and the cell pellet was resuspended in 150 – 250 µl of FACS buffer depending on the type of cells to be analyzed. Unstained cells were used for controls and single stained cells were used for the FACS setup. The probes were analyzed immediately after or stored at 4°C and analyzed the next morning. For analysis of Flt3L-induced DCs, additional isotype controls were used.

TABLE 2.18 *FACS ANTIBODIES WITH DILUTIONS*

DYE/ANTIBODY	DILUTION	FINAL DILUTION
Rat IgG (Fc blocking)	1:100	1:400
Rat anti-mouse BST2-FITC	1:250	1:500
Rat anti-mouse B220-APC	1:100	1:200
Rat anti-mouse B220-FITC	1:200	1:400
Rat anti-mouse CD11b-APC	1:200	1:400
Rat anti-mouse CD11b-FITC	1:100	1:200
Rat anti-mouse CD11c-APC	1:200	1:400
Rat anti-mouse CD11c-PE	1:200	1:400
Rat anti-mouse Flt3-PE	1:100	1:200

Rat anti-mouse F4/80-FITC	1:200	1:400
Rat anti-mouse Ly6C-PE	1:20	1:40
Rat anti-mouse MHC-I-PE	1:200	1:400
Rat anti-mouse MHC-II-PE	1:200	1:400
Rat anti-mouse SiglecH-FITC	1:250	1:500
ToPro3 iodide	1:100	1:200

Used dyes and fluorochrome labeled antibodies and their dilutions for FACS analysis and cell sorting.

For cell-sorting, the cells were washed twice using 1 ml of FACS sorting buffer (without sodium azide) by centrifugation at 1300 rpm at 4°C for 7 min. Unstained and single stained cells were used for the sorting setup. The following steps were carried out under a sterile bench of security class II. Fc-blocking and staining were realized according to the protocol described above. 30 – 150 x 10^6 cells were stained in a large sterile FACS tube (5 ml) using 0.2 – 1 µg/ml of Ab per 5 x 10^6 cells. After two washing steps by centrifugation at 1300 rpm at 4°C for 7 min, the cells were filtered through a 70 µm cell strainer and resuspended in 100 % FCS in a concentration of 20 x 10^6 cells/ml. Subsequently, the stained cells were stored on ice or 4°C (in the cell sorter) and sorted into small reaction tubes (15 ml) at 4°C, which were coated with 100 % FCS before over night at 37°C. 80 µm and 100 µm nozzles were used for cell separation. After purification, the cells were washed by centrifugation at 1300 rpm at 4°C for 7 min and resuspended in medium for stimulation experiments or RNA isolation (see chapter 2.2.7).

2.2.10 RNA ISOLATION OF SORTED PDCS FOR MICROARRAY ANALYSIS

First steps were carried out in a fume hood. Cell pellets of sorted pDCs (~1 x 10^6 cells) from pooled BM cells (see section 2.2.9 for details) of HoxA9$^{-/-}$ and WT mice (4 mice per genotype) were resuspended in 1 ml Trizol and incubated for 5 min at RT. 0.2 µl Chloroform/1 ml Trizol was added and the formulation was shaken for 15 seconds and incubated at RT for 2 – 3 min. After centrifugation at 4000 rpm for 30 min at 4°C, the upper aqueous phase was transferred into a new falcon tube and 0.5 ml Isopropyl/1 ml Trizol was added with subsequent incubation for 10 min at RT. Again, centrifugation was

done at 4000 rpm for 30 min at 4°C. Next steps were done under a sterile bench. The supernatant was discarded and the pellet was washed with 1 ml of 70 % Ethanol/1 ml Trizol. After one last step of centrifugation at 4000 rpm and 4°C for 15 min, the supernatant was discarded and the pellet was dried. 25 µl of RNase free H_2O was used to solve the pellet, which was subsequently stored at -80°C.

RNA was thawed on ice and 1 µl of DNase (10 Units)/50 µg RNA was added. Same volume of 10 x incubation buffer was added and the formulation was incubated at 37°C for 20 min.

After DNase digestion RNA was further purified by precipitation. Chloroform and isoamyl alcohol of the same volume were added followed by shaking and centrifugation at 10.000 rpm at RT for 2 min inducing phase separation. The upper phase was transferred into a new falcon tube adding the same volume Chloroform followed by shaking and centrifugation at 10.000 rpm at RT for 2 min. Again the upper phase was transferred into a new falcon tube and mixed with 2.5-fold volume fraction of 100 % Ethanol and 1/10 volume fraction 3 M sodium acetate (pH 5.0). The formulation was incubated at -80°C for 1 h. Centrifugation with 10.000 rpm at 4°C for 20 min was followed by discarding the supernatant and washing the pellet with 75 % Ethanol. After a last centrifugation step at 10.000 rpm at 4°C for 5 min, the supernatant was discarded and the pellet was dried. Subsequently, the pellet was solved in 50 µl of RNase free H_2O. RNA concentration was determined by photometric measurement at 260 nm using the "Nanodrop". Best purity was considered for samples with a 260/280 ratio of 2.0.

1 µl of RNA of each sample was sent to the "Expression Core Facility" of the Institute for Medical Microbiology, Immunology, and Hygiene of the Technical University of Munich under the direction of Prof. Dr. med. D. H. Busch. RNA was reverse transcribed, amplified, labeled, and hybridized to Affymetrix Mouse Genome 1.0 ST arrays (28.853 probe set) for genome-wide microarray gene expression profiling. To adjust systematic errors, robust multi-array average (RMA) normalization was performed by the software of the "Expression Core Facility".

2.2.11 STATISTICAL ANALYSIS

GraphPad PRISM 6 Software Version 6.05 was used for all statistical analyses. All data are expressed as mean ± standard deviation. The two-tailed paired or unpaired Student's t test were performed for comparison of populations considered to be normally distributed

(Gaussian distribution) such as normalized cytokine levels measured by ELISA of different cell types and cell counts as well as frequencies of cell types determined by FACS, respectively. Welsh's correction was additionally carried out for comparison of populations with clearly different standard deviations such as cell counts of Flt3L-induced DC cultures. For populations that were assumed to be not normally distributed the Mann-Whitney U test was performed (e.g. total BM cell counts). Statistically significant differences were considered for P values < 0.5 (*, $p < 0.5$; **, $p < 0.01$; ***, $p < 0.001$; n.s., not significant).

3. RESULTS

3.1 ANALYSIS OF BM CELLS *EX VIVO*

3.1.1 TOTAL BM CELL NUMBERS OF HOXA9$^{-/-}$ MICE ARE SLIGHTLY REDUCED

BM cells were isolated from 6 – 27 weeks old HoxA9$^{-/-}$ mice and their WT littermates by flushing the dissected femur and tibia of both legs (see section 2.2.3 for details). Total numbers of nucleated BM cells per mouse were determined using the CASY®-1 cell counter after lysis of the erythrocytes. HoxA9$^{-/-}$ mice showed a small, statistically insignificant, mean reduction of 21.89 % (HoxA9$^{-/-}$ [n = 24] versus WT littermates [n = 20]; p = 0.2) including mice of all ages and a mean reduction of 9.27 % (HoxA9$^{-/-}$ [n = 9] versus WT littermates [n = 10]; p = 0.589) in young animals with 6 – 15 weeks of age. BM cells of the latter were further used for functional analysis as for immunological experiments young mice are demanded, whereas experiments with older mice were initially carried out mainly for testing purposes. ***FIGURE 3.1*** illustrates total BM cell numbers shown as scatter plots including statistical analyses. Overall, a big variability was observed in BM cell numbers showing higher mean cell amounts in younger mice (***FIGURE 3.1 B***). Regarding both genotypes, HoxA9$^{-/-}$ mice display a small, statistically insignificant, reduction in total BM cell numbers compared to wild type littermates.

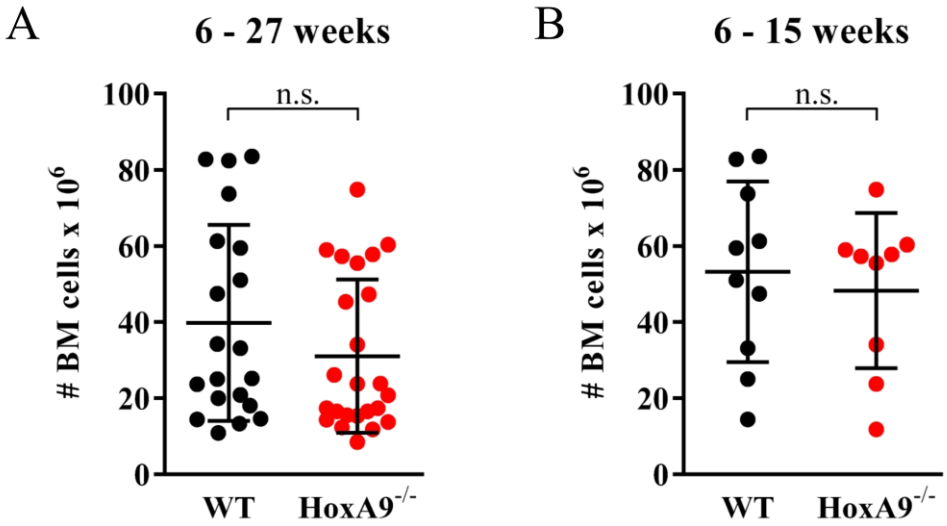

FIGURE 3.1 *TOTAL NUMBERS OF NUCLEATED BM CELLS*
Total numbers of nucleated BM cells per mouse of HoxA9-deficient mice compared to their WT littermates were determined using the CASY®-1 cell counter after lysis of the erythrocytes. ***A*** *Shown are results from mice between 6 – 27 weeks of age (HoxA9$^{-/-}$ [n = 24 ± SD] versus wild type [n = 20 ± SD]; p = 0.2).* ***B*** *Shown are results from mice between 6 – 15 weeks of age (HoxA9$^{-/-}$ [n = 9 ± SD] versus wild type [n = 10 ± SD]; p = 0.589). The Mann-Whitney test was performed for statistical analyses (n.s., not significant). Lines and error bars represent means and standard deviations (SD), respectively.*

3.1.2 HoxA9$^{-/-}$ Mice Develop Normal Quantities of Mature BM DCs But Show Significantly Reduced B Cell Frequencies

To prove the assumption that HoxA9 has no impact on DC development according to previous data (Gwin et al., 2013a), flow cytometric analyses of BM cells using the murine DC-specific cell surface markers B220, CD11c, BST2, and SiglecH were performed in order to determine frequencies of pDCs and cDCs in HoxA9-deficient mice compared to WT control.

The forward scatter (FSC) and side scatter (SSC), which display the size and granularity of the analyzed cells, respectively, were used to roughly discriminate dead cells and cell debris from living cells (***Figure 3.2 A***). The gated living cell fraction was further stained with TO-PRO-3 iodide to detect the remaining dead cells. TO-PRO-3 iodide very sensitively detects nuclear double stranded DNA of dead cells. Therefore, only TO-PRO-3 iodide negative gated events were included for further analysis (***Figure 3.2 B***). The percentages of living cells among all analyzed BM cells did not differ between both genotypes (***Figure 3.2 A - B***). By default, the surface markers B220 and CD11c were used to determine the frequencies of pDCs and cDCs. The protein tyrosine phosphatase B220 (CD45R) is the longest member of the CD45 family and is expressed on the cell surface of murine early B cell precursors and B cells throughout development in the BM and is still retained in mature B cells (Rodig et al., 2005). Therefore, it is used as a pan B cell marker in mice. Additionally, a human B cell subset is known to express B220 (Rodig et al., 2005). However, it can also be found on the plasma membrane of pDCs (Nakano et al., 2001; Nikolic et al., 2002). The name B220 is related to its molecular weight of 220 kDa and the occurrence on B cells. Another cell surface marker of DCs is the integrin alpha x chain CD11c, which is expressed on all subsets of murine DCs (Metlay et al., 1990). B220^{+}CD11c^{+} cell populations represent pDCs, whereas cDCs express CD11c but not B220 on their plasma membrane. B220 single positive cells denote predominantly B cells and precursors throughout the B cell lineage, as already mentioned above. To perform a more precise investigation of the pDC subset in the BM of HoxA9-deficient mice, fluorochrome-labeled antibodies directed against the pDC-specific surface markers BST2 and SiglecH were used to determine frequencies of pDCs. The BM stromal cell antigen 2 (BST2), also known as tetherin, HM1.24, CD317, or mPDCA1 is a very specific marker for pDCs in naïve mice, but is upregulated upon type I IFN stimulation on most cell types (Blasius et al., 2006).

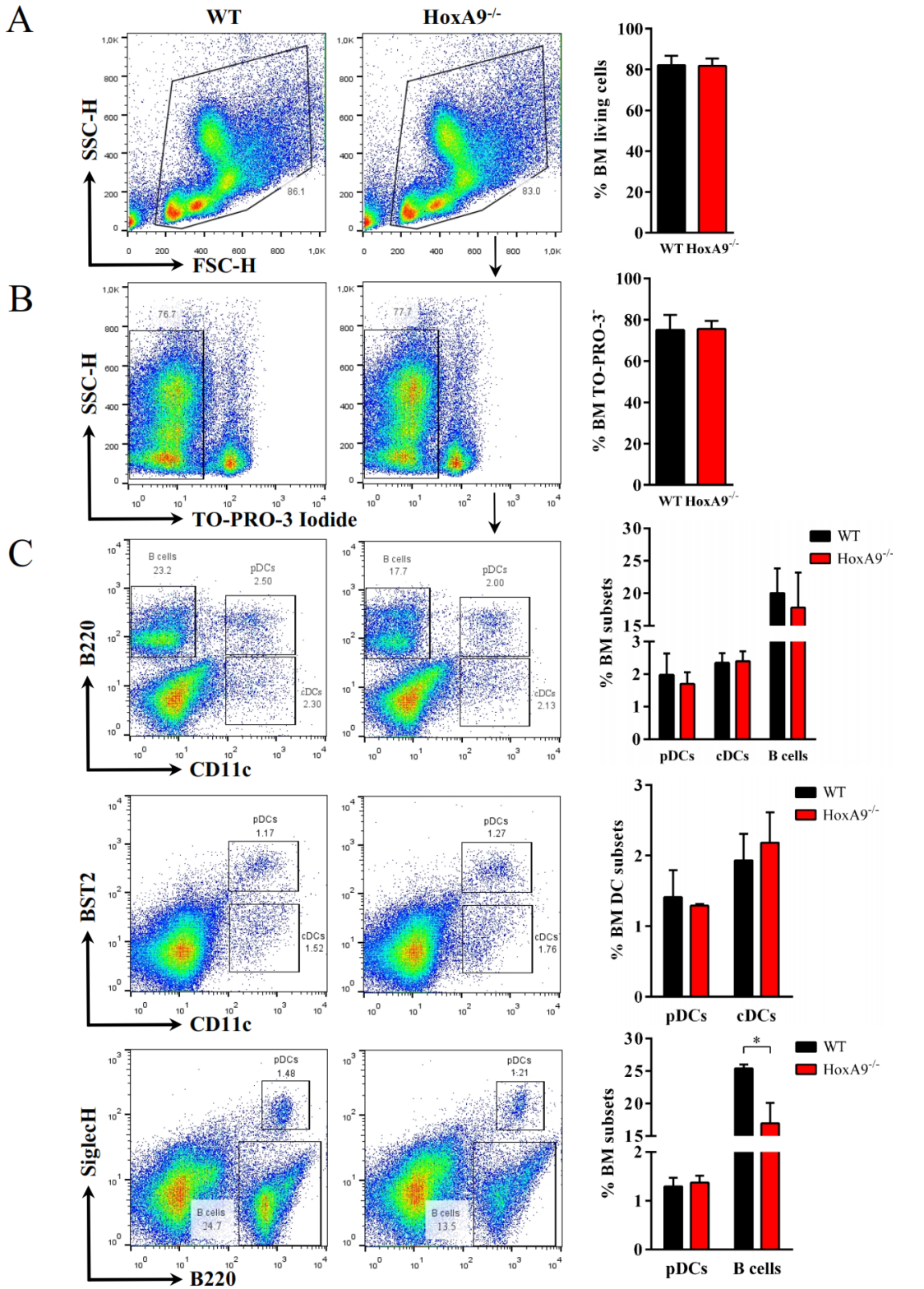

FIGURE 3.2 *FACS ANALYSES OF BM CELLS* EX VIVO

A) *FSC-H (size) and SSC-H (granularity) dot plots were used to discriminate dead cells from living cells.* ***B)*** *TO-PRO-3 Iodide stained cells were excluded from further flow cytometry analysis.* ***C)*** *Antibodies directed against the DC-specific surface receptors B220, CD11c, BST2, and SiglecH were used to determine DC subset and B cell frequencies. PDCs are represented by the $B220^+CD11c^+$, $BST2^+CD11c^+$, or $SiglecH^+B220^+$ population, cDCs reflect single $CD11c^+$ cells, and B cells are shown as single $B220^+$ gated cells. Figures A – B show one representative of five independently performed experiments. In Figure C one representative experiment of five (B220 CD11c gate) or three (BST2 CD11c and SiglecH B220 gate) independently performed experiments is shown. Bars and error bars represent means and standard deviations (n = 5 or 3 ± SD), respectively. The unpaired Student's t test was performed for statistical analyses (*, $p < 0.05$).*

BST2 inhibits the release of virus particles from infected cells (Le Tortorec et al., 2011) and functions as a physiological ligand for the human pDC receptor ILT7, inducing negative regulation of TLR7 and 9 signaling (Cao et al., 2009). SiglecH is a member of the sialic acid binding Ig-like lectin (Siglec) family and is believed to play a role in capturing and delivering pathogens to intracellular TLRs (Blasius and Colonna, 2006). Its signaling through DAP12 is known to induce negative regulation of IRF7 activation in pDCs (Bao and Liu, 2012) (see section 1.3.1.2 for details). Both BST2 and SiglecH are known to be expressed on the plasma membrane of mature murine pDCs (Cisse et al., 2008; Ghosh et al., 2010).

FIGURE 3.2 C depicts one representative experiment of each staining and statistical results of all independently performed experiments. The B220 and CD11c staining displays a very small decrease of pDCs in the knockout genotype and equal percentages of cDCs. $B220^{+}CD11c^{-}$ cells, mainly reflecting B cells and B cell precursors, are slightly reduced among HoxA9-lacking BM cells. Using antibodies directed against BST2 and CD11c, almost equal pDC and slightly increased cDC amounts were determined. SiglecH and B220 double positive pDCs were marginally increased in $HoxA9^{-/-}$ animals on average. Of note, B220 single positive cells, representing B cells in the SiglecH and B220 staining, were significantly reduced when lacking HoxA9. All results of the BM FACS analyses and statistical data are listed in ***TABLE 3.1***.

Taken together, frequencies of both DC subsets display no significant alteration in the HoxA9 knockout genotype regarding surface markers of mature DCs. Frequencies of $B220^{+}$ B cells and precursors are slightly reduced in one and significantly decreased in the other staining under HoxA9 knockout conditions.

TABLE 3.1 *STATISTICAL DATA OF FACS ANALYSES OF BM CELLS* EX VIVO

SUBSET	WT	HOXA9 $^{-/-}$	P VALUE
Cells in the living gate (FSC-H/SSC-H dot plot)	82.08 % ± 4.65 (n = 5 ± SD)	81.74 % ± 3.57 (n = 5 ± SD)	0.90 (n.s.)
TO-PRO-3^{-} gated cells	75.08 % ± 7.18 (n = 5 ± SD)	75.54 % ± 3.82 (n = 5 ± SD)	0.90 (n.s.)
$B220^{+}CD11c^{+}$ pDCs	1.98 % ± 0.66 (n = 5 ± SD)	1.70 % ± 0.36 (n = 5 ± SD)	0.42 (n.s.)

$B220^{-}CD11c^{+}$ cDCs	2.35 % ± 0.30 (n = 5 ± SD)	2.39 % ± 0.31 (n = 5 ± SD)	0.81 (n.s.)
$B220^{+}CD11c^{-}$ B cells	20.04 % ± 3.82 (n = 5 ± SD)	17.80 % ± 5.41 (n = 5 ± SD)	0.47 (n.s.)
$BST2^{+}CD11c^{+}$ pDCs	1.41 % ± 0.38 (n = 3 ± SD)	1.29 % ± 0.02 (n = 3 ± SD)	0.59 (n.s.)
$BST2^{-}CD11c^{+}$ cDCs	1.93 % ± 0.37 (n = 3 ± SD)	2.18 % ± 0.43 (n = 3 ± SD)	0.49 (n.s.)
$SiglecH^{+}B220^{+}$ pDCs	1.29 % ± 0.18 (n = 3 ± SD)	1.37 % ± 0.14 (n = 3 ± SD)	0.59 (n.s.)
$SiglecH^{-}B220^{+}$ B cells	25.40 % ± 0.62 (n = 3 ± SD)	16.97 % ± 3.13 (n = 3 ± SD)	0.01 (*)

After gating the living cell fraction in the FCS-H (size) and SSC-H (granularity) dot plot, staining with TO-PRO-3 Iodide was used to exclude further TO-PRO-3^{+} dead cells or cell debris. DC and B cell frequencies of total BM cells were examined by using fluorochrome-labeled antibodies directed against B220, CD11c, BST2, and SiglecH. Statistical analyses were performed using the unpaired Student's t test (, $p < 0.05$; n.s., not significant).*

3.1.3 HoxA9$^{-/-}$ BM DCs Exhibit Normal Expression of Mature DC-Specific Surface Markers

The expression of additional DC-specific surface marker proteins was examined by further FACS analyses. $B220^{+}CD11c^{+}$ pDCs and $B220^{-}CD11c^{+}$ cDCs were additionally stained with fluorochrome-labeled antibodies directed against BST2, SiglecH, Ly6C, or Flt3 and CD11b or Flt3, respectively. Ly6C (lymphocyte antigen 6 complex, locus C1) is another surface receptor present on murine pDCs, albeit less specific compared to BST2 or SiglecH (Reizis et al., 2011). It is also expressed on multiple other lymphocytes such as monocytes, MΦs, granulocytes, plasma cells, NK cells, and T cell subsets. CD11b is another integrin also known as ITGAM or CR3A and is mainly expressed in myeloid cells including cDCs, whereas pDCs do not express CD11b (Reizis et al., 2011; Watowich and Liu, 2010).

FIGURE 3.3 illustrates representative experiments of each staining. All surface markers were not significantly altered in HoxA9$^{-/-}$ pDCs and cDCs compared to wild type littermates.

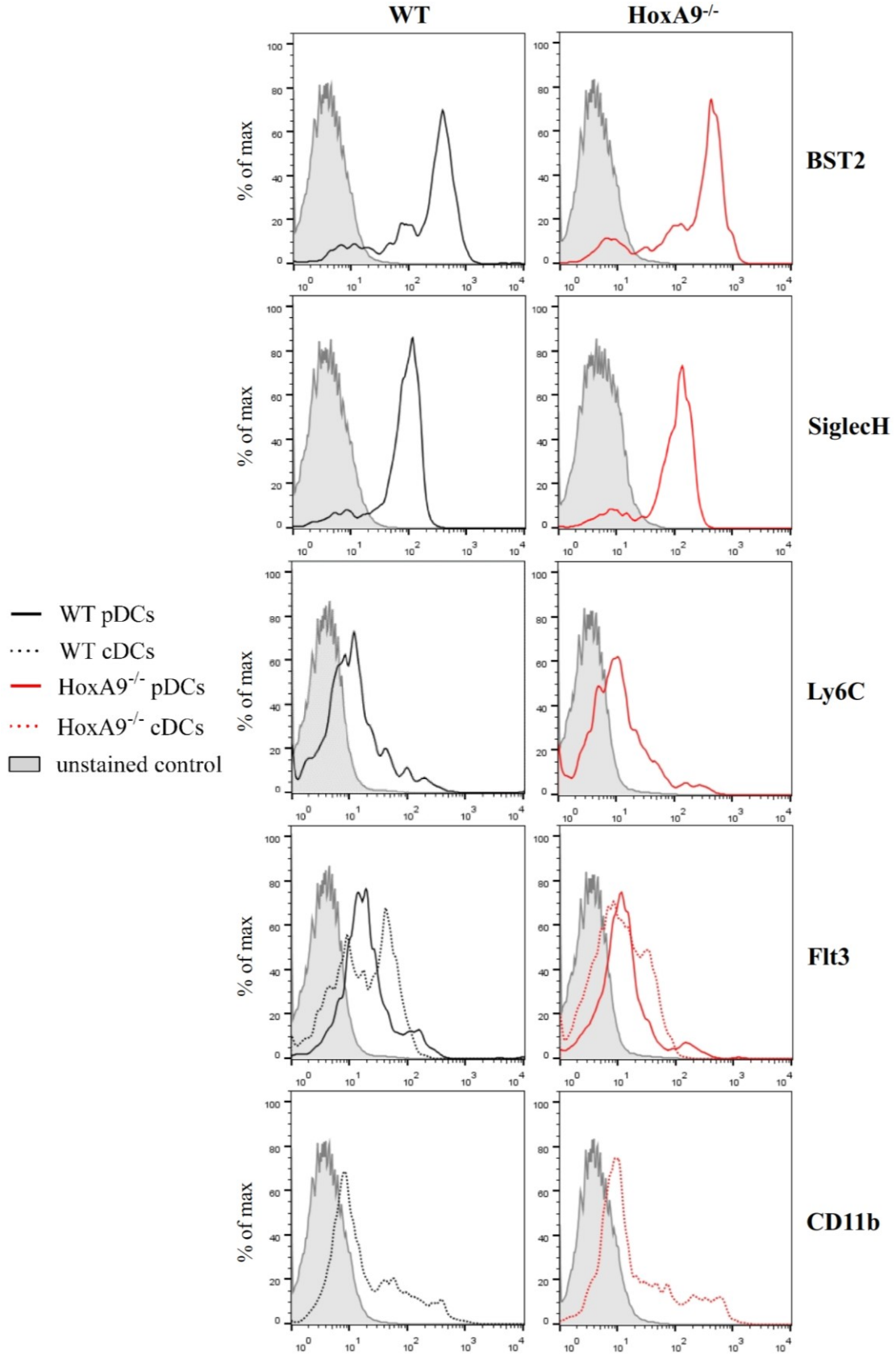

FIGURE 3.3 *FACS ANALYSES OF BM PDCS AND CDCS* EX VIVO

PDCs ($B220^+CD11c^+$ cells) were additionally stained for the surface markers BST2, SiglecH, Ly6C, and Flt3. CDCs ($B220^-CD11c^+$ cells) were additionally stained for the surface markers Flt3 and CD11b. Shaded, black solid lined, black dotted lined, red solid lined, and red dotted lined histograms depict unstained control, WT pDCs, WT cDCs, HoxA9$^{-/-}$ pDCs, and HoxA9$^{-/-}$ cDCs, respectively. Each panel shows one representative experiment of at least two independently performed experiments.

3.1.4 TLR7/9-MEDIATED IFN-α RESPONSES OF HOXA9$^{-/-}$ TOTAL BM CELLS ARE SIGNIFICANTLY IMPAIRED

For functional analysis of HoxA9-deficient DCs, stimulation of primary BM cells *ex vivo* with different TLR-ligands was performed and subsequent cytokine production was measured by ELISA. Activation of TLR7 and 9 in pDCs and cDCs leads to production of proinflammatory cytokines such as IL-6, TNF-α, or IL-12 in both cell types, whereas large quantities of IFN-α/β are uniquely secreted by pDCs (Reizis et al., 2011). Other cell types in the BM are responding to TLR7 and 9 ligation with proinflammatory cytokine production including monocytes, B cells, and also precursors like CDPs. To activate TLR7, the single-stranded ribonucleic acid RNA40 and the imidazoquinoline R848 were used. Two oligonucleotides (ODNs) without containing CpG-motifs called ODN AP-1 and ODN 1720, class A CpG-containing ODN 2216, and class B CpG-containing ODN 1668 were used for TLR9 activation (termed non-CpGAP-1, non-CpG1720, CpG1668,

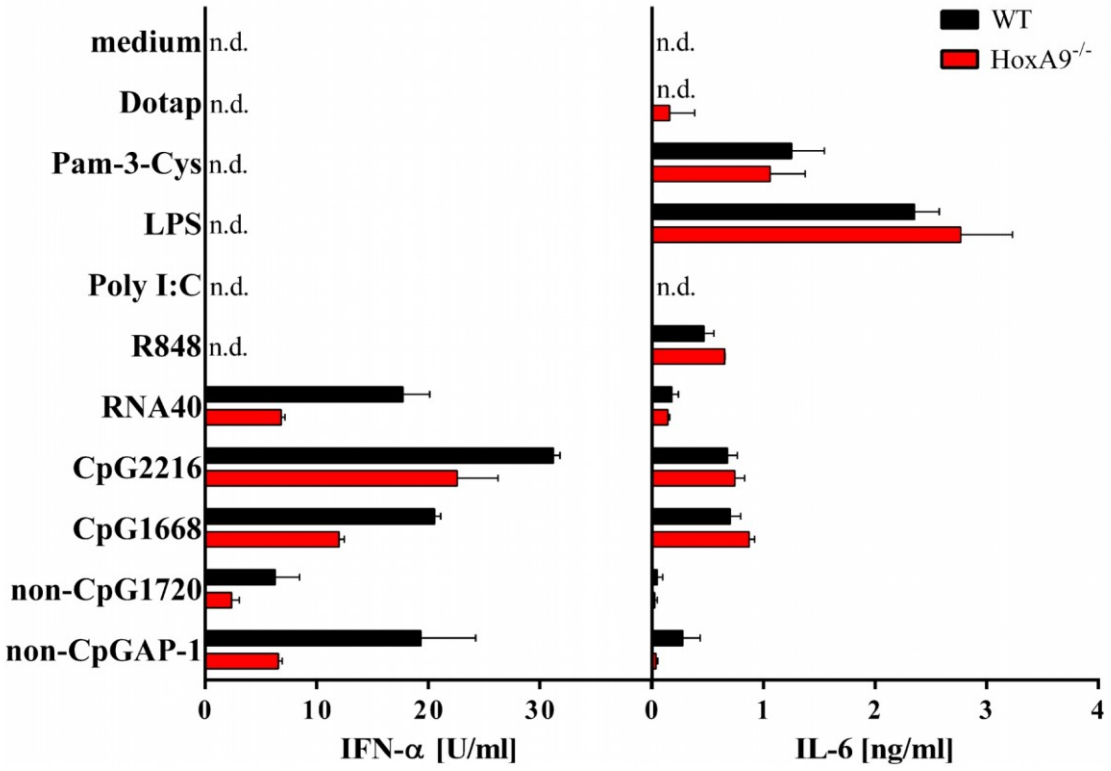

FIGURE 3.4 *TLR STIMULATION OF BM CELLS* EX VIVO

TLR2, 3, 4, 7, and 9 were stimulated with Pam-3-Cys[5µg/ml], Poly I:C[10µg/ml], LPS[1µg/ml], RNA40[10µg/ml]/R848[5µg/ml], and non-CpGAP-1[1µM]/CpG1720[1µM]/CpG1668[1µM]/ CpG2216[1µM], respectively. RNA40, CpG1668, non-CpG1720, non-CpGAP-1, and Poly I:C were complexed to DOTAP. 150.000 cells were suspended in 100 µl medium per well with 100 µl diluted stimulus or medium/DOTAP control in 96-well plates and incubated for 18h overnight. Subsequently, murine IFN-α and IL-6 were detected by ELISA measured in dublicates (n.d., not detectable). Each panel shows one representative experiment of at least three independently performed experiments. Bars and error bars represent means and standard deviations (SD), respectively.

and CpG2216, respectively, in the following passages). In the BM, mainly immature cDCs and monocytes further express TLR2, 3, and 4 with release of proinflammatory cytokines upon ligation of TLR2, 3, and 4 and type I IFN secretion exclusively after TLR3 has been activated. TLR2 stimulation was performed using the synthetic triacetylated lipopeptide Pam-3-Cys (also known as Pam3CSK4). Poly I:C is structurally similar to dsRNA and a synthetic agonist for TRL3, providing IFN-α/β and proinflammatory cytokine release. LPS is generally known to activate TLR4 and thus was used in this study as TLR4 agonist. RNA40, non-CpGAP-1, non-CpG1720, CpG1668, and Poly I:C were complexed to the transfection reagent DOTAP to locate to the endolysosomal compartment. CpG2216 was used with phosphorothioate (PS) backbone and did not need to be complexed to DOTAP. To measure induction of proinflammatory cytokines and type I IFNs, murine IL-6 and IFN-α ELISAs were performed, respectively. 150.000 total BM cells per well were seeded in 96-well plates and suspended in 100 µl medium and further incubated for 18 h overnight after adding 100 µl of diluted stimulus or medium/DOTAP control with subsequent detection of IL-6 and IFN-α (see section 2.2.7 for details).

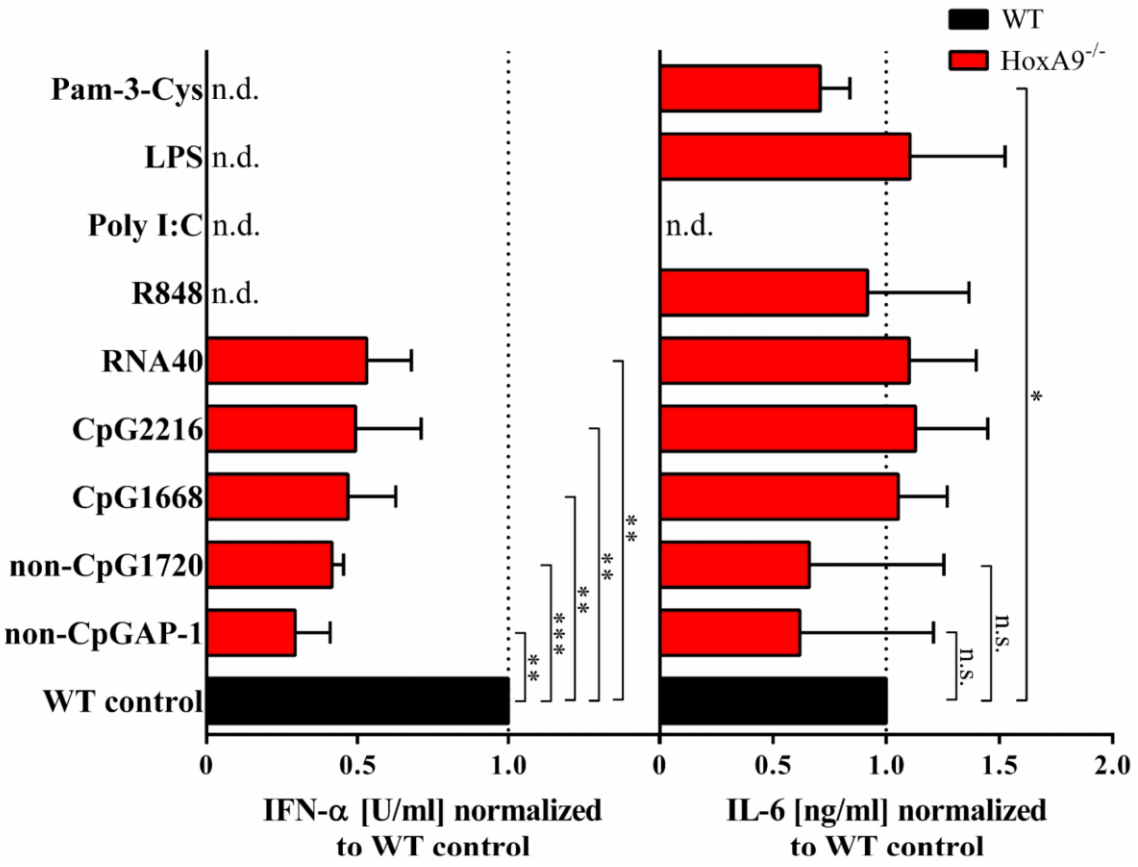

FIGURE 3.5 *STATISTICAL ANALYSIS OF TLR STIMULATION OF BM CELLS* EX VIVO
IFN-α and IL-6 production of HoxA9$^{-/-}$ BM cells were normalized to WT control taken as 1. Statistical analyses of three - five independent experiments of each stimulus were performed using the paired Student's t test (, $p < 0.05$; **, $p < 0.01$; ***, $p < 0.001$; n.s., not significant; n.d., not detectable). Bars and error bars represent means and standard deviations (SD), respectively.*

FIGURE 3.4 shows one representative experiment and ***FIGURE 3.5*** depicts calculated data of at least three independently performed experiments per stimulus with statistical analyses. Absolute cytokine levels of all experiments showed a large variety but stable and reproducible proportions between the KO and WT genotype.

Therefore, IFN-α and IL-6 levels of HoxA9-deficient BM cells were normalized to the corresponding WT control taken as 1 (100 %) and statistical analyses were carried out using the paired Student's *t* test. Upon stimulation with the TLR9 ligands non-CpGAP-1, non-CpG1720, CpG1668, and CpG2216, statistically significant decreased IFN-α levels of 29.41 %, 44.66 %, 46.86 %, and 49.35 % in comparison to WT control, respectively, were observed in HoxA9-deficient BM cells. Moreover, IFN-α induction in response to TLR7 activation with RNA40 revealed 46.94 % mean less IFN-α activity stimulating KO BM cells. In contrast, IL-6 liberation upon TLR7 and 9 stimulation was not significantly different between the WT and KO genotype. Interestingly, the CpG-motif free ODNs non-CpGAP-1 and non-CpG1720 showed reduced IL-6 levels for the KO cells similarly to the proportions seen for IFN-α in three experiments and slightly increased levels in one experiment resulting in a large variability. The TLR7 agonist R848 only prompted IL-6 responses without detectable IFN-α release. Striking differences between both genotypes were not observed in IL-6 levels. As expected, stimulation with the TLR4 ligand LPS induced equivalent amounts of IL-6 in the KO and WT cells but did not lead to IFN-α secretion. Similarly, Pam-3-Cys activated TLR2 and obtained predictable IL-6 but not IFN-α detection. However, IL-6 amounts, after stimulating the KO BM cells with Pam-3-Cys, were reproducibly decreased in small amounts compared to WT control, showing statistical significant differences. Usage of the TRL3 stimulus Poly I:C did astonishingly neither induce detectable levels of IL-6 nor IFN-α.

Summarizing the facts, IFN-α production of primary HoxA9$^{-/-}$ BM cells was significantly diminished upon stimulation of TLR7 and 9, whereas IL-6 levels were detected without significant differences to WT BM cells. TLR4-mediated IL-6 levels were equal in both genotypes, together mainly produced by cDCs (Pre-cDCs), monocytes, and CDPs in the BM of HoxA9 knockout and WT mice. IL-6 levels upon activation of TLR2 display statistically significant reductions for HoxA9-deficient BM cells. Statistical data of all performed experiments is shown in ***TABLE 3.2***.

TABLE 3.2 *STATISTICAL DATA OF TLR STIMULATION OF BM CELLS* EX VIVO

STIMULUS	TLR	CYTOKINE	HOXA9$^{-/-}$ NORMALIZED TO WT CONTROL	P VALUE
non-CpGAP-1 [1µM]	9	IFN-α	0.294 ± 0.116 [n = 4 ± SD]	0.0012 (**)
		IL-6	0.619 ± 0.590 [n = 4 ± SD]	0.288 (n.s.)
non-CpG1720 [1µM]	9	IFN-α	0.417 ± 0.037 [n = 4 ± SD]	< 0.001 (***)
		IL-6	0.661 ± 0.594 [n = 4 ± SD]	0.337 (n.s.)
CpG1668 [1µM]	9	IFN-α	0.467 ± 0.158 [n = 4 ± SD]	0.0068 (**)
		IL-6	1.053 ± 0.217 [n = 4 ± SD]	0.658 (n.s.)
CpG2216 [1µM]	9	IFN-α	0.494 ± 0.218 [n = 5 ± SD]	0.0065 (**)
		IL-6	1.131 ± 0.318 [n = 5 ± SD]	0.411 (n.s.)
RNA40 [10µg/ml]	7	IFN-α	0.531 ± 0.149 [n = 5 ± SD]	0.0021 (**)
		IL-6	1.102 ± 0.296 [n = 5 ± SD]	0.483 (n.s.)
R848 [5µg/ml]	7	IFN-α	not detectable	-
		IL-6	0.918 ± 0.448 [n = 3 ± SD]	0.781 (n.s.)
Poly I:C [10µg/ml]	3	IFN-α	not detectable	-
		IL-6	not detectable	-
LPS [1µg/ml]	4	IFN-α	not detectable	-
		IL-6	1.106 ± 0.419 [n = 5 ± SD]	0.602 (n.s.)
Pam-3-Cys [5µg/ml]	2	IFN-α	not detectable	-
		IL-6	0.701 ± 0.132 [n = 4 ± SD]	0.0215 (*)

Cytokine responses of HoxA9$^{-/-}$ BM cells were normalized to WT control taken as 1 and statistical analyses of three to five independently performed experiments (mean ± SD) were realized using the paired Student's t test (, $p < 0.05$; **, $p < 0.01$; ***, $p < 0.001$; n.s., not significant).*

3.1.5 *EX VIVO* SORTED BM PDCS WITH HOXA9 DEFICIENCY DISPLAY SIGNIFICANTLY DIMINISHED CYTOKINE LEVELS UPON TLR7/9 STIMULATION

Based on the results of section 3.1.4, primary pDCs and cDCs were isolated *ex vivo* from total BM cells of HoxA9-deficient mice and their WT littermates to directly stimulate purified DC fractions. This was realized using a FACSAria™ III cell sorter in cooperation with the "Flow Cytometry Core Facility" of the Institute for Microbiology and Hygiene of the Philipps-University Marburg under the direction of Prof. Dr. med. M. Lohoff. Fluorochrome-labeled antibodies directed against the DC-specific cell surface markers B220 and CD11c were used to sort pDC ($B220^+CD11c^+$) and cDC ($B220^-CD11c^+$) fractions from total BM cells. The more specific pDC markers BST2 and SiglecH are both involved in negative regulation of TLR responses and thus were not used for this purpose. To achieve sufficient cell numbers of both DC subsets, BM cells of three to four mice per genotype were pooled for each experiment. ***FIGURE 3.6 A*** illustrates the sorting process including used gates of one representative experiment. After marking the living cell fraction at the forward (FSC-A) and side scatter (SSC-A), FSC-W/FSC-A and SSC-W/SSC-A gates were used to discriminate single cells from doublets (see section 2.2.9 for details).

The sorted cells were used for TLR stimulation experiments and additionally once for RNA isolation. Purity values of the sort are depicted in ***FIGURE 3.6 B*** for one representative experiment. Mean purity rates of all three experiments are shown in ***FIGURE 3.6 C***. Final purity of both cell strains in all experiments was always > 90 % and overall slightly better for the KO cells (see ***FIGURE 3.6 B***).

For pDCs and cDCs are very rare cell populations in the BM, huge amounts of BM cells had to be sorted to achieve adequate quantities for further analysis. Hence, only a limited number of stimuli could be used to perform TLR stimulation experiments. Sorted pDCs were faced with the TLR7 and 9 agonists RNA40 and CpG2216, respectively, and DOTAP as well as medium control. The cDC subset was additionally stimulated with the TLR2, 3, and 4 activating agents Poly I:C, Pam-3-Cys, and LPS, respectively. Poly I:C and LPS were used in three experiments, whereas Pam-3-Cys was only used in two experiments due to reduced cell amounts. RNA40 and Poly I:C were complexed to DOTAP. One representative TLR stimulation experiment of *ex vivo* sorted pDCs is shown in ***FIGURE 3.7 A***.

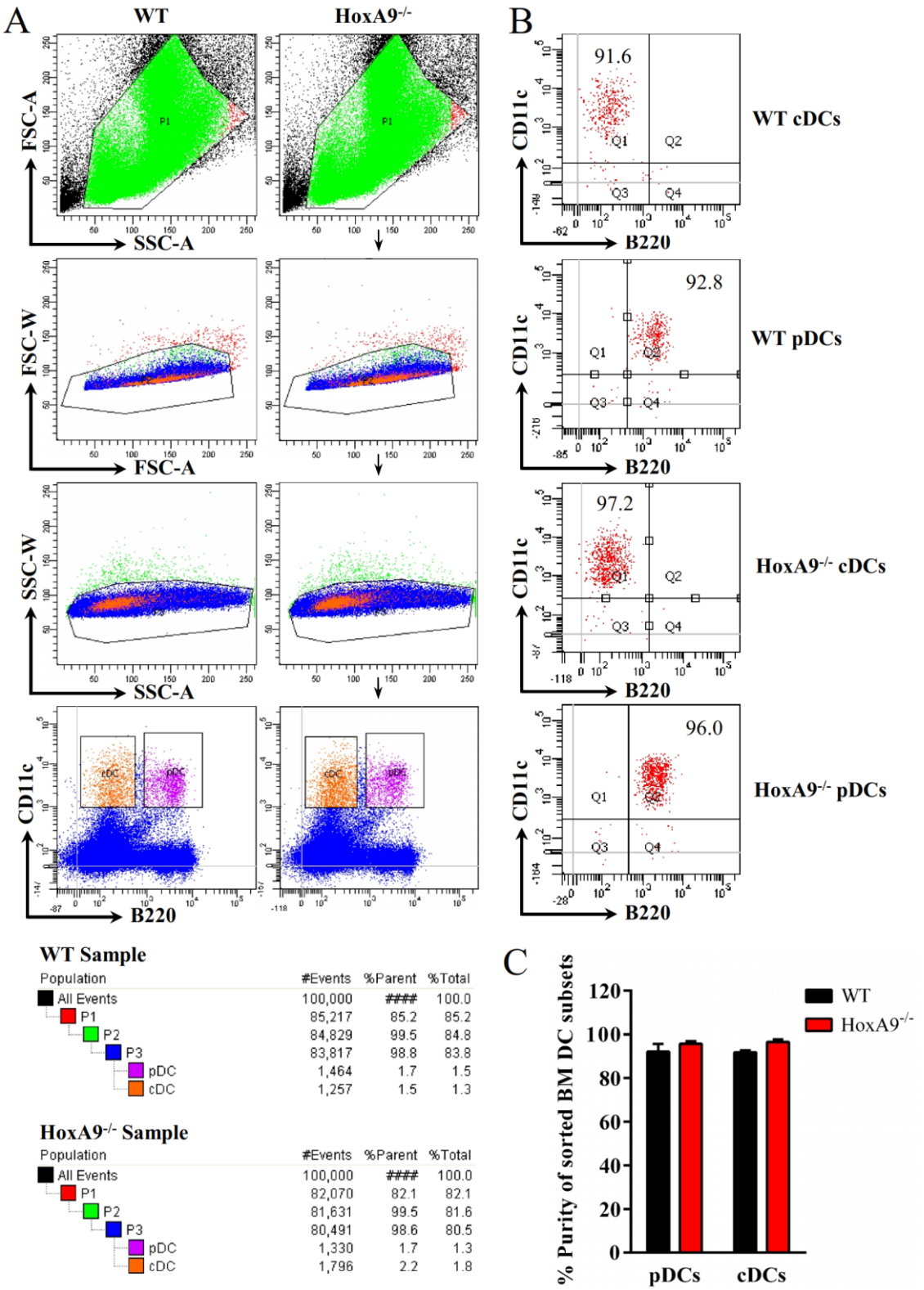

FIGURE 3.6 *FACS-SORT OF BM PDCS AND CDCS*
FACS sort of primary BM-derived pDCs and cDCs was realized using fluorochrome-labeled antibodies directed against B220 and CD11c. PDCs are represented by the $B220^{+}CD11c^{+}$ population and cDCs are characterized by $B220^{-}CD11c^{+}$ cells. ***A)*** *The used sorting process is illustrated exemplarily for one experiment and was carried out in the same way for all experiments. Living cells were gated using the FSC(size)/SSC(granularity) gate. Single cells were further separated from doublets using FSC-A(area)/FSC-W(width) and SSC-A(area)/SSC-W(width) gates.* ***B)*** *Post-sort purities of the sorted DC fractions were measured subsequently. One representative specimen of each DC subset from both genotypes is depicted.* ***C)*** *Mean purities of all sorted samples from all experiments are shown (n = 3 ± SD). Bars and error bars represent means and standard deviations (SD), respectively.*

IFN-α levels upon TLR7 and 9 stimulation of sorted KO pDCs were reproducibly reduced in all experiments, confirming results of total BM cells. One experiment initially displayed higher IFN-α secretion in the KO group. Repetition of this particular experiment with the left over supernatant displayed the result vice versa as observed in the other experiments, indicating a mixing up of the genotypes initially. Statistical data of all three experiments show significantly decreased mean IFN-α levels of 67.74 % and 56.01 % upon TLR7 and 9 stimulation compared to WT control, respectively (***FIGURE 3.7 C***).

Surprisingly, IL-6 production was not detectable at all in two experiments and one experiment exhibited low IL-6 levels (shown in ***FIGURE 3.7 A***). Thus, TLR7 and 9 ligation in sorted pDCs induced massive type I IFN release but only small or not measurable amounts of proinflammatory cytokines represented by IL-6. Sorted cDCs did not show significant differences of IL-6 levels upon TLR7 and 9 ligation (one representative experiment is shown in ***FIGURE 3.7 B*** and calculated data of all three experiments are depicted in ***FIGURE 3.7 C***). Calculated statistics of all three experiments reveal a slight increase of IL-6 after TLR9 activation and nearly equal IL-6 levels after TLR7 stimulation, however, with a huge standard deviation of the latter due to not detectable levels in one and clearly increased levels in another experiment for the KO genotype (184.6 %, 94.84 %, and 0 % compared to WT control).

TLR4-induced IL-6 levels upon LPS stimulation were clearly increased in two experiments and slightly decreased in one experiment (mean differences 65.66 % and 87.12 % higher versus 27.63 % lower). Pam-3-Cys elicited slightly decreased IL-6 amounts in one (***FIGURE 3.7 B***) and marginally increased IL-6 levels in the other experiment (data not shown) for KO cDCs. The TLR3 agonist Poly I:C did surprisingly again not induce any cytokine response at all in both genotypes. All results with statistical analyses are listed in ***TABLE 3.3***.

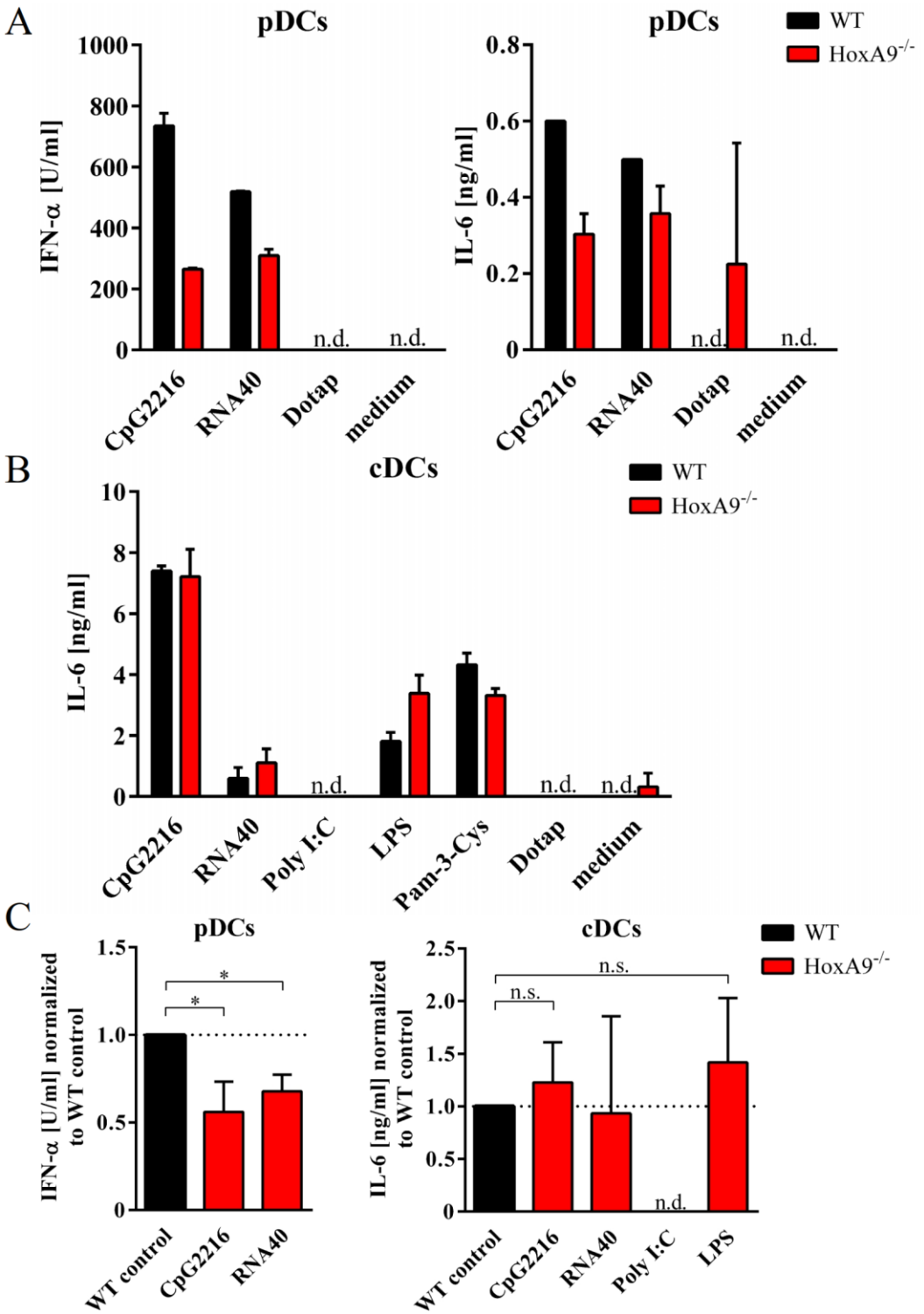

***FIGURE 3.7** TLR STIMULATION OF* EX VIVO *SORTED BM PDCS AND CDCS*

PDCs ($B220^+CD11c^+$) and cDCs ($B220^-CD11c^+$) were sorted ex vivo *from pooled BM cells of three – four mice per genotype and subsequently TLR2, 3, 4, 7, and 9 were stimulated with Pam-3-Cys [5 µg/ml], Poly I:C [10 µg/ml], LPS [1 g/ml], RNA40 [10 pg/ml], and CpG2216 [1 µM], respectively. RNA40 and Poly I:C were complexed to DOTAP. 50.000 cells were suspended in 100 µl medium per well with 100 µl diluted stimulus or medium/DOTAP control in 96-well plates for 18h overnight. Subsequently, murine IFN-α or IL-6 were detected by ELISA measured in dublicates (n.d., not detectable).* ***A)*** *One representative of three independently performed experiments of* ex vivo *sorted pDCs with IFN-α and IL-6 levels is depicted.* ***B)*** *One representative of three independently performed experiments of* ex vivo *sorted cDCs with IL-6 levels is depicted.* ***C)*** *IFN-α and IL-6 production of $HoxA9^{-/-}$ pDCs and cDCs, respectively, were normalized to WT control taken as 1. Statistical analyses of three independent experiments of each stimulus were performed using the paired Student's t test (*, $p < 0.05$; n.s., not significant). Bars and error bars represent means and standard deviations (SD), respectively.*

In summary, *ex vivo* sorted BM-derived HoxA9-deficient pDCs exhibit statistically significant reduced levels of IFN-α upon *in vitro* stimulation of TLR7 and 9, consistent to the results obtained for total nucleated BM cells. IL-6 induction could only be detected in one experiment with rather low amounts, but showed similarly decreased levels for pDCs lacking HoxA9. Results for the cDC subset revealed no significant differences with slightly increased responses for HoxA9$^{-/-}$ cells in IL-6 production, however, with a huge variability for most of the stimuli that complicates interpretation of the data.

TABLE 3.3 *STATISTICAL DATA OF TLR STIMULATION OF* EX VIVO *SORTED BM DCS*

SUBSET	STIMULUS	TLR	CYTOKINE	HOXA9$^{-/-}$ NORMALIZED TO WT CONTROL	P VALUE
pDCs	CpG2216 [1µM]	9	IFN-α	0.560 ± 0.174 [n = 3 ± SD]	0.048 (*)
	RNA40 [10µg/ml]	7	IFN-α	0.677 ± 0.095 [n = 3 ± SD]	0.028 (*)
cDCs	CpG2216 [1µM]	9	IL-6	1.228 ± 0.381 [n = 3 ± SD]	0.409 (n.s.)
	RNA40 [10µg/ml]	7	IL-6	0.932 ± 0.924 [n = 3 ± SD]	0.910 (n.s.)
	Poly I:C [10µg/ml]	3	IL-6	not detectable	-
	LPS [1µg/ml]	4	IL-6	1.417 ± 0.610 [n = 3 ± SD]	0.358 (n.s.)

Cytokine responses of HoxA9$^{-/-}$sorted BM pDCs and cDCs were normalized to WT control taken as 1 and statistical analyses of three independently performed experiments (mean ± SD) were realized using the paired Student's t test (, $p < 0.05$; n.s., not significant).*

3.2 ANALYSIS OF *IN VITRO* GENERATED FLT3L-INDUCED DCS

3.2.1 TOTAL CELL NUMBERS OF HOXA9$^{-/-}$ FLT3L-INDUCED DC CULTURES ARE DECREASED

As mentioned above, DC subsets are rare populations of innate immune cells among total BM cells, which of course complicates further experiments. To generate large amounts of DCs *in vitro*, freshly isolated BM cells were cultured in Flt3L-supplemented medium to induce differentiation of HSCs and beyond precursors into DCs. Brasel et al. first described the *in vitro* generation of DCs by using the cytokine Flt3L (Brasel et al., 2000; Gilliet et al., 2002). DCs developed from these cultures are believed to mainly reflect splenic DCs under homeostatic conditions in terms of expression of transcription factors, cell surface marker profiles, antigen presentation, and cytokine responses including robust type I IFNs by pDCs (Brawand et al., 2002; Gilliet et al., 2002; Naik et al., 2005; Watowich and Liu, 2010). For each culture, 15 x 10^6 BM cells were suspended in Flt3L-supplemented medium and incubated at 37°C, 5 % CO_2, and 100 % humidity (see section 2.2.4 for details). The generated Flt3L-induced DC cultures of both genotypes were harvested after 8 days of incubation and the resulting total cell numbers were determined

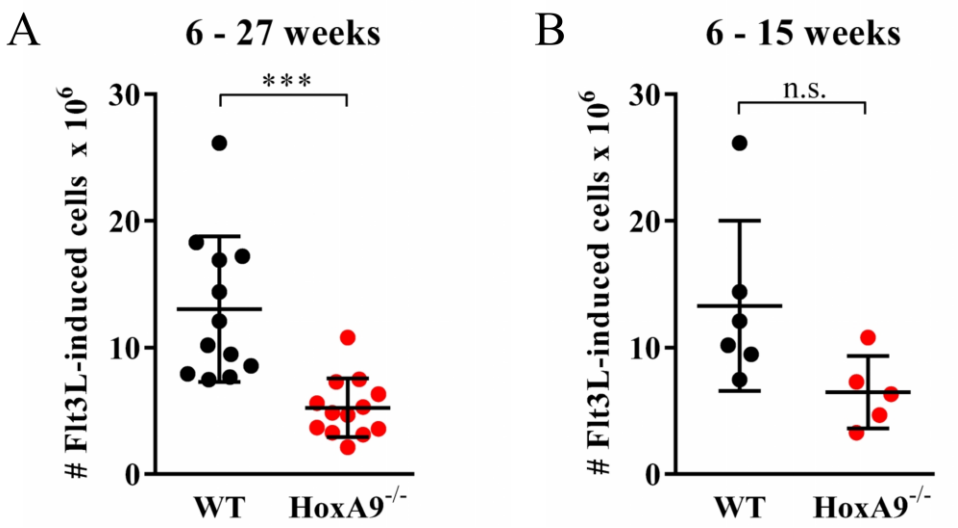

FIGURE 3.8 *TOTAL NUMBERS OF* IN VITRO *GENERATED FLT3L-INDUCED DCS*
Depicted are total cell numbers of in vitro *generated Flt3L-induced cultures of HoxA9$^{-/-}$ animals compared to their WT littermates after 8 days in culture at 37°C, 5 % CO_2, and 100 % humidity. Each culture was prepared using 15 x 10^6 freshly isolated BM cells seeded at a density of 1.5 x 10^6 cells/ml in Flt3L-supplemented medium (see section 2.2.4 for details). The CASY®-1cell counter was used to determine total cell counts.* ***A*** *Shown are results from mice between 6 – 27 weeks of age (HoxA9$^{-/-}$ [n = 13 ± SD] versus WT [n = 12 ± SD]; p = 0.0006).* ***B*** *Shown are results from mice between 6 – 15 weeks of age (HoxA9$^{-/-}$ [n = 5 ± SD] versus WT [n = 6 ± SD]; p = 0.059). The unpaired Student's t test with Welsh's correction was performed for statistical analysis (n.s., not significant; ***, p < 0.001). Lines and error bars represent means and standard deviations (SD), respectively.*

using the CASY®-1 cell counter. Of note, cell counts of HoxA9 knockout cultures from animals of all ages between 6 – 27 weeks were significantly reduced (***FIGURE 3.8 A***). Cultures of young mice from 6 – 15 weeks of age, which were used for further TLR function analysis, show a borderline insignificant (p = 0.059) decrease in cell numbers for the KO genotype (***FIGURE 3.8 B***).

3.2.2 DCs FROM FLT3L- INDUCED CULTURES OF HOXA9$^{-/-}$ MICE EXHIBIT PARTLY ALTERED EXPRESSION PATTERNS AND COMPRISE SIGNIFICANTLY INCREASED CDCS

Samples of WT and HoxA9 knockout Flt3L-induced DC cultures were stained with fluorochrome-labeled antibodies directed against B220, CD11c, BST2, SiglecH, Ly6C,

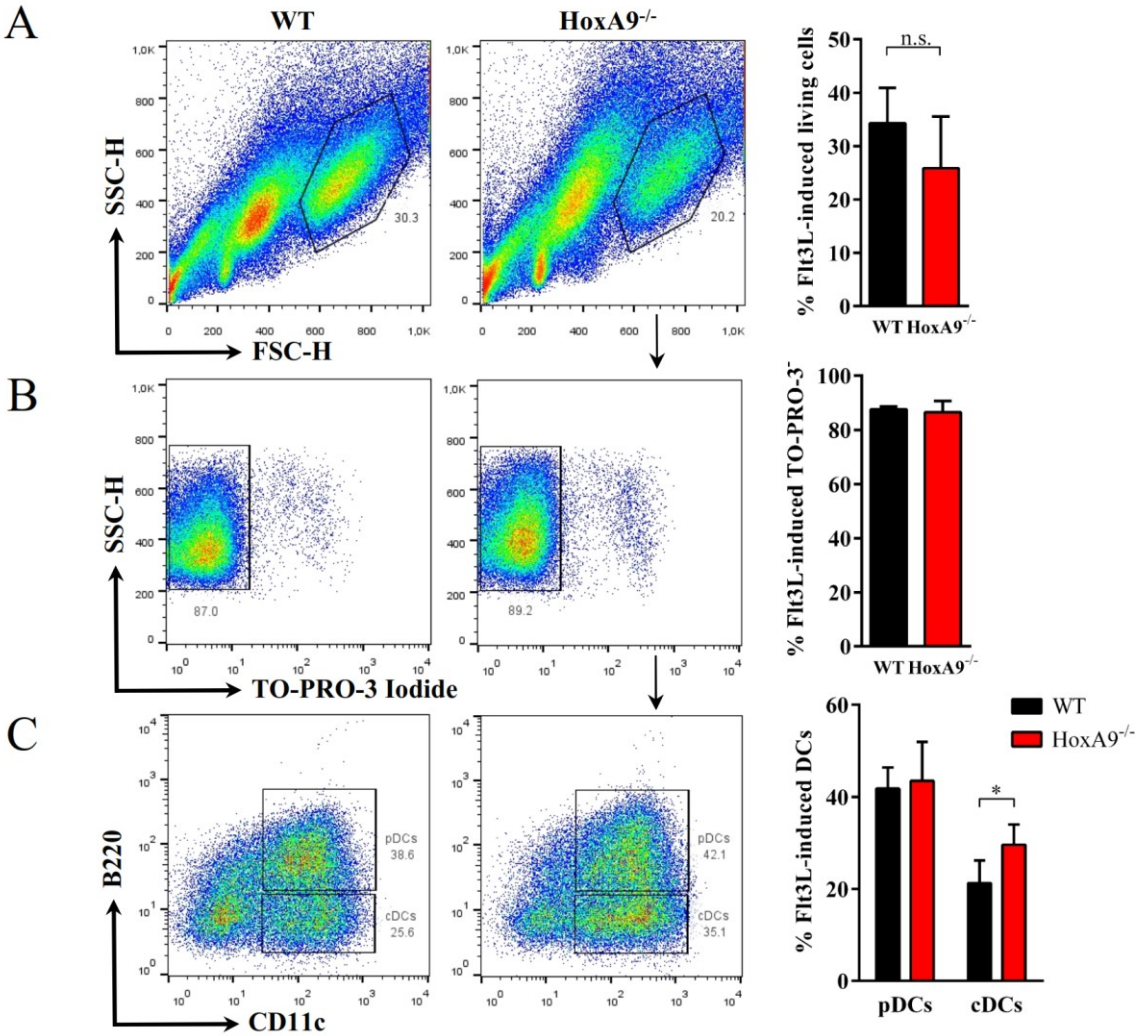

FIGURE 3.9 *FACS ANALYSIS OF* IN VITRO *GENERATED FLT3L-INDUCED DCS*
A) *FSC-H (size) and SSC-H (granularity) gate was used to discriminate dead cells from living cells.* ***B)*** *TO-PRO-3 Iodide positive stained cells were excluded from further flow cytometry analysis.* ***C)*** *Antibodies directed against DC-specific surface receptors B220 and CD11c were used to determine DC subset frequencies of Flt3L-induce cultures. PDCs are represented by the $B220^{+}CD11c^{+}$ population, whereas cDCs are $B220^{-}CD11c^{+}$ events. Figures A – C show one representative of five independently performed experiments. Bars and error bars represent means and standard deviations (n = 5 ± SD), respectively. The unpaired Student's t test was performed for statistical analyses (*, p < 0.05; n.s., not significant).*

Flt3, and CD11b. Living cells were roughly separated from dead cells and cell debris using the size (FSC-H) and granularity (SSC-H) of the cells (***FIGURE 3.9 A***). Interestingly, Flt3L-induced cultures from HoxA9-deficient BM cells reproducibly contained less events in the living cell fraction, albeit not statistically significant (mean, 25.83 % ± 9.69 versus 34.31 % ± 6.64, HoxA9$^{-/-}$ [n = 3 ± SD] versus WT [n = 3 ± SD], respectively; p = 0.145). To exclude the remaining dead cells, only TO-PRO-3 iodide negative gated cells were used for further analysis (***FIGURE 3.9 B***). TO-PRO-3 iodide negative cell populations were equally distributed in both genotypes. Again, B220 and CD11c staining was used to determine pDC and cDC frequencies. Notably, approximately 40 % of the differentiated cells in cultures of both genotypes represented B220^{+}CD11c^{+} pDCs with a marginally mean increase in HoxA9$^{-/-}$ cultures, whereas the cDC fraction (B220^{-}CD11c^{+}) was significantly increased when HoxA9 was lacking (***FIGURE 3.9 C***).

B220^{+}CD11c^{+} pDCs and B220^{-}CD11c^{+} cDCs were additionally stained for the DC-specific surface markers BST2, SiglecH, Ly6C, or Flt3 and CD11b or Flt3, respectively (***FIGURE 3.10***). Expression of BST2 in B220^{+}CD11c^{+} pDCs was not significantly altered in the HoxA9$^{-/-}$ fraction, whereas SiglecH showed a small reduction. Ly6C and Flt3 were not expressed at all in both genotypes. Interestingly, CD11b expression was increased in HoxA9 knockout cDCs and was also upregulated in pDCs, which normally do not express CD11b (Reizis et al., 2011).

In summary, flow cytometry of Flt3L-induced DC cultures from BM cells of HoxA9-deficient animals clearly show a lower percentage of events in the living cell gate (***FIGURE 3.9 A***). Among them, equal amounts of pDCs and a statistically significant increase of cDCs can be found. Further analyses show different expression of CD11b on pDCs and cDCs for HoxA9-deficient cultures.

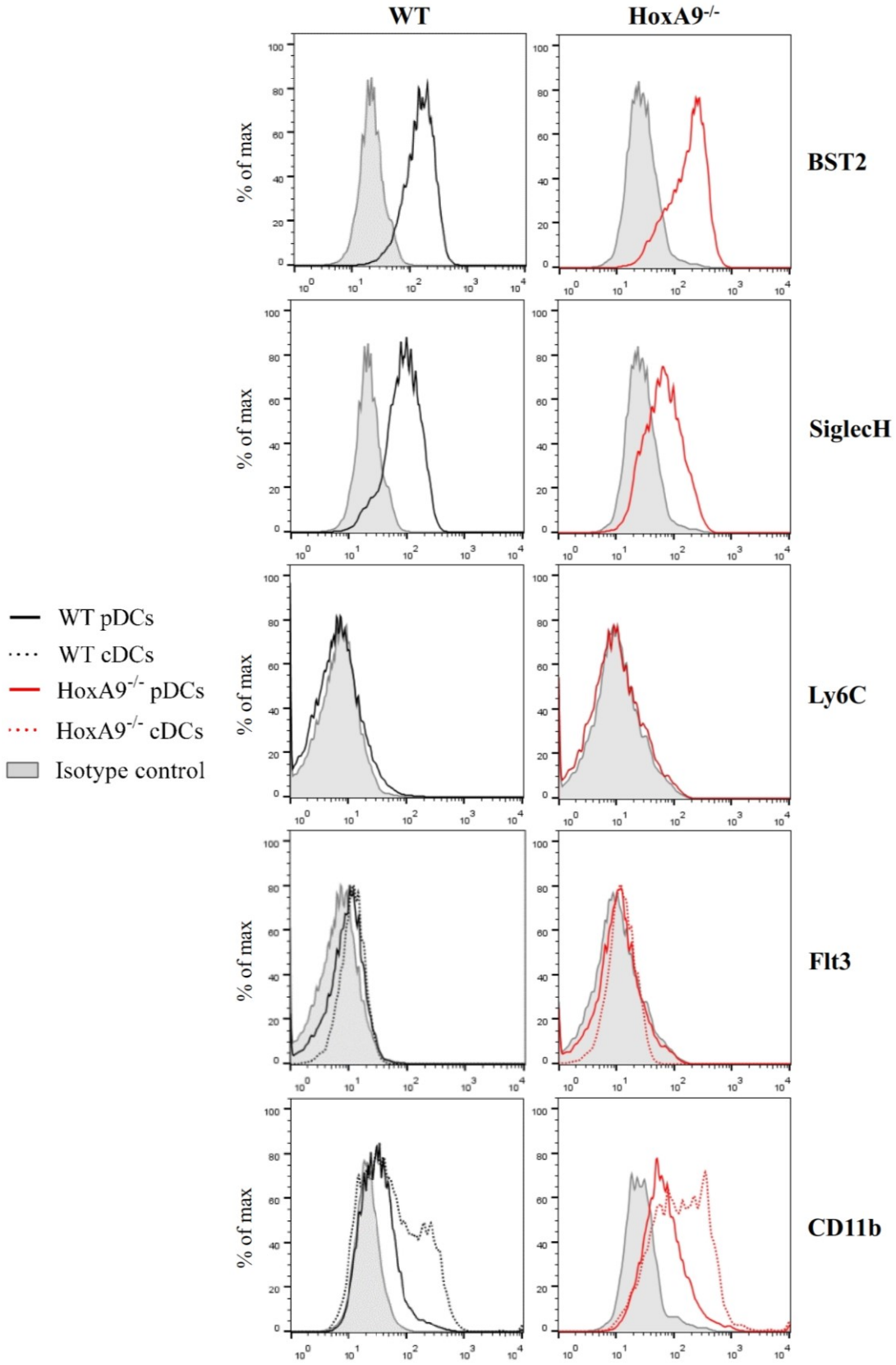

FIGURE 3.10 *ADDITIONAL FACS ANALYSIS OF* IN VITRO *GENERATED FLT3L-INDUCED DCS*
PDCs and cDCs were additionally stained for the surface markers BST2, SiglecH, Ly6C, Flt3, and CD11b. Shaded, black solid lined, black dotted lined, red solid lined, and red dotted lined histograms depict isotype control, WT pDCs, WT cDCs, HoxA9$^{-/-}$ pDCs, and HoxA9$^{-/-}$ cDCs, respectively. Each panel shows one representative experiment of at least 2 independently performed experiments.

3.2.3 TLR STIMULATION OF FLT3L-INDUCED HOXA9-DEFICIENT DCS REVEALS SIGNIFICANTLY ALTERED CYTOKINE RESPONSES

Stimulation of TLR7 and 9 in pDCs and TLR2, 3, 4, 7, and 9 in cDCs was performed for functional analysis of *in vitro* generated Flt3L-induced DC cultures. These experiments were carried out the same way as described for primary BM cells (see section 3.1.3), accept that 100.000 instead of 150.000 cells/well were seeded in 96-well plates.

FIGURE 3.11 A depicts one representative experiment and ***FIGURE 3.11 B*** shows statistical analyses of all three performed experiments. IFN-α responses upon TLR7 and 9 stimulation were almost completely abolished in HoxA9$^{-/-}$ DCs. These proportions were constantly observed throughout all experiments and, therefore, are statistically significant. The corresponding IL-6 levels were clearly reduced as well, however, not in the same amounts as IFN-α and only statistically significant for TLR7-induced IL-6 levels upon RNA40 stimulation. Conversely, TLR4-mediated IL-6 induction was significantly increased in the knockout group. Pam-3-Cys-dependent TLR2 activation led to meanly increased IL-6 levels, but showed a big variability. Poly I:C again did not induce any cytokine responses. ***TABLE 3.4*** includes all statistical data.

Summarizing the facts, functional analyses of DCs in Flt3L-induced *in vitro* cultures reveal a profound block of IFN-α responses and notable reduction of IL-6 upon TLR7/9 ligation when HoxA9 is lacking. TLR4-mediated IL-6 levels are significantly increased in the KO cultures, whereas TLR2-driven IL-6 responses are slightly increased but not significantly altered upon stimulation with Pam-3-Cys.

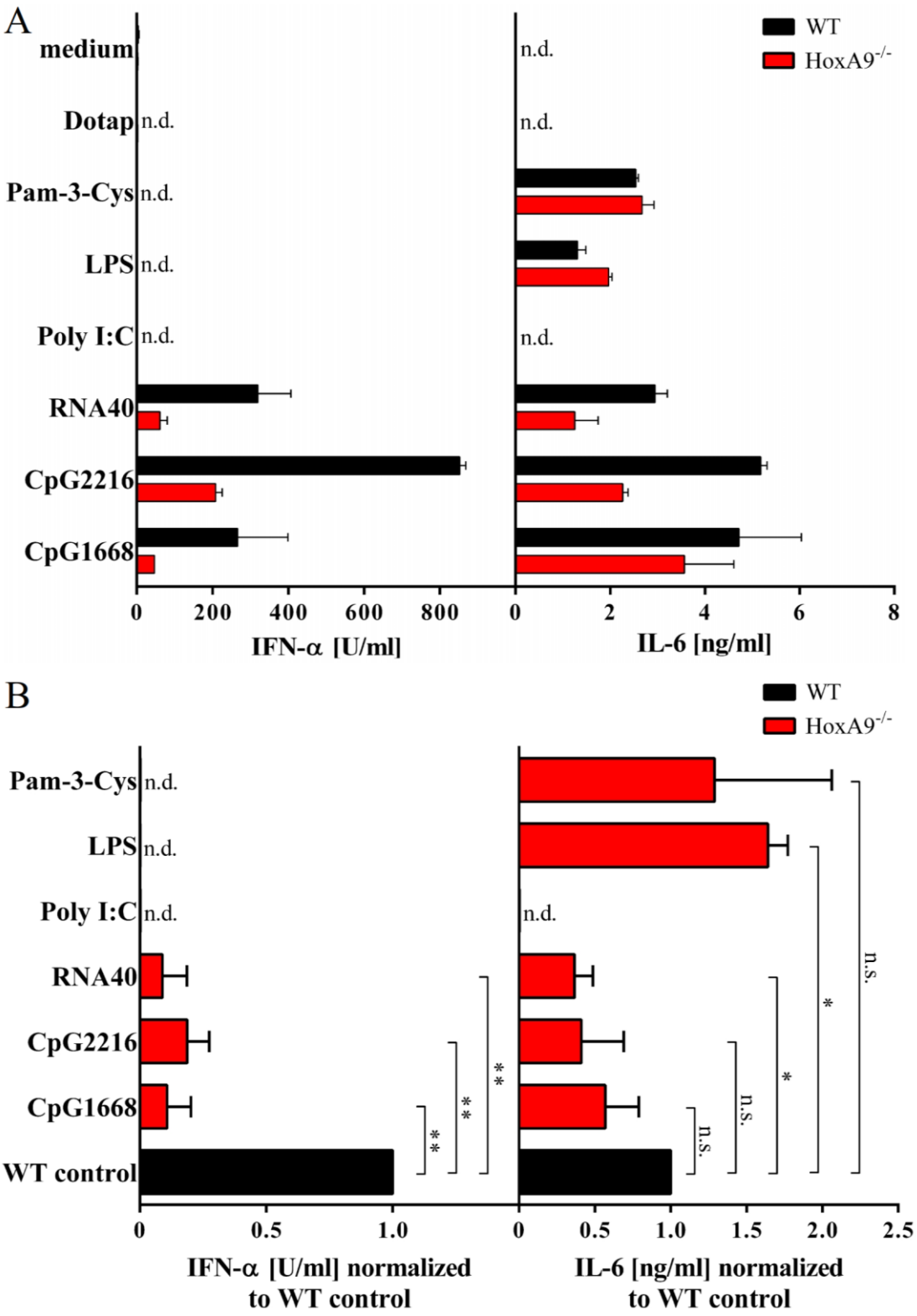

FIGURE 3.11 *TLR STIMULATION OF* IN VITRO *GENERATED FLT3L-INDUCED DCS*
A) *TLR2, 3, 4, 7, and 9 were stimulated with Pam-3-Cys[5µg/ml], Poly I:C[10µg/ml], LPS[1µg/ml], RNA40[10µg/ml], and CpG1668[1µM]/CpG2216[1µM], respectively. 100.000 cells were suspended in 100 µl medium per well and incubated with 100 µl diluted stimulus or medium/DOTAP control in 96-well plates for 18h overnight. Subsequently, murine IFN-α and IL-6 were detected by ELISA measured in dublicates (n.d., not detectable). One representative experiment of three independently performed experiments is shown.* ***B)*** *IFN-α and IL-6 production of HoxA9$^{-/-}$ Flt3L-induced DCs were normalized to WT control taken as 1. Statistical analyses of three independent experiments were performed using the paired Student's t test (*, $p < 0.05$; **, $p < 0.01$; n.s., not significant; n.d., not detectable). Bars and error bars represent means and standard deviations (SD), respectively.*

TABLE 3.4 *STATISTICAL DATA OF TLR STIMULATION OF FLT3L-INDUCED DCS*

STIMULUS	TLR	CYTOKINE	HOXA9$^{-/-}$ NORMALIZED TO WT CONTROL	P VALUE
CpG1668 [1µM]	9	IFN-α	0.108 ± 0.095 [n = 3 ± SD]	0.0037 (**)
		IL-6	0.568 ± 0.221 [n = 3 ± SD]	0.0772 (n.s.)
CpG2216 [1µM]	9	IFN-α	0.187 ± 0.088 [n = 3 ± SD]	0.0039 (**)
		IL-6	0.412 ± 0.279 [n = 3 ± SD]	0.0676 (n.s.)
RNA40 [10µg/ml]	7	IFN-α	0.089 ± 0.097 [n = 3 ± SD]	0.0038 (**)
		IL-6	0.366 ± 0.122 [n = 3 ± SD]	0.0120 (*)
Poly I:C [10µg/ml]	3	IFN-α	not detectable	-
		IL-6	not detectable	-
LPS [1µg/ml]	4	IFN-α	not detectable	-
		IL-6	0.164 ± 0.131 [n = 3 ± SD]	0.0137 (*)
Pam-3-Cys [5µg/ml]	2	IFN-α	not detectable	-
		IL-6	0.129 ± 0.774 [n = 3 ± SD]	0.5844 (n.s.)

Cytokine responses of HoxA9$^{-/-}$ Flt3L-induced DCs were normalized to WT control taken as 1 and statistical analyses of three independently performed experiments (means ± SD) were realized using the paired Student's t test (, $p < 0.05$; **, $p < 0.01$; n.s., not significant).*

3.3 ANALYSIS OF *IN VITRO* GENERATED GM-CSF-INDUCED DCS

3.3.1 GM-CSF-INDUCED HOXA9$^{-/-}$ CDCS DO NOT DIFFER FROM WT CDCS IN SURFACE EXPRESSION PATTERNS AND TLR FUNCTION

GM-CSF-supplemented BM cultures are known to generate inflammatory DCs derived from monocytes (Randolph et al., 1998), reflecting a subtype of cDCs. Furthermore, GM-CSF has the striking ability to inhibit Flt3L-dependent pDC generation (Gilliet et al., 2002; Watowich and Liu, 2010). Therefore, the next step was to use this setting to investigate the impact of HoxA9 on development and TLR function of the cDC subset *in vitro*. GM-CSF has been shown to selectively inhibit Flt3L-induced differentiation of DCs into pDCs via STAT5 (Esashi et al., 2008).

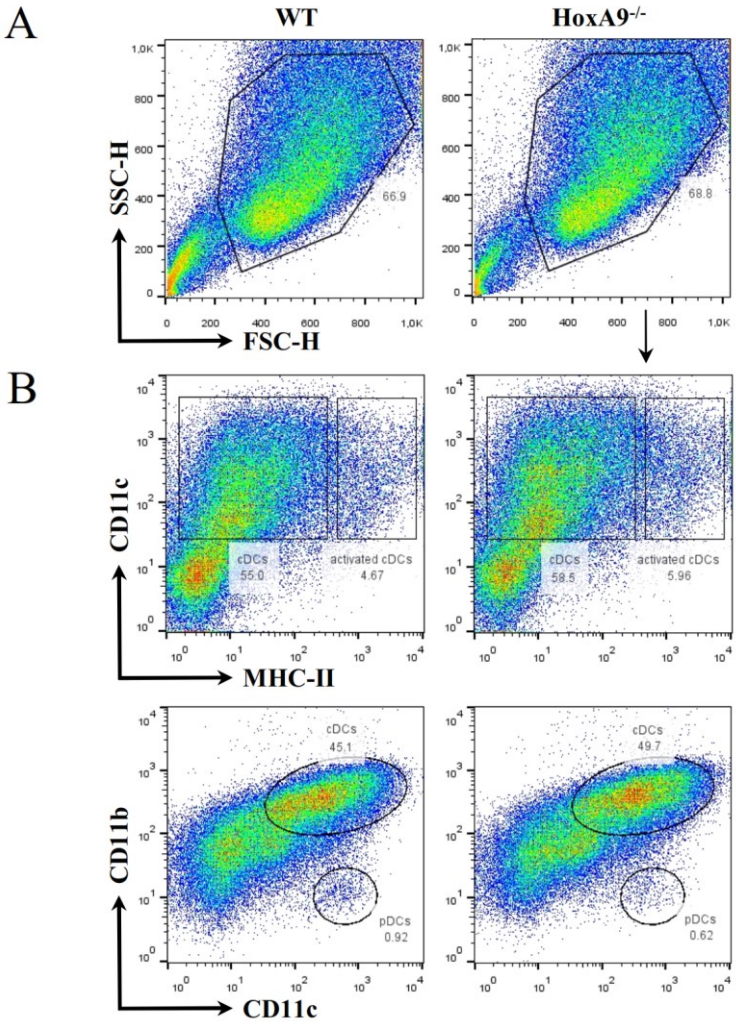

FIGURE 3.12 *FACS ANALYSIS OF* IN VITRO *GENERATED GM-CSF-INDUCED DCS*
A) *The FSC-H (size)/SSC-H (granularity) gate was used to exclude dead cells and cell debris.* ***B)*** *Antibodies directed against CD11c and MHC-II were used to determine frequencies of developed cDCs among GM-CSF-induced HoxA9$^{-/-}$ and WT cultures. Non-activated cDCs are represented by the CD11c^{+}MHC-II^{low} population. Already activated cDCs are depicted as CD11c^{+}MHC-II^{high} cells. The CD11c^{+} population was additionally stained for the integrin alpha chain CD11b. CD11c^{+}CD11b^{-} cells reflect pDCs. For all panels one representative experiment of two independently performed experiments is shown.*

6 x 10^6 freshly isolated BM cells were cultured in GM-CSF supplemented (supernatant of X6310 cell line culture) medium for 6 days at 37°C, 5 % CO_2, and 100 % humidity (see section 2.2.5 for details). Flow cytometric analysis with fluorochrome-labeled antibodies directed against CD11c, MHC-II, and CD11b were used to check the differentiation of the developed cells. Dead cells and cell debris were excluded by using the size (FSC-H) and granularity (SSC-H) of the cells (***FIGURE 3.12 A***). Cultures of both genotypes showed approximately 50 - 60 % $CD11c^+$ and MHC-II^{low} cells, reflecting differentiated non-activated cDCs. A small fraction of 4 - 6 % showed a $CD11c^+$MHC-II^{high} expression, indicating already activated cDCs. Almost all of the $CD11c^+$ cells also expressed CD11b, which is found on the cell surface of cDCs but not pDCs (***FIGURE 3.12 B***). A very small population of $CD11c^+CD11b^-$ cells probably reflect already differentiated BM pDCs before incubation with GM-CSF. ***FIGURE 3.12*** shows one representative out of two performed flow cytometry experiments. According to the results of the FACS analysis shown in ***FIGURE 3.12***, all surface markers are not differentially expressed on the KO cells.

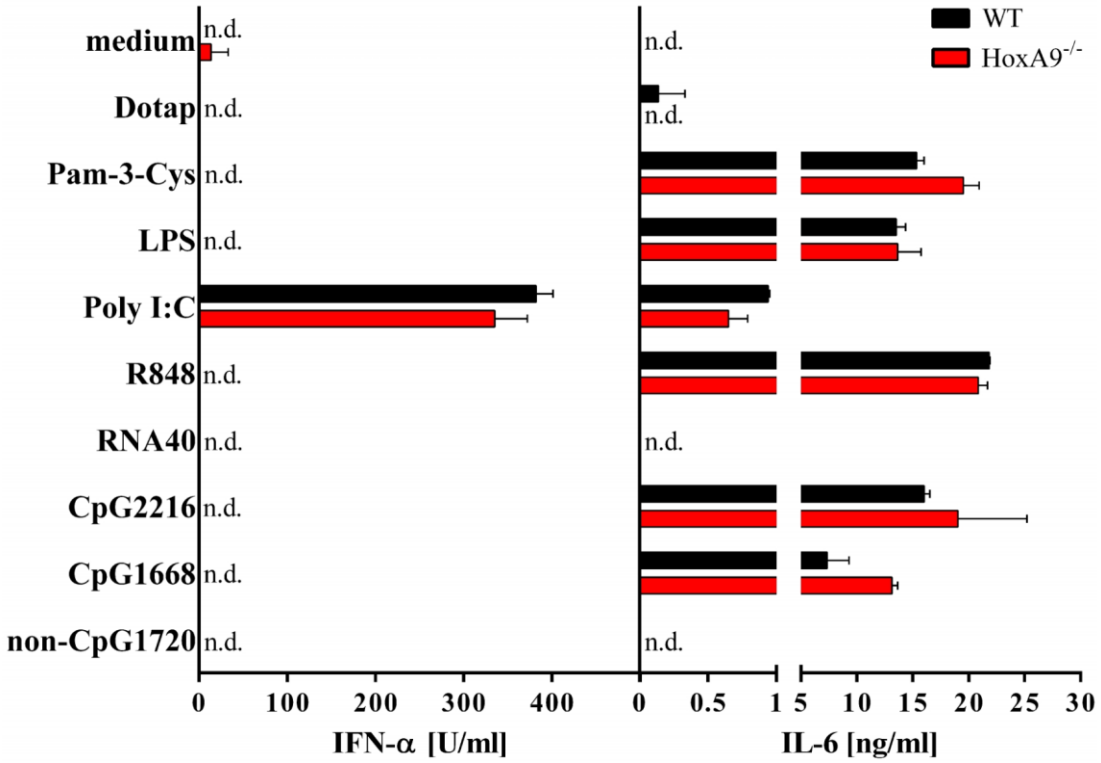

FIGURE 3.13 *TLR STIMULATION OF* IN VITRO *GENERATED GM-CSF-INDUCED DCS*
TLR2, 3, 4, 7, and 9 were stimulated with Pam-3-Cys[5µg/ml], Poly I:C[10µg/ml], LPS[1µg/ml], RNA40[10µg/ml]/R848[5µg/ml], and non-CpG1720[1µM]/CpG1668[1µM]/CpG2216[1µM], respectively. 300.000 cells were suspended in 100 µl medium per well and incubated with 100 µl diluted stimulus or medium/DOTAP control in 96-well plates for 18h overnight. Subsequently, murine IFN-α and IL-6 were detected by ELISA measured in dublicates (n.d., not detectable). Each panel shows one representative of two independently performed experiments. Bars and error bars represent means and standard deviations (SD), respectively.

Functional analysis of TLRs in GM-CSF-derived cDCs were carried out using the same protocol as described above for BM cells and Flt3L-induced DCs. The number of cells seeded per well was 300.000. Stimulation of TLR2, 3, 4, 7, and 9 was performed using Pam-3-Cys, Poly I:C, LPS, RNA40/R848, and non-CpG1720/CpG1668/CpG2216, respectively. IL-6 and IFN-α responses were again measured by ELISA. Poly I:C from Invivogen™, which was used in former experiments, was replaced by Poly I:C from GE healthcare™. For the first time, Poly I:C-mediated IFN-α and IL-6 induction upon TLR3 activation was achieved. The levels of both cytokines were not significantly altered in the KO group compared to the WT ones. All TLR7 and 9 stimuli did not prompt any IFN-α responses. Surprisingly, RNA40 did not induce IL-6 responses at all in both experiments. One representative of two performed experiments is shown in ***FIGURE 3.13***.

Altogether, neither expression patterns of surface markers nor functional analyses by stimulating TLRs display any significant difference between HoxA9-deficient and WT GM-CSF-induced cDCs/inflammatory DCs.

3.4 ANALYSIS OF *IN VITRO* GENERATED M-CSF-INDUCED MΦS AND DCS

3.4.1 M-CSF-DERIVED HOXA9$^{-/-}$ MΦS ARE NORMAL IN TLR FUNCTION AND EXPRESSION OF CELL SURFACE MARKERS

Another cell subset responsible for innate immune reactions are MΦs, which express a broad range of PRRs including many TLRs. The expression profile of the latter in murine MΦs is quite similar to cDCs, especially referring to intracellular TLRs and their signaling pathways (Blasius and Beutler, 2010). TLR7 and 9 activation and further downstream signaling leads to proinflammatory cytokine responses and upregulation of MHC and co-stimulatory molecules via the transcription factor NFκB. Type I IFN production in MΦs is solely dependent on sensing dsRNA via TLR3 and is not mediated by TLR7 or 9, identically to cDCs (Blasius and Beutler, 2010).

To examine TLR function in HoxA9$^{-/-}$ MΦs, freshly isolated BM cells from both genotypes were cultured with medium supplemented with the growth factor M-CSF for 5 days at 37°C, 5 % CO_2, and 100 % humidity (see section 2.2.6 for details). The quality of *in vitro* generated MΦs was tested by FACS analysis using fluorescence-labeled antibodies directed against the best known marker of mature murine macrophages F4/80 (Austyn and Gordon, 1981; Hirsch et al., 1981). F4/80 is a transmembrane protein expressed on several kinds of MΦs and is probably involved in immune tolerance (Lin et al., 2005). An antibody against MHC-I was additionally applied to flow cytometry samples, as MΦs express high amounts of major histocompatibility complexes on their plasma membrane for antigen presentation. Dot plots with FSC-H and SSC-H of both genotypes in ***FIGURE 3.14 A*** depict the gated living cell fractions, which were checked for F4/80 and MHC-I expression shown in ***FIGURE 3.14 B***. MΦs lacking HoxA9 did not significantly differ in cell surface expression of the used markers.

Generated MΦs were functionally analyzed by TLR stimulation experiments according to the protocol described above (see section 2.2.7 for details). 200.000 cells/well were seeded in 96-well plates and stimulated with Pam-3-Cys, Poly I:C, LPS, RNA40/R848, and non-CpG1720/CpG1668/CpG2216 to activate TLR2, 3, 4, 7, and 9, respectively. Subsequent IL-6 and IFN-α responses were detected by ELISA. ***FIGURE 3.14 C*** shows one representative of two performed experiments. Both, IL-6 and IFN-α levels did not prominently differ between the two genotypes, accept IL-6 production upon

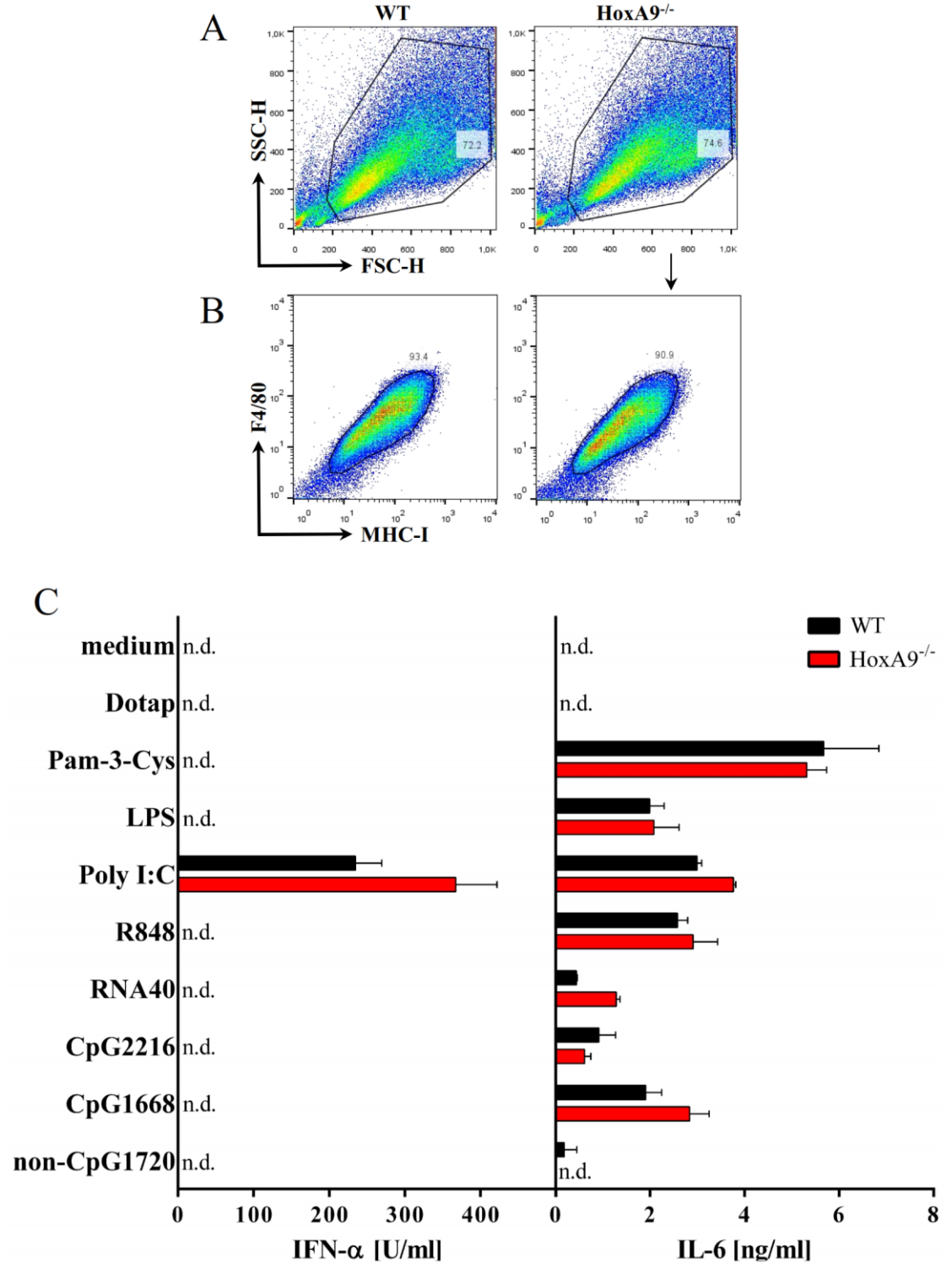

FIGURE 3.14 *FACS ANALYSIS AND TLR STIMULATION OF M-CSF-INDUCED MΦS*
A) *FSC-H (size)/SSC-H (granularity) gate was used to discriminate living cells from dead cells and cell debris* ***B)*** *Fluorochrome-labeled antibodies directed against F4/80 and MHC-I were used to determine quality of developed MΦs of M-CSF-supplemented HoxA9$^{-/-}$ and WT cultures.* ***C)*** *TLR2, 3, 4, 7, and 9 were stimulated with Pam-3-Cys[5µg/ml], Poly I:C[10µg/ml], LPS[1µg/ml], RNA40[10µg/ml]/R848[5µg/ml], and non-CpG1720[1µM]/CpG1668[1µM]/CpG2216[1µM], respectively. 200.000 cells were suspended in 100 µl medium per well with 100 µl diluted stimulus or medium/DOTAP control in 96-well plates for 18h overnight. Subsequently, murine IFN-α and IL-6 were detected by ELISA measured in dublicates (n.d., not detectable). Each panel shows one representative of two independently performed experiments. Bars and error bars represent means and standard deviations (SD), respectively.*

RNA40-induced TLR7 activation, which was increased (289.19 %) in one and reduced (60.34 %) in the other experiment for the KO MΦs. Importantly, IFN-α induction by TLR3 activation was slightly increased in one and slightly decreased in the other experiment, thus showing no significant difference.

In summary, HoxA9-deficient MΦs derived from *in vitro* generated M-CSF-supplemented BM cultures express mature cell surface markers and elicit equal cytokine levels in response to TLR2, 3, 4, 7, and 9 activation compared to wild type MΦs.

3.4.2 FREQUENCIES OF DCS AMONG SUSPENSION CELLS ARE CLEARLY REDUCED IN HOXA9$^{-/-}$ M-CSF-SUPPLEMENTED CULTURES

M-CSF-supplemented BM cultures are capable to drive differentiation from HSCs to MΦs, which are known to be adherent cells with their characteristic morphology. However, numerous cells of these cultures are found to be non-adherent and Francke et al. showed that differentiated cDCs and especially pDCs can be found amongst them (Fancke et al., 2008). Furthermore, M-CSF was shown to generate splenic pDCs and cDCs in Flt3L$^{-/-}$ mice *in vivo* (Fancke et al., 2008). In addition, M-CSF seems to be also important for migratory cDCs found in the gut, peripheral tissues, and Langerhans cells in the skin (Watowich and Liu, 2010). To check involvement of HoxA9 in M-CSF-induced DC generation *in vitro*, all suspension cells were separated from adherent cells (see section 2.2.6 for details) and investigated by flow cytometry analysis using DC-specific surface markers.

After marking the living cell fraction in the FSC-H/SSC-H dot plot, fluorochrome-labeled antibodies directed against B220, CD11c, BST2, and CD11b were used to detect differentiated DCs. ***FIGURE 3.15 A*** shows one of two performed experiments. PDCs were found as B220^{+}CD11c^{+}, BST2^{+}B220^{+}, and CD11c^{+}CD11b^{-} cell populations with a percentage of approximately 3 % in WT and 1.5 % in KO cultures among all suspension cells. In addition, CD11b^{+}CD11c^{+} cells were found in the cultures, reflecting cDCs, with similarly reduced proportions in the KO cultures (***FIGURE 3.15 A*** CD11c/CD11b dot plot). Both experiments exhibited about half as much pDCs and cDCs in cultures lacking HoxA9 compared to WT cultures.

TLR stimulation of total suspension cells was done in the aforementioned way to check functional properties of the developed DC subsets among them. 150.000 cells/well were seeded in 96-well plates and faced with same stimuli used for MΦs. ***FIGURE 3.15 B***

depicts one of two performed experiments. IFN-α induction upon TLR7/9 activation of pDCs was even stronger reduced in the KO samples compared to primary BM cells. Considering approximately 50 % less differentiated pDCs, the decrease of IFN-α was about comparable to the one observed for primary BM cells. The CpG-motif free ODNs AP-1 and 1720 did again also induce less amounts of IFN-α in the KO pDCs as CpG-motif containing ODNs, whereas IL-6 was not detectable. R848 elicited very small amounts of IFN-α in WT cultures, with no response in the KO cultures. IL-6 levels upon TLR7/9 stimulation were less reduced than the IFN-α levels. In view of the differentiated DC proportions, IL-6 was rather slightly increased after stimulation of the KO cultures. Poly I:C-dependent IFN-α and IL-6 levels upon TLR3 stimulation were about equal, as well as Pam-3-Cys- and LPS-induced IL-6 secretion.

Taken together, total M-CSF-induced suspension cells of HoxA9-deficient BM cells contained approximately 50 % less amounts of pDCs as well as cDCs. IFN-α reductions in HoxA9$^{-/-}$ cultures upon TLR7 and 9 stimulation were similar to those found in primary BM cells, considering the differentiated pDC proportions in both genotypes. IL-6 levels were rather slightly increased regarding the reduced DC amounts.

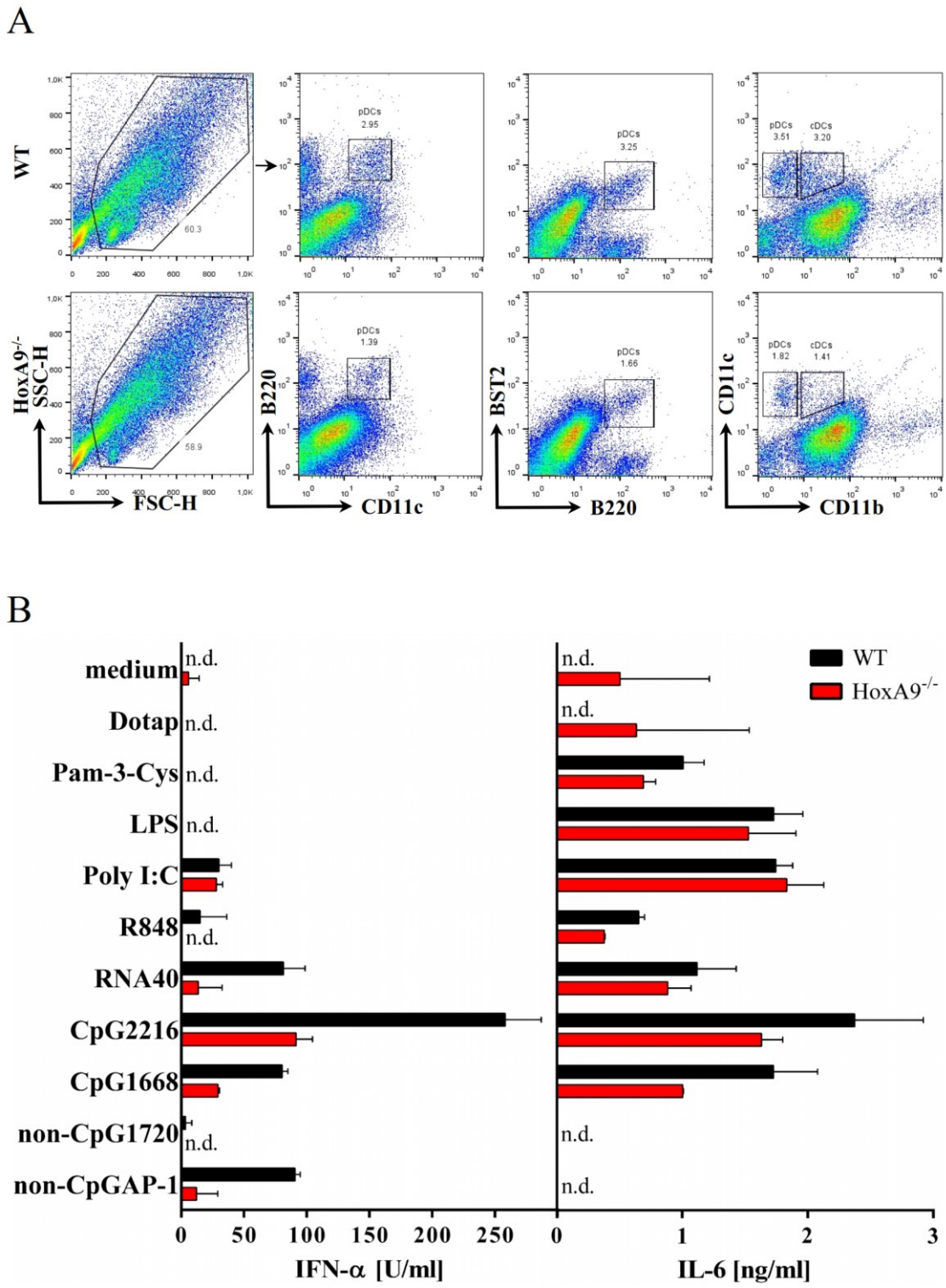

FIGURE 3.15 *FACS ANALYSIS AND TLR STIMULATION OF M-CSF-INDUCED SUSPENSION CELLS*

A) *FSC-H (size)/SSC-H (granularity) gate was used to discriminate living cells from dead cells and cell debris. Fluorochrome-labeled antibodies directed against B220, CD11c, BST2, and CD11b were used to determine percentages of pDCs in M-CSF-induced HoxA9$^{-/-}$ and WT cultures.* ***B)*** *TLR2, 3, 4, 7, and 9 were stimulated with Pam-3-Cys[5µg/ml], Poly I:C[10µg/ml], LPS[1µg/ml], RNA40[10µg/ml]/R848[5µg/ml], and non-CpGAP-1[1µM]/non-CpG1720[1µM]/CpG1668[1µM]/ CpG2216[1µM], respectively. 150.000 cells were suspended in 100 µl medium per well with 100 µl diluted stimulus or medium/DOTAP control in 96-well plates for 18h overnight. Subsequently, murine IFN-α and IL-6 were detected by ELISA measured in dublicates (n.d., not detectable). Each panel shows one representative of two independently performed experiments. Bars and error bars represent means and standard deviations (SD), respectively.*

3.5 ANALYSIS OF SPLENOCYTES *EX VIVO*

3.5.1 SPLENIC DC SUBSETS OF HOXA9$^{-/-}$ ANIMALS EXPRESS MATURE SURFACE MARKERS

Besides the existing DC population in the BM, DCs are of course also found in peripheral tissues and lymphoid organs including the spleen to function as pathogen recognizing "sentinels", able to prompt first line defense mechanisms and to induce long-lasting adaptive immune responses (Watowich and Liu, 2010). To analyze quantities, expression

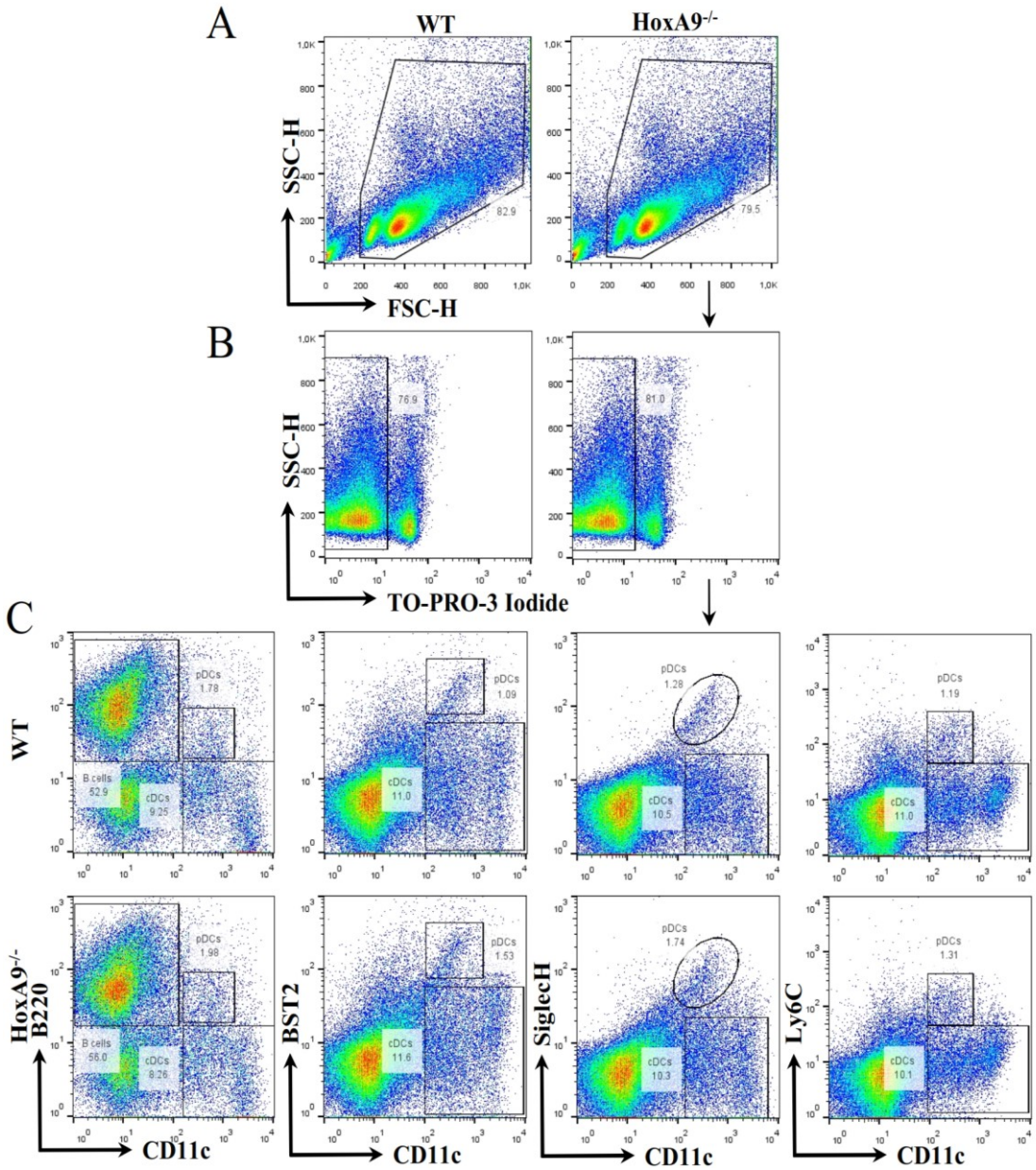

FIGURE 3.16 *FACS ANALYSIS OF SPLENOCYTES* EX VIVO

A) *FSC-H (size)/SSC-H (granularity) gate was used to discriminate living cells from dead cells and cell debris.* ***B)*** *TO-PRO-3 Iodide stained cells were excluded from further flow cytometry analysis.* ***C)*** *Fluorochrome-labeled antibodies directed against B220, CD11c, BST2, SiglecH, and Ly6C were used to determine frequencies of DC subsets among HoxA9$^{-/-}$ and WT splenocytes. PDCs are represented by the B220^{+}CD11c^{+}, BST2^{+}CD11c^{+}, SiglecH^{+}CD11c^{+}, or Ly6C^{+}CD11c^{+} population, whereas single CD11c^{+} cells depict cDCs. Each panel shows one representative of two independently performed stainings.*

patterns, and TLR function of primary resident DCs found in lymphoid organs, total splenocytes were isolated from HoxA9-deficient and WT mice to investigate splenic DC subsets. Total splenocytes of KO and WT mice were isolated by cutting spleens into pieces and incubating the pieces in a special spleen isolation medium including Collagenase D and DNAse for 45 min at 37°C. After mashing the pieces through a 70 µm cell strainer and lysis of the erythrocytes, leucocytes were isolated from the remaining cell fractions by using ficoll gradient separation (see section 2.2.3. for details).

Flow cytometry analyses with the DC-specific markers B220, CD11c, BST2, SiglecH, Ly6C, Flt3, and CD11b were performed to determine frequencies and expression patterns of surface markers. ***FIGURE 3.16 A*** shows separation of living cells from dead cells and cell debris by detecting the size (FSC-H) and granularity (SSC-H) of the cells. TO-PRO-3 iodide staining was used to exclude the remaining dead cells (***FIGURE 3.16 B***). Significant differences between both genotypes regarding proportions of living or dead cells were not observed. ***FIGURE 3.16 C*** depicts one representative of two independently performed experiments of each staining. One experiment showed slightly increased (shown in ***FIGURE 3.16 C***) and the other a rather small decrease (data not shown) of HoxA9-deficient splenic pDCs. The cDC fraction in the spleen was higher (pDC/cDC ratio nearly 1:6) compared to the BM (pDC/cDC ratio nearly 1:1 – 1.5), but equally amounted among WT and KO splenocytes. $B220^+CD11c^+$ pDCs as well as $B220^-$ $CD11c^+$ cDCs were additionally stained for BST2, SiglecH, Ly6C, or Flt3 and Flt3 or CD11b, respectively. Expression patterns of all DC-specific markers were not altered in the KO splenocytes compared to WT (***FIGURE 3.17***). Single $B220^+$ B cells were equally distributed.

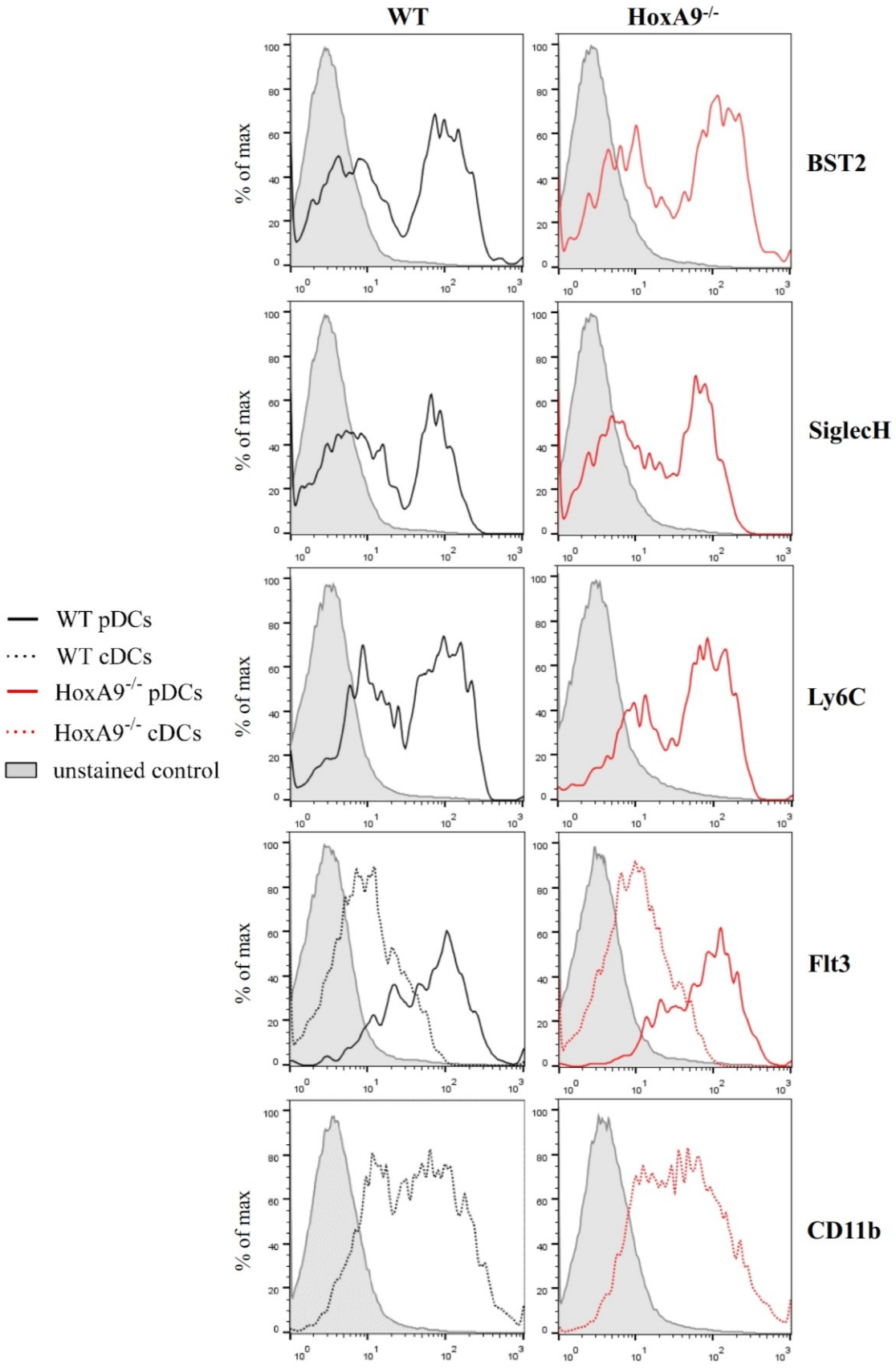

FIGURE 3.17 *ADDITIONAL FACS ANALYSIS OF SPLENOCYTES* EX VIVO

PDCs ($B220^+CD11c^+$ cells) were additionally stained for the surface markers BST2, SiglecH, Ly6C, and Flt3. CDCs ($B220^-CD11c^+$ cells) were additionally stained for the surface markers Flt3 and CD11b. Shaded, black solid lined, black dotted lined, red solid lined, and red dotted lined histograms depict unstained control, WT pDCs, WT cDCs, HoxA9$^{-/-}$ pDCs, and HoxA9$^{-/-}$ cDCs, respectively. Each panel shows one representative experiment of two independently performed experiments.

3.5.2 CYTOKINE RESPONSES UPON TLR7/9 STIMULATION ARE IMPAIRED IN TOTAL SPLENOCYTES *EX VIVO*

Investigation of TLR function of HoxA9$^{-/-}$ DCs was performed by stimulating freshly isolated total splenocytes with TLR agonists according to the protocol described in section 2.2.6. Pam-3-Cys, Poly I:C, LPS, RNA40/R848, and non-CpGAP-1/non-CpG1720/CpG1668/CpG2216 were used to activate TLR2, 3, 4, 7, and 9, respectively. After 18 h of incubation at 37°C, 5 % CO_2, and 100 % humidity, IL-6 and IFN-α production were detected in the cell supernatants by performing ELISA. ***FIGURE 3.18*** illustrates results of one representative out of two performed experiments. Confirming previous data, IFN-α levels detected in the KO samples were clearly diminished upon TLR7 and 9 stimulation of all agonists, whereas TLR3-mediated IFN-α induction was not different to WT control. TLR9-dependent IL-6 secretion of HoxA9$^{-/-}$ splenocytes was slightly reduced after stimulation with CpG1668 and CpG2216 in both experiments, whereas non-CpGAP-1 and non-CpG1720 did not induce detectable IL-6 levels. TLR7-mediated IL-6 production induced by R848 was also slightly increased in KO samples,

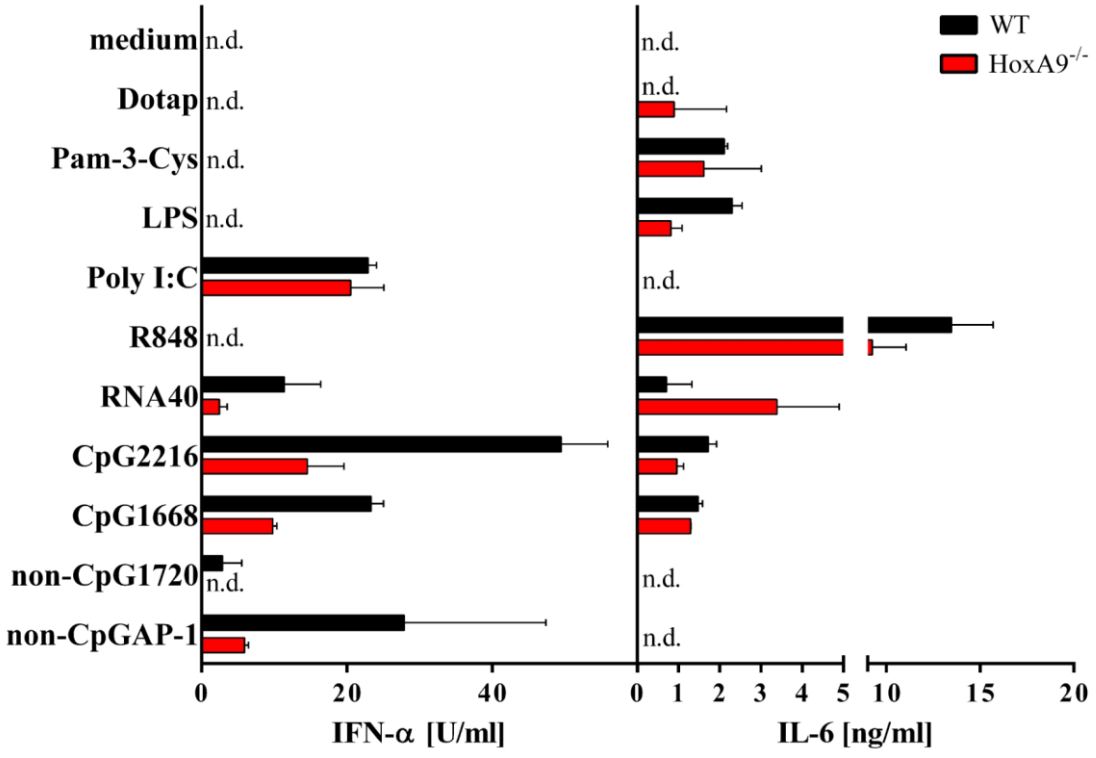

FIGURE 3.18 *TLR STIMULATION OF SPLENOCYTES* EX VIVO
TLR2, 3, 4, 7, and 9 were stimulated with Pam-3-Cys[5µg/ml], Poly I:C[10µg/ml], LPS[1µg/ml], RNA40[10µg/ml]/R848[5µg/ml], and non-CpGAP-1[1µM]/non-CpG1720[1µM]/CpG1668[1µM]/CpG2216, respectively. 200.000 cells were suspended in 100 µl medium per well with 100 µl diluted stimulus or medium/DOTAP control in 96-well plates and incubated for 18h overnight. Subsequently, murine IFN-α and IL-6 were detected by ELISA measured in dublicates (n.d., not detectable). One representative of two independently performed experiments is shown. Bars and error bars represent means and standard deviations (SD), respectively.

whereas RNA40 surprisingly elicited increased IL-6 in both experiments. Stimulation with Pam-3-Cys and LPS as TLR2 and 4 activating agents, respectively, led to equal IL-6 proportions in one and slightly or clearly decreased mean IL-6 levels for the KO splenocytes in the other experiment.

In summary, flow cytometry analyses of *ex vivo* isolated HoxA9$^{-/-}$ splenocytes revealed overall normal amounts of both DC subsets with equal expression of DC-specific surface markers including the cytokine receptor Flt3. Of note, TLR7/9-dependent IFN-α responses were again reproducibly impaired in HoxA9 knockout pDCs, consistent to the findings in BM-derived primary and *in vitro* generated pDCs. TLR3-mediated type I IFN induction was not affected by the KO.

3.6 GENOME-WIDE GENE EXPRESSION PROFILING BY MICROARRAY ANALYSIS OF *EX VIVO* SORTED HOXA9$^{-/-}$ BM PDCS

Several TLR stimulation experiments of different primary and *in vitro* generated DCs collectively indicated dysfunctions of murine HoxA9$^{-/-}$ pDCs upon TLR7/9-dependent IFN-α responses and some evidence suggested also involvement of proinflammatory cytokines, represented by IL-6, as well. As TLR7/9-mediated cytokine responses were not significantly altered in *in vitro* generated cDCs and MΦs, the HoxA9 knockout seems to impact specifically on pDCs. Moreover, alterations in cell counts and surface expression patterns of Flt3L-induced DC cultures *in vitro* implicated HoxA9 in developmental processes, however, which seemed to be compensated *in vivo*. For HoxA9 is known as a transcription factor that was shown to have multiple transcriptional targets and is associated to epigenetic modifications in human hematopoietic cells (Huang et al 2012), genome-wide gene expression profiling of *ex vivo* sorted HoxA9$^{-/-}$ and WT BM pDCs was performed by microarray analysis to identify potential HoxA9 target genes in this particular cell type.

Total RNA from pooled *ex vivo* sorted BM pDCs (B220^{+}CD11c^{+} cells) of HoxA9 KO and WT animals (pooled BM cells of 4 mice per genotype) was purified using Trizol according to the protocol described in section 2.2.10. 1 µg of RNA was sent to the "Expression Core Facility" of the Institute for Medical Microbiology, Immunology, and Hygiene of the Technical University of Munich under the direction of Prof. Dr. med. D. H. Busch. After reverse transcription, amplification, and labeling, the cDNA was hybridized to Affymetrix Mouse Genome 1.0 ST arrays (28.853 probe set) for genome-wide microarray gene expression profiling. Robust Multi-array Average (RMA) normalization was performed to adjust systematic errors.

Pairwise comparison of raw microarray data of sorted HoxA9$^{-/-}$ and WT BM pDCs revealed a total of 68 downregulated genes ≥ 2-fold (WT/KO) and 38 upregulated genes ≤ 0.5-fold (WT/KO) in the knockout pDCs. All down- and upregulated genes are depicted in ***TABLES 3.4*** and ***3.5***, respectively. Underlined genes were shown to be significantly expressed in murine pDCs according to microarray metadata of the Immunological Genome Project consortium (www.immgen.org) (Heng et al., 2008).

TABLE 3.5 *DOWNREGULATED GENES OF SORTED HOXA9$^{-/-}$ BM PDCS*

Gene	Accession (Source)	Fold Change (WT/KO)	Description
Taf1d	BC056964 (GenBank)	8.1	TATA box binding protein (Tbp)-associated factor, RNA polymerase I, D
Rnu12	NR_004432 (RefSeq)	4.3	U12 small nuclear RNA
Snora3	NR_028079 (RefSeq)	4.1	Small nucleolar RNA, H/ACA box 3
Snord34	NR_002455 (RefSeq)	3.6	Small nucleolar RNA, C/D box 34
Snord104	NR_030703 (RefSeq)	3.6	Small nucleolar RNA, C/D box 104
Snora44	NR_034050 (RefSeq)	3.6	Small nucleolar RNA, H/ACA box 44
Snora34	NR_034051 (RefSeq)	3.5	Small nucleolar RNA, H/ACA box 34
Snora69	NR_002900 (RefSeq)	3.5	Small nucleolar RNA, H/ACA box 69
Snora16a	NR_029412 (RefSeq)	3.4	Small nucleolar RNA, H/ACA box 16A
Snord33	NR_001277 (RefSeq)	3.4	Small nucleolar RNA, C/D box 33
Myo9a	NM_173018 (RefSeq)	3	Myosin IXa
Snord35b	NR_000004 (RefSeq)	2.9	Small nucleolar RNA, C/D box 35B
Snhg1	AK051045 (GenBank HTC)	2.9	Small nucleolar RNA host gene 1
Snora7a	NR_028546 (RefSeq)	2.9	Small nucleolar RNA, H/ACA box 7A
Klra10	NM_008459 (RefSeq)	2.8	Killer cell lectin-like receptor subfamily A, member 10
Rnu2	NR_004414 (RefSeq)	2.8	U2 small nuclear RNA
Cdkn1b	NM_009875 (RefSeq)	2.7	Cyclin-dependent kinase inhibitor 1B
Cd8a	NM_001081 110 (RefSeq)	2.7	Cluster of differentiation 8 alpha chain, transcript variant 1
Snord32a	NR_000002 (RefSeq)	2.7	Small nucleolar RNA, C/D box 32A
Snord35a	NR_000003 (RefSeq)	2.7	Small nucleolar RNA, C/D box 35A
Naf1	NM_001163 564 (RefSeq)	2.7	Nuclear assembly factor 1 homolog (S. cerevisiae)
Hsd11b1	NM_008288 (RefSeq)	2.7	Hydroxysteroid 11-beta dehydrogenase 1, transcript variant 1

Uchl3	NM_016723 (RefSeq)	2.6	Ubiquitin carboxyl-terminal esterase L3
Mir421	NR_030558 (RefSeq)	2.6	MicroRNA 421
Hist1h2bb	NM_175664 (RefSeq)	2.5	Histone cluster 1, H2bb
Emp1	NM_010128 (RefSeq)	2.4	Epithelial membrane protein 1
Rnu73b	NR_004418 (RefSeq)	2.4	U73B small nuclear RNA
Dpp4	NM_010074 (RefSeq)	2.3	Dipeptidylpeptidase 4, transcript variant 1
Snord47	NR_028543 (RefSeq)	2.3	Small nucleolar RNA, C/D box 47
Gas5	NR_002840 (RefSeq)	2.3	Growth arrest specific 5, non-coding RNA
Snora20	NR_028479 (RefSeq)	2.3	Small nucleolar RNA, H/ACA box 20
Scrn1	NM_027268 (RefSeq)	2.3	Secernin 1
Gng5	NM_010318 (RefSeq)	2.3	Guanine nucleotide binding protein (G protein), gamma 5
Snora73b	NR_028513 (RefSeq)	2.3	Small nucleolar RNA, H/ACA box 73b
Olfr767	NM_146318 (RefSeq)	2.3	Olfactory receptor 767
Mrpl13	NM_026759 (RefSeq)	2.3	Mitochondrial ribosomal protein L13, nuclear gene encoding mitochondrial protein
Rpgrip1	NM_023879 (RefSeq)	2.2	Retinitis pigmentosa GTPase regulator interacting protein 1, transcript variant 1
Snora73a	NR_028512 (RefSeq)	2.2	Small nucleolar RNA, H/ACA box 73a
D14Abb1e	NM_001114 879 (RefSeq)	2.2	DNA segment, Chr 14, Abbott 1 expressed, transcript variant 1
Ywhaq	NM_011739 (RefSeq)	2.2	Tyrosine 3-monooxygenase/ tryptophan 5-monooxygenase activation protein, theta polypeptide
Apol9b	NM_173743 (RefSeq)	2.2	Apolipoprotein L 9b, transcript variant 2
Myo18b	NM_028901 (RefSeq)	2.2	Myosin XVIIIb
Fam133b	NM_001042 501 (RefSeq)	2.2	Family with sequence similarity 133, member B
Slc44a1	ENSMUST0 0000107651 (ENSEMBL)	2.2	Solute carrier family 44, member 1

Ftl1	NM_010240 (RefSeq)	2.2	Ferritin light chain 1
Rny3	NR_024202 (RefSeq)	2.1	Y3 small cytoplasmic (associated with Ro protein), small cytoplasmic RNA
Gdap10	BC052902 (GenBank)	2.1	Ganglioside-induced differentiation-associated-protein 10
Snord87	NR_004410 (RefSeq)	2.1	Small nucleolar RNA, C/D box 87
Mir297b	NR_030474 (RefSeq)	2.1	MicroRNA 297b
Adam19	NM_009616 (RefSeq)	2.1	A disintegrin and metallopeptidase domain 19 (meltrin beta)
Anxa4	NM_013471 (RefSeq)	2.1	Annexin A4
Rnu3b1	NR_004415 (RefSeq)	2.1	U3B small nuclear RNA 1
Snord82	NR_002851 (RefSeq)	2.1	Small nucleolar RNA, C/D box 82
Cd209d	NM_130904 (RefSeq)	2	Cluster of differentiation 209d
Snord14e	NR_028275 (RefSeq)	2	Small nucleolar RNA, C/D box 14E
Snord49a	NR_028550 (RefSeq)	2	Small nucleolar RNA, C/D box 49A
ND3	ENSMUST00000082411 (ENSEMBL)	2	NADH-ubiquinone oxidoreductase chain 3
Prdm1	NM_007548 (RefSeq)	2	PR domain containing 1, with ZNF domain
Ccdc69	NM_177471 (RefSeq)	2	Coiled-coil domain containing 69
Atp13a3	NM_001128096 (RefSeq)	2	ATPase type 13A3, transcript variant 1
Prkce	NM_011104 (RefSeq)	2	Protein kinase C, epsilon
Scarna17	NR_028560 (RefSeq)	2	Small Cajal body-specific RNA 17
Hoxa5	NM_010453 (RefSeq)	2	Homeobox A5
Rps27	NM_027015 (RefSeq)	2	Ribosomal protein S27, transcript variant 1
Osm	NM_001013365 (RefSeq)	2	Oncostatin M
Eif3m	NM_145380 (RefSeq)	2	Eukaryotic translation initiation factor 3, subunit M
Klri2	NM_177155 (RefSeq)	2	Killer cell lectin-like receptor family I member 2
Etohi1	NM_001177399 (RefSeq)	2	Ethanol induced 1, transcript variant 1

Acat2	NM_009338 (RefSeq)	2	Acetyl-Coenzyme A acetyltransferase 2
Snora23	NR_033336 (RefSeq)	2	Small nucleolar RNA, H/ACA box 23
Tmem222	NM_025667 (RefSeq)	2	Transmembrane protein 222
Ndufc1	NM_025523 (RefSeq)	2	NADH dehydrogenase (ubiquinone) 1, subcomplex unknown, 1
Dld	NM_007861 (RefSeq)	2	Dihydrolipoamide dehydrogenase
Irgm1	NM_008326 (RefSeq)	2	Immunity-related GTPase family M member 1
Ankrd32	NM_134071 (RefSeq)	2	Ankyrin repeat domain 32
Rangrf	NM_021329 (RefSeq)	2	RAN guanine nucleotide release factor
Gtf3c3	NM_001033194 (RefSeq)	2	General transcription factor IIIC, polypeptide 3
Zfp868	NM_172754 (RefSeq)	2	Zinc finger protein 868, transcript variant 1

Shown are downregulated genes in HoxA9$^{-/-}$ BM pDCs compared to WT pDCs. Underlined genes indicate high gene expression in murine pDCs according to microarray data generated by the Immunological Genome Project consortium (www.immgen.org.) (Heng et al., 2008). Sources of gene cDNA sequences comprise RefSeq from NCBI reference sequence database (www.ncbi.nlm.nih.gov/refseq), ENSEMBL database (http://www.ensembl.org), and NCBI GenBank including the high-throughput cDNA (HTC) division (www.ncbi.nlm.nih.gov/genbank).

***TABLE 3.6** UPREGULATED GENES OF SORTED HOXA9$^{-/-}$ BM PDCS*

Gene	Accession (Source)	Fold Change (WT/KO)	Description
Cish	NM_009895 (RefSeq)	0.4	Cytokine inducible SH2-containing protein
Mrps10	ENSMUST00000060752 (ENSEMBL)	0.4	28S ribosomal protein S10, mitochondrial isoform 3
Lpcat2	NM_173014 (RefSeq)	0.4	Lysophosphatidylcholine acyltransferase 2
Slfn4	NM_011410 (RefSeq)	0.4	Schlafen 4
Polr2k	NM_001039368 (RefSeq)	0.5	Polymerase (RNA) II (DNA directed) polypeptide K, transcript variant 1
Parp10	NM_001163575 (RefSeq)	0.5	Poly (ADP-ribose) polymerase family, member 10, transcript variant 1
Lcn2	NM_008491 (RefSeq)	0.5	Lipocalin 2
Tcf19	NM_001163763 (RefSeq)	0.5	Transcription factor 19, transcript variant 1

Olfr1402	NM_146275 (RefSeq)	0.5	Olfactory receptor 1402
Ctse	NM_007799 (RefSeq)	0.5	Cathepsin E
Prnp	NM_011170 (RefSeq)	0.5	Prion protein
Dcxr	NM_026428 (RefSeq)	0.5	Dicarbonyl L-xylulose reductase
Ccnb1	NM_172301 (RefSeq)	0.5	Cyclin B1
Bag3	NM_013863 (RefSeq)	0.5	BCL2-associated athanogene 3
Cd302	NM_025422 (RefSeq)	0.5	Cluster of differentiation 302
Ltf	NM_008522 (RefSeq)	0.5	Lactotransferrin
Minpp1	NM_010799 (RefSeq)	0.5	Multiple inositol polyphosphate histidine phosphatase 1
Net1	NM_019671 (RefSeq)	0.5	Neuroepithelial cell transforming gene 1, transcript variant 1
Stx2	NM_007941 (RefSeq)	0.5	Syntaxin 2
Lasp1	ENSMUST00000148280 (ENSEMBL)	0.5	LIM and SH3 protein 1
Sh3bgrl2	NM_172507 (RefSeq)	0.5	SH3 domain binding glutamic acid-rich protein like 2
Ly6g	ENSMUST00000023246 (ENSEMBL)	0.5	Similar to lymphocyte antigen 6G
Meis1	NM_001193271 (RefSeq)	0.5	Meis homeobox, transcript variant B
Ncf2	NM_010877 (RefSeq)	0.5	Neutrophil cytosolic factor 2
Tns1	NM_027884 (RefSeq)	0.5	Tensin 1
Bcl11b	NM_001079883 (RefSeq)	0.5	B-cell leukemia/lymphoma 11B, transcript variant 1
Alpk1	NM_027808 (RefSeq)	0.5	Alpha-kinase 1
Dock6	NM_177030 (RefSeq)	0.5	Dedicator of cytokinesis 6
Mthfr	NM_001161798 (RefSeq)	0.5	5,10-methylenetetrahydrofolate reductase, transcript variant 1
Ecm1	NM_007899 (RefSeq)	0.5	Extracellular matrix protein 1
Rfc3	NM_027009 (RefSeq)	0.5	Replication factor C (activator 1) 3

Slc10a4	NM_173403 (RefSeq)	0.5	Solute carrier family 10 (sodium/bile acid cotransporter family), member 4
Atad2	NM_027435 (RefSeq)	0.5	ATPase family, AAA domain containing 2
Zfp280b	NM_177475 (RefSeq)	0.5	Zinc finger protein 280B
Eya1	NM_010164 (RefSeq)	0.5	Eyes absent 1 homolog (Drosophila)
Uqcr11	NM_025650 (RefSeq)	0.5	Ubiquinol-cytochrome c reductase, complex III subunit XI
Cdc42ep4	NM_020006 (RefSeq)	0.5	CDC42 effector protein (Rho GTPase binding) 4, transcript variant 1
Lphn2	NM_001081298 (RefSeq)	0.5	Latrophilin 2

Shown are selected genes upregulated in HoxA9$^{-/-}$ BM pDCs compared to WT pDCs. Underlined genes indicate high gene expression in murine pDCs according to microarray data generated by the Immunological Genome Project consortium (www.immgen.org.) (Heng et al., 2008). Sources of gene cDNA sequences comprise RefSeq from NCBI reference sequence database (www.ncbi.nlm.nih.gov/refseq) and ENSEMBL database (http://www.ensembl.org).

4. DISCUSSION

4.1 VARIABILITY OF BM CELL COUNTS

At the outset of this study, I started to isolate BM cells *ex vivo* from HoxA9-deficient mice and the WT littermates by flushing the dissected femur and tibia. After lysis of the erythrocytes, the remaining nucleated BM cells were counted to determine possible variations. However, the data (***FIGURE 3.1***) shows a big variability in BM cell numbers with higher mean cell amounts in younger mice. Consistent with this observation, Sletvold et al. reported about a significantly reduced proliferative capacity of BM cells in older mice (Sletvold and Laerum, 1988). Known circadian variations were handled by doing BM preparations at the same daytime. In addition, also circannual alterations of mouse BM cell proliferation have been observed since the late 1980s (Laerum et al., 1988) and peak in the first part of the year. Interestingly, almost all experiments with young mice were carried out in winter months from December till February, whereas BM cell numbers of old mice were determined in late summer and autumn from August till November. Thus, both age as wells as the time of the year are influencing proliferation in the BM and might therefore be responsible for the large variability in total BM cell counts.

4.2 HOXA9 DEFICIENCY CAUSES REDUCED CELL NUMBERS IN THE BM

The statistical analyses of mean total nucleated cell numbers in the BM revealed reductions for HoxA9-deficient compared to wild type mice, although not statistical significant. However, reduced BM cell numbers in HoxA9$^{-/-}$ animals have been shown in earlier studies. Gwin et al. reported about insignificantly decreased numbers of nucleated BM cells in HoxA9 knockout mice and revealed a significant reduction of lymphohematopoietic progenitors (CLPs), particularly in Flt3^{+} B cell progenitor lineages including Pre-Pro-B and Pro-B precursors (Gwin et al., 2010). Furthermore, Lawrence and colleagues determined normal quantities of nucleated BM cells per femur of HoxA9-deficient mice, however, also with a small decrease of B lymphocytes (Lawrence et al., 1997). Thus, the observed reduction of BM cell numbers, albeit small and statistically not significant, seems to be not simply due to natural variability, instead reflects altered development and differentiation of lymphoid progenitors especially affecting the B cell lineage. This circumstance has been partly linked to transcriptional regulation of Flt3 by

HoxA9 in hematopoietic progenitors through directly binding its promotor region (Gwin et al., 2010; Wang et al., 2006). The cytokine fms-like tyrosine kinase 3 ligand (Flt3L) and its receptor Flt3 are known to be essential factors for lymphoid priming and thus for B cell differentiation (Sitnicka et al., 2002). Nonetheless, they also represent crucial signals for steady-state DC development and the homeostasis of peripheral DCs (Schmid et al., 2010; Waskow et al., 2008). Latest investigations implicate an early contribution of Flt3 in hematopoietic stem cell differentiation including most lineages and probably marking the stage of losing self-renewal potency when expressed (Boyer et al., 2012; Boyer et al., 2011). Flt3 further seems to support the lymphoid and myeloid lineage differentiation rather than the development of erythroid and megakaryocytic cell types (Gwin et al., 2013b). A subgroup of $Flt3^+$ multipotential progenitors (MPPs), which express lymphoid-lineage genes and high levels of Flt3, referred to as lymphoid-primed multipotential progenitors (LMPPs), possess the ability to differentiate into B, T, NK, and DCs through transition into common lymphoid progenitors (CLPs) and beyond subsets (Gwin et al., 2013b). Two studies revealed a synergistic instead of sequential role for HoxA9 and Flt3 in early lymphoid development, since double knockout mice display a profound block in generating lymphoid progenitors destined to become B or T cells and single $HoxA9^{-/-}$ mice show selective impairment in CLP subsets destined to become B cells (Gwin et al., 2013a; Gwin et al., 2013b). Interestingly, neither HoxA9 nor HoxA9/Flt3 deficiency had any impact on lymphoid lineage dependent NK cell development or homeostasis and the quantities of $CD11c^+$ cDCs as well as $B220^+CD11c^+$ pDCs in the BM beyond those observed in single Flt3 knockout mice (Gwin et al., 2013a). Thus, the regulation of Flt3 expression by the transcription factor HoxA9 seems to contribute only in part to the impaired B cell differentiation. One study implicates novel roles for HoxA9 in B cell fate regulation and together with Flt3 cooperative functions in controlling B and T cell lymphoid progeny (Gwin et al., 2013b). Important for this work, HoxA9 seems to be not involved or is completely dispensable in DC development *in vivo*, since normal numbers and frequencies of DC subsets in the BM of HoxA9-deficient mice were reported by the same authors (Gwin et al., 2013a; Gwin et al., 2013b). Consistent to this, *ex vivo* FACS analyses of HoxA9-deficient BM cells in this work displayed reduced frequencies of $B220^+$ B cells but no difference in frequencies of all DC subsets compared to BM cells of wild type littermates. Thus, slightly decreased cell counts of total nucleated BM cells in $HoxA9^{-/-}$ mice are mainly due to impairment of selected lymphoid lineages resulting in altered B cell progeny. In addition, HoxA genes and especially HoxA9 have

been recently shown to generally impact on proliferation rather than differentiation of stem cells and progenitor cells in murine BM (Lebert-Ghali et al., 2016). However, the development of DCs seems to be not affected *in vivo*. One explanation might be the rise of DC precursors from both lymphoid and myeloid progenitor cells (see also ***FIGURE 1.4*** in section 1.3.1.1). The issue of differentiation and development in this context will be further discussed in detail in section 4.6.

4.3 THE HYPOTHESIS THAT HOXA9 FUNCTIONS AS A CO-FACTOR FOR TLR9 IN MURINE PDCS IS UNLIKELY

The initial aim of this work was to clarify whether HoxA9 functions as a co-factor or is basically involved in direct recognition of microbial DNA by TLR9 specifically in mouse pDCs. The fact that murine pDCs are uniquely able to sense DNA via TLR9 in a CpG-motif independent manner and even without containing purine or pyrimidine nucleobases (Bauer, 2013; Haas et al., 2008; Wagner, 2008; Yasuda et al., 2006) raised the question, if TLR9-dependent DNA recognition in pDCs is provided by additional DNA-binding co-factors, which are lacking in other cell types. Unpublished microarray data from the former group of Prof. Bauer in the Institute for Medical Microbiology and Hygiene in Munich revealed prominent expression levels of *hoxa9* mRNA in murine TLR9-stimulated Flt3L-induced pDCs and thus implicated HoxA9 as a potential candidate for pDC-specific TLR9-associated DNA recognition in mice. Furthermore, Philipp Kurbel from our research group was able to show an upregulation of *hoxa9* mRNA in qPCR experiments after TLR9 activation in Flt3L-induced DCs and splenocytes (unpublished data).

Different ODNs either containing or lacking CpG-motifs were used to investigate whether HoxA9-deficient pDCs show different cytokine responses compared to WT pDCs upon TLR9 stimulation. The CpG-motif containing ODN 2216 (CpG2216) belongs to CpG type A ODNs, which are known to trigger a robust IFN-α response, whereas ODN 1668 (CpG1668) is part of type B ODNs believed to induce higher quantities of proinflammatory cytokines including IL-6 via NFκB and strongly drive DC maturation (Hemmi et al., 2003; Verthelyi et al., 2001). However, type A as well as type B ODNs activate both signaling cascades via NFκB and IRF7 in pDCs. The ODNs AP-1 (non-CpGAP-1) and 1720 (non-CpG1720) are free of CpG-motifs and have been shown to induce TLR9 activation exclusively in murine pDCs (Haas et al., 2008; Wagner, 2008).

The results of TLR9 stimulation experiments of several settings including primary BM cells, *ex vivo* sorted BM pDCs, primary splenocytes as well as *in vitro* generated M-CSF-induced suspension cells and Flt3L-induced cultures showed reproducibly reduced IFN-α levels upon stimulation with all TLR9-activating ODNs. Because pDCs are present in all of these settings, CpG-motif containing ODNs as well as ODNs that lack CpG-motifs triggered robust IFN-α secretion in WT cells, whereas KO samples displayed significantly reduced IFN-α responses regardless of the DNA sequence. Unfortunately, Flt3L-induced DC cultures were only stimulated with CpG1668 and CpG2216 but not with ODNs free of CpG-motifs. Future experiments should include TLR9 stimulation with non-CpG ODNs in this cell setting. TLR9-dependent activation of the NFκB pathway and subsequent upregulation of proinflammatory cytokines represented by IL-6 in pDC-containing cell settings showed alterations in total BM cells depending on the ODN (AP-1, 1720), moderately decreased levels in primary splenocytes and M-CSF-induced suspension cells, and displayed a larger decrease in Flt3L-induced cultures and one experiment of *ex vivo* sorted pDCs. Higher IFN-α and IL-6 reductions in Flt3L-induced DC cultures of KO animals compared to other cell settings seem to be mainly due to increased amounts of dead cells ($HoxA9^{-/-}$ cultures gained only 25.85 % mean cells in the life-gate compared to 34.31 % of WT cultures [75.28 % of the WT value]). Conflicting results for IL-6 levels between different cell settings seem to be due to a diverse composition of innate immune cell types that express TLR9 and are differently competent to respond to activating ODNs. Moreover, TLR9 signaling varies depending on the particular cell type. TLR9 activation in murine pDCs drives both signaling cascades via IRF7 and NFκB to induced type I IFNs and proinflammatory cytokines, respectively, whereas murine cDCs, MΦs (monocytes in the BM), and B cells only possess the ability to induce the NFκB pathway (Blasius and Beutler, 2010) (see section 1.2.3.3 and 1.2.3.4 for details). Regarding primary BM cells, equal IL-6 levels were measured constantly in both genotypes upon stimulation with CpG-motif containing ODNs, while agonists with a CpG-motif free sequence exhibited clearly reduced IL-6 amounts in three experiments and increased ones in one experiment. The evidence that only murine pDCs are able to sense DNA regardless of the sequence rather indicates selective impairment of the NFκB pathway in HoxA9-deficient pDCs. The latter suggestion gains support from the fact that one experiment of primary sorted knockout pDCs also showed diminished IL-6 responses (very low levels) upon CpG2216-mediated TLR9 activation and the remaining two experiments provided no detectable IL-6 in both

genotypes while IFN-α was still robustly induced. The observation that TLR9 triggered by CpG-motif containing ODNs in total BM cells reproducibly elicited equivalent IL-6 amounts in the knockout samples compared to wild type, despite significantly reduced $B220^+$ B cell percentages and presumably functionally impaired pDCs, leads to the question whether IL-6 proportions of these two cell subsets contribute only marginally to total IL-6 amounts or other cell types produce higher IL-6 amounts in HoxA9-deficient BM cells for compensation. Percentages of cDCs in the BM determined by flow cytometry were mostly equal but overall showed a tendency to be slightly more frequent among HoxA9-deficient BM cells especially in the BST2 CD11c staining. Sorted primary KO cDCs were competent to elicit IL-6 quantities not significantly different to WT ones with a slight tendency to be higher in KO samples. Other cells present in the BM that are able to produce large amounts of proinflammatory cytokines after triggering TLR9 are monocytes. To fully understand TLR9-induced proinflammatory cytokine responses in BM cells, B cells and monocytes should be investigated more precisely for instance by using FACS analysis of specific surface markers and by stimulating sorted cell fractions with several TLR9 ligands. Moreover, the expression of other proinflammatory cytokines such as TNF-α or IL-12, co-stimulatory molecules including CD80, CD86, or CD40 and MHC-I as well as MHC-II should be examined upon TLR9 activation separately in all cell types mentioned above. TLR9 stimulation of total splenocytes generated similar IL-6 proportions like the BM experiments using CpG1668 and CpG2216. The non-CpG ODNs AP-1 and 1720 did not induce detectable levels of IL-6. Because only two experiments were done, further attempts need to be carried out and TLR9 activation should be examined in detail in sorted cell fractions including DCs, MΦs, and B cells. Regarding pDC-free cell preparations: primary sorted BM cDCs, GM-CSF-generated cDCs as well as M-CSF-induced MΦs did not show significant alterations in IL-6 responses when faced with the TLR9 ligands CpG1668 and CpG2216. As expected, non-CpG1720 did not induce cytokine responses in GM-CSF-induced cDCs and only marginally IL-6 amounts in WT M-CSF-induced MΦs in one experiment. The latter probably occured due to contamination by pDCs found among M-CSF-generated suspension cells. Primary cDCs were not stimulated with non-CpG ODNs due to little cell quantities.

Given that particularly IFN-α inductions by TLR9 agonists were constantly weaker in $HoxA9^{-/-}$ pDC-containing cell settings and sorted primary pDCs, and other cell types including primary and *in vitro* generated cDCs as well as MΦs seem to be not

affected by the KO, the hypothesis that HoxA9 is important for TLR9 function selectively in pDCs becomes more prevalent. Considering the initial hypothesis that HoxA9 might react as a co-factor for TLR9 in pDCs to sense DNA in a sequence independent manner, one would expect that TLR9-dependent cytokine inductions with ODNs that are lacking CpG-motifs should be completely abolished in HoxA9-deficient pDCs or at least show clearly stronger reductions compared to CpG-motif containing ODNs. As this is not the case and TLR7-induced cytokine responses (especially IFN-α) upon stimulation with RNA40 were similarly impaired in KO samples of several pDC-containing cell settings used in this study, it seems more likely that HoxA9 in its known function as a transcription factor influences TLR-mediated cytokine responses particularly in pDCs. Further possible scenarios include direct influence of the HoxA9 protein on translation of genes involved in the TLR machinery (signaling, processing, trafficking, or autophagy) or pDC-specific genes as well as direct inhibition or activation of the gene products. Involvement of HoxA9 in regulating translation of mRNAs through direct binding to the translation initiation factor eIF4E was already shown by Topisirovic and colleagues in hematopoietic cells (Topisirovic et al., 2005). The translation efficiency of cyclin D1 and ornithine decarboxylase (ODC) mRNAs as well as their nuclear transport was enhanced by HoxA9 (Topisirovic et al., 2005). By forming complexes with the ubiquitin ligase core component Roc1-Ddb1-Cul4a with subsequent activation of an E3 ligase resulting in the ubiquitination and thus degradation of the geminin protein, the HoxA9 protein positively influences cell proliferation in hematopoietic cells because geminin inhibits DNA replication (Ohno et al., 2013). These two examples demonstrate that HoxA9 can act on different levels beside its well-known function as a transcription factor. Even both situations, regulating multiple genes and directly control particular actions at several levels, are conceivable as growing evidence shows that Hox genes can adopt multifaceted functions in cooperation with different co-factors and cell type dependent transcription factors (Huang et al., 2012; Rezsohazy et al., 2015). Nonetheless, the most probable explanation lies within altered gene regulation at the level of transcription. Regarding the differential expression of multiple genes found by microarray analysis of pooled primary BM pDCs, I hypothesize that HoxA9 possesses a substantial role within pDC-specific processes in conjunction with TLR7 and 9 and its regulatory circuitry, by acting as transcription factor that enhances and silences multiple genes (see section 4.5 for details). Key prerequisite for this hypothesis is an upregulation of HoxA9 upon TLR activation in pDCs, meaning that HoxA9 is expressed or can be induced in matured differentiated cells

as well. To date, the established scientific doctrine teaches that HoxA9 is highly expressed in early hematopoietic progenitor cells and its expression is subsequently downregulated throughout differentiation resulting in complete inactivity in terminally differentiated cells (Alharbi et al., 2013; Collins and Hess, 2016; Rezsohazy et al., 2015). Similar processes are reported for Hox proteins in embryogenesis. However, the expression of Hox genes along body axes in adult cells has already been reported (Morgan, 2006).

To prove this hypothesis, further investigations should include expression of the HoxA9 protein and mRNA in unstimulated and TLR-stimulated pDCs as well as other mature innate immune cells. Furthermore, regulation of genes on several levels and direct protein-protein interactions of HoxA9 in TLR-associated networks should be studied in the pDC subset in mice and humans.

4.4 HoxA9$^{-/-}$ pDCs are Significantly Impaired in TLR7 and 9 Function

All results of several pDC-containing cell settings used in this study show clearly impaired functions of TLR7 as well as TLR9 in terms of secreted IFN-α quantities in the KO group. This assertion is reinforced by the fact that statistically significant reductions of IFN-α were measured in primary total BM cells and sorted BM pDCs as well as *in vitro* generated Flt3L-induced DC cultures. Other pDC-containing cell settings including primary splenocytes and M-CSF-induced suspension cells also exhibited noticeable lower levels of IFN-α in HoxA9$^{-/-}$ samples, however, statistical analysis in these settings was not carried out due to few experiments. Interestingly, initial experiments using total BM cells of older mice (16 – 27 weeks) for testing purposes displayed no significant alterations in both IFN-α and IL-6 levels in the KO genotype (data not shown). Better compensational mechanisms in older mice might be one explanation of this effect. As for immunological experiments generally young mice are demanded, the data of older mice were not demonstrated and advanced experiments with older mice were not carried out. Nevertheless, further research in this field should take this observation into account. Thus, investigations of age-related influences are the logical consequence.

IL-6 amounts in the same pDC-containing cell settings were inconsistent. As already mentioned before several times, proinflammatory cytokines such as IL-6 are produced by all innate immune cells and secretion takes place after stimulation of all TLRs or other PRRs. In mice, TLR7 and 9 are mainly expressed in DCs, B cells, and monocytes/MΦs, all of which secrete IL-6 after activation of these receptors (Blasius and

Beutler, 2010). Importantly, the quantities of IL-6 differ between different cell types. MΦs and cDCs produce huge amounts of IL-6, whereas pDCs contribute only in small fractions to total IL-6 amounts. Primary total BM cells displayed equal IL-6 levels in both genotypes after TLR7 as well as TLR9 stimulation. Considering that cDCs and monocytes are mainly responsible for total IL-6 quantities and pDCs (and also B cells) have only a small impact on total IL-6 production, the lacking reductions in IL-6 levels compared to IFN-α are explained. On the contrary, sorted BM pDCs and *in vitro* generated cultures that contain solely or higher frequencies of pDCs exhibited lower IL-6 quantities in HoxA9-lacking samples, though statistical significance was only achieved in TLR7-mediated stimulation by RNA40 of Flt3L-induced DCs. Measurable IL-6 levels of *ex vivo* sorted BM pDCs were only found in one experiment showing reductions in the KO group. The remaining experiments revealed no detection of IL-6 at all in both genotypes, suggesting very low quantities outside the ELISA standard range. This observation might be due to the use of the CpG A ODN 2216, which is known to induce predominantly type I IFNs and less proinflammatory cytokines (see sections 1.2.3.2, 1.2.3.4, and 1.3.1.2 for details). Regarding the only experiment with detected IL-6 levels, reductions nearly comparable to those observed for IFN-α upon TRL7 and 9 stimulation were measured for sorted KO pDCs, suggesting that HoxA9-mediated gene regulation might also be impacting on genes associated with NFκB or AP-1 pathways in this DC strain. However, the sorted pDC fraction in this experiment might have also been contaminated by cDCs, which of course induce higher amounts of IL-6 upon TLR7 and 9 activation. The latter scenario would raise the question if the contamination occured in equal amounts for both genotypes. The purity samples of all experiments show a certain amount of contamination for both genotypes, indeed with a marginally increased purity for HoxA9 knockout pDCs (***FIGURE 3.6 C***). However, the contamination in the particular experiment was not higher compared to other experiments. Finally, more cells than intended could have been put into the wells mistakenly.

In general, the reductions observed for IL-6 were constantly lower than those found for IFN-α, but still robustly reproducible. Possible reasons for this observation are found in the FACS data of the mentioned cell populations. Flt3L-induced DC cultures displayed statistically significant higher cDC fractions in the KO group, explaining higher IL-6 amounts after TLR7 and 9 activation, which were still noticeable below WT levels. Further, IL-6 amounts in the same cultures found after TLR2 and TLR4 stimulation, which were solely driven by cDCs, exhibited expectedly higher quantities in HoxA9$^{-/-}$

samples (statistically significant for TLR4). Thus, taken together, IL-6 responses in cell settings containing solely or high frequencies of pDCs, were reproducibly weaker in the KO group, but did not reach results obtained for IFN-α. The fact that IL-6 is produced by all innate immune cells upon TLR7 and 9 activation, in contrast to IFN-α, complicates interpretation of the data. However, the generated data of different cell settings *ex vivo* and *in vitro* together clearly point towards disrupted functions of TLR7 as well as TLR9 particularly in HoxA9 KO pDCs. This raises the question, why measured cytokine levels, especially IFN-α, in HoxA9 knockout cell settings are not completely abolished. Given that the formulated hypothesis from section 4.1 is true, that HoxA9 is upregulated in pDCs after TLR7 and 9 activation and functions as transcription factor in the TLR regulating machinery in this cell type, HoxA9 probably acts in concert with different co-factors and collaborators/general factors via binding to cis-regulatory elements and subsequently silences or enhances the transcription of respective genes. Direct binding to promotor regions of genes is not usually the case according to previous observations. Thus, HoxA9 seems to rather modulate instead of dictate the TLR-mediated immune response in pDCs, probably in cooperation with multiple other factors, which would explain reduced but not completely abolished cytokine levels. Another possible explanation is due to the fact that adjacent Hox genes or co-factors could replace HoxA9. For instance, Meis1, the most important co-factor for HoxA9, was shown to co-bind at multiple (hundreds) binding sites together with HoxA9 (Huang et al., 2012), is a homeobox-containing transcription factor itself, and was upregulated 2-fold in the microarray gene expression profile of HoxA9$^{-/-}$ pDCs. Thus, Meis1 could be "stepped into the breach" to replace, or at least partly replace, HoxA9 in pDCs, resulting in reduced but not completely abrogated cytokine responses. One emphasis in future research in this field should deal with the complex mechanisms how HoxA9 and its multiple co-factors and collaborators act together particularly in TLR-activated pDCs. Very interestingly, Hox proteins have been shown to recruit different other transcription factors depending on the cell type and context (Collins et al., 2014; Collins and Hess, 2016; Huang et al., 2012; Ladam and Sagerström, 2013; Rezsohazy et al., 2015). Transcription factors associated to HoxA9 function in pDCs should be promising targets for further research.

To confirm the postulated functional impairment of TLR7/9 biology in pDCs, I suggest detailed examination of HoxA9$^{-/-}$ pDCs in terms of expression of co-stimulatory proteins such as CD40, CD80, and CD86 as well as MHC-I/MHC-II molecules upon TLR stimulation. Further, additional functional analyses of pDCs

including antigen presentation, priming and cross-priming of T cells, NK cell activation, immune cell recruitment via chemokines, driven plasma cell responses, and induction of immune regulation should be carried out under HoxA9$^{-/-}$ conditions. Experiments using viruses like murine cytomegalovirus (MCMV), lymphocytic choriomeningitis virus (LCMV), or herpes simplex typ 1 (HSV1) would clarify whether HoxA9$^{-/-}$ pDCs are still capable of fighting acute viral infections.

4.5 TLR-MEDIATED CYTOKINE RESPONSES OF CDCS AND MΦS ARE NOT AFFECTED BY THE HOXA9 KNOCKOUT

Besides pDCs, the impact of the HoxA9 KO on TLR-mediated cytokine responses was also checked in cDCs and MΦs. Overall, two significant differences were observed. Firstly, TLR2 stimulation with Pam-3-Cys of total BM cells induced statistically significant less IL-6 in the HoxA9$^{-/-}$ group. Innate immune cells present in the BM that express TLR2 and secrete IL-6 are mainly monocytes and cDC progenitors. IL-6 responses of TLR4, 7, and 9 reproducibly displayed no alteration in BM KO samples. Moreover, TLR2 responses in all other cell settings were stable without differing between the two genotypes. In the first place, this observation seems implausible. However, a lately published study indicates that murine pDCs also express TLR2 (Dasgupta et al., 2014). Dasgupta and colleagues demonstrated that bacterial polysaccharide A (PSA) from *Bacteroides fragilis* induced production of MHC-II, CD86, and ICOSL via TLR2 in mouse pDCs and prompted IL-10 sectretion by CD4+ T cells (Dasgupta et al., 2014). This immunomodulatory effect caused by the commensal *Bacteroides fragilis* triggered protection against colitis (Swiecki and Colonna, 2015). To date, the production of proinflammatory cytokines via TLR2 by pDCs has not been reported. Nevertheless, the reduced IL-6 amounts in total BM cells following TLR2 stimulation might have also been achieved accidentally. Defining a statistical significance level of $p < 0.05$ implies an average incorrect result every 20th calculation.

The second alteration was found for Flt3L-induced DC cultures *in vitro*. IL-6 levels upon TLR4 stimulation were significantly increased for HoxA9$^{-/-}$ cultures compared to WT. TLR4 is not expressed by pDCs, thus IL-6 responses were solely driven by cDCs. Also TLR2-mediated IL-6 liberation showed a small increase in the knockout group, however, not statistically significant. Considering higher cDC amounts in the knockout cultures, increased Pam-3-Cys- and LPS-induced IL-6 levels rather indicate

normal functions of TLR2 and 4, respectively, in cDCs. Comparing these results to the other experiments, the assumption that pDCs rather than both cell types in Flt3L-induced DC cultures are dysfunctional seems to be likely.

TLR2, 3, 4, 7, and 9 stimulation experiments of *in vitro* generated GM-CSF-induced cDCs and M-CSF-induced MΦs did not exhibit any significant differences in IFN-α as well as IL-6 quantities between both genotypes. Interestingly, TLR3-mediated cytokine production via Poly I:C stimulation was measured in both cell settings, whereas primary BM cells, sorted cDCs, and Flt3L-induced DCs did not show any cytokines at all upon TLR3 activation. This observation suggests lacking expression of TLR3 in primary BM cells as wells as Flt3L-induced DCs. However, in the beginning, I used Poly I:C from Invitrogen™, whereas later experiments including those with *in vitro* generated GM-CSF-induced cDCs and M-CSF-induced MΦs were carried out with Poly I:C from GE healthcare™. Thus, Poly I:C from different manufacturers might have made the difference.

4.6 HOXA9 IS IMPACTING ON DC DEVELOPMENT *IN VITRO* BUT NOT *IN VIVO*

As pDCs are the only cell type able to produce large amounts of type I IFNs upon activation of TLR7 and 9, HoxA9 either contributes directly or indirectly (via gene regulation) to mechanistic processes of TLR-mediated functions in pDCs (see section 4.4) or precursors in the BM are not able to fully differentiate and thus lack maturity. The latter aspect is supported by the fact that HoxA9 is generally known to be a crucial player in normal hematopoiesis, responsible for maintenance of the stem cell status in HSCs (Alharbi et al., 2013; Collins and Hess, 2016; Lebert-Ghali et al., 2016). Furthermore, HoxA9 was shown to be the most expressed Hox gene in stem cells and early progenitors (Alharbi et al., 2013; Pineault et al., 2002). Interestingly, a lately published study shows that the whole HoxA gene cluster, including HoxA9 as its most prominent member, is predominantly involved in proliferation and has only subtle influence on differentiation (Lebert-Ghali et al., 2016). As already mentioned above, other findings implicated HoxA9 as a transcriptional regulator of Flt3 in early B cell progenitors (Gwin et al., 2010). Slightly reduced numbers of total BM cells and decreased frequencies of $B220^{+}$ B cells in $HoxA9^{-/-}$ mice (statistically significant in the B220/SiglecH staining) confirm similar results of previous studies (Gwin et al., 2013a; Gwin et al., 2010; Gwin et al., 2013b; Lawrence et al., 2005; Lawrence et al., 1997). In line with these observations, Lawrence

and colleagues reported that HoxA9 knockout mice also display a slight hypocellularity in the spleen and thymus as well as a mild pancytopenia (Lawrence et al., 1997). Total splenocytes of only 2 mice per genotype in my study showed no significant difference ($HoxA9^{-/-}$ [n = 2] 8.2 x 10^6 versus WT [n = 2] 7.2 x 10^6) and a slightly higher average cell amount for the KO group.

The cytokine receptor Flt3 and its ligand Flt3L are essential for DC development (Schmid et al., 2010; Watowich and Liu, 2010), as noted several times before. Huang et al. demonstrated hundreds of DNA binding sites of HoxA9 in hematopoietic cells, which were mostly identified as enhancer regions and only a minority consisted of direct promotor binding sites (Huang et al., 2012). Among them, again Flt3 and multiple other genes involved in hematopoiesis, leukemogenesis, and inflammation were identified (Huang et al., 2012). Flow cytometry analyses of the BM and spleen of HoxA9-deficient animals showed no significant alterations in quantities of matured pDCs and cDCs. Normal expression of the pDC-specific surface markers B220, CD11c, Ly6C, BST2, Flt3, and SiglecH was observed among $HoxA9^{-/-}$ BM cells. Same results were found for CD11c+ cDCs/Pre-cDCs. Previously published data by Gwin et al. also showed no impact on DC subsets in the BM of $HoxA9^{-/-}$ mice using the markers B220 and CD11c (Gwin et al., 2013a). Of note, distinct precursors of NK cells called pre-mNK cells, which have initially been thought to reflect a hybrid cell subset between pDCs and NK cells called interferon-producing killer dendritic cells (IKDCs) (Blasius et al., 2007; Caminschi et al., 2007; Guimont-Desrochers et al., 2012), also express B220 and CD11c on their plasma membrane. Altered differentiation and development of NK cells in HoxA9 deficiency could therefore bias these results. One study states that NK cell development is not different in HoxA9 knockout conditions (Gwin et al., 2013a), however, the authors did not focus on this particular cell type and thus further precise investigations need to be done to rule out this objection. Nonetheless, the results of my study together with previous data indicate a normal differentiation of DCs in HoxA9 knockout mice *in vivo*. According to this, either HoxA9 is not regulating Flt3 in direct precursors of DCs (e.g. CDPs, MDPs, CLPs, and Pre-DCs) in contrast to B cell progenitors or compensational mechanism, e.g. replacement of HoxA9 by adjacent HoxA genes or co-factors such as Meis1, take place *in vivo*. Regarding the first assumption, CDPs, the direct precursors of DCs, have been shown to be normal in HoxA9 knockout mice (Gwin et al., 2013a) and do not express HoxA9 mRNA according to data of the immunological genome project (Heng et al., 2008). Interestingly, the latter assumption demonstrates expression of HoxA9 in MDPs,

CLPs, and almost all prior stem cell and precursor subsets. Looking at the displacement theory, the co-factor Meis1 has been shown to partly substitute HoxA9 function and induce expression of Flt3 in myeloid leukemogenesis models (Wang et al., 2006). Overall, both explanations are likely and might also occur simultaneously.

Reduced cytokine production of BM pDCs is therefore probably not due to incomplete differentiation. However, several studies indicate a complex diversity of pDC subsets within the BM. The pDC-specific surface markers CCR9, SCA1, Ly49Q, and CD9 were found to discriminate certain pDC subsets in the BM differing in degree of maturation as well as ability to produce type I IFNs and proinflammatory cytokines (Swiecki and Colonna, 2015). For instance, $CCR9^+$ subsets represent mature pDCs, whereas $CCR9^-$ populations reflect pDC-like common DC progenitors (CDPs) (Schlitzer et al., 2011). Remarkably, pDC-like CDPs induce stronger type I IFN and proinflammatory cytokine responses that $CCR9^+$ mature pDCs (Schlitzer et al., 2011). The latter can be further subdivided into $SCA1^{low}$ and $SCA1^{high}$ populations. The first of which is able to produce higher amounts of IFN-α and can give rise to the $SCA1^{high}$ subset after being activated by TLR-responses or IFN-α itself (Niederquell et al., 2013; Swiecki and Colonna, 2015). $Ly49Q^-$ pDCs are less capable in eliciting innate immune responses to RNA viruses than $Ly49Q^+$ pDCs (Kamogawa-Schifter et al., 2005). Finally, the $CD9^+$ pDC subset produces large amounts of type I IFNs and possesses a strong ability to prime T cells compared to $CD9^-$ pDCs (Björck et al., 2011). Furthermore, O'Keeffe et al. identified a "nonplasmacytoid" DC subset with high IFN-α producing capacity upon TLR9 activation in the murine BM (O'Keeffe et al., 2012). Consequently, a detailed screening of different pDC subsets in the BM of $HoxA9^{-/-}$ mice is needed to solve whether HoxA9 influences the function of certain subsets while others do not need HoxA9 regulation.

Surprisingly, Flt3L-induced DC cultures generated *in vitro* from HoxA9 knockout BM cells develop clearly decreased numbers of total cells that were differentiated after 8 days in culture, although not statistically significant. Furthermore, the frequencies of differentiated pDCs were nearly equal in both genotypes with a littles tendency to be decreased in the KO group, whereas the cDC fractions were significantly increased in the KO cultures. In addition, the percentage of viable cells was reproducibly lower in HoxA9 KO cultures (~ 75 % of WT), which explains stronger reductions of IFN-α and IL-6 levels in this cell setting compared to primary BM cells. FACS data exhibited a roughly equal expression prolife regarding pDC-specific surface markers with a little tendency of

reduced SiglecH expression in KO pDCs. Prominently stronger CD11b expression was present in both pDCs and cDCs. In line with this, FACS data of suspension cells in M-CSF-induced cultures exhibited reduced frequencies of pDCs as well as cDCs. These observations clearly indicate an involvement of HoxA9 in developmental processes of DCs *in vitro*. Impaired proliferation capacity seems to be present in terms of reduced cell counts in *in vitro* cultures, confirming previously reported findings that HoxA9 is predominantly influencing proliferation rather than differentiation (Lebert-Ghali et al., 2016). Nonetheless, increased cDC fractions and higher CD11b expression in Flt3L-induced DC cultures are pointing towards a shift to the cDC subset in KO cultures, suggesting participation of HoxA9 in maintaining the pDC fate *in vitro*. The fact that the influence on developmental processes was not observed in primary cells again indicates compensational mechanisms *in vivo*.

Besides the known growth factors in DC development Flt3L, GM-CSF, and M-CSF, further factors seem to be involved in this process since KO animals lacking several growth factors are still able to generate DCs (Watowich and Liu, 2010). Interestingly, IFN-α and -β have been shown to be involved in development of DCs by enhancing differentiation into pDCs and inhibiting the cDC subset (Li et al., 2011; Watowich and Liu, 2010). This circumstance is believed to be utilized as an immune-evading mechanism by viruses (e.g measles virus (MV) and lymphocytic choriomeningitis virus (LCMV)) (Hahm et al., 2005; Watowich and Liu, 2010). Both, *in vitro* GM-CSF-induced inflammatory cDCs and Flt3L-induced cDCs as well as *in vivo* Flt3L-induced splenic cDC generation were inhibited by viral infection or by adding rIFN-β to *in vitro* cultures (Hahm et al., 2005). On the contrary, differentiation of the pDC subset seems to be rather promoted by type I IFNs (Li et al., 2011; Watowich and Liu, 2010). Moreover, IFN-α has been linked to hematopoietic processes in the past (Essers et al., 2009). Therefore, reductions of type I IFN levels in HoxA9$^{-/-}$ Flt3L-induced DC cultures could be responsible for the shifted differentiation towards the cDC subset and reduced total numbers of differentiated DCs.

4.7 THE GENE EXPRESSION PROFILE OF HOXA9$^{-/-}$ PDCS DISPLAYS MULTIPLE DIFFERENTIALLY EXPRESSED GENES

Multiple genes were significantly either up- or downregulated in sorted HoxA9$^{-/-}$ BM pDCs compared to WT. Interestingly, among downregulated genes, 21 small nucleolar

RNAs (snoRNAs) of both the box C/D and box H/ACA type, 4 small nuclear RNAs (snRNAs), and 2 microRNAs (miRNAs) can be found. These non-coding RNAs do not serve as protein-coding genes. Instead, their functions include important roles in post-transcriptional gene regulation (e.g. splicing) and translational mechanisms (ribosomal biogenesis through chemical modification of rRNAs) (Boivin et al., 2017). However, especially snoRNAs were shown to be involved in other functions in recent years such as regulating transcript stability, chromatin architecture, and serving as mediators in metabolic processes as well as stress responses (Boivin et al., 2017). The role of HoxA9 in this instance is very unclear. Many non-coding RNAs are "nested" genes, which are located within protein-coding "host" genes and their transcription as well as function depend on the particular "host" gene, while others have their own promotor (Boivin et al., 2017). If and how HoxA9 is influencing the transcription of non-coding RNAs in pDCs or other cell types need to be examined in further research. It is noteworthy that more than one third of the downregulated genes encode non-coding RNAs, while none of these were found among the upregulated genes.

Regarding the downregulated protein-coding genes, some interesting candidates need to be mentioned. The surface marker CD8 with its α and β subunit is expressed on some mouse pDC subsets (Swiecki and Colonna, 2015). The microarray data showed a downregulation of the CD8α subunit mRNA in KO pDCs of nearly one third compared to WT. Lombardi and colleagues reported that the expression of CD8α alone or in combination with the β subunit was found in tolerogenic pDCs that induce Foxp3+ regulatory T cells, whereas the lack of both subunits was restricted to cytokine secreting immunogenic pDCs (Lombardi et al., 2012). In contrast, Brown et al. observed an upregulation of both CD8 subunits in pDCs after TLR7 and 9 stimulation with R848 or CpG1668, respectively, and no stable expression in different pDC subsets. In line with this observation, O'Keeffe et al. reported about CD8 upregulation upon TLR stimulation in pDCs in earlier studies (O'Keeffe et al., 2005; O'Keeffe et al., 2002). The pDCs used for microarray analysis in my study were freshly isolated and not stimulated with TLR agonists prior to RNA purification. Nevertheless, it needs to be clarified whether HoxA9 is involved in the upregulation of CD8 upon TLR activation in pDCs. CD209d, also known as DC-SIGN, is another interesting downregulated gene. It is a PRR and part of the c-type lectin family expressed in MΦs and DCs. According to metadata of the ImmGen consortium, some other downregulated genes in the knockout pDCs show a specific high expression level in different murine pDC subsets, suggesting an important

role in this cell type. These genes include Scrn1, Rpgrip1, and Slc44a. Their functions in pDCs have not been described so far.

Besides Meis1, the most important co-factor of HoxA9 (already mentioned in section 4.4), two other genes among the upregulated genes in the microarray might be of interest. Ctse and Eya1 are both highly expressed in pDCs, thus future examinations should be targeting these genes.

However, the data found in the microarray experiment does not directly explain the reduction of IFN-α levels after TLR stimulation in KO pDCs. Assuming that HoxA9 is not expressed in mature pDCs and is upregulated upon TLR stimulation, this experiment needs to be done with TLR activated pDCs. TLR stimulation should be done using TLR7 and 9 agonists or even naturally infectious agents if possible (e.g. viruses). Furthermore, this experiment was performed only once due to very rare cell material and limited availability of young HoxA9$^{-/-}$ mice. To achieve better validity, at least three independently performed experiments are needed to further confirm the results and prove reproducibility. In addition, statistical analysis can be realized with three independently performed experiments to verify significance of the data. The discovery of a complex heterogeneity of pDC subsets within the BM the last couple of years (see the previous section 4.4 for details) further requires their discrimination by additional FACS markers to investigate a potential impact of HoxA9 on particular subgroups of pDCs. The transcriptome of peripheral pDCs found in the spleen or lymph nodes should be additionally investigated as stimulation experiments of total splenocytes revealed impaired IFN-α responses as well. Finally, research using human pDCs, e.g. isolated from PBMCs, needs to be carried out to prove the impact of HoxA9 on this issue in the human immune system. One approach could be the use of siRNA or small molecules that inhibit HoxA9 and its co-factors to study this system in human pDCs. By doing so, prominent downstream targets of HoxA9 in pDCs could be identified. Their expression should be confirmed with other methods e.g. qPCR and on the protein level using western plots or ELISA. In times of strong decline in sequencing costs, next-generation sequencing (NGS) should be used in the future if possible. Overall, data found in gene expression profiles need to be confirmed for single genes with qPCR and on the protein level.

5. SUMMARY AND FUTURE PROSPECTS

Experiments of *ex vivo* isolated primary BM cells, splenocytes, and sorted BM pDCs as well as *in vitro* generated Flt3L- and M-CSF-induced pDCs reproducibly showed dysfunctional IFN-α responses upon TLR7 and 9 stimulation throughout all cell strains derived from HoxA9$^{-/-}$ mice. These data collectively implicate HoxA9 as an important mediator in TLR-associated functions particularly in pDCs. Reduced IL-6 levels in cell settings with high concentrations of pDCs point towards an impact of HoxA9 on both signaling pathways via NFκB and IRF7 leading to production of proinflammatory cytokines and type I IFNs, respectively. FACS data of the BM and spleen demonstrated no significant influence on frequencies and maturity of pDCs *in vivo* using standard surface expression markers. However, significantly reduced total cell counts and viable cells as well as shifted CD11b expression in Flt3L-induced DC cultures strongly suggest involvement of HoxA9 in DC development *in vitro*, probably in part via transcriptional regulation of the cytokine receptor Flt3. The fact that expression of the latter was only slightly decreased in FACS stainings as well as the microarray expression profil leads to the assumption that other genes might be involved and that compensation takes place *in vivo*. According to recent findings (Lebert-Ghali et al., 2016), it seems likely that HoxA9 largely regulates genes involved in proliferation and has only little influence on differentiation of pDCs, which would explain reduced cell amounts in HoxA9$^{-/-}$ cultures. Other innate immune cells investigated in this study including cDCs and MΦs neither show functional impairment of TLR-mediated immune responses nor developmental alterations.

Hox genes are evolutionary highly conserved genes and represent central players in different very important tasks. HoxA9 has been shown to participate in embryogenesis and hematopoiesis and plays a central role in leukemogenesis (Ramos-Mejía et al., 2014). My results implicate a substantial role for HoxA9 in TLR function particularly in pDCs and participation in DC development *in vitro*, which is dispensable *in vivo*. The upregulated co-factor Meis1 in the knockout pDCs might explain one compensational mechanism. The data generated in this study provides evidence for the involvement of Hox genes in differentiated hematopoietic cells and not only in HSCs and precursors cells, which has not been reported so far to the best of my knowledge. Because HoxA9 was shown to cooperate with different co-factors, general factors, and cell-type dependent transcription factors, future research should investigate the whole machinery associated

with HoxA9 in pDCs. To date, very less in known about the longevity of pDCs. However, it is believed that these cells can last for many months, or even years, in peripheral tissues in mice (Reizis et al., 2011). For HoxA9 and other Hox genes promote maintaining the stem cell status of HSCs, it is supposable that these genes might be involved in keeping some sort of self-renewal of peripheral pDCs when activated by TLRs, which could provide the longevity of this DC subset. Moreover, Hox genes are known to influence the spatiotemporal fate of embryonic tissues. Is it possible that certain expression patterns of Hox genes determine the spatiotemporal fate of pDCs when activated?

The fact that pDCs are not simply IFN producing cells but play crucial roles in initiating different innate immune responses, providing adaptive immune responses, and inducing immune regulation, emphasizes the importance of these cells in physiologic immune mechanisms despite the rarity compared to other cells of the immune system. Recent years revealed the involvement of pDCs in several pathologic conditions such as infections, autoimmune diseases, and different types of cancer. Growing evidence in this field will unveil further knowledge that is needed to understand physiology as well as disease provided by these cells. Novel therapies or diagnostics may proceed from future research.

6. REFERENCES

Abbas, A.K., Lichtman, A.H., and Pillai, S. (2007). Cellular and molecular immunology, 6th edn (Philadelphia, USA: Saunders Elsevier).

Alexopoulou, L., Holt, A.C., Medzhitov, R., and Flavell, R.A. (2001). Recognition of double-stranded RNA and activation of NF-kappaB by Toll-like receptor 3. Nature *413*, 732-738.

Alharbi, R.A., Pettengell, R., Pandha, H.S., and Morgan, R. (2013). The role of HOX genes in normal hematopoiesis and acute leukemia. Leukemia *27*, 1000-1008.

Andrade, W.A., Souza, M.o.C., Ramos-Martinez, E., Nagpal, K., Dutra, M.S., Melo, M.B., Bartholomeu, D.C., Ghosh, S., Golenbock, D.T., and Gazzinelli, R.T. (2013). Combined action of nucleic acid-sensing Toll-like receptors and TLR11/TLR12 heterodimers imparts resistance to Toxoplasma gondii in mice. Cell Host Microbe *13*, 42-53.

Andreeff, M., Ruvolo, V., Gadgil, S., Zeng, C., Coombes, K., Chen, W., Kornblau, S., Barón, A.E., and Drabkin, H.A. (2008). HOX expression patterns identify a common signature for favorable AML. Leukemia *22*, 2041-2047.

Austyn, J.M., and Gordon, S. (1981). F4/80, a monoclonal antibody directed specifically against the mouse macrophage. Eur J Immunol *11*, 805-815.

Avrameas, S., and Guilbert, B. (1971). A method for quantitative determination of cellular immunoglobulins by enzyme-labeled antibodies. Eur J Immunol *1*, 394-396.

Bach, J.F. (2002). The effect of infections on susceptibility to autoimmune and allergic diseases. N Engl J Med *347*, 911-920.

Bao, M., and Liu, Y.J. (2012). Regulation of TLR7/9 signaling in plasmacytoid dendritic cells. Protein Cell.

Barbalat, R., Lau, L., Locksley, R.M., and Barton, G.M. (2009). Toll-like receptor 2 on inflammatory monocytes induces type I interferon in response to viral but not bacterial ligands. Nat Immunol *10*, 1200-1207.

Barton, G.M., Kagan, J.C., and Medzhitov, R. (2006). Intracellular localization of Toll-like receptor 9 prevents recognition of self DNA but facilitates access to viral DNA. Nat Immunol *7*, 49-56.

Basu, S., Campbell, H.M., Dittel, B.N., and Ray, A. (2010). Purification of specific cell population by fluorescence activated cell sorting (FACS). J Vis Exp.

Bauer, S. (2013). Toll-like receptor 9 processing: the key event in Toll-like receptor 9 activation? Immunol Lett *149*, 85-87.

Bauer, S., Kirschning, C.J., Häcker, H., Redecke, V., Hausmann, S., Akira, S., Wagner, H., and Lipford, G.B. (2001). Human TLR9 confers responsiveness to bacterial DNA via species-specific CpG motif recognition. Proc Natl Acad Sci U S A *98*, 9237-9242.

Bei, L., Lu, Y., and Eklund, E.A. (2005). HOXA9 activates transcription of the gene encoding gp91Phox during myeloid differentiation. J Biol Chem *280*, 12359-12370.

BERSON, S.A., and YALOW, R.S. (1959). Quantitative aspects of the reaction between insulin and insulin-binding antibody. J Clin Invest *38*, 1996-2016.

Bhatlekar, S., Fields, J.Z., and Boman, B.M. (2014). HOX genes and their role in the development of human cancers. J Mol Med (Berl) *92*, 811-823.

Biondo, C., Malara, A., Costa, A., Signorino, G., Cardile, F., Midiri, A., Galbo, R., Papasergi, S., Domina, M., Pugliese, M.*, et al.* (2012). Recognition of fungal RNA by TLR7 has a nonredundant role in host defense against experimental candidiasis. Eur J Immunol *42*, 2632-2643.

Björck, P., Leong, H.X., and Engleman, E.G. (2011). Plasmacytoid dendritic cell dichotomy: identification of IFN-α producing cells as a phenotypically and functionally distinct subset. J Immunol *186*, 1477-1485.

Blasius, A.L., Arnold, C.N., Georgel, P., Rutschmann, S., Xia, Y., Lin, P., Ross, C., Li, X., Smart, N.G., and Beutler, B. (2010). Slc15a4, AP-3, and Hermansky-Pudlak syndrome proteins are required for Toll-like receptor signaling in plasmacytoid dendritic cells. Proc Natl Acad Sci U S A *107*, 19973-19978.

Blasius, A.L., Barchet, W., Cella, M., and Colonna, M. (2007). Development and function of murine B220+CD11c+NK1.1+ cells identify them as a subset of NK cells. J Exp Med *204*, 2561-2568.

Blasius, A.L., and Beutler, B. (2010). Intracellular toll-like receptors. Immunity *32*, 305-315.

Blasius, A.L., and Colonna, M. (2006). Sampling and signaling in plasmacytoid dendritic cells: the potential roles of Siglec-H. Trends Immunol *27*, 255-260.

Blasius, A.L., Giurisato, E., Cella, M., Schreiber, R.D., Shaw, A.S., and Colonna, M. (2006). Bone marrow stromal cell antigen 2 is a specific marker of type I IFN-producing cells in the naive mouse, but a promiscuous cell surface antigen following IFN stimulation. J Immunol *177*, 3260-3265.

Boivin, V., Deschamps-Francoeur, G., and Scott, M.S. (2017). Protein coding genes as hosts for noncoding RNA expression. Semin Cell Dev Biol.

Bordon, Y. (2012). Innate immunity: TLR13, unlucky, but just for some. Nat Rev Immunol *12*, 618-619.

Boyer, S.W., Beaudin, A.E., and Forsberg, E.C. (2012). Mapping differentiation pathways from hematopoietic stem cells using Flk2/Flt3 lineage tracing. Cell Cycle *11*, 3180-3188.

Boyer, S.W., Schroeder, A.V., Smith-Berdan, S., and Forsberg, E.C. (2011). All hematopoietic cells develop from hematopoietic stem cells through Flk2/Flt3-positive progenitor cells. Cell Stem Cell *9*, 64-73.

Brasel, K., De Smedt, T., Smith, J.L., and Maliszewski, C.R. (2000). Generation of murine dendritic cells from flt3-ligand-supplemented bone marrow cultures. Blood *96*, 3029-3039.

Brawand, P., Fitzpatrick, D.R., Greenfield, B.W., Brasel, K., Maliszewski, C.R., and De Smedt, T. (2002). Murine plasmacytoid pre-dendritic cells generated from Flt3 ligand-supplemented bone marrow cultures are immature APCs. J Immunol *169*, 6711-6719.

Brooks, J.C., Sun, W., Chiosis, G., and Leifer, C.A. (2012). Heat shock protein gp96 regulates Toll-like receptor 9 proteolytic processing and conformational stability. Biochem Biophys Res Commun *421*, 780-784.

Caminschi, I., Ahmet, F., Heger, K., Brady, J., Nutt, S.L., Vremec, D., Pietersz, S., Lahoud, M.H., Schofield, L., Hansen, D.S.*, et al.* (2007). Putative IKDCs are functionally and developmentally similar to natural killer cells, but not to dendritic cells. J Exp Med *204*, 2579-2590.

Cao, W., and Bover, L. (2010). Signaling and ligand interaction of ILT7: receptor-mediated regulatory mechanisms for plasmacytoid dendritic cells. Immunol Rev *234*, 163-176.

Cao, W., Bover, L., Cho, M., Wen, X., Hanabuchi, S., Bao, M., Rosen, D.B., Wang, Y.H., Shaw, J.L., Du, Q.*, et al.* (2009). Regulation of TLR7/9 responses in plasmacytoid dendritic cells by BST2 and ILT7 receptor interaction. J Exp Med *206*, 1603-1614.

Cao, W., and Liu, Y.J. (2006). Opn: key regulator of pDC interferon production. Nat Immunol *7*, 441-443.

Cao, W., Manicassamy, S., Tang, H., Kasturi, S.P., Pirani, A., Murthy, N., and Pulendran, B. (2008). Toll-like receptor-mediated induction of type I interferon in plasmacytoid dendritic cells requires the rapamycin-sensitive PI(3)K-mTOR-p70S6K pathway. Nat Immunol *9*, 1157-1164.

Cao, W., Rosen, D.B., Ito, T., Bover, L., Bao, M., Watanabe, G., Yao, Z., Zhang, L., Lanier, L.L., and Liu, Y.J. (2006). Plasmacytoid dendritic cell-specific receptor ILT7-Fc epsilonRI gamma inhibits Toll-like receptor-induced interferon production. J Exp Med *203*, 1399-1405.

Casrouge, A., Zhang, S.Y., Eidenschenk, C., Jouanguy, E., Puel, A., Yang, K., Alcais, A., Picard, C., Mahfoufi, N., Nicolas, N.*, et al.* (2006). Herpes simplex virus encephalitis in human UNC-93B deficiency. Science *314*, 308-312.

Caux, C., Dezutter-Dambuyant, C., Schmitt, D., and Banchereau, J. (1992). GM-CSF and TNF-alpha cooperate in the generation of dendritic Langerhans cells. Nature *360*, 258-261.

Chen, F., and Capecchi, M.R. (1997). Targeted mutations in hoxa-9 and hoxb-9 reveal synergistic interactions. Dev Biol *181*, 186-196.

Choi, Y.J., Im, E., Chung, H.K., Pothoulakis, C., and Rhee, S.H. (2010). TRIF mediates Toll-like receptor 5-induced signaling in intestinal epithelial cells. J Biol Chem *285*, 37570-37578.

Cisse, B., Caton, M.L., Lehner, M., Maeda, T., Scheu, S., Locksley, R., Holmberg, D., Zweier, C., den Hollander, N.S., Kant, S.G.*, et al.* (2008). Transcription factor E2-2 is an essential and specific regulator of plasmacytoid dendritic cell development. Cell *135*, 37-48.

Coban, C., Igari, Y., Yagi, M., Reimer, T., Koyama, S., Aoshi, T., Ohata, K., Tsukui, T., Takeshita, F., Sakurai, K.*, et al.* (2010). Immunogenicity of whole-parasite vaccines against Plasmodium falciparum involves malarial hemozoin and host TLR9. Cell Host Microbe *7*, 50-61.

Collins, C., Wang, J., Miao, H., Bronstein, J., Nawer, H., Xu, T., Figueroa, M., Muntean, A.G., and Hess, J.L. (2014). C/EBPα is an essential collaborator in Hoxa9/Meis1-mediated leukemogenesis. Proc Natl Acad Sci U S A *111*, 9899-9904.

Collins, C.T., and Hess, J.L. (2016). Deregulation of the HOXA9/MEIS1 axis in acute leukemia. Curr Opin Hematol *23*, 354-361.

Colonna, M., Trinchieri, G., and Liu, Y.J. (2004). Plasmacytoid dendritic cells in immunity. Nat Immunol *5*, 1219-1226.

Dambuza, I.M., and Brown, G.D. (2015). C-type lectins in immunity: recent developments. Curr Opin Immunol *32C*, 21-27.

Dasgupta, S., Erturk-Hasdemir, D., Ochoa-Reparaz, J., Reinecker, H.C., and Kasper, D.L. (2014). Plasmacytoid dendritic cells mediate anti-inflammatory responses to a gut commensal molecule via both innate and adaptive mechanisms. Cell Host Microbe *15*, 413-423.

Dey, A., Allen, J., and Hankey-Giblin, P.A. (2014). Ontogeny and polarization of macrophages in inflammation: blood monocytes versus tissue macrophages. Front Immunol *5*, 683.

Diebold, S.S., Kaisho, T., Hemmi, H., Akira, S., and Reis e Sousa, C. (2004). Innate antiviral responses by means of TLR7-mediated recognition of single-stranded RNA. Science *303*, 1529-1531.

Dolence, J.J., Gwin, K.A., Shapiro, M.B., and Medina, K.L. (2014). Flt3 signaling regulates the proliferation, survival, and maintenance of multipotent hematopoietic progenitors that generate B cell precursors. Exp Hematol *42*, 380-393.e383.

Dorsam, S.T., Ferrell, C.M., Dorsam, G.P., Derynck, M.K., Vijapurkar, U., Khodabakhsh, D., Pau, B., Bernstein, H., Haqq, C.M., Largman, C., and Lawrence, H.J. (2004). The transcriptome of the leukemogenic homeoprotein HOXA9 in human hematopoietic cells. Blood *103*, 1676-1684.

Dzionek, A., Sohma, Y., Nagafune, J., Cella, M., Colonna, M., Facchetti, F., Günther, G., Johnston, I., Lanzavecchia, A., Nagasaka, T.*, et al.* (2001). BDCA-2, a novel plasmacytoid dendritic cell-specific type II C-type lectin, mediates antigen capture and is a potent inhibitor of interferon alpha/beta induction. J Exp Med *194*, 1823-1834.

Eberle, F., Sirin, M., Binder, M., and Dalpke, A.H. (2009). Bacterial RNA is recognized by different sets of immunoreceptors. Eur J Immunol *39*, 2537-2547.

Enesa, K., Ordureau, A., Smith, H., Barford, D., Cheung, P.C., Patterson-Kane, J., Arthur, J.S., and Cohen, P. (2012). Pellino1 is required for interferon production by viral double-stranded RNA. J Biol Chem *287*, 34825-34835.

Engvall, E., and Perlmann, P. (1971). Enzyme-linked immunosorbent assay (ELISA). Quantitative assay of immunoglobulin G. Immunochemistry *8*, 871-874.

Epelman, S., Lavine, K.J., and Randolph, G.J. (2014). Origin and functions of tissue macrophages. Immunity *41*, 21-35.

Esashi, E., Bao, M., Wang, Y.H., Cao, W., and Liu, Y.J. (2012). PACSIN1 regulates the TLR7/9-mediated type I interferon response in plasmacytoid dendritic cells. Eur J Immunol *42*, 573-579.

Esashi, E., Wang, Y.H., Perng, O., Qin, X.F., Liu, Y.J., and Watowich, S.S. (2008). The signal transducer STAT5 inhibits plasmacytoid dendritic cell development by suppressing transcription factor IRF8. Immunity *28*, 509-520.

Essers, M.A., Offner, S., Blanco-Bose, W.E., Waibler, Z., Kalinke, U., Duchosal, M.A., and Trumpp, A. (2009). IFNalpha activates dormant haematopoietic stem cells in vivo. Nature *458*, 904-908.

Ewald, S.E., Engel, A., Lee, J., Wang, M., Bogyo, M., and Barton, G.M. (2011). Nucleic acid recognition by Toll-like receptors is coupled to stepwise processing by cathepsins and asparagine endopeptidase. J Exp Med *208*, 643-651.

Faber, J., Krivtsov, A.V., Stubbs, M.C., Wright, R., Davis, T.N., van den Heuvel-Eibrink, M., Zwaan, C.M., Kung, A.L., and Armstrong, S.A. (2009). HOXA9 is required for survival in human MLL-rearranged acute leukemias. Blood *113*, 2375-2385.

Fancke, B., Suter, M., Hochrein, H., and O'Keeffe, M. (2008). M-CSF: a novel plasmacytoid and conventional dendritic cell poietin. Blood *111*, 150-159.

Ferrando, A.A., Armstrong, S.A., Neuberg, D.S., Sallan, S.E., Silverman, L.B., Korsmeyer, S.J., and Look, A.T. (2003). Gene expression signatures in MLL-rearranged T-lineage and B-precursor acute leukemias: dominance of HOX dysregulation. Blood *102*, 262-268.

Ferrell, C.M., Dorsam, S.T., Ohta, H., Humphries, R.K., Derynck, M.K., Haqq, C., Largman, C., and Lawrence, H.J. (2005). Activation of stem-cell specific genes by HOXA9 and HOXA10 homeodomain proteins in CD34+ human cord blood cells. Stem Cells *23*, 644-655.

Flajnik, M.F. (2014). Re-evaluation of the immunological Big Bang. Curr Biol *24*, R1060-1065.

Flajnik, M.F., and Du Pasquier, L. (2004). Evolution of innate and adaptive immunity: can we draw a line? Trends Immunol *25*, 640-644.

Gan, T., Jude, C.D., Zaffuto, K., and Ernst, P. (2010). Developmentally induced Mll1 loss reveals defects in postnatal haematopoiesis. Leukemia *24*, 1732-1741.

Ganguly, D., Haak, S., Sisirak, V., and Reizis, B. (2013). The role of dendritic cells in autoimmunity. Nat Rev Immunol *13*, 566-577.

Gay, N.J., and Keith, F.J. (1991). Drosophila Toll and IL-1 receptor. Nature *351*, 355-356.

Geissmann, F., Manz, M.G., Jung, S., Sieweke, M.H., Merad, M., and Ley, K. (2010). Development of monocytes, macrophages, and dendritic cells. Science *327*, 656-661.

Ghosh, H.S., Cisse, B., Bunin, A., Lewis, K.L., and Reizis, B. (2010). Continuous expression of the transcription factor e2-2 maintains the cell fate of mature plasmacytoid dendritic cells. Immunity *33*, 905-916.

Gilliet, M., Boonstra, A., Paturel, C., Antonenko, S., Xu, X.L., Trinchieri, G., O'Garra, A., and Liu, Y.J. (2002). The development of murine plasmacytoid dendritic cell precursors is differentially regulated by FLT3-ligand and granulocyte/macrophage colony-stimulating factor. J Exp Med *195*, 953-958.

Gilliet, M., Cao, W., and Liu, Y.J. (2008). Plasmacytoid dendritic cells: sensing nucleic acids in viral infection and autoimmune diseases. Nat Rev Immunol *8*, 594-606.

Ginhoux, F., Tacke, F., Angeli, V., Bogunovic, M., Loubeau, M., Dai, X.M., Stanley, E.R., Randolph, G.J., and Merad, M. (2006). Langerhans cells arise from monocytes in vivo. Nat Immunol *7*, 265-273.

Golub, T.R., Slonim, D.K., Tamayo, P., Huard, C., Gaasenbeek, M., Mesirov, J.P., Coller, H., Loh, M.L., Downing, J.R., Caligiuri, M.A.*, et al.* (1999). Molecular classification of cancer: class discovery and class prediction by gene expression monitoring. Science *286*, 531-537.

Gorden, K.K., Qiu, X.X., Binsfeld, C.C., Vasilakos, J.P., and Alkan, S.S. (2006). Cutting edge: activation of murine TLR8 by a combination of imidazoquinoline immune response modifiers and polyT oligodeoxynucleotides. J Immunol *177*, 6584-6587.

Gotoh, K., Tanaka, Y., Nishikimi, A., Nakamura, R., Yamada, H., Maeda, N., Ishikawa, T., Hoshino, K., Uruno, T., Cao, Q.*, et al.* (2010). Selective control of type I IFN induction by the Rac activator DOCK2 during TLR-mediated plasmacytoid dendritic cell activation. J Exp Med *207*, 721-730.

Guiducci, C., Ghirelli, C., Marloie-Provost, M.A., Matray, T., Coffman, R.L., Liu, Y.J., Barrat, F.J., and Soumelis, V. (2008). PI3K is critical for the nuclear translocation of IRF-

7 and type I IFN production by human plasmacytoid predendritic cells in response to TLR activation. J Exp Med *205*, 315-322.

Guiducci, C., Ott, G., Chan, J.H., Damon, E., Calacsan, C., Matray, T., Lee, K.D., Coffman, R.L., and Barrat, F.J. (2006). Properties regulating the nature of the plasmacytoid dendritic cell response to Toll-like receptor 9 activation. J Exp Med *203*, 1999-2008.

Guimont-Desrochers, F., Boucher, G., Dong, Z., Dupuis, M., Veillette, A., and Lesage, S. (2012). Redefining interferon-producing killer dendritic cells as a novel intermediate in NK-cell differentiation. Blood *119*, 4349-4357.

Gwin, K., Dolence, J.J., Shapiro, M.B., and Medina, K.L. (2013a). Differential requirement for Hoxa9 in the development and differentiation of B, NK, and DC-lineage cells from Flt3+ multipotential progenitors. BMC Immunol *14*, 5.

Gwin, K., Frank, E., Bossou, A., and Medina, K.L. (2010). Hoxa9 regulates Flt3 in lymphohematopoietic progenitors. J Immunol *185*, 6572-6583.

Gwin, K.A., Shapiro, M.B., Dolence, J.J., Huang, Z.L., and Medina, K.L. (2013b). Hoxa9 and flt3 signaling synergistically regulate an early checkpoint in lymphopoiesis. J Immunol *191*, 745-754.

Gürtler, C., and Bowie, A.G. (2013). Innate immune detection of microbial nucleic acids. Trends Microbiol.

Haas, T., Metzger, J., Schmitz, F., Heit, A., Müller, T., Latz, E., and Wagner, H. (2008). The DNA sugar backbone 2' deoxyribose determines toll-like receptor 9 activation. Immunity *28*, 315-323.

Hahm, B., Trifilo, M.J., Zuniga, E.I., and Oldstone, M.B. (2005). Viruses evade the immune system through type I interferon-mediated STAT2-dependent, but STAT1-independent, signaling. Immunity *22*, 247-257.

Hasan, U., Chaffois, C., Gaillard, C., Saulnier, V., Merck, E., Tancredi, S., Guiet, C., Brière, F., Vlach, J., Lebecque, S.*, et al.* (2005). Human TLR10 is a functional receptor, expressed by B cells and plasmacytoid dendritic cells, which activates gene transcription through MyD88. J Immunol *174*, 2942-2950.

Heil, F., Ahmad-Nejad, P., Hemmi, H., Hochrein, H., Ampenberger, F., Gellert, T., Dietrich, H., Lipford, G., Takeda, K., Akira, S.*, et al.* (2003). The Toll-like receptor 7 (TLR7)-specific stimulus loxoribine uncovers a strong relationship within the TLR7, 8 and 9 subfamily. Eur J Immunol *33*, 2987-2997.

Heil, F., Hemmi, H., Hochrein, H., Ampenberger, F., Kirschning, C., Akira, S., Lipford, G., Wagner, H., and Bauer, S. (2004). Species-specific recognition of single-stranded RNA via toll-like receptor 7 and 8. Science *303*, 1526-1529.

Hemmi, H., Kaisho, T., Takeda, K., and Akira, S. (2003). The roles of Toll-like receptor 9, MyD88, and DNA-dependent protein kinase catalytic subunit in the effects of two distinct CpG DNAs on dendritic cell subsets. J Immunol *170*, 3059-3064.

Hemmi, H., Kaisho, T., Takeuchi, O., Sato, S., Sanjo, H., Hoshino, K., Horiuchi, T., Tomizawa, H., Takeda, K., and Akira, S. (2002). Small anti-viral compounds activate immune cells via the TLR7 MyD88-dependent signaling pathway. Nat Immunol *3*, 196-200.

Hemmi, H., Takeuchi, O., Kawai, T., Kaisho, T., Sato, S., Sanjo, H., Matsumoto, M., Hoshino, K., Wagner, H., Takeda, K., and Akira, S. (2000). A Toll-like receptor recognizes bacterial DNA. Nature *408*, 740-745.

Heng, T.S., Painter, M.W., and Consortium, I.G.P. (2008). The Immunological Genome Project: networks of gene expression in immune cells. Nat Immunol *9*, 1091-1094.

Herzenberg, L.A., Parks, D., Sahaf, B., Perez, O., and Roederer, M. (2002). The history and future of the fluorescence activated cell sorter and flow cytometry: a view from Stanford. Clin Chem *48*, 1819-1827.

Hess, J.L., Bittner, C.B., Zeisig, D.T., Bach, C., Fuchs, U., Borkhardt, A., Frampton, J., and Slany, R.K. (2006). c-Myb is an essential downstream target for homeobox-mediated transformation of hematopoietic cells. Blood *108*, 297-304.

Hidmark, A., von Saint Paul, A., and Dalpke, A.H. (2012). Cutting edge: TLR13 is a receptor for bacterial RNA. J Immunol *189*, 2717-2721.

Hirsch, S., Austyn, J.M., and Gordon, S. (1981). Expression of the macrophage-specific antigen F4/80 during differentiation of mouse bone marrow cells in culture. J Exp Med *154*, 713-725.

Hochrein, H., and Kirschning, C.J. (2013). Bacteria evade immune recognition via TLR13 and binding of their 23S rRNA by MLS antibiotics by the same mechanisms. Oncoimmunology *2*, e23141.

Hoebe, K., Du, X., Georgel, P., Janssen, E., Tabeta, K., Kim, S.O., Goode, J., Lin, P., Mann, N., Mudd, S.*, et al.* (2003). Identification of Lps2 as a key transducer of MyD88-independent TIR signalling. Nature *424*, 743-748.

Holland, P.W. (2013). Evolution of homeobox genes. Wiley Interdiscip Rev Dev Biol *2*, 31-45.

Honda, K., Ohba, Y., Yanai, H., Negishi, H., Mizutani, T., Takaoka, A., Taya, C., and Taniguchi, T. (2005a). Spatiotemporal regulation of MyD88-IRF-7 signalling for robust type-I interferon induction. Nature *434*, 1035-1040.

Honda, K., Yanai, H., Negishi, H., Asagiri, M., Sato, M., Mizutani, T., Shimada, N., Ohba, Y., Takaoka, A., Yoshida, N., and Taniguchi, T. (2005b). IRF-7 is the master regulator of type-I interferon-dependent immune responses. Nature *434*, 772-777.

Hornung, V., Guenthner-Biller, M., Bourquin, C., Ablasser, A., Schlee, M., Uematsu, S., Noronha, A., Manoharan, M., Akira, S., de Fougerolles, A.*, et al.* (2005). Sequence-specific potent induction of IFN-alpha by short interfering RNA in plasmacytoid dendritic cells through TLR7. Nat Med *11*, 263-270.

Hu, Y.L., Fong, S., Ferrell, C., Largman, C., and Shen, W.F. (2009). HOXA9 modulates its oncogenic partner Meis1 to influence normal hematopoiesis. Mol Cell Biol *29*, 5181-5192.

Hu, Y.L., Passegué, E., Fong, S., Largman, C., and Lawrence, H.J. (2007). Evidence that the Pim1 kinase gene is a direct target of HOXA9. Blood *109*, 4732-4738.

Huang, Y., Sitwala, K., Bronstein, J., Sanders, D., Dandekar, M., Collins, C., Robertson, G., MacDonald, J., Cezard, T., Bilenky, M.*, et al.* (2012). Identification and characterization of Hoxa9 binding sites in hematopoietic cells. Blood *119*, 388-398.

Häcker, H., Mischak, H., Miethke, T., Liptay, S., Schmid, R., Sparwasser, T., Heeg, K., Lipford, G.B., and Wagner, H. (1998). CpG-DNA-specific activation of antigen-presenting cells requires stress kinase activity and is preceded by non-specific endocytosis and endosomal maturation. EMBO J *17*, 6230-6240.

Idoyaga, J., and Steinman, R.M. (2011). SnapShot: Dendritic Cells. Cell *146*, 660-660.e662.

Imai, Y., Kuba, K., Neely, G.G., Yaghubian-Malhami, R., Perkmann, T., van Loo, G., Ermolaeva, M., Veldhuizen, R., Leung, Y.H., Wang, H.*, et al.* (2008). Identification of oxidative stress and Toll-like receptor 4 signaling as a key pathway of acute lung injury. Cell *133*, 235-249.

Inaba, K., Inaba, M., Romani, N., Aya, H., Deguchi, M., Ikehara, S., Muramatsu, S., and Steinman, R.M. (1992). Generation of large numbers of dendritic cells from mouse bone marrow cultures supplemented with granulocyte/macrophage colony-stimulating factor. J Exp Med *176*, 1693-1702.

Italiani, P., and Boraschi, D. (2014). From Monocytes to M1/M2 Macrophages: Phenotypical vs. Functional Differentiation. Front Immunol *5*, 514.

Janeway, C.A., and Medzhitov, R. (2002). Innate immune recognition. Annu Rev Immunol *20*, 197-216.

Jin, M.S., and Lee, J.O. (2008). Structures of the toll-like receptor family and its ligand complexes. Immunity *29*, 182-191.

Jung, S., von Thülen, T., Laukemper, V., Pigisch, S., Hangel, D., Wagner, H., Kaufmann, A., and Bauer, S. (2015). A Single Naturally Occurring 2'-O-Methylation Converts a TLR7- and TLR8-Activating RNA into a TLR8-Specific Ligand. PLoS One *10*, e0120498.

Jurk, M., Heil, F., Vollmer, J., Schetter, C., Krieg, A.M., Wagner, H., Lipford, G., and Bauer, S. (2002). Human TLR7 or TLR8 independently confer responsiveness to the antiviral compound R-848. Nat Immunol *3*, 499.

Jöckel, S., Nees, G., Sommer, R., Zhao, Y., Cherkasov, D., Hori, H., Ehm, G., Schnare, M., Nain, M., Kaufmann, A., and Bauer, S. (2012). The 2'-O-methylation status of a

single guanosine controls transfer RNA-mediated Toll-like receptor 7 activation or inhibition. J Exp Med *209*, 235-241.

Kamogawa-Schifter, Y., Ohkawa, J., Namiki, S., Arai, N., Arai, K., and Liu, Y. (2005). Ly49Q defines 2 pDC subsets in mice. Blood *105*, 2787-2792.

Karrich, J.J., Jachimowski, L.C., Uittenbogaart, C.H., and Blom, B. (2014). The plasmacytoid dendritic cell as the Swiss army knife of the immune system: molecular regulation of its multifaceted functions. J Immunol *193*, 5772-5778.

Kato, H., Takeuchi, O., Sato, S., Yoneyama, M., Yamamoto, M., Matsui, K., Uematsu, S., Jung, A., Kawai, T., Ishii, K.J.*, et al.* (2006). Differential roles of MDA5 and RIG-I helicases in the recognition of RNA viruses. Nature *441*, 101-105.

Kawagoe, T., Sato, S., Matsushita, K., Kato, H., Matsui, K., Kumagai, Y., Saitoh, T., Kawai, T., Takeuchi, O., and Akira, S. (2008). Sequential control of Toll-like receptor-dependent responses by IRAK1 and IRAK2. Nat Immunol *9*, 684-691.

Kawai, T., and Akira, S. (2009). The roles of TLRs, RLRs and NLRs in pathogen recognition. Int Immunol *21*, 317-337.

Kawai, T., and Akira, S. (2010). The role of pattern-recognition receptors in innate immunity: update on Toll-like receptors. Nat Immunol *11*, 373-384.

Kawai, T., and Akira, S. (2011). Toll-like receptors and their crosstalk with other innate receptors in infection and immunity. Immunity *34*, 637-650.

Kerkmann, M., Costa, L.T., Richter, C., Rothenfusser, S., Battiany, J., Hornung, V., Johnson, J., Englert, S., Ketterer, T., Heckl, W.*, et al.* (2005). Spontaneous formation of nucleic acid-based nanoparticles is responsible for high interferon-alpha induction by CpG-A in plasmacytoid dendritic cells. J Biol Chem *280*, 8086-8093.

Kim, Y.M., Brinkmann, M.M., Paquet, M.E., and Ploegh, H.L. (2008). UNC93B1 delivers nucleotide-sensing toll-like receptors to endolysosomes. Nature *452*, 234-238.

Kingston, D., Schmid, M.A., Onai, N., Obata-Onai, A., Baumjohann, D., and Manz, M.G. (2009). The concerted action of GM-CSF and Flt3-ligand on in vivo dendritic cell homeostasis. Blood *114*, 835-843.

Konig, H., and Levis, M. (2015). Targeting FLT3 to treat leukemia. Expert Opin Ther Targets *19*, 37-54.

Kumar, H., Kawai, T., and Akira, S. (2009). Toll-like receptors and innate immunity. Biochem Biophys Res Commun *388*, 621-625.

Kumar, H., Kawai, T., and Akira, S. (2011). Pathogen recognition by the innate immune system. Int Rev Immunol *30*, 16-34.

Ladam, F., and Sagerström, C.G. (2013). Hox regulation of transcription: More complex(es). Dev Dyn.

Laerum, O.D., Sletvold, O., and Riise, T. (1988). Circadian and circannual variations of cell cycle distribution in the mouse bone marrow. Chronobiol Int *5*, 19-35.

Lande, R., and Gilliet, M. (2010). Plasmacytoid dendritic cells: key players in the initiation and regulation of immune responses. Ann N Y Acad Sci *1183*, 89-103.

LaRonde-LeBlanc, N.A., and Wolberger, C. (2003). Structure of HoxA9 and Pbx1 bound to DNA: Hox hexapeptide and DNA recognition anterior to posterior. Genes Dev *17*, 2060-2072.

Latz, E., Verma, A., Visintin, A., Gong, M., Sirois, C.M., Klein, D.C., Monks, B.G., McKnight, C.J., Lamphier, M.S., Duprex, W.P.*, et al.* (2007). Ligand-induced conformational changes allosterically activate Toll-like receptor 9. Nat Immunol *8*, 772-779.

Lawrence, H.J., Christensen, J., Fong, S., Hu, Y.L., Weissman, I., Sauvageau, G., Humphries, R.K., and Largman, C. (2005). Loss of expression of the Hoxa-9 homeobox gene impairs the proliferation and repopulating ability of hematopoietic stem cells. Blood *106*, 3988-3994.

Lawrence, H.J., Helgason, C.D., Sauvageau, G., Fong, S., Izon, D.J., Humphries, R.K., and Largman, C. (1997). Mice bearing a targeted interruption of the homeobox gene HOXA9 have defects in myeloid, erythroid, and lymphoid hematopoiesis. Blood *89*, 1922-1930.

Le Tortorec, A., Willey, S., and Neil, S.J. (2011). Antiviral inhibition of enveloped virus release by tetherin/BST-2: action and counteraction. Viruses *3*, 520-540.

Lebert-Ghali, C., Fournier, M., Kettyle, L., Thompson, A., Sauvageau, G., and Bijl, J.J. (2016). Hoxa cluster genes determine the proliferative activity of adult mouse hematopoietic stem and progenitor cells. Blood *127*, 87-90.

Lee, B.L., Moon, J.E., Shu, J.H., Yuan, L., Newman, Z.R., Schekman, R., and Barton, G.M. (2013). UNC93B1 mediates differential trafficking of endosomal TLRs. Elife *2*, e00291.

Lee, H.K., Lund, J.M., Ramanathan, B., Mizushima, N., and Iwasaki, A. (2007). Autophagy-dependent viral recognition by plasmacytoid dendritic cells. Science *315*, 1398-1401.

Lee, J., Chuang, T.H., Redecke, V., She, L., Pitha, P.M., Carson, D.A., Raz, E., and Cottam, H.B. (2003). Molecular basis for the immunostimulatory activity of guanine nucleoside analogs: activation of Toll-like receptor 7. Proc Natl Acad Sci U S A *100*, 6646-6651.

Lehnertz, B., Pabst, C., Su, L., Miller, M., Liu, F., Yi, L., Zhang, R., Krosl, J., Yung, E., Kirschner, J*., et al.* (2014). The methyltransferase G9a regulates HoxA9-dependent transcription in AML. Genes Dev *28*, 317-327.

Lemaitre, B., Nicolas, E., Michaut, L., Reichhart, J.M., and Hoffmann, J.A. (1996). The dorsoventral regulatory gene cassette spätzle/Toll/cactus controls the potent antifungal response in Drosophila adults. Cell *86*, 973-983.

Leng, S.X., McElhaney, J.E., Walston, J.D., Xie, D., Fedarko, N.S., and Kuchel, G.A. (2008). ELISA and multiplex technologies for cytokine measurement in inflammation and aging research. J Gerontol A Biol Sci Med Sci *63*, 879-884.

Li, H.S., Gelbard, A., Martinez, G.J., Esashi, E., Zhang, H., Nguyen-Jackson, H., Liu, Y.J., Overwijk, W.W., and Watowich, S.S. (2011). Cell-intrinsic role for IFN-α-STAT1 signals in regulating murine Peyer patch plasmacytoid dendritic cells and conditioning an inflammatory response. Blood *118*, 3879-3889.

Li, X.D., and Chen, Z.J. (2012). Sequence specific detection of bacterial 23S ribosomal RNA by TLR13. Elife *1*, e00102.

Lin, H.H., Faunce, D.E., Stacey, M., Terajewicz, A., Nakamura, T., Zhang-Hoover, J., Kerley, M., Mucenski, M.L., Gordon, S., and Stein-Streilein, J. (2005). The macrophage F4/80 receptor is required for the induction of antigen-specific efferent regulatory T cells in peripheral tolerance. J Exp Med *201*, 1615-1625.

Litman, G.W., Cannon, J.P., and Dishaw, L.J. (2005). Reconstructing immune phylogeny: new perspectives. Nat Rev Immunol *5*, 866-879.

Litvak, V., Ratushny, A.V., Lampano, A.E., Schmitz, F., Huang, A.C., Raman, A., Rust, A.G., Bergthaler, A., Aitchison, J.D., and Aderem, A. (2012). A FOXO3-IRF7 gene regulatory circuit limits inflammatory sequelae of antiviral responses. Nature *490*, 421-425.

Lombardi, V., Speak, A.O., Kerzerho, J., Szely, N., and Akbari, O. (2012). $CD8\alpha^{+}\beta^{-}$ and $CD8\alpha^{+}\beta^{+}$ plasmacytoid dendritic cells induce $Foxp3^{+}$ regulatory T cells and prevent the induction of airway hyper-reactivity. Mucosal Immunol *5*, 432-443.

Lund, J.M., Alexopoulou, L., Sato, A., Karow, M., Adams, N.C., Gale, N.W., Iwasaki, A., and Flavell, R.A. (2004). Recognition of single-stranded RNA viruses by Toll-like receptor 7. Proc Natl Acad Sci U S A *101*, 5598-5603.

Mancuso, G., Gambuzza, M., Midiri, A., Biondo, C., Papasergi, S., Akira, S., Teti, G., and Beninati, C. (2009). Bacterial recognition by TLR7 in the lysosomes of conventional dendritic cells. Nat Immunol *10*, 587-594.

Matsushima, N., Tanaka, T., Enkhbayar, P., Mikami, T., Taga, M., Yamada, K., and Kuroki, Y. (2007). Comparative sequence analysis of leucine-rich repeats (LRRs) within vertebrate toll-like receptors. BMC Genomics *8*, 124.

Medzhitov, R., Preston-Hurlburt, P., and Janeway, C.A. (1997). A human homologue of the Drosophila Toll protein signals activation of adaptive immunity. Nature *388*, 394-397.

Metlay, J.P., Witmer-Pack, M.D., Agger, R., Crowley, M.T., Lawless, D., and Steinman, R.M. (1990). The distinct leukocyte integrins of mouse spleen dendritic cells as identified with new hamster monoclonal antibodies. J Exp Med *171*, 1753-1771.

Michallet, M.C., Rota, G., Maslowski, K., and Guarda, G. (2013). Innate receptors for adaptive immunity. Curr Opin Microbiol *16*, 296-302.

Mishra, B.P., Zaffuto, K.M., Artinger, E.L., Org, T., Mikkola, H.K., Cheng, C., Djabali, M., and Ernst, P. (2014). The histone methyltransferase activity of MLL1 is dispensable for hematopoiesis and leukemogenesis. Cell Rep *7*, 1239-1247.

Miyake, K. (2006). Roles for accessory molecules in microbial recognition by Toll-like receptors. J Endotoxin Res *12*, 195-204.

Morgan, R. (2006). Hox genes: a continuation of embryonic patterning? Trends Genet *22*, 67-69.

Mullighan, C.G., Kennedy, A., Zhou, X., Radtke, I., Phillips, L.A., Shurtleff, S.A., and Downing, J.R. (2007). Pediatric acute myeloid leukemia with NPM1 mutations is characterized by a gene expression profile with dysregulated HOX gene expression distinct from MLL-rearranged leukemias. Leukemia *21*, 2000-2009.

Murphy, K.P., Janeway, C.A.J., Travers, P., Walport, M., Mowat, A., and Weaver, C.T. (2012). Janeway's immunobiology, 8th edn (New York, USA: Garland Science, Taylor & Francis Group, LLC).

Nagasawa, M., Schmidlin, H., Hazekamp, M.G., Schotte, R., and Blom, B. (2008). Development of human plasmacytoid dendritic cells depends on the combined action of the basic helix-loop-helix factor E2-2 and the Ets factor Spi-B. Eur J Immunol *38*, 2389-2400.

Nagel, S., Venturini, L., Marquez, V.E., Meyer, C., Kaufmann, M., Scherr, M., MacLeod, R.A., and Drexler, H.G. (2010). Polycomb repressor complex 2 regulates HOXA9 and HOXA10, activating ID2 in NK/T-cell lines. Mol Cancer *9*, 151.

Nagi, R.S., Bhat, A.S., and Kumar, H. (2014). Cancer: A Tale of Aberrant PRR Response. Front Immunol *5*, 161.

Naik, S.H., Proietto, A.I., Wilson, N.S., Dakic, A., Schnorrer, P., Fuchsberger, M., Lahoud, M.H., O'Keeffe, M., Shao, Q.X., Chen, W.F.*, et al.* (2005). Cutting edge: generation of splenic CD8+ and CD8- dendritic cell equivalents in Fms-like tyrosine kinase 3 ligand bone marrow cultures. J Immunol *174*, 6592-6597.

Nakano, H., Yanagita, M., and Gunn, M.D. (2001). CD11c(+)B220(+)Gr-1(+) cells in mouse lymph nodes and spleen display characteristics of plasmacytoid dendritic cells. J Exp Med *194*, 1171-1178.

Negishi, H., Fujita, Y., Yanai, H., Sakaguchi, S., Ouyang, X., Shinohara, M., Takayanagi, H., Ohba, Y., Taniguchi, T., and Honda, K. (2006). Evidence for licensing of IFN-gamma-induced IFN regulatory factor 1 transcription factor by MyD88 in Toll-like receptor-dependent gene induction program. Proc Natl Acad Sci U S A *103*, 15136-15141.

Niederquell, M., Kurig, S., Fischer, J.A., Tomiuk, S., Swiecki, M., Colonna, M., Johnston, I.C., and Dzionek, A. (2013). Sca-1 expression defines developmental stages of mouse pDCs that show functional heterogeneity in the endosomal but not lysosomal TLR9 response. Eur J Immunol *43*, 2993-3005.

Nikolic, T., Dingjan, G.M., Leenen, P.J., and Hendriks, R.W. (2002). A subfraction of B220(+) cells in murine bone marrow and spleen does not belong to the B cell lineage but has dendritic cell characteristics. Eur J Immunol *32*, 686-692.

O'Keeffe, M., Fancke, B., Suter, M., Ramm, G., Clark, J., Wu, L., and Hochrein, H. (2012). Nonplasmacytoid, high IFN-α-producing, bone marrow dendritic cells. J Immunol *188*, 3774-3783.

O'Keeffe, M., Grumont, R.J., Hochrein, H., Fuchsberger, M., Gugasyan, R., Vremec, D., Shortman, K., and Gerondakis, S. (2005). Distinct roles for the NF-kappaB1 and c-Rel transcription factors in the differentiation and survival of plasmacytoid and conventional dendritic cells activated by TLR-9 signals. Blood *106*, 3457-3464.

O'Keeffe, M., Hochrein, H., Vremec, D., Caminschi, I., Miller, J.L., Anders, E.M., Wu, L., Lahoud, M.H., Henri, S., Scott, B.*, et al.* (2002). Mouse plasmacytoid cells: long-lived cells, heterogeneous in surface phenotype and function, that differentiate into CD8(+) dendritic cells only after microbial stimulus. J Exp Med *196*, 1307-1319.

O'Neill, L.A., Fitzgerald, K.A., and Bowie, A.G. (2003). The Toll-IL-1 receptor adaptor family grows to five members. Trends Immunol *24*, 286-290.

Obermann, H.L., and Bauer, S. (2012). Toll-like receptor 9, what o'clock is it? Immunity *36*, 159-161.

Ohno, Y., Yasunaga, S., Janmohamed, S., Ohtsubo, M., Saeki, K., Kurogi, T., Mihara, K., Iscove, N.N., and Takihara, Y. (2013). Hoxa9 transduction induces hematopoietic stem and progenitor cell activity through direct down-regulation of geminin protein. PLoS One *8*, e53161.

Oldenburg, M., Krüger, A., Ferstl, R., Kaufmann, A., Nees, G., Sigmund, A., Bathke, B., Lauterbach, H., Suter, M., Dreher, S.*, et al.* (2012). TLR13 recognizes bacterial 23S rRNA devoid of erythromycin resistance-forming modification. Science *337*, 1111-1115.

Ordureau, A., Enesa, K., Nanda, S., Le Francois, B., Peggie, M., Prescott, A., Albert, P.R., and Cohen, P. (2013). DEAF1 is a Pellino1-interacting protein required for interferon production by Sendai virus and double stranded RNA. J Biol Chem.

Ozinsky, A., Underhill, D.M., Fontenot, J.D., Hajjar, A.M., Smith, K.D., Wilson, C.B., Schroeder, L., and Aderem, A. (2000). The repertoire for pattern recognition of pathogens by the innate immune system is defined by cooperation between toll-like receptors. Proc Natl Acad Sci U S A *97*, 13766-13771.

Paludan, S.R., and Bowie, A.G. (2013). Immune sensing of DNA. Immunity *38*, 870-880.

Park, B., Buti, L., Lee, S., Matsuwaki, T., Spooner, E., Brinkmann, M.M., Nishihara, M., and Ploegh, H.L. (2011). Granulin is a soluble cofactor for toll-like receptor 9 signaling. Immunity *34*, 505-513.

Park, B.S., Song, D.H., Kim, H.M., Choi, B.S., Lee, H., and Lee, J.O. (2009). The structural basis of lipopolysaccharide recognition by the TLR4-MD-2 complex. Nature *458*, 1191-1195.

Parroche, P., Lauw, F.N., Goutagny, N., Latz, E., Monks, B.G., Visintin, A., Halmen, K.A., Lamphier, M., Olivier, M., Bartholomeu, D.C.*, et al.* (2007). Malaria hemozoin is immunologically inert but radically enhances innate responses by presenting malaria DNA to Toll-like receptor 9. Proc Natl Acad Sci U S A *104*, 1919-1924.

Pauls, E., Shpiro, N., Peggie, M., Young, E.R., Sorcek, R.J., Tan, L., Choi, H.G., and Cohen, P. (2012). Essential role for IKKβ in production of type 1 interferons by plasmacytoid dendritic cells. J Biol Chem *287*, 19216-19228.

Perfetto, S.P., Chattopadhyay, P.K., and Roederer, M. (2004). Seventeen-colour flow cytometry: unravelling the immune system. Nat Rev Immunol *4*, 648-655.

Pifer, R., Benson, A., Sturge, C.R., and Yarovinsky, F. (2011). UNC93B1 is essential for TLR11 activation and IL-12-dependent host resistance to Toxoplasma gondii. J Biol Chem *286*, 3307-3314.

Pineault, N., Helgason, C.D., Lawrence, H.J., and Humphries, R.K. (2002). Differential expression of Hox, Meis1, and Pbx1 genes in primitive cells throughout murine hematopoietic ontogeny. Exp Hematol *30*, 49-57.

Rahim, M.M., Tai, L.H., Troke, A.D., Mahmoud, A.B., Abou-Samra, E., Roy, J.G., Mottashed, A., Ault, N., Corbeil, C., Goulet, M.L.*, et al.* (2013). Ly49Q positively regulates type I IFN production by plasmacytoid dendritic cells in an immunoreceptor tyrosine-based inhibitory motif-dependent manner. J Immunol *190*, 3994-4004.

Ramos-Mejía, V., Navarro-Montero, O., Ayllón, V., Bueno, C., Romero, T., Real, P.J., and Menendez, P. (2014). HOXA9 promotes hematopoietic commitment of human embryonic stem cells. Blood *124*, 3065-3075.

Randolph, G.J., Beaulieu, S., Lebecque, S., Steinman, R.M., and Muller, W.A. (1998). Differentiation of monocytes into dendritic cells in a model of transendothelial trafficking. Science *282*, 480-483.

Reizis, B., Bunin, A., Ghosh, H.S., Lewis, K.L., and Sisirak, V. (2011). Plasmacytoid dendritic cells: recent progress and open questions. Annu Rev Immunol *29*, 163-183.

Rezsohazy, R., Saurin, A.J., Maurel-Zaffran, C., and Graba, Y. (2015). Cellular and molecular insights into Hox protein action. Development *142*, 1212-1227.

Roach, J.C., Glusman, G., Rowen, L., Kaur, A., Purcell, M.K., Smith, K.D., Hood, L.E., and Aderem, A. (2005). The evolution of vertebrate Toll-like receptors. Proc Natl Acad Sci U S A *102*, 9577-9582.

Rodig, S.J., Shahsafaei, A., Li, B., and Dorfman, D.M. (2005). The CD45 isoform B220 identifies select subsets of human B cells and B-cell lymphoproliferative disorders. Hum Pathol *36*, 51-57.

Saiki, R.K., Scharf, S., Faloona, F., Mullis, K.B., Horn, G.T., Erlich, H.A., and Arnheim, N. (1985). Enzymatic amplification of beta-globin genomic sequences and restriction site analysis for diagnosis of sickle cell anemia. Science *230*, 1350-1354.

Saitoh, T., and Akira, S. (2010). Regulation of innate immune responses by autophagy-related proteins. J Cell Biol *189*, 925-935.

Saitoh, T., Satoh, T., Yamamoto, N., Uematsu, S., Takeuchi, O., Kawai, T., and Akira, S. (2011). Antiviral protein Viperin promotes Toll-like receptor 7- and Toll-like receptor 9-mediated type I interferon production in plasmacytoid dendritic cells. Immunity *34*, 352-363.

Sasai, M., Linehan, M.M., and Iwasaki, A. (2010). Bifurcation of Toll-like receptor 9 signaling by adaptor protein 3. Science *329*, 1530-1534.

Sawai, C.M., Sisirak, V., Ghosh, H.S., Hou, E.Z., Ceribelli, M., Staudt, L.M., and Reizis, B. (2013). Transcription factor Runx2 controls the development and migration of plasmacytoid dendritic cells. J Exp Med *210*, 2151-2159.

Schlitzer, A., Loschko, J., Mair, K., Vogelmann, R., Henkel, L., Einwächter, H., Schiemann, M., Niess, J.H., Reindl, W., and Krug, A. (2011). Identification of CCR9-murine plasmacytoid DC precursors with plasticity to differentiate into conventional DCs. Blood *117*, 6562-6570.

Schmid, M.A., Kingston, D., Boddupalli, S., and Manz, M.G. (2010). Instructive cytokine signals in dendritic cell lineage commitment. Immunol Rev *234*, 32-44.

Schmid, M.A., Takizawa, H., Baumjohann, D.R., Saito, Y., and Manz, M.G. (2011). Bone marrow dendritic cell progenitors sense pathogens via Toll-like receptors and subsequently migrate to inflamed lymph nodes. Blood *118*, 4829-4840.

Schmitz, F., Heit, A., Guggemoos, S., Krug, A., Mages, J., Schiemann, M., Adler, H., Drexler, I., Haas, T., Lang, R., and Wagner, H. (2007). Interferon-regulatory-factor 1

controls Toll-like receptor 9-mediated IFN-beta production in myeloid dendritic cells. Eur J Immunol *37*, 315-327.

Schraml, B.U., and Reis e Sousa, C. (2015). Defining dendritic cells. Curr Opin Immunol *32*, 13-20.

Schroeder, J.T., Bieneman, A.P., Xiao, H., Chichester, K.L., Vasagar, K., Saini, S., and Liu, M.C. (2005). TLR9- and FcepsilonRI-mediated responses oppose one another in plasmacytoid dendritic cells by down-regulating receptor expression. J Immunol *175*, 5724-5731.

Schwandner, R., Dziarski, R., Wesche, H., Rothe, M., and Kirschning, C.J. (1999). Peptidoglycan- and lipoteichoic acid-induced cell activation is mediated by toll-like receptor 2. J Biol Chem *274*, 17406-17409.

Segura, E., Wong, J., and Villadangos, J.A. (2009). Cutting edge: B220+CCR9- dendritic cells are not plasmacytoid dendritic cells but are precursors of conventional dendritic cells. J Immunol *183*, 1514-1517.

Shah, K.M., Stewart, S.E., Wei, W., Woodman, C.B., O'Neil, J.D., Dawson, C.W., and Young, L.S. (2009). The EBV-encoded latent membrane proteins, LMP2A and LMP2B, limit the actions of interferon by targeting interferon receptors for degradation. Oncogene *28*, 3903-3914.

Shah, N., and Sukumar, S. (2010). The Hox genes and their roles in oncogenesis. Nat Rev Cancer *10*, 361-371.

Shi, Z., Cai, Z., Sanchez, A., Zhang, T., Wen, S., Wang, J., Yang, J., Fu, S., and Zhang, D. (2011). A novel Toll-like receptor that recognizes vesicular stomatitis virus. J Biol Chem *286*, 4517-4524.

Shinohara, M.L., Lu, L., Bu, J., Werneck, M.B., Kobayashi, K.S., Glimcher, L.H., and Cantor, H. (2006). Osteopontin expression is essential for interferon-alpha production by plasmacytoid dendritic cells. Nat Immunol *7*, 498-506.

Silver, A.C., Arjona, A., Walker, W.E., and Fikrig, E. (2012). The circadian clock controls toll-like receptor 9-mediated innate and adaptive immunity. Immunity *36*, 251-261.

Silverstein, A.M. (2003). Cellular versus humoral immunology: a century-long dispute. Nat Immunol *4*, 425-428.

Sitnicka, E., Bryder, D., Theilgaard-Mönch, K., Buza-Vidas, N., Adolfsson, J., and Jacobsen, S.E. (2002). Key role of flt3 ligand in regulation of the common lymphoid progenitor but not in maintenance of the hematopoietic stem cell pool. Immunity *17*, 463-472.

Sletvold, O., and Laerum, O.D. (1988). Alterations of cell cycle distribution in the bone marrow of aging mice measured by flow cytometry. Exp Gerontol *23*, 43-58.

Soshnikova, N. (2014). Hox genes regulation in vertebrates. Dev Dyn *243*, 49-58.

Staffas, A., Arabanian, L.S., Wei, S.Y., Jansson, A., Ståhlman, S., Johansson, P., Fogelstrand, L., Cammenga, J., Kuchenbauer, F., and Palmqvist, L. (2016). Upregulation of Flt3 is a passive event in Hoxa9/Meis1-induced acute myeloid leukemia in mice. Oncogene.

Stanley, E.R., Chen, D.M., and Lin, H.S. (1978). Induction of macrophage production and proliferation by a purified colony stimulating factor. Nature *274*, 168-170.

Steger, J., Füller, E., Garcia-Cuellar, M.P., Hetzner, K., and Slany, R.K. (2015). Insulin-like growth factor 1 is a direct HOXA9 target important for hematopoietic transformation. Leukemia *29*, 901-908.

Steinman, R.M., and Cohn, Z.A. (1973). Identification of a novel cell type in peripheral lymphoid organs of mice. I. Morphology, quantitation, tissue distribution. J Exp Med *137*, 1142-1162.

Steinman, R.M., and Idoyaga, J. (2010). Features of the dendritic cell lineage. Immunol Rev *234*, 5-17.

Sun, L., Wu, J., Du, F., Chen, X., and Chen, Z.J. (2013a). Cyclic GMP-AMP synthase is a cytosolic DNA sensor that activates the type I interferon pathway. Science *339*, 786-791.

Sun, M., Song, C.X., Huang, H., Frankenberger, C.A., Sankarasharma, D., Gomes, S., Chen, P., Chen, J., Chada, K.K., He, C., and Rosner, M.R. (2013b).

HMGA2/TET1/HOXA9 signaling pathway regulates breast cancer growth and metastasis. Proc Natl Acad Sci U S A *110*, 9920-9925.

Svingen, T., and Tonissen, K.F. (2006). Hox transcription factors and their elusive mammalian gene targets. Heredity *97*, 88-96.

Swiecki, M., and Colonna, M. (2015). The multifaceted biology of plasmacytoid dendritic cells. Nat Rev Immunol *15*, 471-485.

Tabeta, K., Hoebe, K., Janssen, E.M., Du, X., Georgel, P., Crozat, K., Mudd, S., Mann, N., Sovath, S., Goode, J.*, et al.* (2006). The Unc93b1 mutation 3d disrupts exogenous antigen presentation and signaling via Toll-like receptors 3, 7 and 9. Nat Immunol *7*, 156-164.

Tai, L.H., Goulet, M.L., Belanger, S., Toyama-Sorimachi, N., Fodil-Cornu, N., Vidal, S.M., Troke, A.D., McVicar, D.W., and Makrigiannis, A.P. (2008). Positive regulation of plasmacytoid dendritic cell function via Ly49Q recognition of class I MHC. J Exp Med *205*, 3187-3199.

Takaoka, A., Yanai, H., Kondo, S., Duncan, G., Negishi, H., Mizutani, T., Kano, S., Honda, K., Ohba, Y., Mak, T.W., and Taniguchi, T. (2005). Integral role of IRF-5 in the gene induction programme activated by Toll-like receptors. Nature *434*, 243-249.

Takeda, A., Goolsby, C., and Yaseen, N.R. (2006). NUP98-HOXA9 induces long-term proliferation and blocks differentiation of primary human CD34+ hematopoietic cells. Cancer Res *66*, 6628-6637.

Takeshita, F., Leifer, C.A., Gursel, I., Ishii, K.J., Takeshita, S., Gursel, M., and Klinman, D.M. (2001). Cutting edge: Role of Toll-like receptor 9 in CpG DNA-induced activation of human cells. J Immunol *167*, 3555-3558.

Takeuchi, O., and Akira, S. (2010). Pattern recognition receptors and inflammation. Cell *140*, 805-820.

Talukder, A.H., Bao, M., Kim, T.W., Facchinetti, V., Hanabuchi, S., Bover, L., Zal, T., and Liu, Y.J. (2012). Phospholipid scramblase 1 regulates Toll-like receptor 9-mediated type I interferon production in plasmacytoid dendritic cells. Cell Res *22*, 1129-1139.

Tanimura, N., Saitoh, S., Matsumoto, F., Akashi-Takamura, S., and Miyake, K. (2008). Roles for LPS-dependent interaction and relocation of TLR4 and TRAM in TRIF-signaling. Biochem Biophys Res Commun *368*, 94-99.

Tenoever, B.R., Ng, S.L., Chua, M.A., McWhirter, S.M., García-Sastre, A., and Maniatis, T. (2007). Multiple functions of the IKK-related kinase IKKepsilon in interferon-mediated antiviral immunity. Science *315*, 1274-1278.

Tomai, M.A., Miller, R.L., Lipson, K.E., Kieper, W.C., Zarraga, I.E., and Vasilakos, J.P. (2007). Resiquimod and other immune response modifiers as vaccine adjuvants. Expert Rev Vaccines *6*, 835-847.

Topisirovic, I., Kentsis, A., Perez, J.M., Guzman, M.L., Jordan, C.T., and Borden, K.L. (2005). Eukaryotic translation initiation factor 4E activity is modulated by HOXA9 at multiple levels. Mol Cell Biol *25*, 1100-1112.

Trinchieri, G. (2010). Type I interferon: friend or foe? J Exp Med *207*, 2053-2063.

Tun-Kyi, A., Finn, G., Greenwood, A., Nowak, M., Lee, T.H., Asara, J.M., Tsokos, G.C., Fitzgerald, K., Israel, E., Li, X.*, et al.* (2011). Essential role for the prolyl isomerase Pin1 in Toll-like receptor signaling and type I interferon-mediated immunity. Nat Immunol *12*, 733-741.

Uematsu, S., Fujimoto, K., Jang, M.H., Yang, B.G., Jung, Y.J., Nishiyama, M., Sato, S., Tsujimura, T., Yamamoto, M., Yokota, Y.*, et al.* (2008). Regulation of humoral and cellular gut immunity by lamina propria dendritic cells expressing Toll-like receptor 5. Nat Immunol *9*, 769-776.

Velu, C.S., Chaubey, A., Phelan, J.D., Horman, S.R., Wunderlich, M., Guzman, M.L., Jegga, A.G., Zeleznik-Le, N.J., Chen, J., Mulloy, J.C.*, et al.* (2014). Therapeutic antagonists of microRNAs deplete leukemia-initiating cell activity. J Clin Invest *124*, 222-236.

Verthelyi, D., Ishii, K.J., Gursel, M., Takeshita, F., and Klinman, D.M. (2001). Human peripheral blood cells differentially recognize and respond to two distinct CPG motifs. J Immunol *166*, 2372-2377.

Wagner, H. (2008). The sweetness of the DNA backbone drives Toll-like receptor 9. Curr Opin Immunol *20*, 396-400.

Wang, G.G., Pasillas, M.P., and Kamps, M.P. (2006). Persistent transactivation by meis1 replaces hox function in myeloid leukemogenesis models: evidence for co-occupancy of meis1-pbx and hox-pbx complexes on promoters of leukemia-associated genes. Mol Cell Biol *26*, 3902-3916.

Ward, A.E., and Rosenthal, B.M. (2014). Evolutionary responses of innate immunity to adaptive immunity. Infect Genet Evol *21*, 492-496.

Waskow, C., Liu, K., Darrasse-Jèze, G., Guermonprez, P., Ginhoux, F., Merad, M., Shengelia, T., Yao, K., and Nussenzweig, M. (2008). The receptor tyrosine kinase Flt3 is required for dendritic cell development in peripheral lymphoid tissues. Nat Immunol *9*, 676-683.

Watarai, H., Sekine, E., Inoue, S., Nakagawa, R., Kaisho, T., and Taniguchi, M. (2008). PDC-TREM, a plasmacytoid dendritic cell-specific receptor, is responsible for augmented production of type I interferon. Proc Natl Acad Sci U S A *105*, 2993-2998.

Watowich, S.S., and Liu, Y.J. (2010). Mechanisms regulating dendritic cell specification and development. Immunol Rev *238*, 76-92.

Weber, F., Wagner, V., Rasmussen, S.B., Hartmann, R., and Paludan, S.R. (2006). Double-stranded RNA is produced by positive-strand RNA viruses and DNA viruses but not in detectable amounts by negative-strand RNA viruses. J Virol *80*, 5059-5064.

Weighardt, H., Jusek, G., Mages, J., Lang, R., Hoebe, K., Beutler, B., and Holzmann, B. (2004). Identification of a TLR4- and TRIF-dependent activation program of dendritic cells. Eur J Immunol *34*, 558-564.

West, A.P., Brodsky, I.E., Rahner, C., Woo, D.K., Erdjument-Bromage, H., Tempst, P., Walsh, M.C., Choi, Y., Shadel, G.S., and Ghosh, S. (2011). TLR signalling augments macrophage bactericidal activity through mitochondrial ROS. Nature *472*, 476-480.

Wu, J., Sun, L., Chen, X., Du, F., Shi, H., Chen, C., and Chen, Z.J. (2013). Cyclic GMP-AMP is an endogenous second messenger in innate immune signaling by cytosolic DNA. Science *339*, 826-830.

Yamamoto, M., Sato, S., Hemmi, H., Hoshino, K., Kaisho, T., Sanjo, H., Takeuchi, O., Sugiyama, M., Okabe, M., Takeda, K., and Akira, S. (2003). Role of adaptor TRIF in the MyD88-independent toll-like receptor signaling pathway. Science *301*, 640-643.

Yarovinsky, F., Zhang, D., Andersen, J.F., Bannenberg, G.L., Serhan, C.N., Hayden, M.S., Hieny, S., Sutterwala, F.S., Flavell, R.A., Ghosh, S., and Sher, A. (2005). TLR11 activation of dendritic cells by a protozoan profilin-like protein. Science *308*, 1626-1629.

Yasuda, K., Rutz, M., Schlatter, B., Metzger, J., Luppa, P.B., Schmitz, F., Haas, T., Heit, A., Bauer, S., and Wagner, H. (2006). CpG motif-independent activation of TLR9 upon endosomal translocation of "natural" phosphodiester DNA. Eur J Immunol *36*, 431-436.

Yoshizaki, M., Tazawa, A., Kasumi, E., Sasawatari, S., Itoh, K., Dohi, T., Sasazuki, T., Inaba, K., Makrigiannis, A.P., and Toyama-Sorimachi, N. (2009). Spatiotemporal regulation of intracellular trafficking of Toll-like receptor 9 by an inhibitory receptor, Ly49Q. Blood *114*, 1518-1527.

Yu, P., Lübben, W., Slomka, H., Gebler, J., Konert, M., Cai, C., Neubrandt, L., Prazeres da Costa, O., Paul, S., Dehnert, S.*, et al.* (2012). Nucleic acid-sensing Toll-like receptors are essential for the control of endogenous retrovirus viremia and ERV-induced tumors. Immunity *37*, 867-879.

Yu, Y., and Hayward, G.S. (2010). The ubiquitin E3 ligase RAUL negatively regulates type i interferon through ubiquitination of the transcription factors IRF7 and IRF3. Immunity *33*, 863-877.

Zhang, J., Han, B., Li, X., Bies, J., Jiang, P., Koller, R.P., and Wolff, L. (2016). Distal regulation of c-myb expression during IL-6-induced differentiation in murine myeloid progenitor M1 cells. Cell Death Dis *7*, e2364.

7. TABLE OF ACADEMIC TEACHERS

My academic teachers in Marburg:

Adamkiewicz, Afanou, Aigner, Albert, Alter, Arabin, Aumüller, Bahr, Barth, Bartsch, Basler, Bauer, Baum, Baumann, Becker, Bender, Benes, Berger, Bette, Bien, Brehm, Bürk, Carl, Cetin, Czubayko, Daut, del Rey, Dietrich, Dinges, Dodel, Donner-Banzhoff, Droutsas, Eberhart, Efe, Eggert, Eivazi, Ellenrieder, El-Zayat, Eming, Engenhart-Cabillic, Ermisch, Fendrich, Feuser, Figiel, Frink, Fuchs-Winkelmann, Geks, Goeze, Görg, Gress, Grosse, Grundmann, Grzeschik, Hadji, Hahn, Häußermann, Hegele, Heinis, Hertl, Heyse, Höffken, Hoffmann, Hofmann, Hoyer, Hundt, Jablonski-Momeni, Jacob, Jerrentrup, Kann, Kanngießer, Kaufmann, Kerzel, Kircher, Kiriazidis, Kirschbaum, Klose, Koch, Koczulla, König, Konrad, Koolman, Kratz, Krause, Kroh, Krüger, Kühne, Kühnert, Langer, Leonhardt, Leube, Lill, Linhart, Löffler, Lohoff, Lorch, Lüers, Maier, Maisch, Maisner, Mandic, Mandrek, Mann, Mayer, Mennel, Michl, Milani, Mittag, Moll, Moosdorf, Mueller, Müller, Mutters, Neubauer, Nimsky, Oertel, Olbert, Pagenstecher, Plöger, Pfestroff, Plant, Preisig-Müller, Ramaswamy, Rausch, Reese, Renz, Richter, Rohlfs, Röhm, Röper, Rosenow, Ruchholtz, Rupp, Rüsch, Schade, Schäfer, Schlosser, Schmidt, Schofer, Schoner, Schu, Schulze, Schütz, Sehrbundt, Seitz, Sekundo, Sesterhenn, Sevinc, Sommer, Steinbach-Hundt, Steinfeldt, Steiniger, Stiewe, Strauch, Strempel, Strik, Suske, Tackenberg, Teigelkamp, Teymoortash, Vogelmeier, Vogt, Wagner, Waldegger, Waldmann, Weber, Weihe, Werner, Westermann, Wilhelm, Woernle, Wulf, Yang, Ziring, Zettl, Zoremba, Zovko

My academic teachers in Frankenberg:

Cassebaum, Dylla, Hübner, Ludoph

My academic teachers in Kassel:

Deeb, Deventer, von Ditfurth, Faß, de Haan, Khalid, Loer, Raible, Ruten, Spiller

8. ACKNOWLEDGEMENTS

A big thanks goes to Prof. Dr. Stefan Bauer for giving me the opportunity to do such an interesting and challenging work in his department. Furthermore, I want to express special gratitude to Dr. Andreas Kaufmann for is guidance and patience during the whole work. I will never forget your dry sense of humor – yes the "lost son" has finally done it. All the staff from AG Kaufmann helped me a lot in learning the methods and getting on with laboratory work to realize this project. I would like to mention especially Jenny Großmann, Steffi Jung, Steffi Jöckel, Viktoria Laukemper, and Hannah-Lena Obermann for their support and friendship during this time. A special thanks goes to AG Schnare for providing the GM-CSF-induced DC cultures as well as the use of Poly I:C for several experiments. The FACS sorting experiments would not have been possible without Hartmann Raifer from the Institute for Microbiology and Hygiene – thanks a lot for your instructions, patience, and evenings you have spent with me at the FACSAria sorter.

This thesis would never have been possible without the help of my family. First of all, I thank my wonderful wife Jessica Bleyl for her outstanding patience and perseverance during approximately 6 years of our lifetime that this work needed to be eventually finished after several setbacks. My wife and my parents Karla and Fritz Bleyl made it possible for me to become a physician because of constant loving understanding and always being there encouraging me not to give up in difficult times. My mother Karla died suddenly in July 2015. She was the best mother one can imagine. This doctoral thesis is dedicated to her. I thank the rest of my family for supporting me during this time.

Official licenses were obtained for all pictures and figures used from other publications. Permission to reproduce this copyrighted material in this dissertation was granted by the respective publishers. The following table lists figures, license numbers, and references.

FIGURE	LICENSE NUMBER	REFERENCE
1.1	4210691375899	Reprinted from Immunity, Vol 34/ Issue 5, Taro Kawai and Shizuo Akira, Toll-like Receptors and Their Crosstalk with Other Innate Receptors in Infection and Immunity, Pages 637 - 650, Copyright (2011), with permission from Elsevier.
1.2	4210710901003	Reprinted from Immunity, Vol 32/ Issue 3, Amanda L. Blasius and Bruce Beutler, Intracellular Toll-like Receptors, Pages 305 - 315, Copyright (2010), with permission from Elsevier.
1.3 B	4210720903022	Reprinted from The Journal of Experimental Medicine (JEM), Vol 204/ Issue 10, Hema Bashyam, Ralph Steinman: Dendritic cells bring home the Lasker, Pages 2245 - 2248, Copyright (2007), with permission from Rockefeller University Press.
1.3 A and B	4210731170302	Reprinted from Nature Medicine, Vol 9/ Issue 1, Nina Bhardwaj and Bruce D. Walker, Immunotherapy for AIDS virus infections: Cautious optimism for cell-based vaccine, Pages 13 - 14, Copyright (2003), with permission from Nature Publishing Group.
1.3 A	4210740409361	Reprinted from Nature Immunology, Vol 5/ Issue 12, Marco Colonna, Giorgio Trinchieri, and Yong-Jun Liu, Plasmacytoid dendritic cells in immunity, Pages 1219 - 1226, Copyright (2004), with permission from Nature Publishing Group.
1.5 and 1.6	4210760675326	Reprinted from Development, Vol 142/ Issue 7, René Rezsohazy, Andrew J. Saurin, Corinne Maurel-Zaffran, and Yacine Graba, Cellular and molecular insights into Hox protein action, Pages 1212 - 1227, Copyright (2015), with permission from Company of Biologists.